eman ta zabal zazu

Universidad del País Vasco

Euskal Herriko Unibertsitatea

Azole resistance mechanisms in *Candida albicans*. Exposure to fluconazole and the role of the Erg11 Y477C, Tac1 S758F and Mrr2 A311V new mutations by CRISPR-Cas9 gene editing.

Pilar Menéndez-Manjón Tartiere

Supervisors: María Dolores Moragues Tosantos and

Inés Arrieta Aguirre

Department of Nursing I

Department of Immunology, Microbiology and Parasitology

Leioa

2022

Abbreviations and acronyms

5FC	Flucytosine
5FdUMP	5-fluorodeoxyuridine monophosphate
5FU	5-fluorouracil
5FUTP	5-fluorouridine triphosphate
A	Adenine
A	Alanine
A230	Absorbance at 230 nm
A260	Absorbance at 260 nm
A280	Absorbance at 280 nm
ABC	ATP-binding cassette
ABCD	Amphotericin B complexed with cholesteryl sulfate
ABD	Amphotericin B complexed with deoxycholate
ABLC	Amphotericin B lipid complex
AD1	Distal activation domain 1
AmB	Amphotericin B
AFG	Anidulafungin
ARE	Azole-responsive element
ATCC	American Type Culture Collection
ATP	Adenosine-5'-triphosphate
BEE	Basal expression element
BLAST	Basic Alignment Search Tool
bp	Base pair
BRE	Benomyl responsive element
C	Cytosine
C	Cysteine
Cap1	*C. albicans AP-1*
Cas	CRISPR-associated protein
cas	CRISPR-associated gene
CFG	Caspofungin
CDC	US Center of Disease Control and Prevention
cDNA	Complementary DNA
Cdr1	*Candida* drug resistance 1
Cdr2	*Candida* drug resistance 2
CDS	Coding sequence
Chr5L	Left arm of chromosome 5
Chr	Chromosome
CLSI	Clinical and Laboratory Standards Institute
CLT	Clotrimazole
Cq	Quantification cycle

CRISPR Clustered regularly interspaced short palindromic repeats

crRNA	Short CRISPR RNA
Cys	Cysteine
D	Aspartic acid
DBD	DNA-binding domain
DMSO	Dimethyl sulfoxide
DNA	Deoxyribonucleic acid
DRE	Drug responsive element
DSB	Double-stranded break
DTT	Dithiothreitol
E	Glutamic acid
EDTA	Ethylenediaminetetraacetic acid
F	Phenylalanine
FC	Fold-change
Fks	FK506-supersensitive/β-1,3-D-glucan synthase
FLC	Fluconazole
Flp	Flippase (tyrosine site-specific recombinase)
FO	Flip-out
FRT	Flp recognition target
FSL	Fungus-specific loop
G	Glycine
G	Guanine
GOF	Gain-of-function
GPI	Glycosyl phosphatidylinositol
gRNA	Guide-RNA
GTP	Guanosine-5'-triphosphate
H	Histidine
h	Hours
HDR	Homology-directed repair
HR	Homologous recombination
HRE	H_2O_2 response element
Hsp90	Heat shock protein 90
I	Isoleucine
ID1	Inhibitory domain
IDSA	Infectious Diseases Society of America
IDT	Integrated DNA Technologies
IFI	Invasive fungal infection
indel	Insertion and deletion
INV	Inverted repeat sequence
IPC	Inter-plate calibrator
ITC	Itraconazole

K	Lysine
kb	Kilobase
KDAC	Lysine deacetylases
L	Leucine
L-AmB	Amphotericin B lipid formulation
LB	Luria-Bertani
LBD	Ligand-binding domain
LOF	Loss-of-function
LOH	Loss of heterozygosity
MAPK	Mitogen-activated protein kinase
Mb	Megabase
Mdr1	Multidrug resistance 1
MFG	Micafungin
MFS	Major Facilitator
MHR	Middle homology region
MIC	Minimal inhibitory concentration
MMEJ	Microhomology-mediated end joining
MOPS	3-(N-Morpholino)propanesulfonic acid
mRNA	Messenger RNA
Mrr1	Multidrug resistance regulator 1
Mrr2	Multidrug resistance regulator 2
MTL	Mating type-like locus
N	Asparagine
NAC	Non-*albicans Candida*
NBD	Nucleotide binding domain
NCBI	National Center for Biotechnology Information
NHEJ	Nonhomologous end joining
NLS	Nuclear localization signal
NRE	Negative regulator element
NT	Nourseothricin
nt	Nucleotide
OD	Optical density
OD_{600}	Optical density at 600 nm
ON	Over-night
P	Proline
PAM	Protospacer adjacent motif
PBS	Phosphate buffered saline
PCR	Polymerase chain reaction
PDK1	Phosphoinositide-dependent kinase 1
Pdr	Pleiotropic drug resistance

PKC	Protein kinase C
Pap1	Poly(A) polymerase
POS	Posaconazole
Q	Glutamine
R	Arginine
Rep1	Regulator of efflux pump 1
RNA	Ribonucleic acid
RNP	CRISPR RNA-Cas9 protein complex
rpm	Revolutions per minute
RT	Reverse transcription
RT-qPCR	Quantitative reverse transcription PCR
RTe	Repair template
S	Serine
SD	Standard deviation
SDD	Susceptible-dose dependent
SDS	Sodium dodecyl sulfate
sgRNA	Single-guide RNA
SMG	Supra-MIC growth
SNP	Single nucleotide polymorphism
SRE	Sterol response element
SRE	Steroid responsive element
T	Threonine
T	Thymine
Tac1	Transcriptional activator of *CDR* genes
TAD	Transcriptional activation domain
Tm	Melting temperature
TMD	Transmembrane domain
TOR	Target of rapamycin
tracrRNA	Trans-activating RNA
Tris	Tris(hydroxymethyl)aminomethane
tRNA	Transfer RNA
Upc2	Uptake control 2
UPV/EHU	Universidad del País Vasco/Euskal Herriko Unibertsitatea
USA	United States of America
UTP	Uridine triphosphate
V	Valine
VRC	Voriconazole
W	Tryptophan
WT	Wild type
Y	Tyrosine

YEPD	Yeast Extract Peptone Dextrose
YNB	Yeast Nitrogen Base
Zn	Zinc

Index

INTRODUCTION

1. INTRODUCTION

Fungal infections are estimated to affect more than one billion people worldwide (Bongomin et al., 2017) comprising from mucocutaneous to severe systemic infections. Superficial infections of the skin and nails are the most common fungal diseases in humans and affect around 25% of the general population worldwide (Bongomin et al., 2017; Havlickova et al., 2008). Mucosal infections of the oral and genital tracts are also common, especially vulvovaginal candidiasis. In fact, 50 to 75% of women in their childbearing years suffer from at least one episode of vulvovaginitis, and 5 to 8% (~75 million women) have at least four episodes annually (Gamarra et al., 2014; Sobel, 2007). On the other hand, even though invasive fungal infections (IFIs) have a much lower incidence than superficial infections, which are estimated to affect between 150-300 million people worldwide (Bongomin et al., 2017; Geddes-McAlister & Shapiro, 2018), are of great concern because they are associated with extremely high mortality rates (Bongomin et al., 2017; Brown et al., 2012). According to current estimates, 1.6 million people die every year from invasive diseases caused by different fungal species, almost the same as for tuberculosis (Bongomin et al., 2017; Brown et al., 2012). Therefore, fungal pathogens are being recognized as a major human threat (Geddes-McAlister & Shapiro, 2018).

The current incidence of invasive diseases is largely a result of the increase in immunosuppressive infections, such as HIV/AIDS, and modern immunosuppressive treatments (cancer patients, transplant recipients) and invasive medical interventions (Brown et al., 2012; Castanheira et al., 2017; Pfaller et al., 2019). Additionally, the increase in the numbers of individuals in the elderly, neonate, and patient populations requiring invasive therapies also contributes to the higher rates of IFIs (Castanheira et al., 2017; Pfaller et al., 2019).

Among the fungi that can cause IFIs, *Candida* yeast species are the primary threat, particularly in health care settings, where they are among the top four most common nosocomial bloodstream pathogens (Lamoth et al., 2018; McCarty & Pappas, 2016).

1.1. *Candida* infections

Candida species are commensals and part of the normal human microbiota of skin, gastrointestinal and genital tracts; however, they can trigger either superficial and mucosal infections or invasive infections. Superficial infections can affect immunocompetent patients, while invasive infections are found in susceptible patients such as elderly and immunocompromised people (Bhattacharya et al., 2020). And it has also been associated with the use of medical devices such as central venous catheters, cardiovascular devices and urinary catheters (Kojic & Darouiche, 2004).

Candida species are the most common fungal etiological agent of life-threatening invasive infections (Brown et al., 2012; Kullberg & Arendrup, 2015; Magill et al., 2014; Pfaller & Castanheira, 2016). More than 400,000 candidiasis cases are estimated per year, with mortality rates ranging from 46 to 75% (Brown et al., 2012). Nonetheless, a worldwide candidemia rate is difficult to establish due to the variability of criteria followed in each study, of incidence rates in different countries and year-periods, as well as to the scarce number of studies in other regions other than Europe and North America. In addition, many patients with candidemia have underlying medical conditions that make difficult to distinguish between mortality due to *Candida* infection and all-cause mortality (Lamoth et al., 2018). There have been reports of 30% mortality in USA or Spain (Cleveland et al., 2012; Puig-Asensio et al., 2014) while in other settings it reached values as high as 60% in South Africa (Kreusch & Karstaedt, 2013) or 72% in Brazil (Doi et al., 2016).

More than a dozen *Candida* species can cause disease, but *Candida albicans* is the predominant one, representing 53.5% of the isolates in Europe and around 43% in North America (Pfaller et al., 2019) and Canada (McTaggart et al., 2020). The other four most common species of *Candida* in decreasing order of frequency are *Nakaseomyces glabrata* (formerly known as *Candida glabrata*), *Candida parapsilosis*, *Candida tropicalis* and *Pichia kudriavzevii* (formerly known as *Candida krusei*) (Pfaller et al., 2019).

1.2. *Candida albicans*

Candida albicans is a species of the genus *Candida*, clade CTG, order *Saccharomycetales*, class *Saccharomycetes*, subphylum *Saccharomycotina* and phylum *Ascomycota*. Furthermore, most of the clinically relevant *Candida* species belong to the CTG clade, which translates the CTG codon as serine instead of leucine (McManus & Coleman, 2014).

Candida albicans is a diploid polymorphic yeast that can form true hyphae, along with *Candida dubliniensis*, which is the closest relative to *C. albicans* (Jones et al., 2004; McManus & Coleman, 2014). Hyphae are considered a virulence factor due to their implication in adhesion and tissue invasion (McManus & Coleman, 2014). Usually, it reproduces clonally but can undergo a parasexual cycle (Bennett & Johnson, 2003) that contributes to genomic recombination, revelation of recessive traits by loss of heterozygosity (LOH), aneuploidy and copy number variation. This ability to generate genomic diversity provides another way to adapt to the environment (Berman & Hadany, 2012; Forche et al., 2008).

1.3. *Candida albicans* parasexual cycle

The parasexual cycle of *C. albicans* is regulated by the mating type-like locus (*MTL*), located on chromosome 5, with two idiomorphs, type a and type α, and they encode transcription factors that regulate the mating type characteristics (Hull & Johnson, 1999; McManus & Coleman, 2014). Mating only occur between cells that have phenotypically switched from the normal "white" form to the "opaque" mating competent form. Mating-competent cells are naturally homozygous at the *MTL* locus. When two cells of opposite mating type mate, they form tetraploid zygotes by conjugation, which subsequently undergo concerted chromosome loss until they reach a diploid state with high levels of homozygosity and high frequencies of aneuploidy (Figure 1.1). This process is a parasexual cycle due to the absence of meiosis. Mating is a rare phenomenon and is thought to occur only under stressful environmental conditions (McManus & Coleman, 2014).

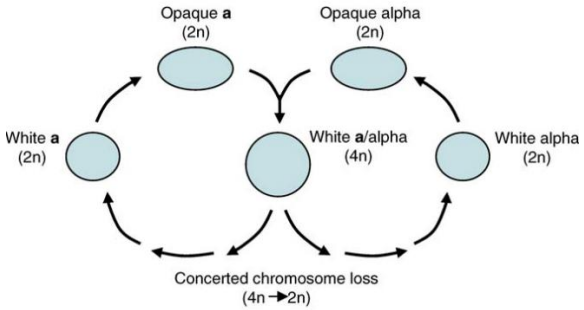

Figure 1.1. The mating cycle in *C. albicans* (Forche et al., 2008).

1.4. The genome of *Candida albicans*

Candida albicans genome's length is between 14.3 and 14.8 Mb (Cuomo et al., 2019; Jones et al., 2004; van het Hoog et al., 2007) and consists of eight pairs of chromosomes, ranging in size from 0.94 to 3.19 Mb (van het Hoog et al., 2007). The GC content is 33.5% (Cuomo et al., 2019). The genome sequence is highly polymorphic, with approximately 4 polymorphisms/kb of the genome, of which more than 89% are made up of single base substitutions (Jones et al., 2004). In fact, a genome analysis of two *C. albicans* strains revealed an average of 1 heterozygous single nucleotide polymorphism (SNP) every 330-390 base pairs (bp) (Butler et al., 2009). However, this heterozygosity is not evenly distributed through the genome, and their frequency varies considerably among isolates (Ene et al., 2019).

1.5. Antifungal drugs

Candida infections can be treated with antifungals that belong to different classes of drugs and target different cellular processes, and cause growth inhibition (fungistatic) or killing (fungicidal) of these pathogenic yeasts. Since the discovery of the first antifungal, amphotericin B (AmB) (Figure 1.2), only four main classes of antifungal drugs for systemic treatment are available to date: polyenes, pyrimidine analogues (5-flucytosine), azoles, and echinocandins (Bhattacharya et al., 2020).

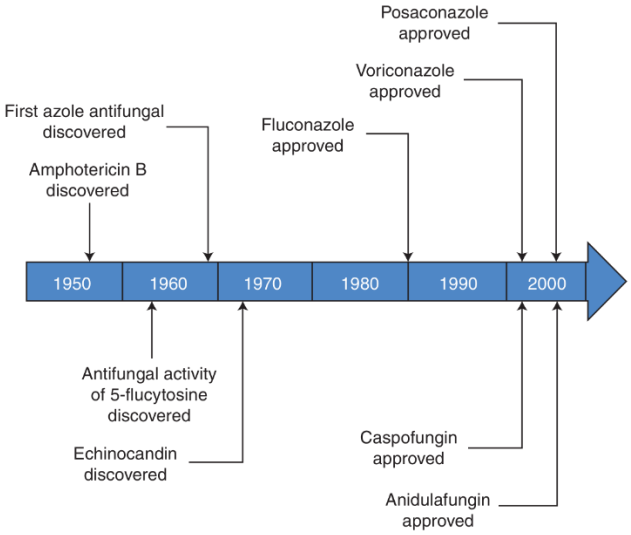

Figure 1.2. Timeline of antifungal drugs development (Roemer & Krysan, 2014).

1.5.1. Polyenes

Polyenes are natural products that were first introduced in the 1950s (Figure 1.2). These drugs consist of a hydrophobic polyene hydrocarbon chain and a hydrophilic polyhydroxyl chain (Figure 1.3) (Robbins et al., 2016). They include AmB and nystatin, but only AmB is used for systemic treatment.

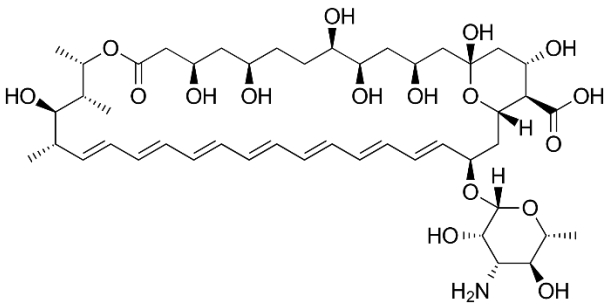

Figure 1.3. Chemical structure of amphotericin B.

They exert fungicidal activity by sequestering the ergosterol from the cell membrane and forming sponges on the outside of the cell destabilizing the membrane (Figure 1.4) (Anderson et al., 2014).

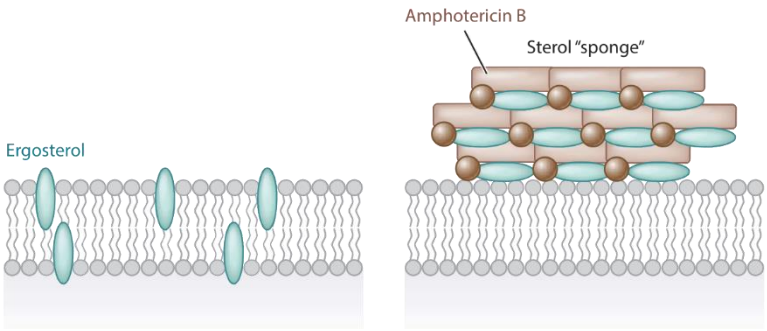

Figure 1.4. Mode of action of polyenes (modified from Robbins et al., 2017).

Even though ergosterol is more sensitive to AmB than cholesterol, the common mammalian sterol, making this drug highly selective towards fungal cells, it still affects mammalian cells. Consequently, they are last in line in antifungal treatment (Ostrosky-Zeichner et al., 2010). To decrease its toxicity, the conventional AmB, which is complexed with sodium deoxycholate (ABD), has been modified as a cholesteryl sulfate complex (ABCD), as a lipid complex (ABLC), and as a liposomal formulation (L-AmB) (Hamill, 2013).

Despite the limited use of AmB for the treatment of invasive candidiasis, it is mostly chosen when the *Candida* spp. are resistant to other drug classes or the drugs do not penetrate into the relevant niche (Bhattacharya et al., 2020). Resistance against this class of antifungals is rarely encountered and has a high fitness cost in the fungus (Vincent et al., 2013).

1.5.2. Pyrimidine analogues

The next antifungal drug discovered was flucytosine (5-fluorocytosine), introduced in the 1960s (Figure 1.2), and it belongs to the pyrimidine analogues (Robbins et al., 2016).

Flucytosine is a synthetic fluorinated analogue of cytosine (Figure 1.5) that is imported into the cell via the cytosine permease enzyme, then converted to 5-fluorouracil (5FU) by fungal specific cytosine deaminases, and finally it is metabolized to 5-fluorouridine triphosphate (5FUTP). 5FUTP is incorporated into the fungal RNA instead of uridine triphosphate (UTP), thereby affecting protein translation. Alternatively, 5FU can be converted to 5-fluorodeoxyuridine monophosphate (5FdUMP) that inhibits thymidylate synthase, an important enzyme in DNA biosynthesis (Vermes et al., 2000).

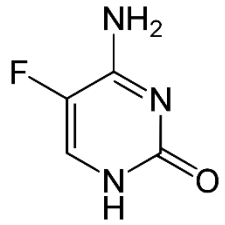

Figure 1.5. Chemical structure of 5-fluorocytosine.

However, due to the rapid development of resistance against it, this drug cannot be used as monotherapy and are only administered in combination with other drugs (Robbins et al., 2016).

1.5.3. Azoles

Azoles are the most used antifungal drugs because of their safety profile and their range of formulations (Robbins et al., 2016), and they are widely used for the treatment of candidiasis (Pappas et al., 2016).

Azoles are divided into two subclasses, triazoles (three nitrogen atoms in the azole ring) and imidazoles (two nitrogen atoms) (Bhattacharya et al., 2020). Triazoles are the largest and most common type of azoles administered in the clinical setting and comprises fluconazole (FLC), voriconazole (VRC), posaconazole (POS), itraconazole (ITC) and isavuconazole (Figure 1.6), while imidazoles are mainly composed of clotrimazole (CLT) and ketoconazole (Figure 1.7), which are generally formulated for topical use (Robbins et al., 2016).

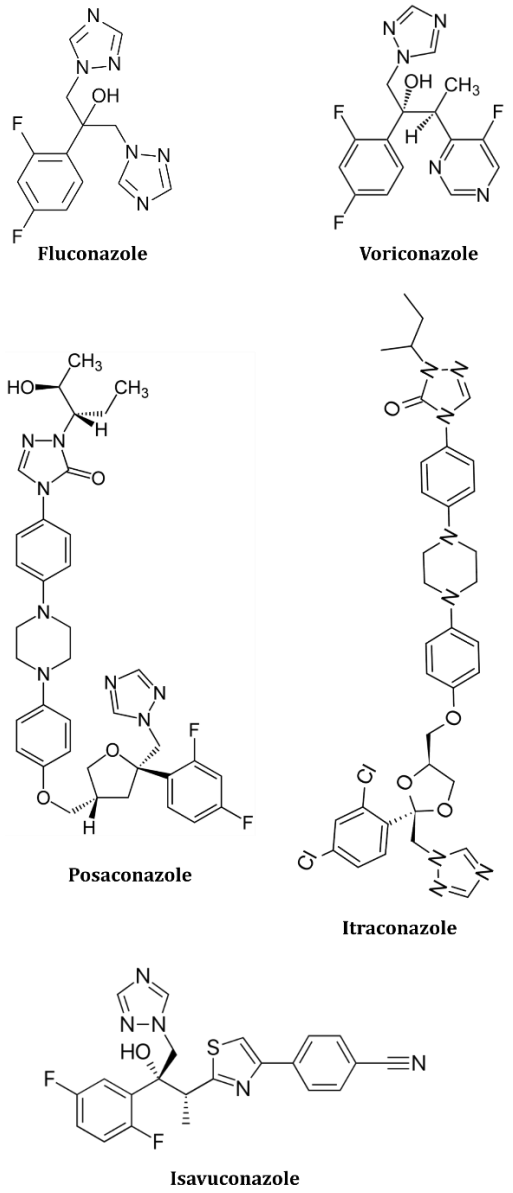

Figure 1.6. Chemical structure of the triazole's group.

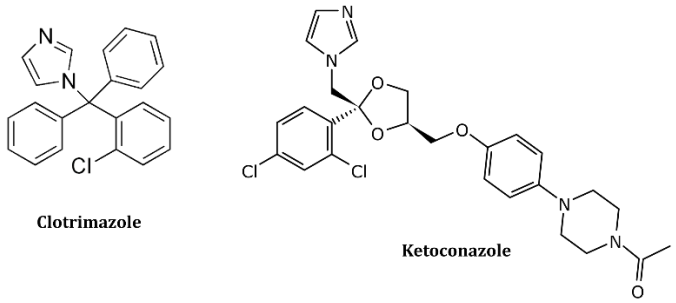

Figure 1.7. Chemical structure of the imidazole's group.

All azoles carry a five-membered nitrogen-containing heterocyclic moiety, which binds to an iron atom in the heme group located in the active site of the drug target, the 14α-lanosterol demethylase or Erg11, encoded by the *ERG11* gene (Robbins et al., 2016). This enzyme is a member of the cytochrome P450 superfamily and is involved in the biosynthesis of ergosterol, a fundamental sterol in fungal membranes. In particular, 14α-lanosterol demethylase catalyses the oxidative removal of the 14α methyl group from lanosterol (Strzelczyk et al., 2013).

Ergosterol is the major sterol component of fungal cell membranes, including the plasma and mitochondrial membranes, whose structure and function are vital for fungi maintenance. Together, sterols and sphingolipids form lipid rafts in the cell membrane that contain many biologically important proteins involved in signalling, response to stress, mating, and nutrient transport (Bhattacharya et al., 2018; Kodedová & Sychrová, 2015).

Ergosterol biosynthesis is catalysed by a cascade of 25 different enzymes (Figures 1.8 and 1.9 A) (Bhattacharya et al., 2020). When Erg11 is inhibited by azoles, the levels of ergosterol are reduced, destabilizing the cell membrane (Figure 1.9 B(a)) and other enzymes in the ergosterol pathway (Erg6, Erg25, Erg26, Erg27 and Erg3) synthesize toxic methylated sterols (14 methylergosta 8-24-28 dienol) (Figure 1.9 B(b)) (Bhattacharya et al., 2018), which contribute to damaging the cell membrane, altering its stability, permeability and the action of membrane-bound enzymes (Figure 1.9 B(c)) (Odds et al., 2003; Shapiro et al., 2011), and thus hindering cell growth and division. In *Candida* species azoles have fungistatic activity, while for *Aspergillus* spp. voriconazole is fungicidal (Perlin et al., 2017; Robbins et al., 2016).

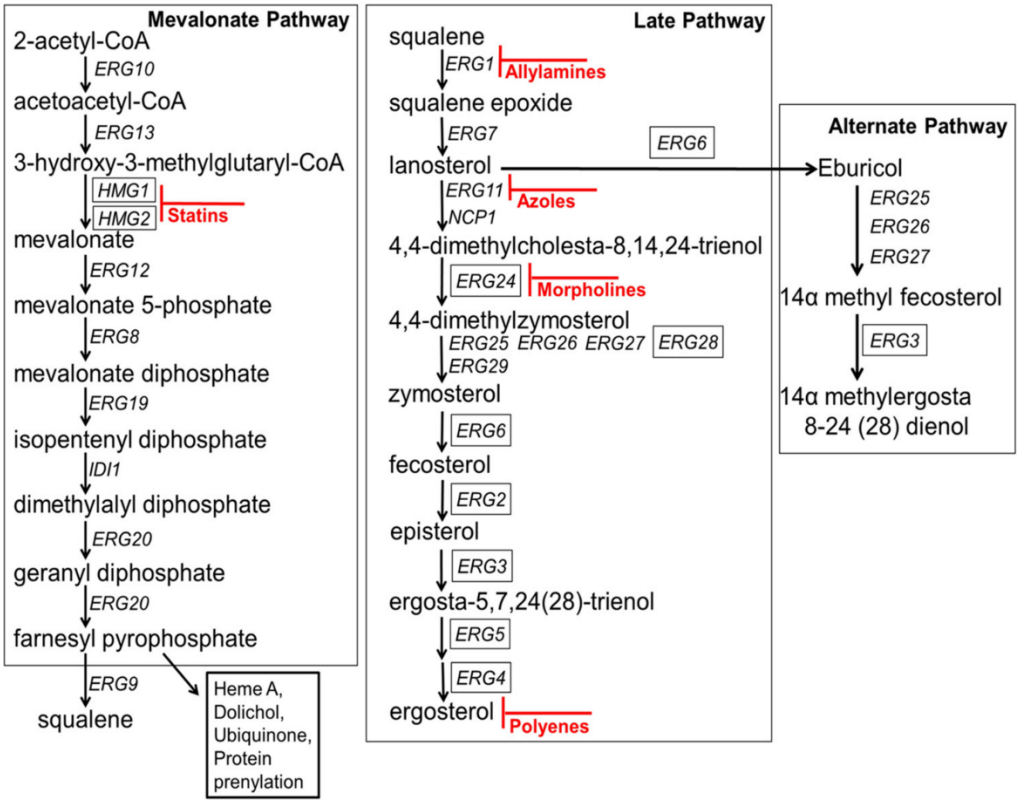

Figure 1.8. Ergosterol biosynthetic pathway. The mevalonate pathway, on the left, supplies products for different biosynthetic pathways. The late pathway, in the middle, leads to the synthesis of ergosterol. The alternate pathway, on the right, leads to the toxic fungistatic sterol 14α methylergosta 8-24-28 dienol. Boxed gene names denote nonessential genes. Antifungal drugs are shown in red (Bhattacharya et al., 2018).

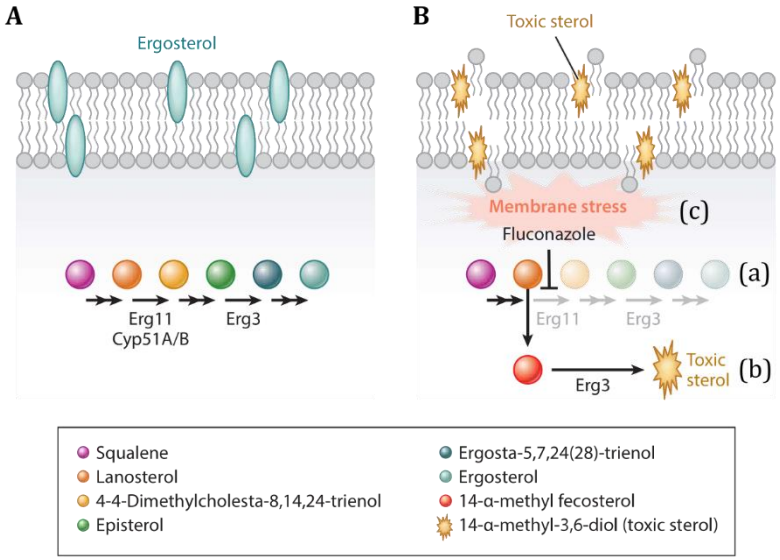

Figure 1.9. Mode of action of azole drugs. A) Ergosterol biosynthesis pathway requires several enzymes (black arrows) that transform squalene (purple circle) into ergosterol (light blue circle and ellipses). B) Azoles inhibit Erg11, so the ergosterol synthesis is inhibited (a), leading to the synthesis of toxic sterols (b) that destabilize the cell membrane (c) (Robbins et al., 2017).

Even though echinocandins are recommended as first-line therapy treatment for candidemia, prior to species identification and susceptibility testing, FLC is still largely used in the clinical practice. As reported in the 2016 Infectious Diseases Society of America (IDSA) guidelines, FLC remains an acceptable empirical alternative for patients who are not critically ill or at risk of fluconazole resistance (Bassetti et al., 2018).

Fluconazole is the azole most commonly used in therapy, probably due to its oral presentation high availability and tolerability by patients (Delarze & Sanglard, 2015). Second generation of triazoles that include VRC, POS, ITC and isavuconazole are more potent against resistant pathogens. Isavuconazole is a novel azole, as effective as voriconazole, but less toxic. And with a toxicity profile similar to that of FLC, but more active (Falci & Pasqualotto, 2013; Wilson et al., 2016). However, the use of triazoles is greatly limited due to interactions with statins, corticosteroids and other drugs (Brown et al., 2012).

1.5.4. Echinocandins

Echinocandins are the most recent type of antifungals developed (Figure 1.2) and are composed of anidulafungin, micafungin and caspofungin (Figure 1.10). They are cyclic hexapeptides that inhibit noncompetitively the β-1,3-D-glucan synthase or Fks (FK506-supersensitive) (Figure 1.11). This protein is a multisubunit enzyme complex that is involved in the synthesis of β-1,3-D-glucan, the major component of the cell wall (Perlin, 2011; Robbins et al., 2016). The enzyme complex has at least two subunits, Fks and Rho (Douglas et al., 1994; Kondoh et al., 1997). Fks is the catalytic subunit (Schimoler-O'rourke et al., 2003) and is encoded by three related genes, *FKS1*, *FKS2* and *FKS3* (Perlin, 2011). Rho is a GTP-binding protein in the Rho/Rac subfamily of Ras-like GTPases and regulates the activity of glucan synthase (Mazur & Baginsky, 1996).

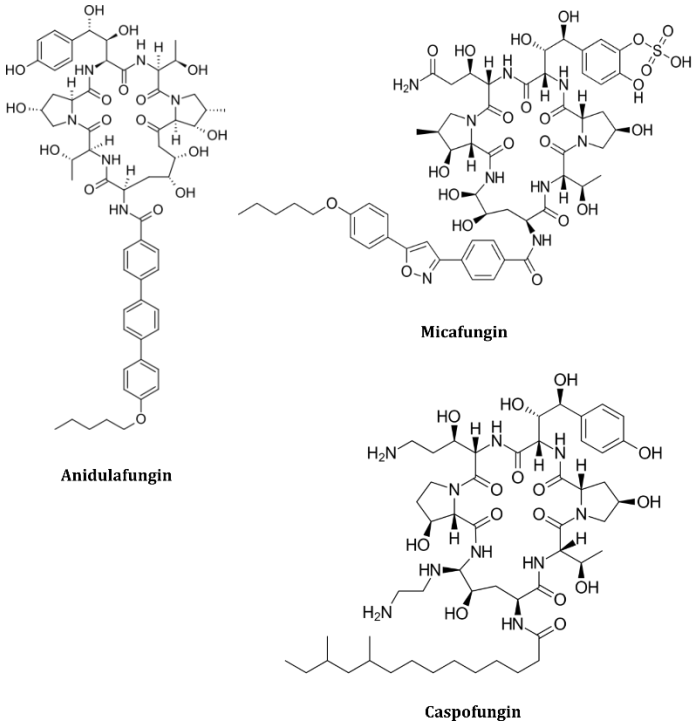

Figure 1.10. Chemical structure of echinocandins.

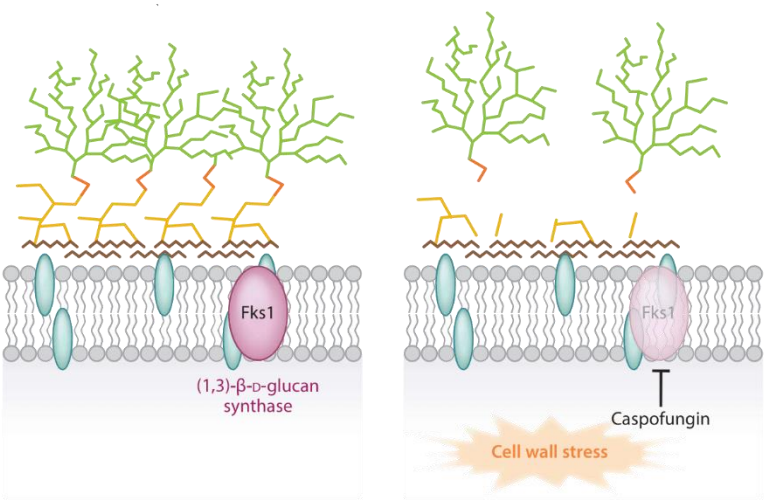

Figure 1.11. Echinocandins mode of action. Fungal cell walls are composed of β-1,3-D-glucans (yellow chains) covalently linked to β-1,6-D-glucans (orange chains) as well as chitin (brown), mannans (green), and cell wall proteins. When Fks is inhibited by echinocandins synthesis of β-1,3-D-glucans is inhibited disrupting the cell wall structure (Robbins et al., 2017).

These drugs are usually fungicidal and commonly chosen because they exhibit low toxicity for humans. Echinocandins are usually administered to patients with moderately severe to severe illness or to patients with prior exposure to azoles (Pappas et al., 2016). However, their use is limited due to the absence of oral formulations and the need for daily administration (Bassetti et al., 2018).

1.5.5. Other antifungal drugs

Besides the antifungal drugs available for treatment of invasive infections, there are other antifungals of topical use for the treatment of superficial mycosis (Perfect, 2017). Allylamines and thiocarbamates inhibit Erg1 or squalene-epoxidase, an enzyme involved in ergosterol biosynthesis whose inhibition leads to membrane rupture and squalene accumulation (Bhattacharya et al., 2020; White et al., 1998). Morpholines also thwart ergosterol biosynthesis by inhibiting two enzymes of the pathway, C-14 sterol reductase and C-8 sterol isomerase, encoded by the *ERG24* and *ERG2* genes, respectively (Bhattacharya et al., 2020; de Oliveira Santos et al., 2018; White et al., 1998). And additionally, griseofulvin interferes with microtubule formation during mitosis (de Oliveira Santos et al., 2018).

Efforts in the development of new antifungal drugs have provided us with several molecules, like new triazoles ravuconazole, albaconazole and isavuconazole (de Oliveira Santos et al., 2018). Albaconazole is being studied for superficial infections, while isavuconazole was approved for its use in the clinic in 2015 (Ellsworth & Ostrosky-Zeichner, 2020; Perfect, 2017). Other structurally different compounds are currently being evaluated in clinical trials for their utility in treatment of fungal infections. Two of them are in early phases of testing, such as T-2307, an arylamine that inhibits the mitochondrial membrane potential causing a profound fungicidal effect (Bassetti et al., 2018; Perfect, 2017) and is in phase I development (Bassetti et al., 2018); and OSU-0312, an inhibitor of phosphoinositide-dependent kinase 1 (PDK1) whose antifungal activity relies on the disruption of cell wall signalling (McCarthy et al., 2017). Other compounds are in more advanced phases like VL2397, a natural cyclic hexapeptide siderophore that disrupts intracellular fungal biochemical machinery (Perfect, 2017), and is in phase II studies for first-line treatment of invasive aspergillosis (Sanguinetti et al., 2019). Other drugs in phase II clinical trials are: rezafungin, a more stable modified echinocandin, allowing for topical use in the treatment of skin and vaginal infections (Perfect, 2017; Sanguinetti et al., 2019) and extended interval dosing (Bassetti et al., 2018; Garcia-Effron, 2020); fosmanogepix is a prodrug converted to manogepix that inhibits the synthesis of glycosyl phosphatidylinositol (GPI) hindering the attachment of adhesion proteins to the cell wall, which in turn results in diminished cell wall integrity (McCarthy et

al., 2017; Sanguinetti et al., 2019; Shaw & Ibrahim, 2020); and VT-1161, a modified azole with fewer drug-drug interactions than other azoles in phase II clinical trials for treatment of vaginal candidiasis (Perfect, 2017; Sanguinetti et al., 2019).

Of note is the SCY078, a derivative of enfumafungin, currently named ibrexafungerp (Jallow & Govender, 2021). This is the first compound of the triterpene antifungal drug class, it has oral bioavailability and is in phase II and III trials for invasive and mucocutaneous candidiasis (Bassetti et al., 2018; Perfect, 2017; Sanguinetti et al., 2019). In phase III clinical trials it showed to be effective for treatment of acute vulvovaginal candidiasis (Jallow & Govender, 2021), and has recently been approved for its treatment (Lee, 2021). This drug, similarly to echinocandins, inhibits Fks1, which in turn precludes the biosynthesis of β-1,3-D-glucan in the fungal cell wall (Jallow & Govender, 2021).

1.6. Resistance to antifungal drugs

Resistance against antifungal drugs is defined as the combination of clinical and microbiological resistance (Nishimoto et al., 2020; Pfaller et al., 2019). Clinical resistance refers to failure in clearing an infection caused by an in vitro susceptible microorganism despite adequate treatment (Costa-de-Oliveira & Rodrigues, 2020; Nishimoto et al., 2020). This type of resistance is usually due to several factors, such as the severity of the infection, the existence of foreign material that can support biofilm formation, immune host status, suboptimal dosing, drug interactions, pharmacokinetics or the fungal burden.

On the other hand, microbiological resistance is identified by determining minimal inhibitory concentrations (MICs) in vitro for a given antifungal and interpreting this value according to established clinical breakpoints (Morio et al., 2017; Pfaller et al., 2019). Resistant strains have MICs above the breakpoint and are more likely to cause a therapeutic failure than susceptible strains with MICs below the breakpoint (Berman & Krysan, 2020; Nishimoto et al., 2020). Importantly, there is not an absolute association between in vitro MIC and clinical response. To address the problem of response variability, drug resistance is assessed as high probability of treatment success, uncertain effect of treatment, or high probability of treatment failure (Perlin et al., 2017).

Microbiological drug resistance can be either primary (intrinsic) or secondary (acquired). Primary drug resistance is found naturally among some fungi without previous exposure to antifungal drugs, and often involves the same mechanism as that which causes acquired resistance (Cowen et al., 2015), although unknown mechanisms can also be implicated (Morio et al., 2017; Perlin et al., 2017). Secondary resistance develops following exposure to antifungal drugs and can be either reversible, due to transient adaptation, or persistent because of one or several genetic alterations (Costa-de-Oliveira & Rodrigues, 2020). Transient resistance can appear because of changes in chromatin organization or in gene expression. Alternatively, resistance can also be transient because of genetic modifications with negative fitness costs for the resistant strain compared to the wild type (WT), which would overrun the mutant when the antibiotic pressure is lifted (Vale-Silva, 2015).

Since the introduction of the first antifungal compounds, resistant fungal isolates have been reported worldwide and, as a result, the incidence of invasive infections caused by resistant fungi has increased over the past decades. This increase has been observed specially among *Aspergillus fumigatus* and non-*albicans Candida* (NAC) species, such as *N. glabrata* or *Candida auris* (Hokken et al., 2019; Perlin et al., 2017; Wiederhold, 2017). Moreover, the development of less toxic drugs, which can be applied safely in a range of patients with various conditions, has contributed to the expansion of antifungal use for prophylaxis, empirical and directed therapy, which has in turn led to increased drug resistance (Perlin et al., 2017).

Similar to antibiotics for bacterial infection, emergence of antifungal resistance among *Candida* species is a serious threat to public health worldwide. According to the USA Centers for Disease Control and Prevention (CDC) 2019 report of antibiotic resistance threat, more than 34,000 cases and 1700 deaths annually were due to drug-resistant *Candida* spp. (Bhattacharya et al., 2020). In addition, the rise in acquired resistance to any drug class is of great concern due to the limited spectrum of antifungals available for treatment of fungal infections (Perlin et al., 2017).

Overall, antifungal resistance remains relatively low (McTaggart et al., 2020); however, there is evidence suggesting that acquired resistance may be an emerging and underdiagnosed entity, as shown in two different studies, in which quite high azole resistance rates among mucosal *C. albicans* isolates (20% and 15%) were

reported (Arendrup, 2014; Cuenca-Estrella et al., 2011). On the contrary, a study carried out in two USA cities for *C. albicans*, *C. tropicalis* and *C. parapsilosis* bloodstream isolates reported low incidences of FLC resistance, 2%, 6% and 4%, respectively (Lockhart et al., 2012). In another epidemiological study from the SENTRY Antifungal Surveillance Program, the *C. albicans* resistance rate for FLC was of 0.3% and showed little variation throughout the years (Pfaller et al., 2019).

Resistance to all antifungal drugs have been reported, and different mechanisms have been shown to be implicated. Nonetheless, we will focus on azole resistance because they are the most used antifungal drugs (Robbins et al., 2017).

1.6.1. Azole resistance mechanisms

Azole resistance among *Candida* spp. involves several well-defined mechanisms, including alteration or overexpression of the drug target, upregulation of drug transporters, alteration of ergosterol biosynthesis, genome plasticity and activation of stress response pathways (Figure 1.12) (Berkow & Lockhart, 2017; Bhattacharya et al., 2020; Hokken et al., 2019; Ksiezopolska & Gabaldón, 2018; Morio et al., 2017; Murphy & Bicanic, 2021; Perlin et al., 2017; Robbins et al., 2017; Whaley et al., 2017). These mechanisms can occur either alone or concurrently in a single isolate (Morio et al., 2017; Murphy & Bicanic, 2021; Robbins et al., 2017) and can produce additive effects or lead to cross-resistance among azole drugs (Perlin et al., 2017).

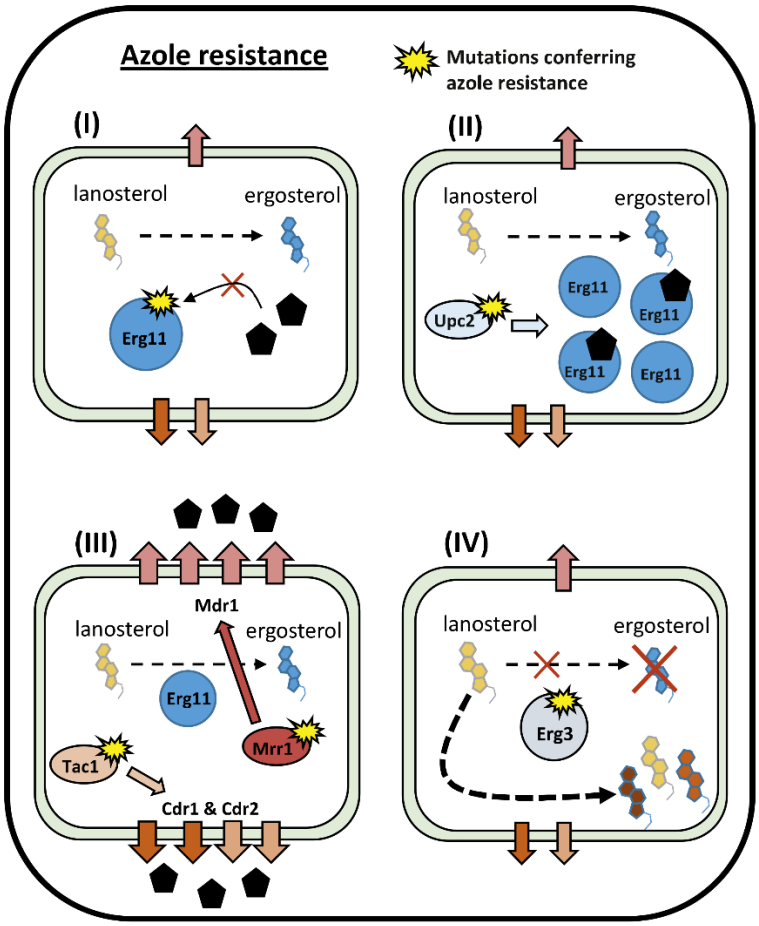

Figure 1.12. Most common mechanisms of azole resistance in *C. albicans*. (I) Mutations in azoles (black pentagons) target enzyme, Erg11, reduce its affinity to azoles avoiding inhibition. (II) Hyperactivating mutations in Upc2, the transcriptional activator of *ERG11*, induce high expression of the target protein increasing the amount of azole drug necessary for inhibition. (III) Hyperactivating mutations in the transcription factors Tac1, regulating the expression of Cdr1 and Cdr2 efflux pumps (dark and light brown arrows, respectively), and Mrr1, regulating Mdr1 pump (light red arrows), confer constitutive high expression of the corresponding drug efflux pumps reducing the intracellular azole concentration. (IV) Inactivating mutations in Erg3 abolish the synthesis of the toxic sterols that destabilize the cell membrane when ergosterol biosynthesis is inhibited by azoles (Morio et al., 2017).

1.6.1.1. Modification of the drug target

This mechanism is broadly documented in the literature, in which a great number of non-synonymous nucleotide polymorphisms are registered in *ERG11* alleles from *C. albicans* clinical isolates resistant to azoles (Nishimoto et al., 2020; Perlin et al., 2017; Robbins et al., 2017). More than 140 different mutations have been described, but only a few have been directly associated to resistance (Arendrup & Patterson, 2017; Berkow & Lockhart, 2017; Berman & Hadany, 2012; Ksiezopolska & Gabaldón, 2018; Morio et al., 2017; Murphy & Bicanic, 2021). Up to date, 26 amino acid

substitutions have been empirically linked to azole resistance either alone or in combination: A61V, A114S, T123I, F126L, Y132F, Y132H, K143E, K143Q, K143R, Y257H, S279F, T315A, S405F, N435V, D446E, D446N, G448E, G448V, F449S, F449V, G450E, G464S, R467K, R467I, I471T and D502E (Chau et al., 2004; Favre et al., 1999; Flowers et al., 2015; Kakeya et al., 2000; Kelly, Lamb, Loeffler et al., 1999; Kelly, Lamb, & Kelly, 1999; Lamb et al., 1997; Lamb et al., 2000; Liu et al., 2015; Perea et al., 2001; Sanglard et al., 1998; Warrilow et al., 2012; White, 1997b; Wu et al., 2017; Xiang et al., 2013; Zhao et al., 2013).

The relatively low number of resistance-associated mutations in *ERG11* is due to the difficulty of determining the influence of each mutation on resistance, as they usually appear in combinations of two to four in the same allele, and there is some uncertainty if some mutations only result in resistance when they appear in combination (Arendrup & Patterson, 2017). These mutations confer resistance by altering the binding site between azoles and their target in a way that azoles bind Erg11 with less affinity (Morio et al., 2017; Nishimoto et al., 2020).

1.6.1.2. Overexpression of the drug target

Overexpression of Erg11 can be due to gene duplication (Selmecki et al., 2008) as a consequence of the duplication of chromosome 5 or the formation of an isochromosome of its left arm, where the genes *ERG11* and *TAC1* (*CDR1* and *CDR2* transcription factor) are located (Selmecki et al., 2006; Selmecki et al., 2008); or to constitutive activation of its transcription factor Upc2 (uptake control 2) (Dunkel, Liu et al., 2008; Flowers et al., 2012; Silver et al., 2004).

Regarding Upc2, it belongs to the zinc cluster transcription factor protein family, which is characterized by a conserved Zn_2-Cys_6 DNA-binding domain in their amino end unique to the kingdom Fungi. The zinc finger domain is flanked by multiple nuclear localization signals. The carboxy-terminal region of these proteins contains a ligand-binding domain (LBD) that regulates its transcriptional activity and its ligand-dependent cellular localization (Figure 1.13) (Silver et al., 2004; Yang et al., 2015). It is involved in its own regulation after azole exposure as well as in that of many genes of the ergosterol biosynthetic pathway under ergosterol starvation but not in basal conditions (MacPherson et al., 2005; Silver et al., 2004). When sterols are abundant, Upc2 is present in the cytoplasm bound to ergosterol and inactivated,

while at low amounts of ergosterol, Upc2 is free and active, and is transported to the nucleus to exert its transcriptional activity on target genes (Figure 1.14) (Yang et al., 2015). Upc2 binds to regulatory elements of the *ERG11* (and other genes of the ergosterol biosynthetic pathway) and of its own promoter called ARE (azole-responsive element), which is composed of a SRE (sterol response element), and an inverted repeat sequence called INV (Oliver et al., 2007).

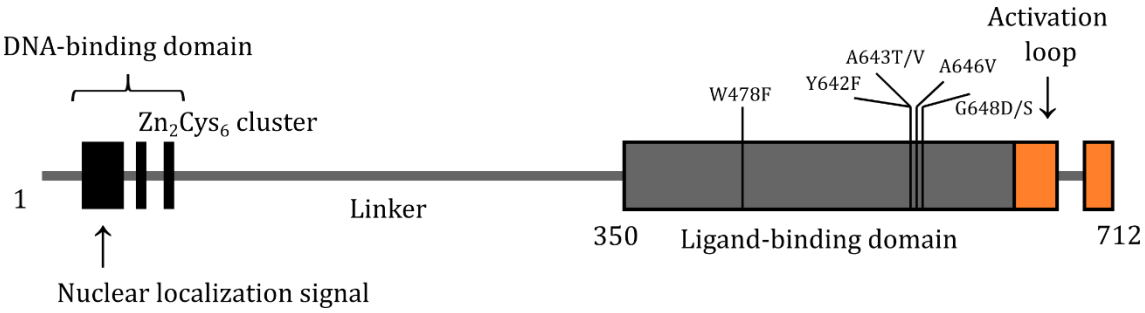

Figure 1.13. Schematic representation of the domain structure of *C. albicans* Upc2 and localization of described gain-of-function (Yang et al., 2015).

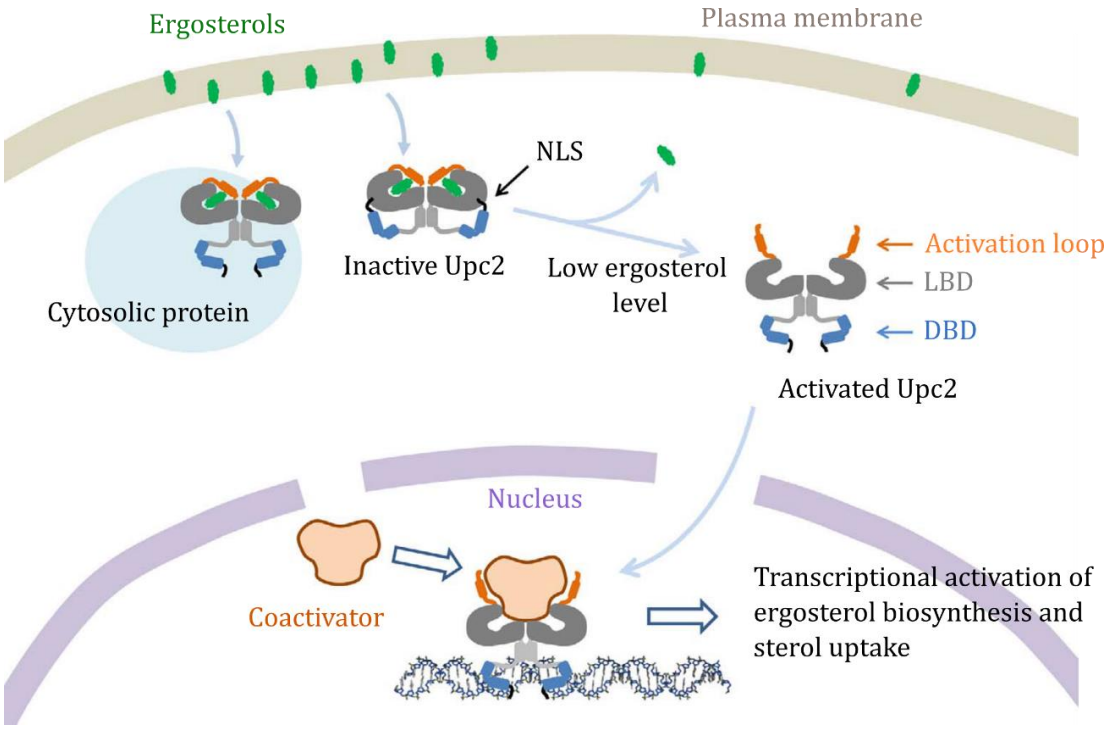

Figure 1.14. In a sterol-rich condition, Upc2 binds to ergosterol and stays in the cytosol as a repressed form [by hiding NLS (nuclear localization signal) or by being captured with a cytosolic protein]. On ergosterol depletion, ligan-free Upc2 undergoes conformational activation and moves to nucleus for transcriptional activation of related genes. LBD, ligand-binding domain; DBD, DNA-binding domain (Yang et al., 2015).

The Upc2-mediated overexpression of *ERG11* is caused by gain-of-function (GOF) mutations that hyperactivate the transcriptional regulator, of which, seven have been related to resistance: W478F, Y642F, A643T, A643V, A646V, G648D and G648S (Figure 1.13) (Dunkel et al., 2008; Flowers et al., 2012; Heilmann et al., 2010; Hoot et al., 2011). All these mutations are located at the carboxyl end and result in a constitutive activation of the regulator. However, this activation imposes a metabolic burden, so in non-selective environments, without antifungal, is a disadvantage to the fungus (Yang et al., 2015). Maybe explaining why, even though many azole-resistant *C. albicans* isolates show increased *ERG11* expression, not all the cases can be associated to GOF mutations in Upc2, implicating additional regulators (Flowers et al., 2012).

1.6.1.3. Enhanced efflux of azoles

Enhanced efflux is the most common resistance mechanism against azoles among *C. albicans* strains (Berman & Krysan, 2020; Costa-de-Oliveira & Rodrigues, 2020; Morio et al., 2017; Murphy & Bicanic, 2021; Perlin et al., 2017). Fungi have two types of efflux pumps that are located at the cell membrane, ATP-binding cassette (ABC) transporters, which employ ATP (Rees et al., 2009), and Major Facilitator (MFS), whose energy source is the proton gradient across the cell membrane (Berkow & Lockhart, 2017; Bhattacharya et al., 2020; Costa-de-Oliveira & Rodrigues, 2020; Morio et al., 2017; Murphy & Bicanic, 2021; Perlin et al., 2017).

- *ABC transporters*

The 28 members of the ABC protein superfamily can be grouped into five subfamilies. The Pdr (pleiotropic drug resistance) subfamily comprises Cdr1 (*Candida* drug resistance 1) and its close homologue Cdr2 (*Candida* drug resistance 2) (Coleman & Mylonakis, 2009; Prasad & Goffeau, 2012), both involved in azole resistance (Prasad et al., 1995; Sanglard et al., 1997).

ABC proteins are made up of two transmembrane domains (TMDs) and two cytoplasmic nucleotide binding domains (NBDs). They can be arranged as dimers in a forward topology, where the TMDs precede the NBDs (TMD_6-$NBD)_2$, while in a reverse topology the NBDs come first (NBD-$TMD_6)_2$. Yeast Pdr subfamily possesses the reverse topology (Figure 1.15) (Prasad & Goffeau, 2012).

Typically, the TMDs comprise 12 transmembrane α-helices segments (TMSs) interlinked with six extracellular and four intracellular loops, whereas the ABC domain is formed by Walker A and Walker B motifs and an ABC signature motif (Prasad & Goffeau, 2012).

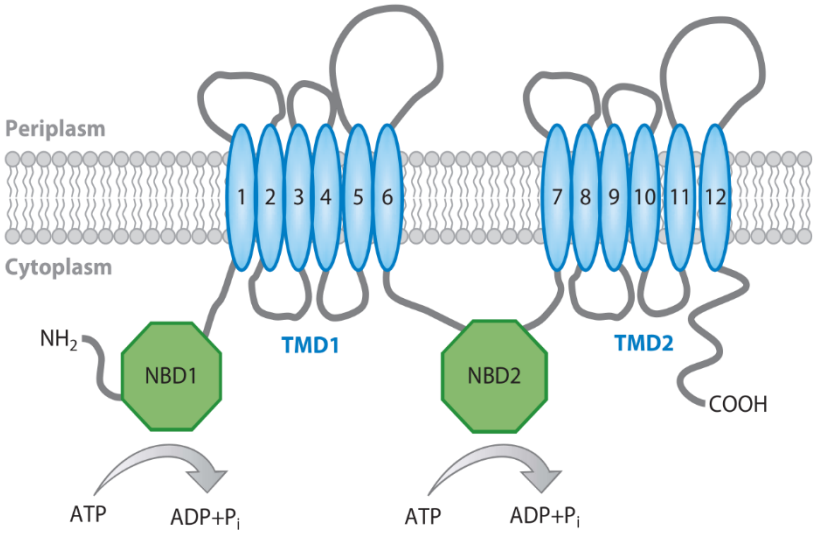

Figure 1.15. Yeast Pdr subfamily topology. The nucleotide binding domain (NBD) and the transmembrane domain (TMD) are arranged as dimers. The α-helices of the TMDs are represented in blue, while the extracellular and intracellular loops are in grey (Prasad & Goffeau, 2012).

Both Cdr1 and Cdr2 are able to transport several types of azoles (Coleman & Mylonakis, 2009). In fact, deletion of *CDR1* in *C. albicans* resulted in enhanced intracellular FLC levels and increased susceptibility of the mutant to FLC and many other drugs, providing genetic evidence that *CDR1* is a multidrug resistance gene in *C. albicans* (Sanglard et al., 1996). In contrast, inactivation of *CDR2* had no effect on FLC accumulation and did not influence the susceptibility of the mutants to FLC, but this was attributed to the absence or extremely low *CDR2* expression in susceptible isolates (Sanglard et al., 1997). In fact, it has been proposed that Cdr1 makes a much greater functional contribution to FLC resistance in *C. albicans* than Cdr2 (Holmes et al., 2008). Nonetheless, disruption of *CDR2* in a Δ*cdr1* mutant background further increased the susceptibility to FLC and other drugs (Sanglard et al., 1997). Upregulation of both *CDR1* and *CDR2* mediates azole resistance by enhanced drug efflux and reduced azole accumulation (Nishimoto et al., 2020; Tsao et al., 2009).

In order to identify the transcription factor involved in the regulation of *CDR1* and *CDR2* genes, their promoters were analysed, and 5 regulatory elements were

identified: basal expression element (BEE), responsible for basal expression; drug responsive element (DRE), required for expression in response to certain drugs (de Micheli et al., 2002); two steroid responsive elements (SRE), involved in response to steroid hormones (Karnani et al., 2004); and a negative regulator element (NRE) (Figure 1.16) (Gaur et al., 2004). Only the DRE is associated to both transient and constitutive overexpression in resistant clinical isolates of *C. albicans* (de Micheli et al., 2002). Since this region presents two CGG triplets that are recognized by zinc cluster transcription factors, Coste and collaborators (Coste et al., 2004) explored the *C. albicans* genome for genes encoding putative regulators with zinc finger motifs, of which Tac1 (transcriptional activator of *CDR* genes) was identified as the main regulator of ABC transporters expression. Tac1 induces the expression of these transporters in response to steroids and some toxic chemical compounds or can become hyperactivated due to GOF mutations. Moreover, higher levels of resistance are achieved when the *TAC1* hyperactive allele becomes homozygous. This is usually coupled with *MTL* homozygosity since both genes are located in the left arm of chromosome 5 (Chr5L) (Coste et al., 2006).

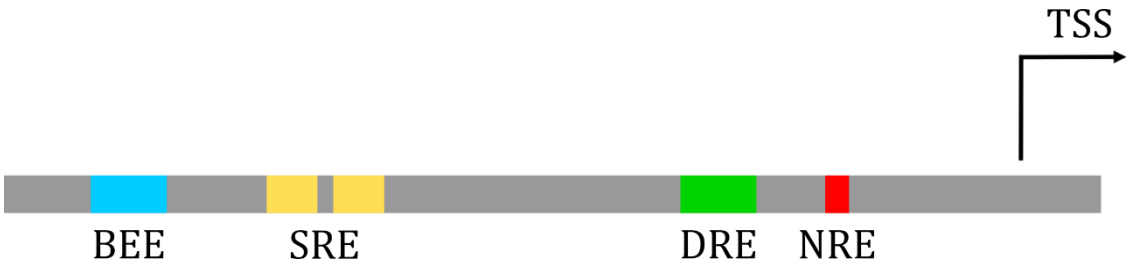

Figure 1.16. Structure of the promoter region of the *CDR* genes. BEE, basal expression element; SRE, sterol responsive element; DRE, drug responsive element; NRE, negative regulator element; TSS, transcription start site.

Twenty-one different Tac1 mutations have been confirmed as GOF: T225A, W239L, I255stop, H263Y, E461K, R673Q, ΔM677, R693K, A736T, A736V, A790V, I794V, H839Y, ΔL962-N969, P971S, N972D, N972I, N972S, N977D, G980E and G980W (Coste et al., 2006; Coste et al., 2007; Coste et al., 2009; Sitterlé et al., 2020; Znaidi et al., 2007). These mutations are usually located within Tac1 middle (MHR, middle homology region) and activation domains (TAD, transcriptional activation domain at the carboxy end). In fact, it has been proposed that the Tac1 middle region exerts

an inhibitory effect on the TAD region and that GOF mutations in either domain weaken this interaction (Figure 1. 17) (Liu & Myers, 2017).

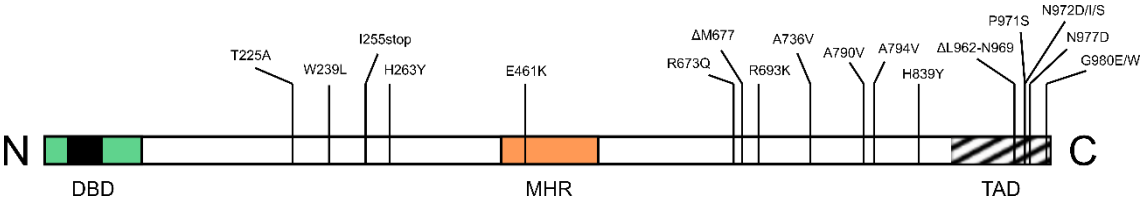

Figure 1.17. Location of identified GOF mutations in Tac1. The green area (DBD) contains the DNA binding domain, the zinc cluster motif is indicated in black shading, the hatched area depicts the transcription activation domain (TAD), and the orange area the middle homology region (MHR). (Modified from Nishimoto et al., 2020).

Recently, another transcription factor that regulates Cdr1 has been discovered and it has been proposed as a new player in the development of resistance (Schillig & Morschhäuser, 2013). It was called Mrr2 (multidrug resistance regulator 2) and was shown to be essential for the basal expression of *CDR1* but was not involved in *CDR2* regulation. Up to date, only three studies have aimed at establishing its involvement in resistance but with opposing results (Feng et al., 2019; Nishimoto et al., 2019; Wang et al., 2015). So far 21 non-synonymous mutations have been described in *MRR2* and 6 of them have been associated to azole resistance by Wang and collaborators (Wang et al., 2015) and Feng and collaborators (Feng et al., 2019): H358N, E439N, S466L, A468G, S469T and T470N.

- *The MFS transporters*

The most relevant member of the Major Facilitator transporters in resistance to azoles is Mdr1 (multidrug resistance 1) (Berkow & Lockhart, 2017; Gaur et al., 2008), encoded by *MDR1* (previously termed *BEN*^{r} for conferring resistance to benomyl) (Fling et al., 1991; Franz et al., 1998), which is more specific towards FLC and VRC than the other azole class members (Cheng et al., 2007; Sanglard et al., 1995; Sanglard & Coste, 2016).

The *C. albicans* genome sequence predicts 95 MFS transporters classified in 17 families, and all of them have around 12 to 14 transmembrane segments and no NBDs (Gaur et al., 2008). *MDR1* encodes an MFS transporter of the DHA1 family that leads to enhanced azole efflux and azole resistance when overexpressed. When it was disrupted in *MDR1* overexpressing *C. albicans* isolates the mutants exhibited

increased susceptibility to FLC (Wirsching, Michel, & Morschhäuser, 2000). As with *CDR2*, even though *MDR1* expression is very low in azole-susceptible *C. albicans* clinical isolates (Morschhäuser et al., 2007), its overexpression has been linked to azole resistance (Gaur et al., 2008).

Constitutive overexpression of *MDR1* in azole-resistant *C. albicans* strains was also linked to mutations in *trans*-regulatory factors (Wirsching, Michel, Köhler et al., 2000). Analysis of the *cis*-acting elements present in the *MDR1* promoter region revealed that multiple transcription factors regulate *MDR1* expression (Hiller et al., 2006). For example, a benomyl response element (BRE) is required for benomyl-dependent *MDR1* upregulation and necessary for constitutive high expression. This element contains a consensus binding sequence for the Mcm1 transcription factor. A second element, the H_2O_2 response element (HRE) is required for H_2O_2-dependent *MDR1* upregulation but dispensable for constitutive high expression and is thought to be recognized by Cap1, a bZip transcription factor (Rognon et al., 2006). Upc2 has also been linked to *MDR1* regulation (Znaidi et al., 2008), however, the zinc cluster transcription factor Mrr1 (multridrug resistance regulator 1) was identified as the central regulator of *MDR1* expression and GOF mutations in this transcriptional regulator were linked to *MDR1* overexpression and FLC resistance (Morschhäuser et al., 2007). Sixteen different Mrr1 GOF mutations have been reported causing constitutive upregulation of *MDR1*: K335N, Q350L, T360I, T381I, P683H, P683S, N803D, R873T, V877F, G878E, A880E, W893R, T896I, G963S, G997V and L998F (Figure 1.18) (Dunkel et al., 2008; Eddouzi et al., 2013; Lohberger et al., 2014; Morschhäuser et al., 2007).

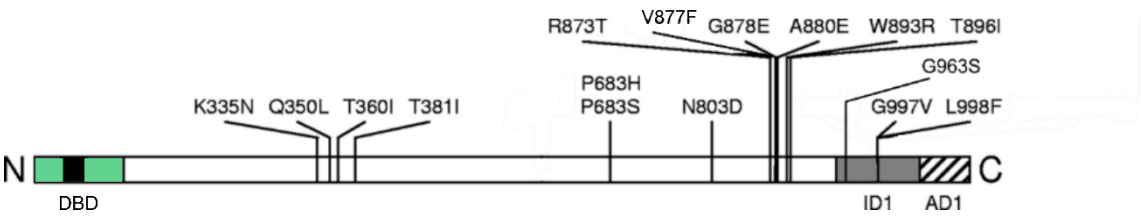

Figure 1.18. Location of identified GOF mutations in Mrr1. The green area (DBD; amino acids 1 to 106) contains the DNA binding domain and represents the region that is sufficient for the activation of the *MDR1* promoter, the zinc cluster motif (amino acids 31 to 59) is indicated in black, the hatched area (AD1; amino acids 1051 to 1108) depicts the distal activation domain 1, and the grey area (ID1; amino acids 951 to 1050) is defined as an inhibitory domain (Modified from Schubert, Barker et al., 2011).

1.6.1.4. Alteration of the ergosterol biosynthesis pathway

This mechanism consists of loss-of-function (LOF) mutations in the enzyme Δ5,6 sterol desaturase or Erg3, involved in the ergosterol biosynthesis pathway and encoded by the *ERG3* gene. When Erg11 is inhibited by azoles, this enzyme synthesizes the toxic 14α-methylergosta-8,24(28)-dien-3β,6α-diol (Figure 1.8), which inhibits fungal cell growth (Bhattacharya et al., 2020; Nishimoto et al., 2020; Whaley et al., 2017). However, inactivation of Erg3 by LOF mutations prevents formation of this toxic compound, causing azole resistance (Berkow & Lockhart, 2017; Hokken et al., 2019; Nishimoto et al., 2020; Whaley et al., 2017). The inhibition of Erg3 also leads to a depletion of ergosterol and accumulation of 14α-methylfecosterol, which allows continued growth in the presence of azole despite altered membrane composition (Kelly et al., 1997). Moreover, mutations in Erg3 are associated with cross-resistance to polyenes, likely caused by the depletion of the target ergosterol (Ksiezopolska & Gabaldón, 2018; Morio et al., 2017; Nishimoto et al., 2020). In some cases, this mechanism has been associated with attenuated virulence due to impaired filamentation (Chau et al., 2005), possibly explaining why it is rarely encountered among azole-resistant *C. albicans* clinical isolates (Berkow & Lockhart, 2017; Nishimoto et al., 2020; Whaley et al., 2017), but some *erg3*Δ mutants have been reported to maintain the ability to form hyphae (Vale-Silva et al., 2012). In this way, a recent study shows that changes within the *ERG3* promoter that affect expression and activity may be sufficient to confer azole resistance in niche-specific instances without affecting *C. albicans* pathogenicity, which implies that changes in *ERG3* locus may be more clinically relevant than previously believed (Luna-Tapia et al., 2018). Nonetheless, it has also been reported that the loss of Erg3 activity confers a distinct phenotype from azole resistance, and shares some characteristics of the trailing growth, which is defined as reduced but persistent growth at azole concentrations above the MIC (Luna-Tapia et al., 2019), increasing the uncertainty to the relevance of Erg3 loss of function in azole resistance.

1.6.1.5. Genome plasticity

Besides deregulation of expression and modification of cellular targets, many resistant strains suffer genomic reorganization in the forms of loss of heterozygosity (LOH) events or aneuploidies (Morio et al., 2017). In fact, aneuploidy was observed

in 50% of the strains that developed FLC resistance (Selmecki et al., 2006; Selmecki et al., 2009). Loss of heterozygosity events are frequently observed in chromosome 5, where *TAC1* and *ERG11* genes reside, both playing a major role in azole resistance (Selmecki et al., 2006). They have also been reported in *MRR1*, located in chromosome 3 (Schubert, Popp et al., 2011). These processes are of great importance in the evolution of resistance since it was shown that homozygous mutations conferred higher resistance levels than heterozygous ones (Coste et al., 2007).

The most frequent aneuploidy relies on two extra copies of Chr5L containing *ERG11* and *TAC1*, which correlates with azole resistance due to an amplification of the copy number of these genes (Selmecki et al., 2006; Selmecki et al., 2009). Several other chromosome aneuploidies related to azole resistance have been described, such as those of chromosomes 3, 4, 6 and 7. Trisomy of chromosome 3 has been reported after azole exposure. This chromosome hosts the pump encoding genes *CDR1* and *CDR2* as well as *MRR1*, thus, chromosome 3 increased copy number causes increased *CDR1* and *CDR2* expression and facilitates resistance development (Mount et al., 2018; Selmecki et al., 2009). The azole resistance associated with chromosome 4 trisomy was neither attributed to increased efflux pump activities nor to altered ergosterol biosynthesis in clinical isolates. Thus, this need to be further studied in the future (Anderson et al., 2017). Other studies reported that azole-resistant strains that exhibited substantial overexpression of *MDR1* were also found trisomic for chromosome 6, which carries the *MDR1* gene (Perepnikhatka et al., 1999; Selmecki et al., 2009). In addition, Mount and collaborators (Mount et al., 2018) have shown that amplification of chromosome 3 and 7 enables the evolution of antifungal drug resistance, likely through the upregulation of multiple genes involved in efflux and stress response signalling. In the amplified region of chromosome 3, three genes with annotated roles in response to azoles or membrane transport were identified: orf19.344 (upregulated in azole-resistant strains and thought to be regulated by Tac1), orf19.304 (putative transporter similar to *MDR* proteins), and Npr2 (putative urea transporter). The latter was implicated as a mediator of azole resistance in the absence of *RGD1*, which encodes an RHO-GTPase activating protein that had not been previously implicated in azole resistance in *C. albicans*. In chromosome 7, the genes coding for the cellular stress response regulator Hsp90 (heat shock protein

90), the MFS transporter Flu1, and sugar transporters as Hgt12 and Hgt13 were identified.

It has been reported that azole exposure causes aberrant cell cycle regulation in *C. albicans* with a tetraploid intermediate preceding aneuploidy formation (Harrison et al., 2014), and promoting whole-chromosome LOH via unusual mitotic divisions (chromosome duplications and losses) (Forche et al., 2011; Harrison et al., 2014). Interestingly, both LOH and aneuploidy occur at a much higher frequency than point mutations (Forche et al., 2011).

1.6.1.6. Stress responses

Cellular stress-response circuitry provides a critical strategy for fungi to survive the cell membrane stress induced by exposure to azoles. A leading example of a global cellular regulator that governs stress responses crucial for azole resistance is the molecular chaperone Hsp90. This protein is a conserved and essential chaperone that regulates cellular signalling by stabilizing a myriad of client proteins, many of which are signal transducers such as the protein phosphatase calcineurin and some kinases in the Pkc1 signalling cascade (Figure 1.19) (Cowen & Lindquist, 2005; Cowen et al., 2009; LaFayette et al., 2010; Singh et al., 2009). Compromise of Hsp90 function blocks the evolution of azole resistance, the resistance caused by the loss of function of Erg3 and reduces the resistance of isolates that evolved resistance in a human host by multiple mechanisms (Cowen & Lindquist, 2005; Cowen et al., 2009; Robbins et al., 2017).

Calcineurin is a Ca^{2+}-calmodulin-activated protein phosphatase that is involved in the regulation of cell cycle progression, cation homeostasis, morphogenesis, and responses to environmental stress. In *C. albicans* is formed by a heterodimer composed of a catalytic subunit, Cna1, and a regulatory subunit, Cnb1 (Figure 1.19). When activated, it initiates a signalling cascade leading to the dephosphorylation and activation of the major transcription factor Crz1 (Figure 1.19) (Iyer et al., 2022). It has also been shown that calcineurin is essential for tolerating cell membrane stresses elicited by azoles (Cruz et al., 2002; Sanglard et al., 2003). Hsp90 physically interacts and stabilizes the catalytic subunit of calcineurin, such that depletion of Hsp90 leads to depletion of calcineurin (Singh et al., 2009). Therefore, similarly to Hsp90, calcineurin's role in azole resistance is mainly associated with resistance

mechanisms that do not avert the toxic effect of the antifungal drug, such as LOF mutations in Erg3 (Cowen & Lindquist, 2005).

Hsp90 also stabilizes core components of the protein kinase C (PKC) pathway, which is critical to cell wall homeostasis, morphogenesis, and responses to cell wall and cell membrane stress. Pkc1 is a core kinase that acts upstream of the terminal mitogen-activated protein kinase (MAPK) signalling cascade, comprising Bck1, Mkk1 and Mkc1 kinases (Figure 1.19) (Iyer et al., 2022). Deletion of *PKC1* in *C. albicans* confers hypersensitivity to the azoles and renders the azoles fungicidal, while deletion of *MKC1* does not, suggesting that Pkc1 has other downstream targets involved in membrane stress responses (LaFayette et al., 2010).

Other Hsp90 interacting proteins have been implicated in drug tolerance and resistance, that is the case of the Hsp90 co-chaperone Sgt1 (Figure 1.19). This protein is important for regulating antifungal-induced stress, as depletion of *SGT1* abrogates azole tolerance and resistance (Shapiro et al., 2012). Hsp90 function was also found to be regulated by acetylation such that pharmacological inhibition of lysine deacetylases phenocopies inhibition of Hsp90, blocking the evolution of azole resistance and reducing resistance of *C. albicans* that evolved in a human host (Robbins et al., 2012).

Nonetheless, all of these stress response pathways have also been associated to azole tolerance, which might indicate that they do not confer true resistance (MIC above the clinical breakpoints) but enables the yeast to continue growing even in the presence of elevated drug concentrations.

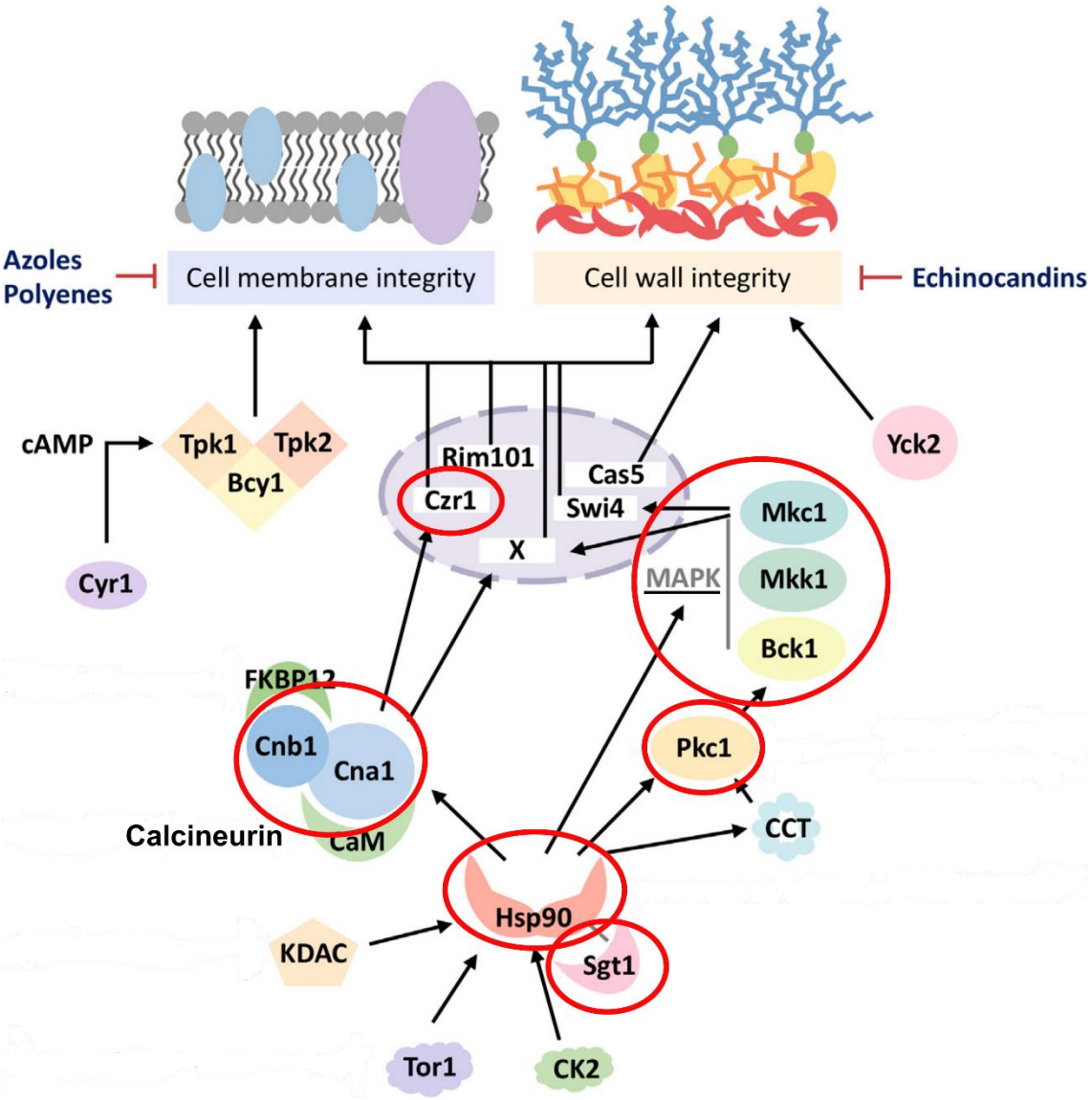

Figure 1.19. Cellular stress response pathways activated after compromise of cell membrane integrity upon azole exposure. Azoles inhibit the biosynthesis of ergosterol, resulting in ergosterol depletion in the cell membrane and thus, cell membrane stress. The central cellular regulator modulating stress responses is Hsp90, which is post-translationally regulated by lysine deacetylases (KDAC). Hsp90 interacts with several proteins such as its co-chaperone Sgt1, calcineurin and components of the PKC pathway (Pkc1, Bck1, Mkk1 and Mkc1). These two signalling cascades activate transcription factors and additional regulators yet to be identified that are located in the nucleus. Preponderant factors involved in azole resistance and tolerance are circled in red (Modified from Iyer et al., 2022).

1.6.1.7. Alternative resistance mechanisms

Despite the already mentioned mechanisms, several reports suggest that other mechanisms must exist since azole-resistant *C. albicans* clinical isolates that lack any of the established mechanisms have been reported (Berkow & Lockhart, 2017; Ksiezopolska & Gabaldón, 2018), highlighting the need for further research in this

area. Moreover, sequencing of the genes associated to azole resistance in *C. albicans* clinical isolates continues to reveal new putative GOF mutations (Garnaud et al., 2015; Sitterlé et al., 2020; Spettel et al., 2019).

Another promising area of research is the transporter involved in azole uptake. Azoles are imported by facilitated diffusion in an energy independent manner. Different azole uptake rates have been reported in azole-resistant *C. albicans* clinical isolates, but the transporter remains to be discovered (Mansfield et al., 2010; Nishimoto et al., 2020).

A recent study has demonstrated that the Mlt1p vacuolar ABC transporter is implicated in the import of azoles into vacuoles and its deletion causes susceptibility to azoles in *C. albicans* (Khandelwal et al., 2019).

Besides genetic alterations, epigenetics have also been associated to azole-resistance development. In *C. albicans* deacetylating enzymes have been shown to be overexpressed in resistant isolates during resistance acquisition, and was attributed to the activity of Hsp90, which has to be deacetylated in order to interact with its client proteins (Chang et al., 2019).

An additional mechanism that contributes to azole resistance is enhanced mRNA stability. Analysis of two matched pairs of azole-susceptible and resistant isolates revealed that the half-life of *CDR1* mRNA was threefold higher in the resistant isolates compared with their susceptible counterparts (Manoharlal et al., 2008) and the poly(A) tail of *CDR1* mRNA was 35%-50% hyperadenylated in the resistant isolates (Manoharlal et al., 2010). mRNA adenylation is controlled by poly(A) polymerase (Pap1), which is encoded by two distinct alleles, *PAP1-a* and *PAP1-α*, located in close proximity to the *MTL*. Whereas the susceptible isolates were heterozygous for *PAP1*, the resistant isolates where homozygous for the *PAP1-α* allele. *PAP1-a* has a repressive effect on *CDR1* transcript polyadenylation and stability, while *PAP1-α* homozygosity contributes to azole resistance (Manoharlal et al., 2010).

1.6.2. Tolerance

Tolerance is defined as the ability of a subpopulation from 5 to 90% of the cells to grow slowly in the presence of an antifungal drug at concentrations above the MIC

and differs from resistance in that is less dependent on the drug concentration and is affected by environmental conditions such as pH and temperature. The size of the subpopulation of tolerant cells determines the tolerance level of the isolate together with the colony forming rate at supra-MIC concentrations of the drug (Rosenberg et al., 2018).

Tolerance has been associated to several stress response pathways elements such as Hsp90 (Cowen & Lindquist, 2005), calcineurin (Sanglard et al., 2003), target of rapamycin (TOR) (Khandelwal et al., 2018) and Rim (pH response pathway) (Garnaud et al., 2018). Their inhibition eliminates tolerance without affecting the MIC and greatly increases the fungicidal activity of FLC across a diverse set of isolates with different tolerance levels (Berman & Krysan, 2020). Other cellular components that have been linked to tolerance are the vacuoles. In this regard, defects in vacuolar transport were shown to enhance growth at supra-MIC levels (Berman & Krysan, 2020; Luna-Tapia et al., 2015; Luna-Tapia et al., 2016; Mount et al., 2018). Also, the final transcription factor of the Rim pathway, Rim101, may influence tolerance by regulating the transcription of key components of the vacuolar trafficking pathway (Berman & Krysan, 2020; Cornet et al., 2005).

It has been proposed that tolerance may increase the frequency of antifungal resistance (Cowen & Lindquist, 2005) since tolerant strains are able to divide more frequently in the presence of azoles than susceptible ones, its population will be predominant and, therefore, will have a higher probability to acquire new mutations (Berman & Krysan, 2020).

Another common term used for referring growth at supra-MIC concentrations of drug is trailing growth. Trailing is defined as reduced but persistent visible growth at drug concentrations above the MIC (Marcos-Zambrano et al., 2016). Like tolerance, trailing growth is sensitive to growth conditions (Agrawal et al., 2007; Coenye et al., 2008; Marr et al., 1999). Therefore, it is thought that tolerance and trailing growth probably reflect the same phenomenon (Berman & Krysan, 2020; Nishimoto et al., 2020).

The clinical importance of tolerance is still under debate, although lately it has been proposed to be a contributor to recurrent or persistent infections (Berman & Krysan, 2020; Nishimoto et al., 2020; Rosenberg et al., 2018).

1.7. CRISPR-Cas9

In order to improve drug discovery and therapeutic guidelines is important to understand the mechanisms of resistance encountered in resistant clinical isolates (McTaggart et al., 2020). Efficient genetic manipulation tools may help to this end but they have often been time-consuming and cumbersome in fungi, particularly in species with diploid genomes that lack a sexual cycle. Additional factors hampering genetic manipulation are low efficiency of transformation and/or homologous recombination (HR), the absence of natural plasmids, and the lack of cloning vectors or the limited number of dominant markers available for selection (Morio et al., 2020).

The *CRISPR* (clustered regularly interspaced short palindromic repeats) locus was first reported in 1987 in *Escherichia coli* (Ishino et al., 1987) and years later was also discovered in archaea by Mojica and collaborators (Mojica et al., 1993). This same group together with those of Bolotin and Pourcel reported in 2005 that part of the sequences contained in the *CRISPR* loci, the spacers (Figure 1.20), derived from microbial pathogens and foreign genetic elements, such as bacteriophages, archaeal viruses and plasmids, providing evidence that these genetic elements acted as a microbial immune system (Bolotin et al., 2005; Mojica et al., 2005; Pourcel et al., 2005). Moreover, analysis of the flanking regions of the *CRISPR* loci elicited the discovery of four genes that were homologous in different bacterial and archaeal species and were named CRISPR-associated (*cas*) genes and were predicted to act together with *CRISPR* loci (CRISPR-Cas systems) working as an acquired immune system (Jansen et al., 2002; Makarova et al., 2006).

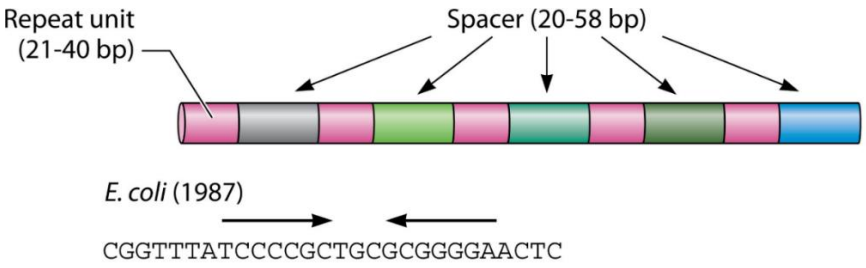

Figure 1.20. Structure of *CRISPR* loci. The *CRISPR* loci are composed of two elements: the repeat sequences (pink) that usually include a palindromic structure (exemplified by the *Escherichia coli* sequence shown below), and the spacer regions with no homology with each other (grey, green and blue) (Modified from Ishino et al., 2018).

It was later discovered that the RNA transcripts of the *CRISPR* loci are processed into short CRISPR RNAs (crRNA) that contain the repeat and spacer sequences. The spacer sequence, also termed guide, is complementary to the invading DNA. When the crRNAs are complexed with the Cas proteins, they recognize the target sequence, called protospacer, by base pairing, inducing sequence-specific cleaving (Gasiunas et al., 2012). Also, CRISPR-Cas systems have a mechanism to distinguish between foreign and self DNA via the protospacer adjacent motif (PAM), which is only present in the invading DNA (Hille et al., 2018).

The potential of CRISPR-associated protein Cas9 for genome editing was first reported in 2012 (Gasiunas et al., 2012; Jinek et al., 2012). There are two classes of CRISPR-Cas systems based on the architecture of the effector complex, which carries out DNA cleaving, class 1 and class 2, each subdivided into three types. Class 2 systems have a single multidomain effector protein and thus it was the system of choice to develop the genomic editing technology. The best studied is the Cas9 protein, a class 2 type II RNA-guided endonuclease, which forms a ribonucleoprotein complex with the crRNA and a trans-activating RNA (tracrRNA) essential for target recognition (Figure 1.21) (Ishino et al., 2018). Among Cas9 proteins, the most common variant used for genome editing is the *Streptococcus pyogenes* Cas9 (SpCas9) (Komor et al., 2017).

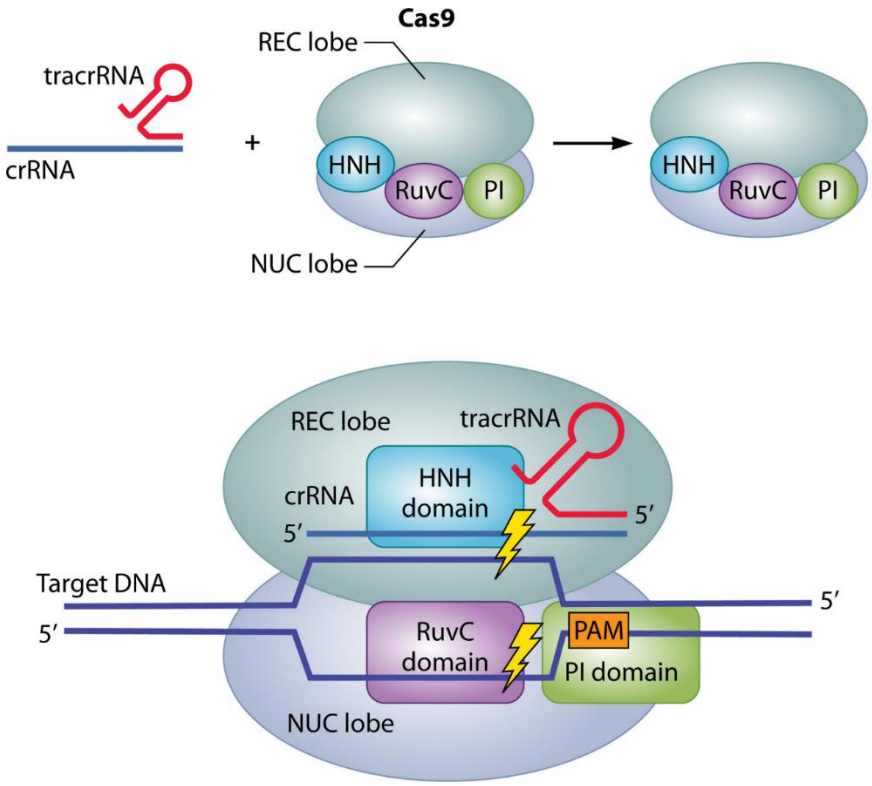

Figure 1.21. Structure of Cas9-crRNA-tracrRNA complex and DNA cleaving mechanism. The Cas9-crRNA-tracrRNA complex binds to foreign DNA containing the PAM, where Cas9 binds and starts to unwind the double strand of the foreign DNA to induce duplex formation of crRNA and foreign DNA. Cas9 consists of two regions, called the REC (recognition) and the NUC (nuclease) lobes. The REC lobe is responsible for nucleic acid recognition. The NUC lobe contains the HNH and RuvC nuclease domains and a C-terminal region containing a PAM-interacting (PI) domain. The HNH and the RuvC domains cleave the DNA strand, forming a duplex with crRNA and the other DNA strand, respectively, so that double-strand break occurs in the target DNA (Ishino et al., 2018).

The CRISPR-Cas9 editing tool directs Cas9 to the target site by a single-guide RNA (sgRNA), which comprises the roles of the crRNA and tracrRNA in the native system, where Cas9 will introduce a double-stranded break (DSB) 3 bp upstream of the PAM (NGG for SpCas9, where N stands for any base (A, T, C, G)). The DSB can be repaired by nonhomologous end joining (NHEJ), usually resulting in insertions or deletions leading to frame shift of the reading frame and premature stop codons. Microhomology-mediated end joining (MMEJ) is an alternative, also an error-prone repair pathway requiring short homology regions (2-40 bp). If a donor template with appropriate homology regions is available (e.g., the second allele in diploid genomes, or exogenous DNA), repair may occur by homology-directed repair (HDR). Precise editing exploits HDR machinery providing the cell with donor DNA molecules harbouring the intended mutation flanked by homology arms (Figure 1.22). Although conventional methods can also be used to introduce mutations by

HDR, DSBs significantly increase the rate of these events by up to 4000-fold (Morio et al., 2020).

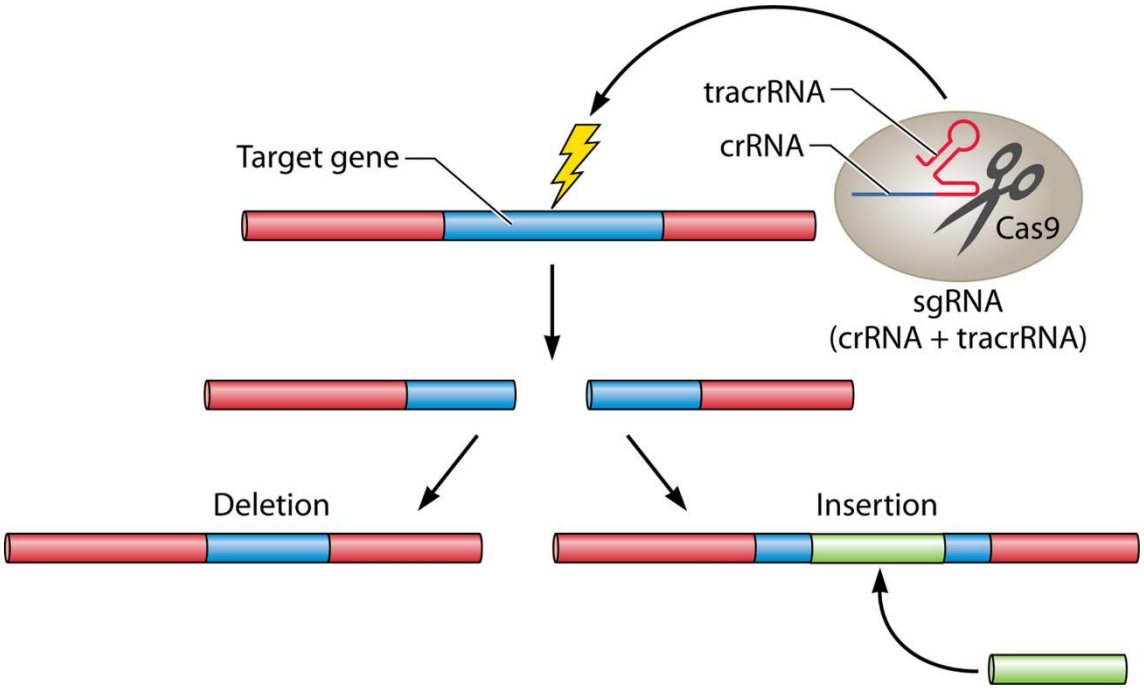

Figure 1.22. Genome editing by CRISPR-Cas9. Cas9 is directed by sequence homology between the crRNA of the sgRNA and the target gene (in blue), which is then cleaved. The Cas9-induced cut generates a double-stranded break (DSB) that has to be repaired by the cell. There are two main repair mechanisms involved: the non-homologous end joining (NHEJ) that usually implies short deletions or insertions (left), and the homology-directed repair (HDR) that repairs the DSB by recombination with the other allele or, if present, with a donor DNA template (green bar; right) (Ishino et al., 2018).

Several methods for CRISPR-Cas9 editing in *C. albicans* have been developed in the recent years. Almost all of them relied on the expression of Cas9 by the yeast and on the use of selection markers (Huang & Mitchell, 2017; Liu et al., 2022; Min et al., 2016; Ng & Dean, 2017; Nguyen et al., 2017; Shapiro et al., 2018; Vyas et al., 2015; Vyas et al., 2018). They were focused on generating deletion mutants, but they can also be adapted to introduce different genetic changes (single-nucleotide mutation, stop codon insertion, barcoding, fluorescent tagging, etc.) in coding as well as noncoding regions. Moreover, they allow engineering of heterozygous mutations in diploid species (Morio et al., 2020).

OBJECTIVES

2. OBJECTIVES

Fungal infections have become a serious concern in the clinical setting due to their associated high mortality rates that are related, on the one hand, to the affected population, generally immune compromised or debilitated, and, on the other hand, to the increase in recent years of these patients, which has also been accompanied by an increase in the isolation of strains resistant to antifungal drugs. The main causative agents of fungal infections worldwide belong to *Candida* species, of which *Candida albicans* represent the majority of the isolates. This species can cause from superficial to invasive infections that are commonly treated with antifungal drugs of the azole class, which exert a fungistatic effect on these yeasts. Even though the resistance rates to these agents among *Candida* species are not very high, their occurrence are of great concern due to the limited spectra of antifungal drugs available for treatment. Furthermore, although there are several well-established resistance mechanisms, there is evidence of the existence of alternative factors yet to be linked to azole resistance. Besides bona fide resistance, tolerance to antifungal drugs has also gained interest since it has been proposed as a precursor of acquired resistance and a cause of recurrent or persistent infections. Therefore, research on resistance and tolerance mechanisms is still of utmost importance to expand the knowledge of all the factors involved in resistance development and establishment, which in turn can aid on improving therapeutic guidelines and drug discovery.

The objectives of this thesis were:

1. Evaluation of azole susceptibility in clinical isolates of *C. albicans* from the UPV/EHU collection.

2. Identification of the most common resistance mechanisms in azole-resistant and susceptible *C. albicans* strains by sequencing target regions of the genes *ERG11*, *TAC1*, *UPC2*, *MRR1* and *MRR2*; and measuring expression levels of *CDR1*, *CDR2* and *MDR1* genes.

3. Evaluation of the role in azole resistance of new mutations by CRISPR-Cas9 gene editing.

4. Follow-up on the adaptation to fluconazole exposure in vitro of azole-susceptible *C. albicans* strains.

MATERIAL AND METHODS

3. MATERIAL AND METHODS

3.1. Microorganisms

The *Candida albicans* reference strains and clinical isolates used in this thesis are listed in Tables 3.1 and 3.2. Subcloning Efficiency™ DH5α™ Competent Cells (Invitrogen, USA) were used for cloning the plasmid pV1524 (Vyas et al., 2018) and its derivatives (See Section 3.7.6).

Table 3.1. *Candida* reference strains.

Species	Strain	Sample origin
Candida albicans	ATCC® MYA-2876™ (SC5314)	-
Candida albicans	ATCC® 64124™	Oral
Candida albicans	ATCC® 64450™	Skin
Candida parapsilosis	ATCC® 22019™	-
Candida krusei	ATCC® 6258™	Sputum

ATCC: American Type Culture Collection

Table 3.2. *Candida albicans* clinical isolates.

Identity	Sample origin	Source
BE-AZ	Vulvovaginal	Bombero-Etxaniz Health Centre (Bilbao)
BE-32	Vulvovaginal	Bombero-Etxaniz Health Centre (Bilbao)
BE-47	Vulvovaginal	Bombero-Etxaniz Health Centre (Bilbao)
BE-48	Vulvovaginal	Bombero-Etxaniz Health Centre (Bilbao)
BE-90	Vulvovaginal	Bombero-Etxaniz Health Centre (Bilbao)
BE-113	Vulvovaginal	Bombero-Etxaniz Health Centre (Bilbao)
BE-114	Vulvovaginal	Bombero-Etxaniz Health Centre (Bilbao)
06-100	Necrotizing cellulitis	UPV/EHU Collection (Leioa)
06-114	Oral	UPV/EHU Collection (Leioa)
06-116	Prosthesis	UPV/EHU Collection (Leioa)
08-105	Oral lichen planus	UPV/EHU Collection (Leioa)
08-187	Oral lichen planus	UPV/EHU Collection (Leioa)
09-297	Oral lichen planus	UPV/EHU Collection (Leioa)
10-166	Unknown	UPV/EHU Collection (Leioa)

Table 3.2. Continued.

Identity	Sample origin	Source
10-168	Unknown	UPV/EHU Collection (Leioa)
15-155	Unknown	Hospital de la Santa Creu i Sant Pau (Barcelona)
10-169	Unknown	UPV/EHU Collection (Leioa)
10-170	Unknown	UPV/EHU Collection (Leioa)
10-171	Unknown	UPV/EHU Collection (Leioa)
10-221	Oral lichen planus	UPV/EHU Collection (Leioa)
10-280	Oral	UPV/EHU Collection (Leioa)
10-294	Oral	UPV/EHU Collection (Leioa)
10-295	Oral	UPV/EHU Collection (Leioa)
15-153	Urine nephrostomy	Hospital de la Santa Creu i Sant Pau (Barcelona)
15-154	Blood culture	Hospital de la Santa Creu i Sant Pau (Barcelona)
15-156	Vitreous humor	Hospital de la Santa Creu i Sant Pau (Barcelona)
15-157	Oral mucosa	Hospital de la Santa Creu i Sant Pau (Barcelona)
15-158	Blood culture	Hospital de la Santa Creu i Sant Pau (Barcelona)
15-159	Wound	Hospital de la Santa Creu i Sant Pau (Barcelona)
15-160	Unknown	Hospital de la Santa Creu i Sant Pau (Barcelona)
15-161	Blood culture	Hospital de la Santa Creu i Sant Pau (Barcelona)
15-176	Unknown	Hospital Universitari I Politècnic de la Fe (Valencia)
15-178	Unknown	Hospital Universitari I Politècnic de la Fe (Valencia)
15-179	Unknown	Hospital Universitari I Politècnic de la Fe (Valencia)
16-091	Vaginal exudate	Hospital Universitario Severo-Ochoa (Madrid)
16-092	Sputum	Hospital Universitario Severo-Ochoa (Madrid)
16-122	Vaginal	Hospital Universitario Severo-Ochoa (Madrid)
16-123	Vaginal	Hospital Universitario Severo-Ochoa (Madrid)
16-132	Pharyngeal	Hospital Universitario Severo-Ochoa (Madrid)
16-133	Vaginal	Hospital Universitario Severo-Ochoa (Madrid)
16-134	Vaginal	Hospital Universitario Severo-Ochoa (Madrid)
16-135	Vaginal	Hospital Universitario Severo-Ochoa (Madrid)
16-138	Broncho aspirate	Hospital Universitario Severo-Ochoa (Madrid)

3.2. Plasmid pV1524

The vector pV1514 constructed by Vyas and colleagues (Vyas et al., 2018) contains all the elements necessary for CRISPR-Cas9 editing in *C. albicans*. Namely, the *CAS9* gene, the guide-RNA scaffold, which links Cas9 and the guide-RNA (gRNA), and a cloning site for gRNAs. Additionally, all genes required for the editing system are flanked by two sequences homologous to the 5' and 3' ends of the *NEUT5L* locus, respectively, and two Flp recognition target (FRT) sequences. The former will direct integration of the CRISPR cassette in this locus by homologous recombination, while the latter are recognized by a tyrosine site-specific recombinase (flippase, Flp), which will excise the cassette. The gene *FLP* in the plasmid is under the control of the maltose-inducible *MAL2p* promoter (Figure 3.1).

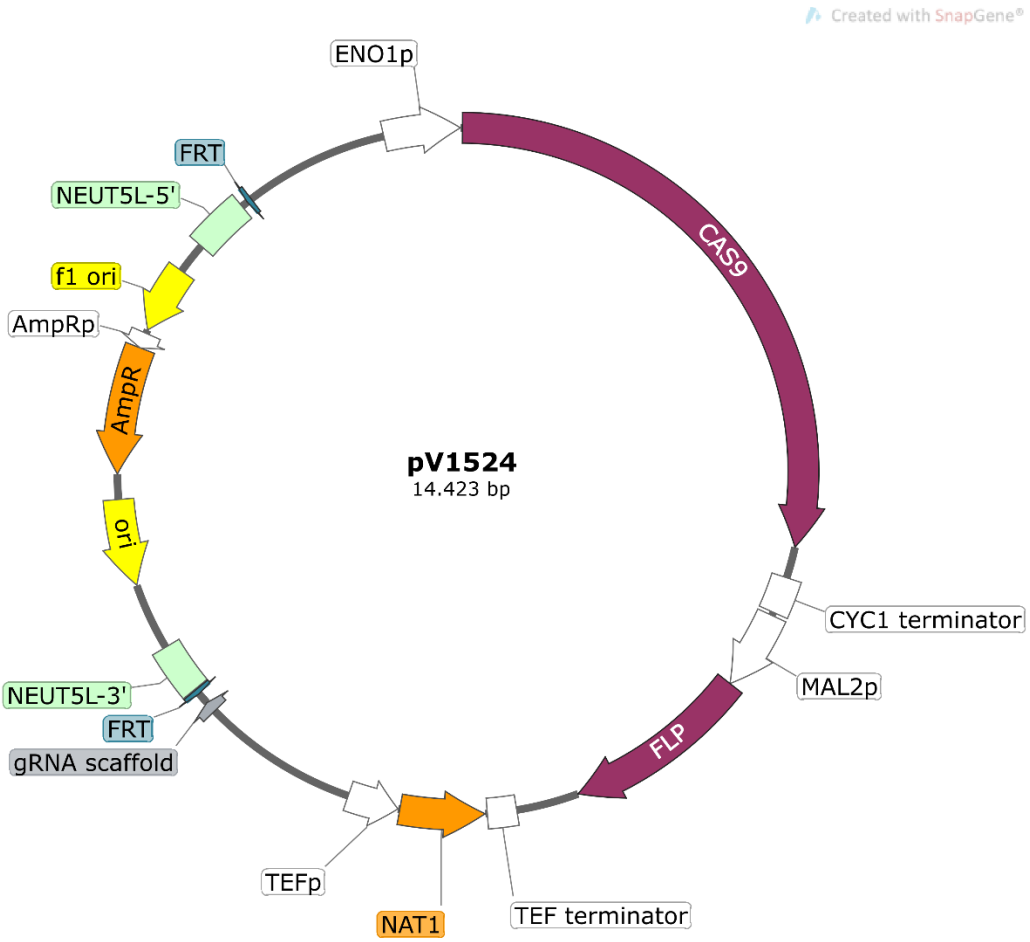

Figure 3.1. Simplified map of plasmid pV1524. Purple, *CAS9* and *FLP* genes; orange, resistance marker genes (*NAT1* and *AmpR*); white, promoters and terminators; yellow, replication origins; green; *NEUT5L* homologous regions; blue, FRT sequences; grey, gRNA scaffold.

3.3. Media and culture conditions

3.3.1. Culture media for *Candida*

— Sabouraud Dextrose Agar EP/USP/ISO (Condalab, Spain)

Suspend 65 g of powder in 1 l of distilled water and sterilize in autoclave at 121°C for 15 minutes. The final medium contains:

- Dextrose 40 g/l
- Mixture of peptic digest of animal tissue and pancreatic digest of casein (1:1) 10 g/l
- Bacteriological agar 15 g/l

— Candida Chromogenic Agar (Condalab, Spain)

Suspend 45.9 g of medium in 1 l of previously sterilized and cooled distilled water and take it to boiling point three times. The final medium contains:

- Glucose 20 g/l
- Chloramphenicol 0.5 g/l
- Peptone 10 g/l
- Bacteriological agar 15 g/l
- Chromogenic mixture 0.4 g/l

— RPMI-1640 (Sigma-Aldrich, USA)

This medium contains glucose (2 g/l) and L-Glutamine (0.3 g/l), besides other components, and lacks Sodium Bicarbonate. Suspend 10.4 g of powder in 900 ml of cooled down sterilized and distilled water, complete with 0.164 M 3-(N-Morpholino)propanesulfonic acid (MOPS) (Scharlab, Spain), adjust pH to 7±0.1 with NaOH 5 M and add sterile distilled water up to 1 l. Finally, sterilize by filtration (0.2 µm aPES membrane; Fisher Scientific, USA).

This medium was used for susceptibility testing (see Section 3.4) and the evolution experiment (see Section 3.8).

— Yeast Extract Peptone Dextrose (YEPD) broth/agar

- Yeast extract 10 g
- Peptone 20 g
- Dextrose 20 g
- Bacteriological agar (for YEPD agar) 16 g

Suspend in 1 l of distilled water and sterilize in autoclave at 121°C for 15 minutes.

— YEPD + 10NT

This medium was prepared for flip-out (FO) screening (see Section 3.7.12). After sterilizing, YEPD agar was cooled down to 50°C in a water bath and then supplemented with 10 μg/ml of nourseothricin (NT) (Jena Bioscience, Germany).

— YEPD + NT

This medium was used for transformants selection and flip-out screening (see Sections 3.7.10 and 3.7.12). In this case, YEPD agar was supplemented with 100 μg/ml of NT.

— YEP + 2% maltose broth/agar

This medium was used for flip-out induction (see Section 3.7.12). It was prepared as YEPD but without adding dextrose and separately, a solution of 20% maltose (w/v) was prepared in distilled water and sterilized by filtration (0.2 μm; Sarstedt, Germany). After sterilization, YEP was cooled down to 50°C in a water bath and 2% maltose (v/v) was added.

— YEP + 4% maltose broth/agar

This medium was prepared as above, except for the final maltose concentration, which was 4% (v/v).

— Yeast Nitrogen Base (YNB) + 2% maltose broth/agar

A 100 ml solution containing 10X YNB and 20% maltose (w/v) was prepared and sterilized by filtration (0.2 μm; Sarstedt, Germany). The final broth medium was prepared by dilution of this solution with 900 ml of sterile distilled water. If agar plates were to be made, 1.6 g/l of bacteriological agar was added to 900 ml of water,

autoclaved at 121°C for 15 minutes and cooled down to 50°C in a water bath before adding the concentrated solution of YNB+maltose (10X).

— YNB + 4% maltose broth

This medium was prepared as above, except for the maltose concentration, which was 4% (v/v).

— YNB supplemented with fluconazole (YNB+FLC)

YNB medium was prepared as explained above using glucose (2% final concentration) instead of maltose as carbon source and was supplemented with the appropriate fluconazole (FLC) concentration (0.125, 0.25, 0.5, 1, 2, 4, 8, 10, 16, 32, 64 µg/ml). This medium was used for Spot Assays (see Sections 3.7.13.2 and 3.8.7)

3.3.2. Culture media for *Escherichia coli*

– Luria-Bertani (LB) (Lennox) broth (Condalab, Spain)

Suspend 20 g of the medium in 1 l of distilled water and sterilize in autoclave at 121°C for 15 minutes. The final composition is:

- Tryptone 10 g/l
- Yeast Extract 5 g/l
- Sodium Chloride 5 g/l

– LB + NT broth/agar

For LB broth, 50 µg/ml of NT were supplemented to each culture flask just before inoculation. In the case of LB agar, it was prepared with LB Agar (Lennox) (Condalab, Spain) suspending 35 g of powder in 1 l of distilled water. Then it was sterilized in autoclave at 121°C for 15 minutes and cooled down to 50°C before adding 50 µg/ml of NT.

3.3.3. Culture conditions

Unless otherwise stated, yeasts were usually grown in Sabouraud agar or YEPD agar at 37°C for 24h for strain maintenance.

Escherichia coli was grown in LB + NT broth at 37°C and 200 rpm for 12-16h for plasmid purification (see Section 3.7.3) and in LB + NT agar at 37°C for 24h for transformants selection (see Section 3.7.6).

3.4. In vitro susceptibility to antifungal drugs

3.4.1. M27-A3 method by CLSI

Susceptibility testing against FLC (Sigma-Aldrich, USA) of *Candida* reference strains and clinical isolates was performed by the standardized broth microdilution method according to the Clinical and Laboratory Standards Institute's (CLSI) M27-A3 document (Clinical and Laboratory Standards Institute, 2008) and M27-S4 (Clinical and Laboratory Standards Institute, 2012), containing FLC in a 0.12-64 μg/ml concentration range. Strains were classified as either resistant (MIC ≥ 8 μg/ml), susceptible-dose dependent (SDD) (MIC = 4 μg/ml) or susceptible (MIC ≤ 2) according to the MIC breakpoints published in the M27-S4 document (Clinical and Laboratory Standards Institute, 2012).

Clotrimazole (CLT) antifungal activity testing is not standardized, so the protocol of Pelletier and collaborators (Pelletier et al., 2000) based on the CLSI's M27-A3 document with modifications was followed. The stock solution of CLT 10000 μg/ml of dimethyl sulfoxide (DMSO; Sigma-Aldrich, USA) was diluted to 1600 μg/ml with sterile distilled water. Then, serial dilutions of CLT (16 to 0.03 μg/ml) were prepared in sterile distilled water. The growth control contained the highest DMSO concentration (16%) possible to discard fungal growth inhibition by this compound. The cut-off value 0.5 μg/ml was used to determine if clinical isolates are susceptible or resistant. The plates were sealed with parafilm and stored at -80°C for a maximum of 6 months covered with aluminium foil until used.

3.4.2. Sensititre YeastOne® Y010 method

Other antifungal drugs (posaconazole (POS), itraconazole (ITC), voriconazole (VRC), flucytosine (5FC), anidulafungin (AFG), caspofungin (CFG), micafungin (MFG) and amphotericin B (AmB)), along with FLC, were assayed with the commercial method Sensititre YeastOne® Y010 (Trek Diagnostic Systems, United Kingdom). *Candida parapsilosis* ATCC 22019 and *C. krusei* ATCC 6258 were used as reference strains.

This is a colorimetric dilution method that contains a growth indicator based on the oxidation of the Alamar blue dye, which facilitates endpoint reading by a colour change. Each plate includes serial dilutions of nine dehydrated antifungals: AFG (0.015-8 µg/ml), MFG (0.008-8 µg/ml), CFG (0.008-8 µg/ml), 5FC (0.06-64 µg/ml), POS (0.008-8 µg/ml), VRC (0.008-8 µg/ml), ITC (0.015-16 µg/ml), FLC (0.12-256 µg/ml) and AmB (0.12-8 µg/ml). The assay was carried out following manufacturer's instructions.

3.5. Characterization of *ERG11*, *TAC1*, *UPC2*, *MRR1* and *MRR2* genes in *Candida albicans* strains

3.5.1. Primer design

The primers used for amplification of target regions of *ERG11*, *TAC1* and *UPC2* genes were described by Arrieta Aguirre (Arrieta Aguirre, 2018), and for the *MRR2* gene by Wang and collaborators (Wang et al., 2015). For *MRR1* we performed a search in NCBI's Nucleotide database of the *MRR1* gene in *C. albicans*. An alignment was done with sequences comprising the complete coding sequence (CDS) with Clustal Omega at EMBL-EBI (McWilliam et al., 2013). Based on the alignment, three pairs of primers were designed to amplify three regions of the *MRR1* gene rich in gain-of-function (GOF) mutations that were previously published (Dunkel et al., 2008; Eddouzi et al., 2013; Lohberger et al., 2014; Morschhäuser et al., 2007). Primers were designed at conserved regions to avoid polymorphisms and to assure correct annealing to their DNA target. Criteria described by Sambrook and Russel (Sambrook & Russell, 2001) was followed: primers must be 18-25 nucleotide long, guanine and cytosine proportion must not exceed 60%, three or more guanines or cytosines in the 5 last nucleotides of the 3' end must be avoided, and preferably they should have a melting temperature (Tm) between 52 and 58°C.

The quality of the selected primers was evaluated with the Oligo Analyzer 3.1 program of IDT (Integrated DNA Technologies) (https://eu.idtdna.com/pages/tools/oligoanalyzer). The design was made to avoid hairpin, self-dimer and hetero-dimer formation.

Primers used for amplification and sequencing of *C. albicans* resistance-associated genes target regions are listed in Table 3.3.

3.5.2. DNA purification

– PBS (Phosphate buffered saline)

- NaH_2PO_4 (Panreac, Spain) 0.386 g
- Na_2HPO_4 (Panreac, Spain) 1.02 g
- NaCl (Panreac, Spain) 8.5 g
- Distilled water 1 l

Adjust pH to 7.2 and sterilize by autoclave at 121°C for 15 minutes.

– Lysis buffer

- Tris-HCl pH8 (Sigma-Aldrich, USA) 50 mM
- Na-EDTA (Sigma-Aldrich, USA) 20 mM
- NaCl (Panreac Quimica, Spain) 75 mM
- Lyticase (Sigma-Aldrich, USA) 50U/ml

DNA was extracted using the DNeasy® Plant Mini Kit (Qiagen, Germany) following manufacturer's instructions with modifications. Briefly, 4-5 colonies grown in Sabouraud agar over-night (ON) at 37°C were resuspended in 400 µl of sterile PBS, 90 mg of sterile glass beads (Sigma-Aldrich, USA) were added and vortexed for 5 minutes. The supernatant was transferred to another tube, and 300 µl of lysis buffer were added. The mixture was incubated at 30°C for 20 minutes. Then, 4 µl of RNase (100 mg/ml) (Qiagen, Germany) was added and incubated at 37°C for 20 minutes. Then 100 µl of SDS 10% (Bio-rad, USA) and 40 µl of Proteinase K (20 mg/ml) (Roche, Switzerland) were added and incubated at 55°C for 20 minutes. Finally, the kit protocol was followed from the fourth step. DNA concentration and purity were determined by measuring absorbance at 230, 260 and 280 nm with NanoDrop 1000 (ThermoFisher Scientific, USA). Values between 1.6 and 2 of A260/280 and A260/230 ratios indicate a high purity level. DNA samples were stored at -20°C until use.

Table 3.3. Primers for amplification and sequencing of *C. albicans* resistance-associated genes target regions.

Target region and Primer	Sequence (5'-3')	Annealing temperature (°C)	Reference
***TAC1* 673-1383**			
Zinc2-1123	GATGCCAACGAATTATTGA	63	Coste et al., 2009
Tac1-Rv3-461	TGGTAGTGACATCGTTGGTATTG		Arrieta Aguirre, 2018
***TAC1* 2017-2940**			
Tac1-Fw3-673	ACCTCAGTTCAAGCAAGTACTG	59	Arrieta Aguirre, 2018
Tac1-Rv2-980	CCTTTGATAGGAAAAAATATATGAAAC		
***ERG11* 83-746**			
Erg11-F2	GGGTTCCATTTGTTTACAACTTAGT	57	Arrieta Aguirre, 2018
Erg11-R1	GCAGCATCACGTCTCCAATAA		
***ERG11* 639-1554**			
Erg11-F3	TGACCGTTCATTTGCTCAACTA	57	Arrieta Aguirre, 2018
Erg11-R4	GATTTCTGCTGGTTCAGTAGGT		
***UPC2* 1804-2094**			
Upc2-Fw	GGCCATGCGGATAATGAGA	57	Arrieta Aguirre, 2018
Upc2-Rv	ATTACTGGTAAGGACGCTTGG		
***MRR1* 908-1174**			
Mrr1-F-335	GAGACTTTAGAAGAGTGAATCA	58	This study
Mrr1-R-381	TGTCATAGGGAACAACATCAT		
***MRR1* 1151-2114**			
Mrr1-F-381	TCAATGATGTTGTTCCCTATGA	58	This study
Mrr1-R-683	CGTCTCGATACGCTAAGAA		
***MRR1* 2266-3200**			
Mrr1-F-803	AAATCATTCTTGGTGTCAGTAT	58	This study
Mrr1-R-1037	AAAGGTGTATTGCCATAGTAA		

Table 3.3. Continued.

Target region and Primer	Sequence (5'-3')	Annealing temperature (°C)	Reference
MRR2			
Mrr2-1F	GCAGAAGCGAGGGAACTTGAAA	58	Wang et al., 2015
Mrr2-1R	AGCACGGAGTGTGTCGTAGGAA		
Mrr2-2F	TGATCCCCATCATAGACGAAAC		
Mrr2-2R	TAGGTCCCTTGAATAAGTAGAGCG		
Mrr2-3F	AGTAGAAACCAAACTCCAAGCC		
Mrr2-3R	CGAAACTTCTGCCATCCTCAAT		

3.5.3. Amplification protocol

The amplification was carried out in a GeneAmp® PCR System 9700 (Applied Biosystems, USA). The PCR mixture contained each primer pair described in Table 3.3 in a final reaction volume of 25 µl (Table 3.4).

Table 3.4. PCR reaction mixture for amplification of resistance-associated genes.

Reagents	Volume (µl)
Phusion High-Fidelity PCR Master Mix with GC Buffer (2X) (ThermoFisher Scientific, USA)	12.5
Forward primer (25 µM)	0.5
Reverse primer (25 µM)	0.5
DNA (5 ng/µl)	2
H_2O	up to 25 µl

The PCR thermal cycling conditions were constant for all gene fragments except the annealing temperature, which varied depending on the gene fragment being amplified (Table 3.3), and consisted of:

Initial denaturation	98°C – 30 s	
Denaturating stage	98°C – 5 s	30 cycles
Annealing stage	Table 3.3 – 30 s	
Elongation stage*	72°C – 30 s	
Final elongation	72°C – 5 min	

*TAC1 2017-2940 fragment's elongation step was set for 15 s at 72°C.

Sequences were obtained at the Sequencing and Genotyping Service SGIker of the University of the Basque Country UPV/EHU. The sequences were analysed with Chromas 2.5.1 software (Technelysium) to identify heterozygous mutations, and BioEdit Sequence Alignment Editor 7.2.5 to align them with the reference sequences DQ393587 for *TAC1*, EU583451 for *UPC2*, X13296 for *ERG11*, XM_711520 for *MRR1* and XM_705846 for *MRR2*, downloaded from the NCBI's Nucleotide database.

3.6. Gene expression analysis by quantitative reverse transcription PCR (RT-qPCR)

The expression levels of *CDR1*, *CDR2* and *MDR1* genes were measured by RT-qPCR in all resistant isolates and SC5314, BE-047, BE-090 and 15-161 susceptible strains. Primers for each gene were selected and efficiency of each pair of primers was determined. cDNA was synthesized by reverse transcription from RNA extracted from *C. albicans* strains and amplified by RT-qPCR. Expression levels of target genes were normalized with reference to that of reference genes (actin, *ACT1*, and plasma membrane H^+-ATPase genes, *PMA1*) (Morio et al., 2012). Primers for cDNA amplification were obtained from the literature and are listed in Table 3.5.

Table 3.5. Primers for gene expression analysis by RT-qPCR.

Primer	Sequence (5'-3')	Concentration (µM)*	Reference
CDR1-Fw	ATTCTAAGATGTCGTCGCAAGATG	0.5	Flowers et al., 2012
CDR1-Rv	AGTTCTGGCTAAATTCTGAATGTTTTC	0.5	
CDR2-Fw	TAGTCCATTCAACGGCAACATT	0.3 (0.5)	
CDR2-Rv	CACCCAGTATTTGGCATTGAAA	0.1 (0.3)	
MDR1-Fw	ACATAAATACTTTGCCCATCCAGAA	0.5	
MDR1-Rv	AAGAGTTGGTTTGTAATCGGCTAAA	0.3 (0.5)	
ACT1-Fw	ACGGTGAAGAAGTTGCTGCTTTAGTT	0.5 (0.3)	
ACT1-Rv	CGTCGTCACCGGCAAAA	0.3 (0.1)	
PMA1-Fw	TTGAAGATGACCACCCAATCC	0.5 (0.3)	Morio et al., 2012
PMA1-Rv	GAAACCTCTGGAAGCAAATTCG	0.3 (0.1, 0.5)	

*For the expression analysis of the CRISPR-Cas9 transformants and the in vitro evolution experiment populations, the primer concentrations were adjusted as specified in brackets.

3.6.1. RNA purification

3.6.1.1. Sample preparation

Yeasts were first incubated in Sabouraud agar at 37°C for 24h, and a single colony was used to inoculate 3 ml of Sabouraud broth that was incubated at 30°C and 200 rpm ON. Optical density at a wavelength of 600 nm (OD_{600}) of ON cultures was measured and 10 ml of fresh Sabouraud broth were inoculated with 10^6 cells/ml. The latter cultures were incubated at 30°C and 120 rpm for approximately 6 hours to reach the exponential phase ($OD_{600} \simeq$ 2-3), and 1.5 ml of mid-log cultures were harvested by centrifugation at 16800 g for 2 min.

3.6.1.2. RNA extraction

Total RNA was extracted from mid-log cells using the MasterPure™ Yeast RNA Purification Kit (Epicentre Biotechnologies, USA) following manufacturer's instructions with modifications; proteinase K treatment was carried out at 50°C for 20 minutes and DNase treatment was prolonged up to 30 minutes. RNA was quantified with NanoDrop 1000 (ThermoFisher Scientific, USA). The quality and integrity of RNA was determined with Bioanalyzer at the Gene Expression Service SGIker of the University of the Basque Country UPV/EHU. RNA was stored at -80°C until use.

3.6.2. cDNA synthesis

cDNA was synthesized by reverse transcription from RNA extracted from *C. albicans* strains with PrimeScript™ RT reagent Kit (Perfect Real Time) (Takara) following manufacturer's instructions. In addition, negative controls of the reverse-transcription were performed, which consisted of a pool of RNA samples and all the kit reagents except for the reverse transcriptase. In total four RNA pools were prepared mixing equal volumes of each sample, one corresponded to the susceptible strains RNA while the other three were made up of the resistant strains RNA. cDNA was stored at -80°C until use.

3.6.3. Efficiency determination

The cDNA of the genes whose primers are specified in Table 3.5 was amplified from RNA of the SC5314 *C. albicans* strain, and for efficiency determination, a standard

curve was performed with six 1/5 serial dilutions (from 40 ng/µl to 0.0128 ng/µl). Primer concentration was adjusted until all efficiencies were between 0.8 and 1.1 and no primer dimers were formed. Efficiency is calculated with the following equation: $E = \left[10^{(-1/m)}\right] - 1$; where m stands for the slope of the linear regression of representing the quantification cycle (C_q) versus the logarithm of cDNA concentration (Bustin et al., 2009).

3.6.4. Reference genes stability analysis

Stability of the two reference genes used for normalization was calculated with geNorm (Vandesompele et al., 2002).

3.6.5. Amplification by RT-qPCR

RT-qPCR was performed in an ABI 7300 Real-Time PCR System (Applied Biosystems) with the following conditions. The 20 µl PCR reaction mixture composition is shown in Table 3.6 where primers volume varied in accordance with the final concentration specified in Table 3.5.

Table 3.6. RT-qPCR reaction mixture for gene expression analysis.

Reagents	Volume (µl)
SYBR® Premix ExTaq™ (Tli RNaseH Plus) (Takara) (2X)	10
ROX (50X)	0.4
Forward primer (25 µM)	*
Reverse primer (25 µM)	*
cDNA (20 ng/µl)	2
H_2O	up to 20 µl

* Variable volume in accordance with the final concentration specified in Table 3.5 for the different primer pairs.

The PCR thermal cycling conditions were as follows:

Initial denaturation	95°C – 30 s	
Denaturating stage	95°C – 5 s	40 cycles
Annealing and elongation stage	60°C – 30 s	
Dissociation curve	95°C – 15 s 60°C – 1 min 95°C – 15 s 60°C – 15 s	

Each resistant and susceptible strain was tested in triplicate and for each gene a non-template control was included. Additionally, the SC5314 strain RNA sample was used as an inter-plate calibrator (IPC) and was included in all PCR plates.

3.6.6. Data analysis

The fluorescence data obtained were analysed with the 7300 System SDS Software Version 1.4.0.27 supplied by Applied Biosystems. The software automatically set the base line for each sample, which indicates the absence of detectable amplification. When fluorescence exceeds significantly the base line, the threshold was fixed manually to 0.2. Then, C_q was automatically calculated, which corresponds to the amplification cycle where the fluorescence overcomes the threshold in logarithmic scale (Figure 3.2).

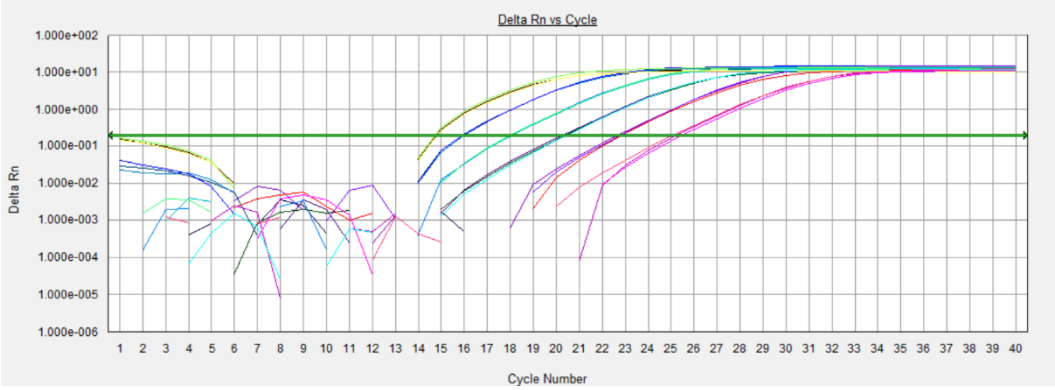

Figure 3.2. Graphic representation of the emitted fluorescence relative intensity versus the PCR cycle number.

To calculate the fold-change (FC) in gene expression the following steps were followed:

a. Quality control: technical replicates that deviated > 0.5 SD were eliminated.

b. Inter-plate calibration was calculated with the next equation: $Cq_{norm} = Cq - \overline{Cq} + \overline{IPC}$, where Cq represents the C_q value of each replicate in each plate, $\overline{Cq}$ is the average Cq of the three replicates in its corresponding plate and $\overline{IPC}$ is the average Cq of all the IPCs.

c. Normalization: C_q of our target genes (tg) was normalized against the geometric average of those of the reference genes (ref) as follows: $\Delta Cq = Cq_{tg} - \overline{Cq}_{ref}$. The ΔCq of resistant isolates (r) was compared with the average ΔCq of the susceptible ones (s) ($\Delta\Delta Cq = \Delta Cq_r - \overline{\Delta Cq_s}$).

The FC was calculated with the $2^{-\Delta\Delta Cq}$ equation, as described by Livak and Schmittgen (Livak & Schmittgen, 2001). Overexpression was arbitrarily considered significant when the FC was greater than 2 (Torelli et al., 2008).

3.7. Single-base editing mediated by CRISPR-Cas9 system

The genome editing by CRISRP-Cas9 followed in this work is outlined in Figure 3.3. First, specific gRNA sequences for each mutated gene were searched and cloned into pV1524 plasmid, then the recombinant plasmids were transformed into *E. coli* competent cells to obtain multiple copies of each plasmid (Figure 3.3 A). After selection and verification of correct clones, the recombinant vector together with a repair template (RTe) containing the desired mutation was introduced in *C. albicans* SC5314 by electroporation (Figure 3.3 B). Finally, the integrated vector was removed by Flp activity induction (Figure 3.3 D).

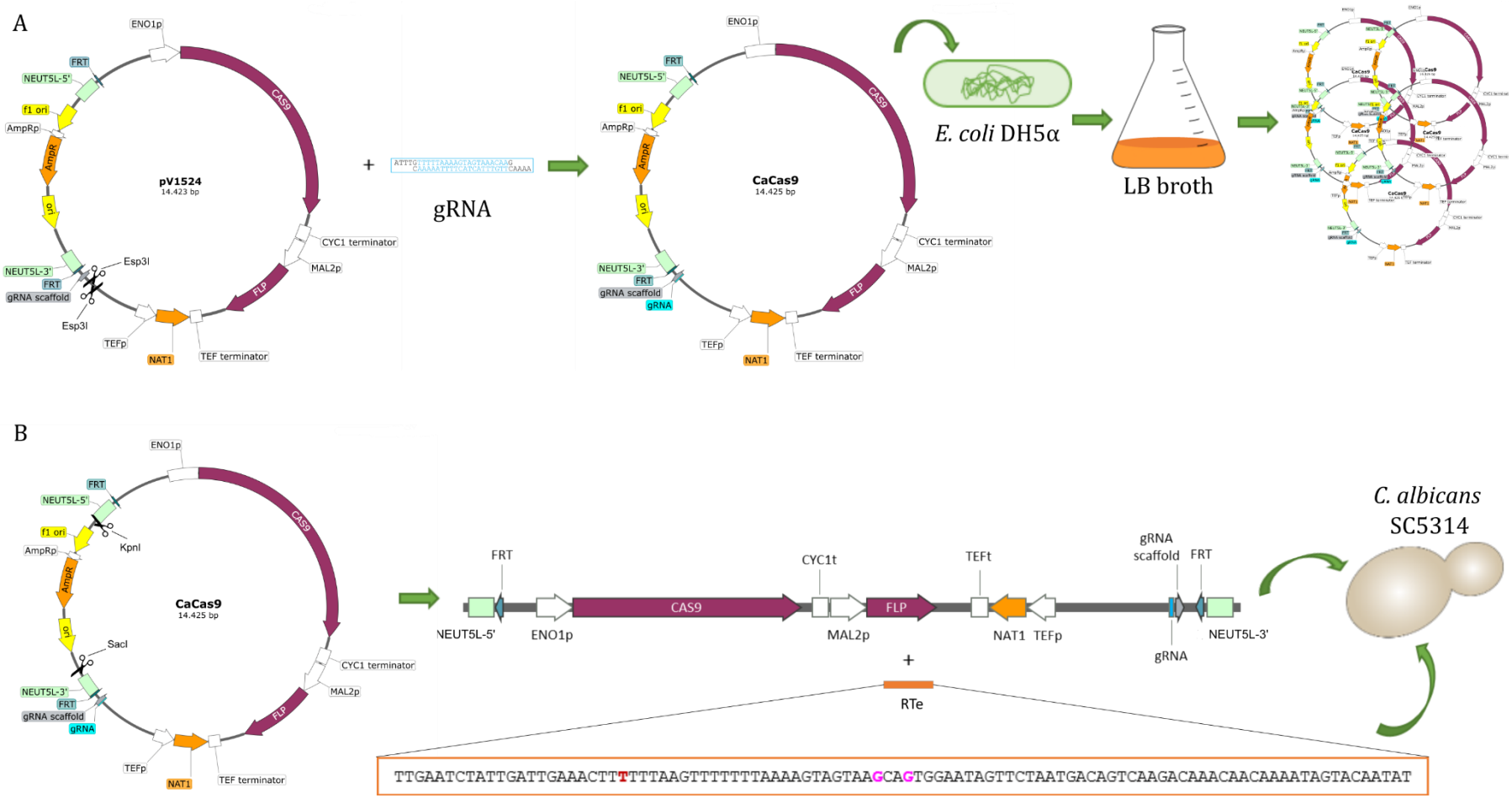

Figure 3.3. Schematic CRISPR-Cas9 editing process in *C. albicans*. A, gRNA cloning into pV1524 plasmid after excision with Esp3I; B, *C. albicans* transformation with linearized recombinant pV1524 excised with KpnI and SacI and RTe; C, integration of CRISPR-Cas9 cassette into *C. albicans* chromosome 5 *NEUT5L* locus and CRISPR-Cas9-mediated editing; D, induction of flippase activity and excision of CRISPR-Cas9 cassette.

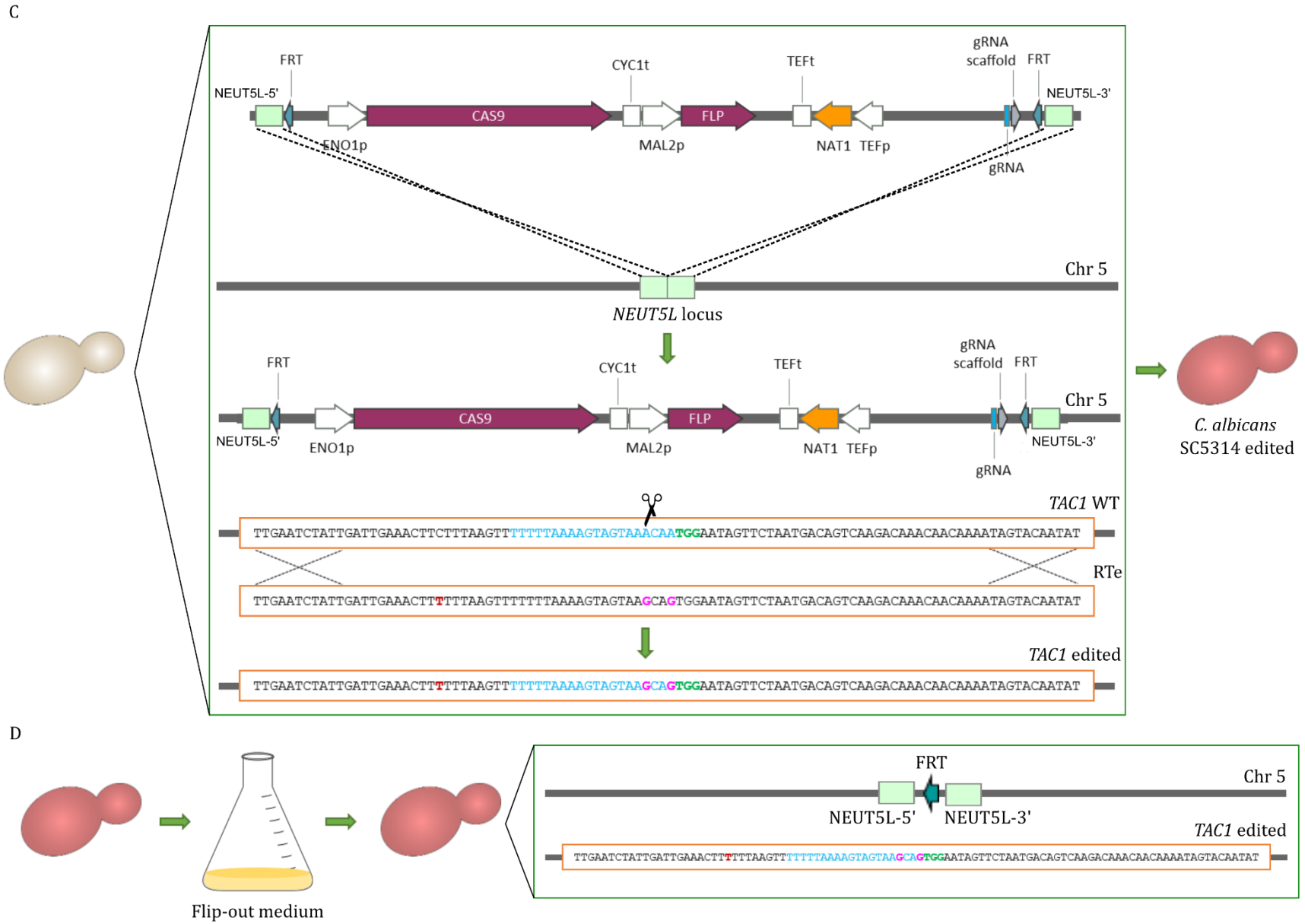

Figure 3.3. Continued.

3.7.1. Experimental design

3.7.1.1. Guide-RNA design

CRISPR-Cas9 editing relies on the endonuclease activity of Cas9, which catalyses the formation of double-stranded breaks (DSBs). Its activity is sequence-specific and is guided by a 20 bp RNA molecule called gRNA that needs to be adjacent in its 3' end to a PAM (protospacer adjacent motif). The PAM sequence recognized by Cas9 is composed of three bases, 5'-NGG-3'. Therefore, for our experiment, we first searched for PAM sequences near to each of the desired mutations. In order to do so, the complete CDS of *TAC1*, *ERG11* and *MRR2* genes of *C. albicans* SC5314 were downloaded from NCBI's Nucleotide database and Cas9's PAM motifs surrounding the single nucleotide polymorphism (SNP) were searched both in the coding and complementary sequences. Then, the following 20 bp towards the 5' end were annotated, which would be the gRNA sequences. Each gRNA was evaluated for its specificity with BLAST (Basic Alignment Search Tool, https://blast.ncbi.nlm.nih.gov/Blast.cgi) against the reference genome sequence of *C. albicans* SC5314 and for hairpin formation with Oligo Analyzer 3.1 program. Based on those two results and their distance to the mutation, a gRNA for each gene was selected.

3.7.1.2. Repair template design

After Cas9 enzyme cuts the DNA double strand, *C. albicans* will repair the DSB primarily by homologous recombination (HR) (Legrand et al., 2019). In order to introduce small genome changes we can take advantage of this repair mechanism and introduce into *C. albicans* competent cells a RTe, together with the Cas9-containing vector, that carries the desired SNP and is homologous to both ends of the DSB. Thus, we designed two RTes specific for each gRNA selected, since they have to be centred over the cleaving site (3-4 bp 5' of the PAM sequence). One contained the desired mutation (mutated RTe) while the other one had the wild type (WT RTe) sequence as control. In addition to the desired mutation, we included in the RTe sequence two silent mutations in the 7 nucleotides adjacent to the PAM, in order to avoid post-modification cleavage of the genome and undesired cuts in the RTe. All RTe's were designed to be 100 bp long to allow HR.

3.7.2. Guide-RNA preparation

– Annealing buffer

- Tris pH 7.5 10 mM
- NaCl 50 mM
- EDTA 1 mM

The gRNA was prepared by annealing two oligonucleotides phosphorylated at their 5'-ends (Table 3.7) in the following conditions: both oligonucleotides were resuspended in annealing buffer to a final concentration of 100 µM, 10 µl of each were mixed and were incubated at 95°C for 5 minutes. Then, it was left to cool at room temperature for 1 hour.

Table 3.7. Primer sequences for gRNA synthesis.

Primer	gRNA	Sequence (5'-3')
Tac1-758-g2F	Tac1-758-g2	ATTTGTTTTTAAAAGTAGTAAACAAG
Tac1-758-g2R		AAAACTTGTTTACTACTTTTAAAAAC
Erg11-477-g4F	Erg11-477-g4	ATTTGCAATTTGCTTATGTTCAATTG
Erg11-477-g4R		AAAACAATTGAACATAAGCAAATTGC
Mrr2-311-g1F	Mrr2-311-g1	ATTTGCCACTCGCTCACTGCCCTCCG
Mrr2-311-g1R		AAAACGGAGGGCAGTGAGCGAGTGGC

gRNA sequence is highlighted in blue. The rest of the primer sequence corresponds to plasmid sequence.

3.7.3. Plasmid purification

Plasmid pV1524 was ordered from the Addgene repository in a bacterial stab, which was subcultured upon reception in LB agar + NT at 37° for 24 h. From a single colony two ON cultures were initiated in LB + NT at 37°C and 200 rpm. One of these cultures was used for storage at -80°C in 25% glycerol and the other one for plasmid purification.

Plasmids were extracted with GeneJET Plasmid Miniprep Kit (ThermoFisher Scientific) following manufacturer's instructions with modifications. Briefly, the pelleted cells were thoroughly resuspended with 250 µl of the Resuspension Solution by vortexing and incubated for 15 min at 37°C. Then 250 µl of the Lysis Solution were added, the tubes were inverted 5 times, and incubation was prolonged up to 5 min. Subsequently, 350 µl of the Neutralization Solution were

incorporated, the tubes were again inverted 5 times and incubated in ice for 5 min. The mix was centrifuged at maximum revolutions and the supernatant was passed through the column 6 times by centrifugation for 30 s at 5000 g. Washing was performed two times with 500 µl of Wash Solution, followed by an additional centrifugation for 1 min at 12000 g. After incubating for 1 min at room temperature with pre-warmed Elution buffer at 60°C, plasmids were eluted by centrifugation for 2 min at 12000 g. The eluate was passed through the column a second time and purified plasmids were quantified with NanoDrop 1000.

3.7.4. Restriction digestion of pV1524 for gRNA cloning

The plasmid pV1524 was digested with BsmBI (Esp3I) (ThermoFisher Scientific) restriction enzyme. The digestion was carried out in 40 µl reaction volume (Table 3.8) and was incubated at 37°C for 2 hours.

Table 3.8. Restriction digestion with BsmBI mixture.

Reagent	Volume (µl)	Final concentration
Vector	*	5 µg/40 µl
Tango Buffer (10X)	4	-
BsmBI (Esp3I) (10 U/µl)	2	0.5 U/µl
DTT (20 mM)	2	1 mM
Milli-Q water	up to 40 µl	

* Variable volume depending on the concentration of the vector sample.

The digestion product was migrated in an agarose gel at 0.8% stained with Ethidium Bromide 0.2 µg/ml for 1 hour at 100 V (Figure 3.4). Then, the desired band was excised from the gel with a clean scalpel and was extracted with GeneClean III Kit (MP Biomedicals) with the following modifications: the DNA was incubated with EZ-GLASSMILK® for 5 min at 55°C and another 5 min at room temperature; the bound DNA was washed 3 times with 600 µl of New Wash; and elution was performed in two steps with TE buffer pre-warmed at 55°C and incubation for 2 min at room temperature. The final centrifugation step was carried out at 14000 g for 1 min. Plasmid restriction digests were quantified by gel electrophoresis and image analysis with a Molecular Imager® ChemiDoc™ XRS System and Quantity One Analysis Software 4.5.0 (BioRad, USA).

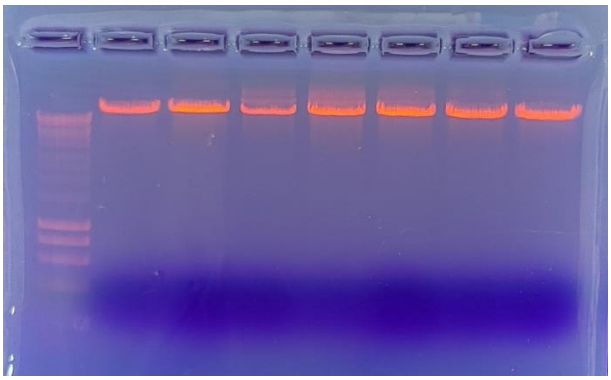

Figure 3.4. Agarose gel of pV1524 digested with BsmBI.

3.7.5. Ligation

The gRNAs and the digested plasmids were ligated in a 3:1, 5:1 or 7:1 molar ratio in a final volume of 20 µl (Table 3.9). The reaction was incubated at 16°C ON.

Table 3.9. Ligation reaction mixture.

Reagent	Volume (µl)	Final concentration
Vector	*	5 ng/µl
gRNA[a]	*	0.624 ng (3:1), 1.040 ng (5:1), 1.456 ng (7:1) or 0.153 ng (3:4) / 20 µl
T4 DNA Ligase buffer (10x)	2	-
T4 DNA ligase (5 U/µl)	0.2	1 U/20 µl
Milli-Q water	up to 20 µl	

[a]gRNA input amount was calculated with NEBioCalculator® (http://nebiocalculator.neb.com/#!/ligation), * Variable volume

3.7.6. Transformation of *E. coli* competent cells

The ligation product was transformed into *E. coli* Subcloning Efficiency™ DH5α™ Competent Cells (Invitrogen, USA) following manufacturer's instructions. Transformants were selected by cultivation in LB agar + NT at 37°C for 24-72h.

3.7.7. Screening of correct transformants

Ligation was confirmed by colony PCR (Table 3.10) and sequencing. Prior to PCR, a colony was suspended in 20 µl of water and boiled for 20 minutes, and 2 µl of the lysate were used for amplification. Positive transformants were grown in LB

broth + NT for plasmid purification and subsequent sequencing. The primers used for PCR and sequencing are shown in Table 3.11.

Table 3.10. Colony PCR reaction mixture.

Reagents	Volume (µl)
BioMix™ 2X (Meridian Bioscience™)	10
Forward primer (25 µM)	0.4
Reverse primer (25 µM)	0.4
Colony lysate	2
Water	up to 20 µl

Table 3.11. Primer sequences for gRNA transformants screening and sequencing.

Primer	gRNA	Sequence (5'-3')
PCR COLONY		
Tac1-758-g2-5'	Tac1-758-g2	CGAGACTTGCGTAAACTATTTTTAATTTGTTT
Tac1-758-g2-3'		CTTGCTATTTCTAGCTCTAAAACTTGTTT
Erg11-477-g4-5'	Erg11-477-g4	GCGTAAACTATTTTTAATTTGCAATTTG
Erg11-477-g4-3'		TTCTAGCTCTAAAACAATTGAAC
Mrr2-311-g1-5'	Mrr2-311-g1	GCGTAAACTATTTTTAATTTGCCACTC
Mrr2-311-g1-3'		TGCTATTTCTAGCTCTAAAACGGAG
SEQUENCING		
gRNAseq-Fw	All	GAAGCATCTAATCAACTCCCAGATCA
gRNAseq-Rv		AACTGAATTGTGCTTGAATACCA

gRNA sequences are highlighted in blue

The thermocycling steps were:

Initial denaturation	94°C – 5 min	
Denaturating stage	94°C – 30 s	25 cycles
Annealing stage	61°C – 30 s	
Elongation stage	72°C – 5 s	
Final elongation	72°C – 3 min	

3.7.8. Repair template synthesis

The RTe were synthesized by primer extension of two overlapping primers (Table 3.12) in 50 µl reaction volume (Table 3.13).

Table 3.12. Primer sequences for RTe synthesis.

Primer	RTe	Sequence (5'-3')
Tac1-758-RTe2 Fw	Tac1-758-RTe2	TTGAATCTATTGATTGAAACTTTTTAAGTTTTTTTA
		AAAGTAGTAAGCAGTGGAATAGT
Tac1-758-RTe2 Rv		ATATTGTACTATTTTGTTGTTTGTCTTGACTGTCATT
		AGAACTATTCCACTGCTTACTAC
Tac1-WT-RTe2 Fw	Tac1-WT-RTe2	TTGAATCTATTGATTGAAACTTCTTTAAGTTTTTTTA
		AAAGTAGTAAGCAGTGGAATAGT
Tac1-WT-RTe2 Rv		ATATTGTACTATTTTGTTGTTTGTCTTGACTGTCATT
		AGAACTATTCCACTGCTTACTAC
Erg11-477-RTe4 Fw	Erg11-477-RTe4	TTTGGTGGTGGTAGACATAGATGTATTGGGGAACAAT
		TTGCTTGTGTCCAGTTAGGAACC
Erg11-477-RTe4 Rc		CAATAGTCCATCTTAAATTATAAACAAAAGTAGTTAA
		AATGGTTCCTAACTGGACACAAG
Erg11-WT-RTe4 Fw	Erg11-WT-RTe4	TTTGGTGGTGGTAGACATAGATGTATTGGGGAACAAT
		TTGCTTATGTCCAGTTAGGAACC
Erg11-WT-RTe4 Rv		CAATAGTCCATCTTAAATTATAAACAAAAGTAGTTAA
		AATGGTTCCTAACTGGACATAAG
Mrr2-311-RTe1 Fw	Mrr2-311-RTe1	AACCATCATGAAAGAGTTTGACATTACCAAAACCCAC
		TCGCTCACTGCTCTTCAGGTAGA
Mrr2-311-RTe1 Rv		CAGTTCTGGTGCCACGATTTTATAGAACCTAAGCATG
		ATTTCTACCTGAAGAGCAGTGAG
Mrr2-WT-RTe1 Fw	Mrr2-WT-RTe1	AACCATCATGAAAGAGTTTGACATTACCAAAACCCAC
		TCGCTCACTGCTCTTCAGGCAGA
Mrr2-WT-RTe1 Rv		CAGTTCTGGTGCCACGATTTTATAGAACCTAAGCATG
		ATTTCTGCCTGAAGAGCAGTGAG

Bold red, base change to trigger single base editing; yellow, coding triplet for the amino acid change; bold pink, silent mutations; green, PAM. The overlapping sequence between the two primers is underlined.

Table 3.13. RTe synthesis reaction mixture.

Reagents	Volume (µl)
Phusion High-Fidelity PCR Master Mix with GC Buffer (2X) (ThermoFisher Scientific, USA)	25
Forward primer (25 µM)	2
Reverse primer (25 µM)	2
Water	up to 50 µl

The PCR cycling conditions were:

Initial denaturation	98°C – 30 s	
Denaturating stage	98°C – 5 s	30 cycles
Annealing stage	71°C – 15 s	
Elongation stage	72°C – 15 s	
Final elongation	72°C – 5 min	

PCR products were purified with QIAquick® PCR Purification Kit (Qiagen, Germany) following manufacturer's instructions.

3.7.9. Restriction digestion of recombinant pV1524 for *C. albicans* transformation

Before transformation of *C. albicans* with recombinant pV1524 plasmids containing the gRNAs, the vectors had to be linearized to facilitate integration in the host genome. They were double digested with KpnI and SacI restriction enzymes in 40 µl of reaction volume (Table 3.14), and the digestion mixture was incubated at 37°C for 2 h.

Table 3.14. Double restriction with KpnI and SacI reaction mixture.

Reagents	Volume (µl)	Final concentration
Vector (200 ng/µl)	25	5 µg/40 µl
Tango Buffer (10X)	4	1 X
KpnI (10 U/µl)	2	0.5 U/µl
SacI (10 U/µl)	2	0.5 U/µl
Milli-Q water	up to 40 µl	

The restriction sites for KpnI and SacI in plasmid pV1524 are located next to the *NEUT5L* locus sequences, leaving two fragments, one of 11552 bp that contains all the elements necessary for integration, genome editing and vector removal; and another one of 2871 bp with the elements used for cloning in *E. coli*.

Digested plasmids were dialysed against Milli-Q water for 1 h with Nitrocellulose membranes MF™ 0.025µm VSWP (Millipore, USA).

3.7.10. Transformation of *C. albicans* by electroporation

– Transformation Mix (for 10 ml):

- 10X TE Buffer pH 7.5 1 ml
- 1M Lithium Acetate pH 7.5 1 ml
- Milli-Q water 8 ml

A hybrid lithium acetate/electroporation protocol was used for transformation of *C. albicans*. First, an ON culture was established at 30°C and 200 rpm in YEPD broth. Next day 50 ml of YEPD broth were inoculated with 100 µl of the ON culture and was incubated at 30°C and 200 rpm until an OD_{600} of 1.6-2.2 was reached. The culture was then centrifuged for 5 min at 3000 g at 4°C. The supernatant was discarded, and the pellet was resuspended in 10 ml of cold Transformation Mix followed by incubation for 1 hour at 30°C and 150 rpm. Then, 250 µl of 1 M DTT freshly prepared was added and incubation was prolonged for 30 minutes. Here after, 40 ml of cold sterile Milli-Q water was added and after mixing, the mixture was centrifuged at 4°C and 3000 g for 5 min. From this point onwards the tubes were kept on ice. The supernatant was discarded, and the pellet was resuspended in 25 ml of cold sterile Milli-Q water by gently mixing. The centrifugation step was repeated, and the supernatant was discarded. The pellet was resuspended in 1 ml of sterile cold 1 M sorbitol and centrifuged again. After discarding the supernatant, the cells were resuspended in the remaining volume to obtain a dense suspension.

In a pre-cooled 0.2 cm electroporation cuvette 40 µl of cell suspension were mixed with 5 µg of the gRNA containing plasmid linearized with KnpI and SacI and dialysed, and 6 µg of purified RTe. Electroporation was carried out in a Gene Pulser® II Electroporation System (BioRad, USA) at a voltage of 1.8 kV, a capacitance of 25 µF and a resistance of 200 Ω. After electroporation, 1 ml of cold YEPD broth was added and the electroporated cells were transferred to a 2 ml Eppendorf tube. The volume was divided into two tubes (transformation 1 and 2) and cells were incubated for 4 hours at 30°C and 250 rpm, then they were centrifuged 5 min at 3000 g, and 800 µl of the supernatant were removed to concentrate the cell suspension. We plated 100 µl of each tube in YEPD+NT agar plates and were incubated at 37°C for 5 days.

3.7.11. Screening of transformants

Every colony of the transformation plates were transferred to YEPD+NT agar plates and were incubated at 37°C for 24-48h. If evident growth was achieved each transformant was analysed for vector integration at the *NEUT5L* locus by colony PCR as described in Section 3.7.7, with the exception that *C. albicans* lysates were obtained in NaOH 20 mM. Three pair of primers were designed to check the correct integration of plasmid pV1524 at *NEUT5L* (Figure 3.5 and Table 3.15). It has to be noted that if pV1524 were integrated homozygously into the genome, then the *NEUT5L* locus could not be amplified due to the long size of the resulting amplicon (around 11 kb).

Additionally, in order to detect if the transformants had acquired the desired mutation, or not in the case of the controls, allele-specific primers were designed for each mutation (Table 3.15). These primers were paired with those used for sequencing the corresponding gene fragment (Table 3.3).

Figure 3.5. Schematic view of the location of primers used for integration screening. Neut5LUp-Fw and Neut5LDown-Rv are located upstream and downstream, respectively, from the *NEUT5L* locus in Chr5, and they are paired with ENO1Up-Rv and Neut5L3'Up-Fw that are located inside the plasmid sequence. These two primer pairs will only give a PCR product when the plasmid is integrated into chromosome 5 of *C. albicans* SC5315. The other two primers, Neut5L-Fw and Neut5L-Rv, are directed to the 5' and 3' ends of the *NEUT5L* locus and will generate a PCR product when the plasmid is absent.

Table 3.15. Primers for screening of transformants.

Primer	Amplification target/Size (bp)	Sequence (5'-3')
INTEGRATION		
Neut5LUp-Fw	Locus 5' end/826	TTGTCTAATATACAGGATCTG
ENO1Up-Rv		GTCTATAGTGAAGATGATCA
Neut5L3'Up-Fw	Locus 3' end/979	TATCGAGTGTTTAAGGATAATG
Neut5LDown-Rv		ATCTATATTGTCAAGCCAAGAC
Neut5L-Fw	Whole locus/953(or 11779)*	ATGAAGAATGCTGAATCAC
Neut5L-Rv		CTTTAGCTTCTTCTACCGTATG
MUTATION		
Tac1-S758Fesp-Fw	Mutated allele	CCAATTTGAATCTATTGATTGAAACTT**T**
Tac1-S758WTesp-Fw	WT allele	CCAATTTGAATCTATTGATTGAAACTTC
Tac1-980-Rv2		Table 3.3
Erg11-Y477Cesp-Fw	Mutated allele	TGGGGAACAATTTGCTT**G**
Erg11-Y477WTesp-Fw	WT allele	GTATTGGGGAACAATTTGCTTA
Erg11-R4		Table 3.3
Mrr2-A311V-Fw		CAGATCGACGGACATTAC
Mrr2-A311Vesp-Rv	Mutated allele	GAACCTAAGCATGATTTCT**A**
Mrr2-A311WTesp-Rv	WT allele	GAACCTAAGCATGATTTCTG

The base specific for the introduced mutation is highlighted in red. *When the pV1524 is integrated into the *NEUT5L* locus the amplification product from the primer pair Neut5L-Fw and Neut5L-Rv would be around 11 kb so it would not be amplified by the Taq polymerase.

The cycling conditions for integration screening were:

Initial denaturation	95°C – 5 min	
Denaturating stage	95°C – 30 s	30 cycles
Annealing stage	49°C – 1 min	
Elongation stage	72°C – 1 min	
Final elongation	72°C – 5 min	

For amplification of the whole *NEUT5L* locus:

Initial denaturation	95°C – 5 min	
Denaturating stage	95°C – 30 s	30 cycles
Annealing stage	53°C – 30 s	
Elongation stage	72°C – 30 s	
Final elongation	72°C – 5 min	

For detection of WT allele in Tac1 transformants:

Initial denaturation	94°C – 5 min	
Denaturating stage	94°C – 30 s	30 cycles
Annealing stage	64°C – 30 s	
Elongation stage	72°C – 15 s	
Final elongation	72°C – 5 min	

For detection of WT allele in Erg11 transformants:

Initial denaturation	95°C – 5 min	
Denaturating stage	95°C – 30 s	25 cycles
Annealing stage	66°C – 30 s	
Elongation stage	72°C – 15 s	
Final elongation	72°C – 5 min	

For detection of mutated allele in Mrr2 transformants:

Initial denaturation	94°C – 5 min	
Denaturating stage	94°C – 30 s	30 cycles
Annealing stage	65°C – 30 s	
Elongation stage	72°C – 15 s	
Final elongation	72°C – 5 min	

Only integrative mutants were sequenced to confirm the mutation. The PCR conditions for sequencing were the same used in Section 3.5.3, but cell lysates were used instead of purified DNA as template. In this case, only the mutation-containing

region was amplified. Therefore, for amplification of *TAC1*, *ERG11* and *MRR2* the following pairs of primers were used, respectively:

- *TAC1*: Tac1-673-Fw3 and Tac1-980-Rv2

- *ERG11*: Erg11-F3 and Erg11-R4

- *MRR2*: Mrr2-2F and Mrr2-2R

The amplicon sequences were obtained from the Sequencing and Genotyping Service SGIker of the University of the Basque Country UPV/EHU.

3.7.12. Flip-out (FO)

To eliminate the CRISPR-Cas9 genes and the resistance marker, the Flp recombinase was induced. Induction conditions had to be adjusted for each mutant. Two types of media were used, YEP and YNB, supplemented either with 2% or 4% maltose. In addition, different times of incubation were sustained; usually cultures were maintained for 48 h at 30°C and 200 rpm in any of those media. When this strategy failed, ON cultures were set up in YEPD at 30°C and 200 rpm, and 50 µl of the ON cultures were transferred to 25 ml of YEPD and were incubated at 30°C and 200 rpm until they reached an $0D_{600}$ = 1.6-2. Then, 500 µl of the latter culture were transferred to 25 ml YEP with 2% maltose and incubated at 37°C and 200 rpm for 4 h.

After the induction phase, we plated 300 cells onto YEPD, YEPD+10NT and YEPD+NT agar plates that were incubated at 37°C between 24 and 48 hours. Only the small colonies grown in YEPD+10NT were analysed for FO (Figure 3.6). The selected colonies were streaked in YEPD and YEPD+NT agar plates and incubated at 37°C for 24 hours. The colonies that only grew in YEPD agar (Figure 3.7) were confirmed by colony PCR, as was done to verify integration of the plasmid into *Candida*'s genome, and sequencing (see Section 3.7.11).

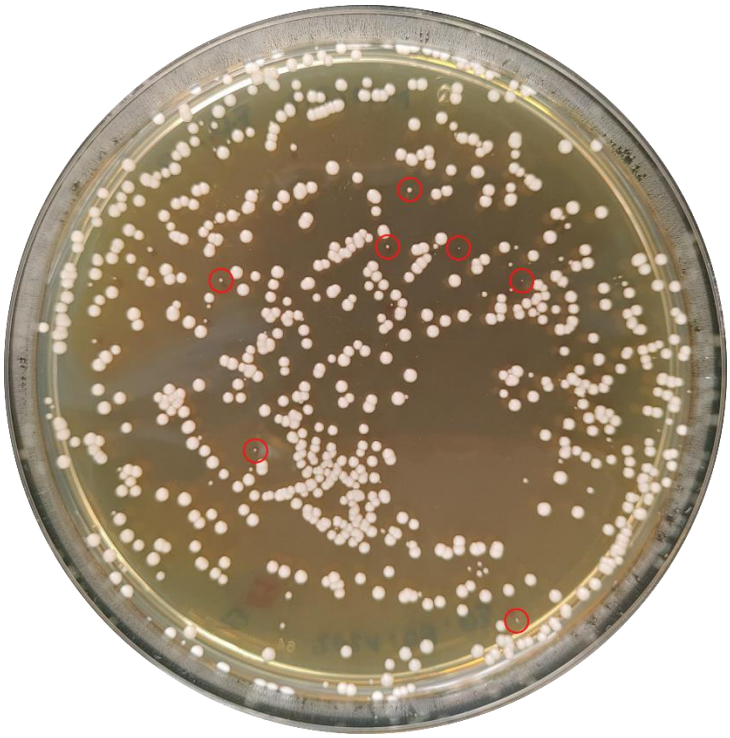

Figure 3.6. Colonies grown on YEPD+10NT agar plates after flip-out induction. Red circles mark small colonies that would be further analysed.

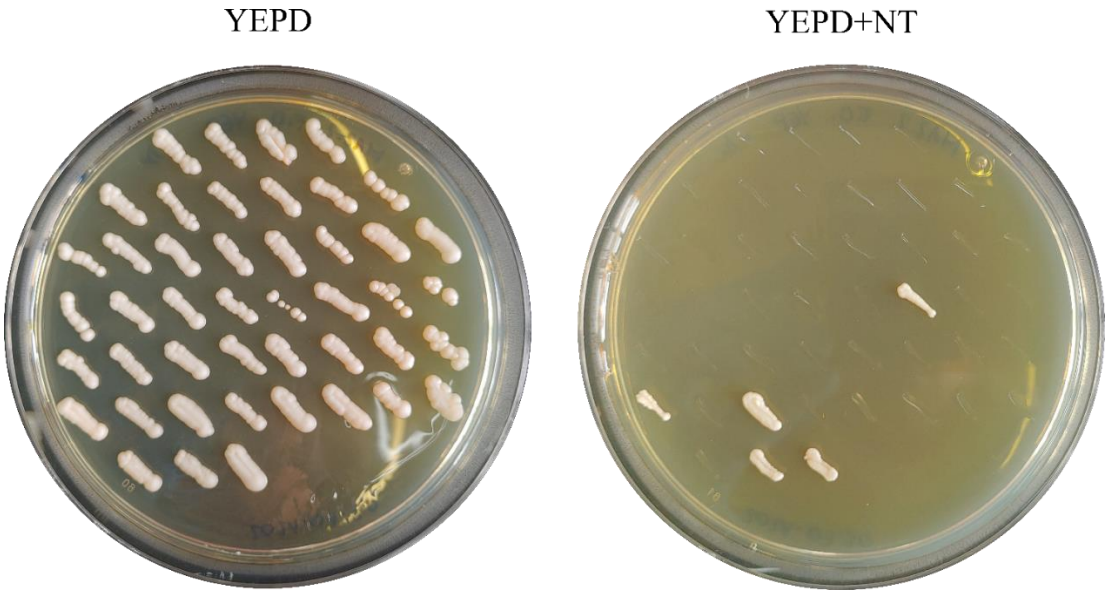

Figure 3.7. Small colonies obtained from YEPD+10NT agar plates (Fig. 3.6) streaked onto YEPD (left) and YEPD+NT (right) agar plates.

3.7.13. Phenotypic characterization of mutants

Two mutants from independent transformations were selected and their susceptibility phenotype was assessed by CLSI method and Spot Assay. Mutants of transcription factors Tac1 and Mrr2 were also assayed for *CDR1* and *CDR2* gene expression by RT-qPCR.

3.7.13.1. CLSI

Susceptibility to FLC was assessed by the CLSI method as explained in Section 3.4.1. Plates were incubated at 37°C or 25°C for 48h or up to 72h when little growth was seen after 24h of incubation.

3.7.13.2. Spot Assay

For Spot Assay, ON cultures in YNB at 30°C and 200 rpm were adjusted to OD_{600} = 1 and then five 5-fold serial dilutions were prepared. Five microliters of each dilution were spotted onto duplicate YNB and YNB+FLC agar plates. Plates were incubated at 25°C for 72h or at 37°C for 48 h.

3.7.13.3. Gene expression

Expression of the *CDR1* and *CDR2* genes for the Tac1 and Mrr2 mutants was measured by RT-qPCR as explained in section 3.6. In this case, in addition to *ACT1* and *PMA1*, five additional genes proposed by Nailis and collaborators (Nailis et al., 2006), namely *RPPB2* (cytosolic ribosomal acidic protein P2B), *LSC2* (succinyl-CoA synthetase β-subunit fragment), *CPA1* (carbamoyl-phosphate synthetase small subunit), *IMH3* (inosine-5'-monophosphate dehydrogenase fragment) and *RIP* (ubiquinol cytochrome-c reductase complex component) were evaluated as possible reference genes.

The primers for cDNA amplification of the new reference genes are in Table 3.16.

RNA extraction and cDNA synthesis were performed in triplicate for each sample, and they were carried out as explained in Sections 3.6.1 and 3.6.2.

The efficiency of RT-qPCR was estimated for each gene with a standard curve of one fifth serial dilutions of SC5314 cDNA (from 50 ng/µl to 0.016 ng/µl). Primer concentration was adjusted to obtain an efficiency between 0.8 and 1.1 and to avoid

the formation of primer dimers. The efficiency values were calculated as explained in Section 3.6.3.

Stability of the reference genes was assessed with the web-based RefFinder tool (https://www.heartcure.com.au/reffinder/), which allows analysing stability by geNorm (Vandesompele et al., 2002), NormFinder (Andersen et al., 2004) and BestKeeper (Pfaffl et al., 2004) calculations.

The RT-qPCR was carried out as explained in Section 3.6.5, using the primers as stated in Tables 3.5 and 3.16.

Each sample was tested in triplicate and non-template controls were included.

Data analysis was done as detailed in Section 3.6.6. In this case, an unpaired two-tailed t-test with Welch's correction was used to determine if differences in expression between mutants and control or parental strains were statistically significant ($p < 0.05$).

Table 3.16. Primers for gene expression analysis by RT-qPCR.

Primer	Sequence (5'-3')	Concentration (µM)*	Reference
RPP2B-Fw	TGCTTACTTATTGTTAGTTCAAGGTGGTA	0.1 (0.3)	Nailis et al., 2006
RPP2B -Rv	CAACACCAACGGATTCCAATAAA	0.1	
LSC2-Fw	CGTCAACATCTTTGGTGGTATTGT	0.3 (0.5)	
LSC2-Rv	TTGGTGGCAGCAATTAAACCT	0.1 (0.3)	
CPA1-Fw	TCTGGTGTTGCTGCCATAACTG	0.5	
CPA1-Rv	AATTCTCCCCAATGATGAACCTT	0.3 (0.5)	
IMH3-Fw	TATTCATATGGCATTATTGGGTGGTA	0.3 (0.5)	
IMH3-Rv	AACCATTTCTGCTTGTTCTTCAGA	0.1 (0.5)	
RIP-Fw	TGTCACGGTTCCCATTATGATATTT	0.3 (0.5)	
RIP-Rv	TGGAATTTCCAAGTTCAATGGA	0.1 (0.5)	

*The primer concentrations in brackets refer to the ones used in the gene expression analysis of the in vitro evolution experiment.

3.8. In vitro evolution of azole resistance

Candida albicans reference strain SC5314 and the clinical isolate BE-47, both susceptible to azoles (FLC MIC 0.25 µg/ml), were subjected to an in vitro evolution experiment with FLC to check for acquisition of resistance and development of GOF mutations. The yeasts were freshened up in Sabouraud agar at 37°C ON. Then, two flasks with 10 ml of RPMI 1640 medium, one of them supplemented with FLC 0.25 µg/ml, were inoculated each with one yeast colony and incubated at 37°C and 140 rpm for 24 hours. OD_{600} was measured and 10^6 cells were transferred into 10 ml of their corresponding fresh medium, with FLC 0.25 µg/ml (experimental populations) or without it (control populations), every day for three consecutive days (samples t1, t2 and t3). From that point on, experimental populations were transferred daily to fresh medium with FLC, whose concentration was doubled once they reached an $OD_{600} \geq 1$, up to FLC 64 µg/ml on day 15 (samples t4, t5…t15), and they were maintained in this medium with FLC 64 µg/ml until day 23 (samples t16-t23), with daily changes. Following the exposition to FLC, both SC5314 and BE-47 experimental populations were subcultured in RPMI medium without FLC for an additional 32-day period (until day 55; samples t24-t55) in order to evaluate if the acquired resistance was due to transient or permanent mechanisms. Parallel control samples were transferred daily into RPMI medium and incubated in the same conditions (Figure 3.8).

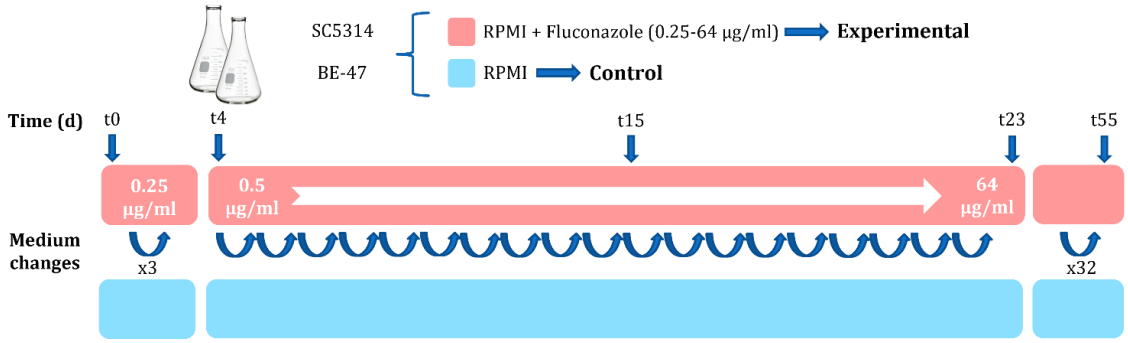

Figure 3.8. Schematic representation of the evolution experiment process.

Throughout the experiment, aliquots of every inoculum of experimental and control populations were mixed with an equal volume of glycerol 50% and stored at -80°C.

A summary of the experimental populations' samples and their corresponding FLC concentration is shown in Table 3.17.

Table 3.17. Summary of experimental populations' samples and their corresponding FLC concentration.

Experimental populations' samples	t0	t1-t3	t4	t5	t6	t7	t8-t9	t11	t13	t15-t23	t24-t55
FLC concentration (µg/ml)	0	0.25	0.5	1	2	4	8	16	32	64	0

3.8.1. Susceptibility testing of the experimental and control populations

The susceptibility against azole drugs of the SC5314 and BE-47 derived populations was assayed as described in Section 3.4 with modifications. Since we were working with the whole population, the inoculum was prepared from ON cultures at 37°C and 200 rpm in RPMI medium and adjusted to the cell density recommended by the CLSI and Sensititre YeastOne® methods.

3.8.2. Sequencing of *TAC1*, *ERG11*, *UPC2*, *MRR1* and *MRR2* genes

DNA was extracted from selected experimental and control populations of SC5314 and BE-47 strains (Section 3.5.2), and sequencing of the target regions of the *TAC1*, *ERG11*, *UPC2*, *MRR1* and *MRR2* genes (Section 3.5.3) was performed. The selected populations were SC5314_t0, t4, t7, t15, t23, t26 and t55 and BE-47_t0, t7 and t23.

3.8.3. RNA extraction and RT-qPCR

The expression level of *CDR1*, *CDR2, MDR1* and *ERG11* genes were measured in SC5314 and BE-47 strains and their derived populations. The *ACT1*, *PMA1*, *RPPB2, LSC2*, *CPA1*, *IMH3* and *RIP* were evaluated as possible reference genes. The primers for cDNA amplification of *ERG11* are listed in Table 3.18.

Table 3.18. Primers for gene expression analysis by RT-qPCR.

Primer	Sequence (5'-3')	Concentration (µM)	Reference
ERG11-Fw	AACTACTTTTGTTTATAATTTAAGATGGACTATTGA	0.5	Morio et al., 2012
ERG11-Rv	AATGATTTCTGCTGGTTCAGTAGGT	0.5	

RNA extraction and cDNA synthesis were performed twice for each sample, and they were carried out as explained in Sections 3.6.1 and 3.6.2.

The efficiency of RT-qPCR was estimated as explained in Section 3.7.13.3 and primer concentrations were adjusted. The efficiency values were calculated as explained in Section 3.6.3.

Stability of the reference genes was assessed as in Section 3.7.13.3.

The RT-qPCR was carried out as explained in Section 3.6.5, using the primers as stated in Tables 3.5, 3.16 and 3.18.

Each sample was tested in triplicate and non-template controls were included. Additionally, the SC5314_t0 population was used as IPC and was included in all PCR plates.

Data analysis was done as detailed in Section 3.6.6 and 3.7.13.3. In this case, expression between experimental and control populations was compared.

3.8.4. Zygosity of the *MTL* locus

Mating-type like (*MTL*) locus zygosity was determined in control and experimental populations of both *C. albicans* strains, as well as in 10 random colonies from each population, as described by Rustad and collaborators (Rustad et al., 2002).

3.8.5. Fitness determination

Fitness of the populations obtained at the different time points of the assay were estimated from their doubling time (g). Briefly, frozen yeast stocks of each population were grown ON in RPMI at 37°C and 30°C, and 200 rpm. OD_{600} was adjusted to 0.2 with fresh medium and five wells of two 100-well plates (Bioscreen) were loaded with 200 µl of the adjusted suspensions of each population. Five control wells contained only RPMI. Each plate was incubated at 37°C or 30°C for 24 h in Labsystems Bioscreen C, and OD (420-580 nm) was registered every 30 minutes, after 10 seconds of low intensity shaking.

The doubling time (g) was calculated for each population ($g = \ln 2/\mu$, where µ stands for the linear regression slope of the exponential phase of the corresponding growing curve, built with natural logarithm of OD data). Then, fitness was estimated as the ratio (quotient) between g values of the initial populations (SC5314_t0 and

BE47_t0) and their correspondent control or experimental populations. Statistical differences between control and exposed populations were analysed with the one-way ANOVA with Tukey's test for multiple comparisons (GraphPad Prism 8). Values of $p < 0.05$ were considered statistically significant.

3.8.6. Tolerance to fluconazole

Tolerance to fluconazole of control and experimental populations was estimated as explained by Rosenberg and collaborators (Rosenberg et al., 2018). Population samples stored at -80°C were cultured in 10 ml of RPMI medium at 30°C and 200 rpm for 16 to 48h (until cultures reached and $OD_{600} \geq 1$). Cultures were adjusted at an $OD_{600} = 0.25$ in RPMI medium, and then diluted 1/1000 to prepare an inoculum similar to the one established by CLSI. Flat bottom 96-well plates containing serial dilutions of fluconazole from 64 µg/ml to 0.125 µg/ml according to the CLSI protocol were inoculated with 100 µl of the diluted inoculum and incubated at 25 or 37°C for 48-72h. After mixing each well by pipetting, OD was measured every 24h with a BIO-TEK® ELx808 plate reader at 450 nm.

MIC was determined after 24h of incubation and tolerance after 48h. If the control well OD was below 0.1 after 24h, then the plate was incubated for 72h, and the MIC was determined after 48h and tolerance after 72h. MIC was calculated as the concentration of fluconazole at which the OD was equal or less than the 50% of the control well.

Tolerance was estimated as established by Rosenberg and collaborators (Rosenberg et al., 2018), with a parameter named supra-MIC growth (SMG) that was calculated as the mean OD of all the wells above the MIC relative to the control well after 48h

$$SMG = \frac{Mean\ OD\ in\ wells\ above\ the\ MIC}{OD\ control\ well}.$$

3.8.7. Spot Assay

Similar to the tolerance assay, population samples stored at -80°C were cultured in 10 ml of YNB+glucose 2% at 30°C and 200 rpm for 16 to 48h. Cultures were then adjusted at an $OD_{600} = 0.25$ and diluted 1/1000. Five microliters of the diluted inoculum were plated onto YNB+FLC (from 0 to 64 µg/ml) and plates were incubated at 25 or 37°C for 72h. Pictures of the plates were taken every 24h.

RESULTS

4. RESULTS

4.1. Susceptibility to azoles of the *Candida albicans* strains

We measured the susceptibility against azole drugs of 43 clinical isolates and 3 reference strains following the CLSI M27-A3 and Sensititre YeastOne® Y010 methods. The strains were classified as resistant, susceptible dose-dependent (SDD) or susceptible according to the cut-offs established by CLSI M27-S4 for all azoles except clotrimazole (CLT). According to Pelletier and collaborators (Pelletier et al., 2000) isolates were considered resistant to CLT when their MICs were > 0.5 mg/l. Susceptibility results are summarized in Table 4.1.

All the strains that showed either fluconazole (FLC) or CLT resistance with CLSI's method were also assayed with Sensititre, together with the two azole-susceptible strains that were used for the evolution experiment (Section 3.8), SC5314 and BE-47, and two isolates that showed inconsistent results in CLSI, 06-100 and 10-171. In total, 21 out of the 46 strains (46%) showed reduced susceptibility to one or more azoles, of which five only exhibited FLC resistance (BE-114, 06-114, 10-168, 10-221 and 16-134) while 6 showed reduced susceptibility against all classes (ATCC 64124, ATCC 64550, 15-154, 15-176, 16-092 and 16-138). The rest of the isolates were either SDD or resistant to two, three or four azole types. Six isolates had reduced azole susceptibility against two azole types; three of them were resistant to FLC and CLT (10-170, 15-156 and 15-157); one was resistant to FLC and posaconazole (POS) (15-159); another was resistant to FLC and SDD to voriconazole (VOR) (16-091) and the last one was resistant to FLC and SDD to itraconazole (ITC) (16-135). Three isolates were less susceptible to three azole classes; one was SDD to FLC, ITC and VOR (16-122); another was resistant to FLC and VOR, and SDD to ITC (16-123); and the other one was resistant to FLC, ITC and POS (16-132). Only the BE-113 isolate was found to have reduced susceptibility to four azoles, it was classified as SDD to FLC and VOR, and resistant to ITC and POS.

The Sensititre YeastOne® Y010 method also measures the activity of the echinocandin group (caspofungin, micafungin and anidulafungin), 5-fluorocytosin and amphotericin B. None of the isolates showed reduced susceptibility to any of these antifungal compounds.

Table 4.1. MIC values of azole drugs at 24h measured either by CLSI or Sensititre YeastOne® methods of *C. albicans* clinical isolates of the UPV/EHU collection and three reference strains.

Strain[a]	CLSI (MIC)[b]		Sensititre YeastOne® (MIC)			
	FLC	CLT	FLC	ITC	POS	VOR
BE-47	0.12	0.03	0.5	0.03	0.015	0.008
BE-AZ	0.12	0.03	-	-	-	-
BE-32	0.12-0.25	0.03	-	-	-	-
BE-48	0.12-0.25	0.03	-	-	-	-
09-297	0.12-0.25	0.03	-	-	-	-
10-166	0.12	0.03	-	-	-	-
10-294	0.12-1	0.03-0.06	-	-	-	-
15-158	0.12	0.03	-	-	-	-
15-178	0.12	0.03	-	-	-	-
SC5314	0.12	0.03	0.12-0.25	0.03-0.06	0.008	0.008-0.03
BE-90	0.12	0.12	-	-	-	-
06-116	0.25-0.5	0.03-0.06	-	-	-	-
10-169	0.12-0.25	0.03-0.06	-	-	-	-
10-295	0.12-0.25	0.03	-	-	-	-
15-153	2	0.03	-	-	-	-
15-155	0.12-0.25	0.03-0.06	-	-	-	-
15-161	0.12-0.25	0.03-0.06	-	-	-	-
15-179	0.12-0.25	0.03	-	-	-	-
10-171	0.12-0.5	0.03-0.12	0.12	0.03	0.015	0.008
10-280	0.12-0.5	0.03-0.12	-	-	-	-
08-187	0.25-0.5	0.03-0.06	-	-	-	-
08-105	0.25-0.5	0.03-0.06	-	-	-	-
15-160	0.25	0.03-0.06	-	-	-	-
06-100	0.12-0.5	0.03-0.06	0.5	0.03	0.03	0.008
16-133	0.5	0.12	-	-	-	-
16-135 (48h)[c]	1 (**64**)	(0.12)	0.5 (2)	**0.5** (**16**)	0.03 (**8**)	0.015 (0.03)
16-132 (48h)[c]	0.5 (**64**)	0.12 (0.25)	0.5 (**256**)	0.06 (**16**)	0.015 (**8**)	0.015 (0.06)
15-159	2	0.03	2	**16**	**8**	0.06
16-122	2-**4**	0.03	**8**	**0.25**	0.06	**0.5**
16-123	**8**	0.03	**4**	0.12	0.03	**0.5**
10-168	2-**64**	0.25	0.25	0.03	0.015	0.008
06-114	2-**64**	0.12-**2**	0.25	0.03	0.015	0.008
BE-114	**4**-**64**	0.25-**1**	2	0.06	0.03	0.03
10-221	**64**	0.25	0.25	0.03	0.015	0.008
16-134	**64**	0.25	0.5	0.03	0.015	0.008
15-156	**64**	0.25-**2**	0.5	0.06	0.03	0.008
15-157	**64**	**2**	0.5	0.03	0.015	0.008
10-170	**64**	**1-2**	0.12	0.03	0.008	0.008
BE-113	2-**4**	0.25-**0.5**	**8**	**16**	**8**	**1**
16-091	**64**	0.03	**8**	0.12	0.03	**0.5**
ATCC 64550	**16**	**2**	**32**	**0.25**	**0.5**	**0.5**
15-154	**32-64**	**0.5**	**32**	**16**	**8**	**0.5**
15-176	**16-64**	**2-4**	**64**	**0.5**	**0.5**	**1**
ATCC 64124	-	-	**256**	**16**	**1**	**8**
16-092	**64**	**0.5**	**256**	**16**	**8**	**8**
16-138	**64**	**1**	**256**	**16**	**8**	**8**

[a] Reference strains are indicated in purple. [b] More than one MIC value reflects the range of values obtained in different experiments. [c] Measurement after 48h in brackets.
MIC values above the resistance cut-off are shown in bold red and those in the SDD range are highlighted in bold black.

4.2. Expression level of *CDR1*, *CDR2* and *MDR1* genes of azole resistant clinical isolates

The Mrr1 and Mrr2 transcription factors regulate, respectively, *MDR1* and *CDR1* gene expression (Morschhäuser et al., 2007; Schillig & Morschhäuser, 2013) and gain-of-function (GOF) mutations have been described for both genes (Dunkel et al., 2008; Eddouzi et al., 2013; Feng et al., 2019; Lohberger et al., 2014; Morschhäuser et al., 2007; Schubert et al., 2011; Wang et al., 2015). Therefore, we decided to analyse the expression of *CDR1* and *MDR1* genes in our collection of *C. albicans* strains. *CDR2* was also included to see if Tac1 GOF mutations were associated to overexpression of *CDR1* or *CDR2* alone, or both.

4.2.1. RT-qPCR efficiency

The efficiency of the RT-qPCR reaction for each of the genes is shown in Table 4.2. We were unable to determine the efficiency for *CDR2* gene due to its low expression level.

Table 4.2. Efficiency values of the amplification reaction for each gene.

Gene	Gene name	Efficiency
CDR1	Candida Drug Resistance 1 – ABC efflux pump	0.96
CDR2	Candida Drug Resistance 2 – ABC efflux pump	-
MDR1	Multidrug Resistance 1 – Major Facilitator pump	0.92
ACT1	Actin	1
PMA1	Plasma membrane H^+-ATPase	0.96

4.2.2. Reference genes' stability

The M stability value calculated by GeNorm was 0.051 for the two genes (*ACT1* and *PMA1*).

4.2.3. Fold-change in gene expression

Expression level of *CDR1*, *CDR2* and *MDR1* genes was measured by RT-qPCR in the clinical isolates classified as resistant in this study in order to identify which ones could harbour GOF mutations in Mrr1 and Mrr2 transcription factors. Their mRNA

transcript level was compared to that displayed by four susceptible isolates of the same collection (SC5314, BE-47, BE-90 and 15-161). Each gene was considered to be overexpressed when it showed at least a two-fold increase in its mRNA transcript levels (Torelli et al., 2008).

Ten out of the 19 tested isolates overexpressed the *CDR1* gene (Figure 4.1). The resistant reference strains ATCC 64550 and 64124 showed the greatest overexpression (x16.32 and x16.79, respectively), while the rest of the overexpressing isolates ranged between x2.09 and x6.01.

The *CDR2* gene was overexpressed in 5 isolates and displayed the highest increment in expression level among the three genes studied (Figure 4.1). The highest increase was shown by ATCC 64124 (x272.24) followed in descending order by 15-176 (x148.09), ATCC 64550 (x74.93), BE-113 (x3.25) and 16-132 (x2.41).

The *MDR1* gene was overexpressed in isolates 06-114, 15-176, 16-132 and ATCC 64550 with a fold-change of x5.97, x117.12, x3.86 and x14.11, respectively (Figure 4.1). Except for 06-114, the other isolates were also overexpressing the other two efflux pumps.

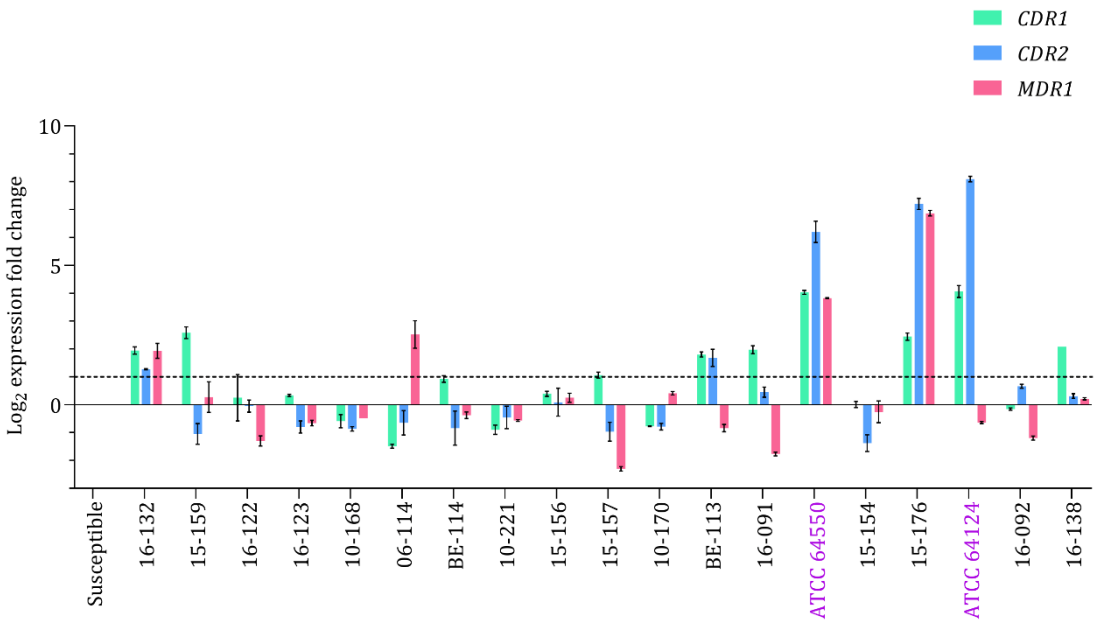

Figure 4.1. *CDR1*, *CDR2* and *MDR1* mRNA expression level in azole resistant clinical isolates measured by RT-qPCR relative to a group of four susceptible isolates. Error bars indicate standard deviations (SD) of three technical replicates. The dotted line indicates a two-fold increase of expression. Reference strains are indicated in purple.

In light of these results, *MRR1* gene was sequenced for the *MDR1* overexpressing strains (06-114, 15-176, 16-132 and ATCC 64550), together with the two azole resistant vulvovaginal isolates (BE-113 and BE-114), while the *MRR2* gene was sequenced for all the *CDR1* overexpressing strains and six randomly chosen susceptible isolates.

4.3. Characterization of *ERG11*, *TAC1*, *UPC2*, *MRR1* and *MRR2* genes

To investigate the molecular mechanisms behind azole resistance in our resistant isolates we amplified and sequenced some target regions of Erg11, Tac1, Upc2, Mrr1 and Mrr2 encoding genes of the *C. albicans* collection under study (Table 3.3).

4.3.1. Erg11 amino acid substitutions

For Erg11, 27 distinct non-synonymous mutations were identified among susceptible and resistant isolates (Table 4.3). Six of them were previously described as GOF mutations (A114S, Y132H, K143R, Y257H, G450E, and R467K) and 11 were new substitutions (R47K, W57L, R76C, A149D, F217L, D225N, P236H, F319L, V402F, Y477C and Q479E). Most of them appeared in susceptible isolates, however, W57L and F217L were only present in one resistant strain (16-122) in heterozygosis, and the amino acid substitution Y477C was found in strain 16-134 in homozygosis. Eight out of the 46 strains studied did not harbour any mutations, the rest of them contained from one to four non-synonymous amino acid substitutions. Only seven out of the 21 azole resistant isolates harboured GOF mutations in Erg11. Besides the non-synonymous mutations, we also identified 23 different single nucleotide polymorphisms (SNPs) that did not lead to changes in the amino acid sequence (Supplementary material Table I). In combination, most of the strains exhibited between 8 and 16 polymorphisms, of which the majority were synonymous.

Table 4.3. Amino acid substitutions found in Erg11 of azole-susceptible and resistant isolates of the UPV/EHU collection.

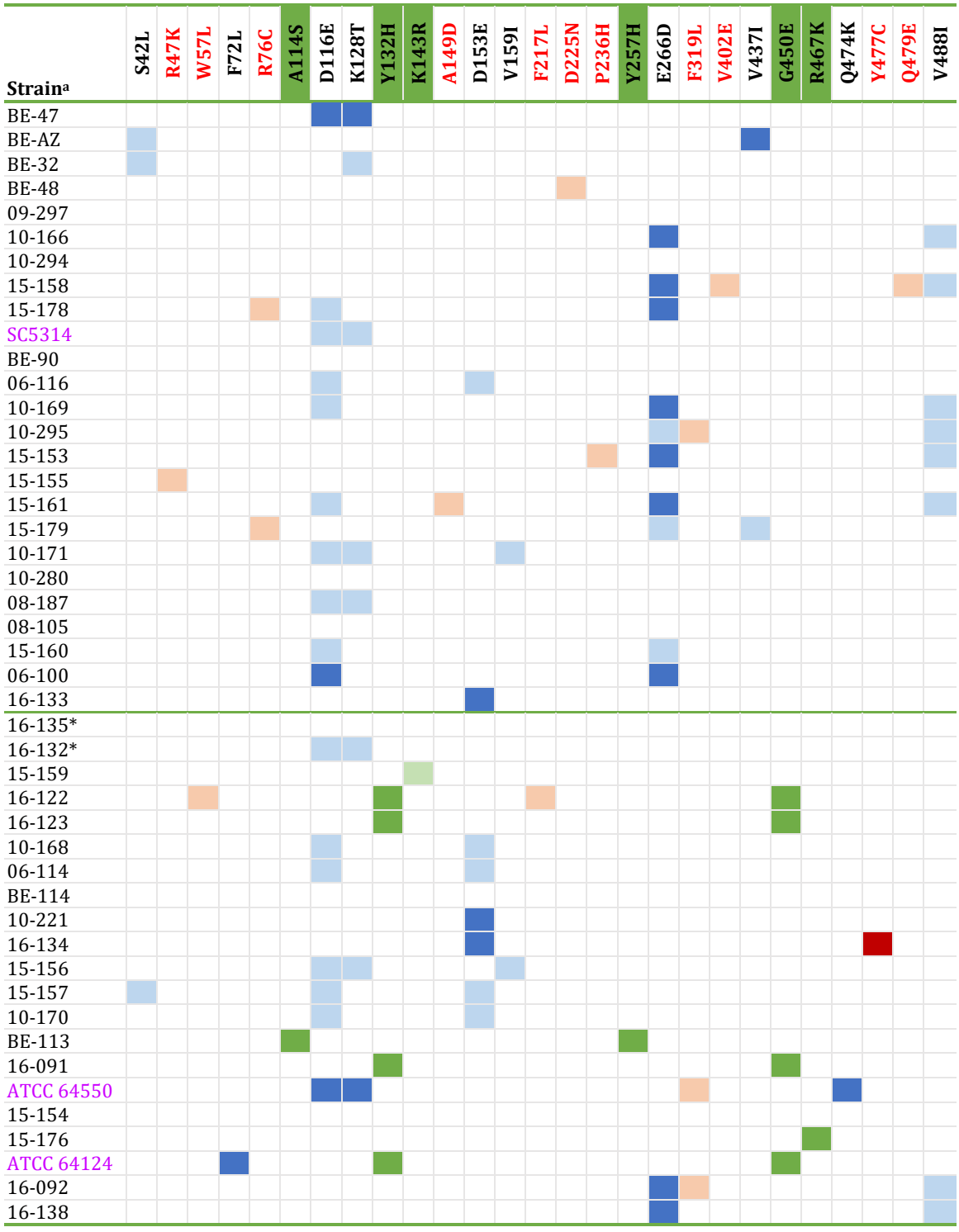

Blue: previously described mutations; green: previously described mutations associated to resistance; red: new mutations found in this work; light colour: mutations in heterozygosis; dark colour: mutations in homozygosis. [a] Reference strains are highlighted in purple.

4.3.2. Tac1 amino acid substitutions

For Tac1, we identified 27 non-synonymous mutations, of which 14 were described as not associated to resistance (R206H, V207A, A377V, N396S, N772K, D776N, N823K, E829Q, C858Y, R869Q, I895T, N896S, S935L and S941P), four as GOF (A736V, H839Y, ΔL962-N969 and N977D) and 9 are introduced for the first time in this study (G245A, E265K, E319K, R341G, Q404P, E423D, Y449H, S758F and N881S) (Table 4.4). All new mutations found were harboured by susceptible isolates, except for S758F, which was only present in homozygosis in the BE-113 resistant strain. All isolates studied contained from one to ten mutations. Only two of the resistant strains harboured previously described GOF mutations in Tac1 (15-176 and ATCC 64124), each presenting two GOF mutations in heterozygosis. In addition to the non-synonymous mutations, we also identified 41 synonymous SNPs, with most of strains presenting a high number of polymorphisms of both types, many harbouring between 17 and 22 SNPs (Supplementary material Table II).

Table 4.4. Amino acid substitutions found in Tac1 of azole susceptible and resistant isolates of the UPV/EHU collection.

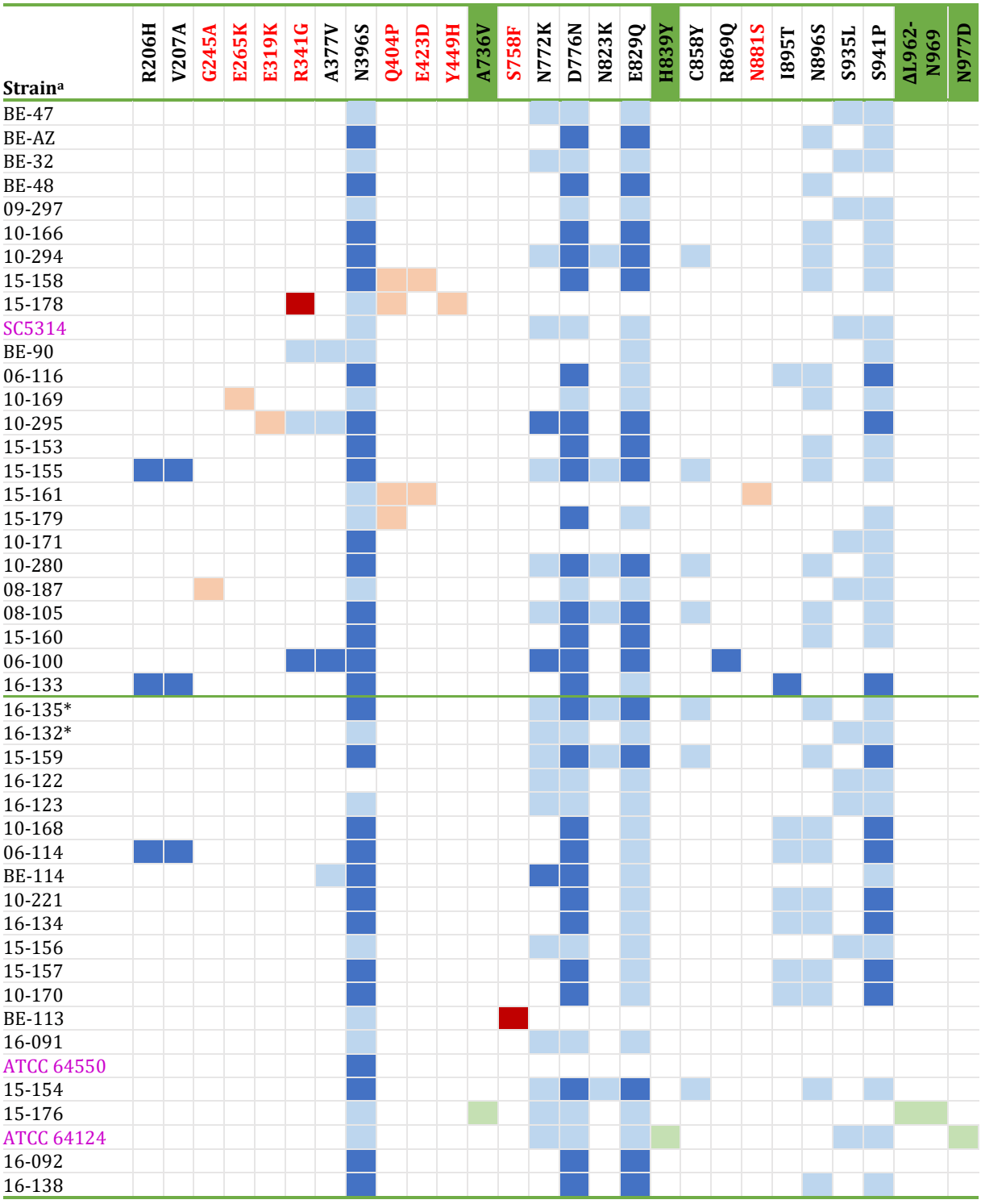

Blue: previously described mutations; green: previously described mutations associated to resistance; red: new mutations found in this work; light colour: mutations in heterozygosis; dark colour: mutations in homozygosis. [a] Reference strains are highlighted in purple.

4.3.3. Upc2 amino acid substitutions

For Upc2, we only found two GOF mutations both in heterozygosis, A643V in isolate 15-176 and G648S in isolates 16-091, 16-122 and 16-123 (Table 4.5). These substitutions were previously described in association to azole resistance. In this case, no synonymous mutations were identified in the sequenced region of *UPC2* (Supplementary material Table III).

4.3.4. Mrr1 amino acid substitutions

We sequenced the target regions of *MRR1* gene of the isolates that overexpressed *MDR1* (06-114, 15-176, 16-132 and ATCC 64450), and the BE-113 and BE-114 vulvovaginal resistant isolates. Additionally, despite not being able to measure the expression of the efflux pumps in the 16-134 and 16-135 resistant isolates, we also sequenced the *MRR1* gene of these isolates. We identified four amino acid substitutions already described in the literature, and one of them, G947S, has been associated to azole resistance (Table 4.5). This mutation was harboured in homozygosis by isolate 15-176. For *MRR1* we found many synonymous mutations that were common among the sequenced isolates (Supplementary material Table IV).

Table 4.5. Amino acid substitutions found in Upc2 and Mrr1 of azole susceptible and resistant isolates of the UPV/EHU collection.

	Upc2		Mrr1			
Strain[a]	**A643V**	**G648S**	V341E	L592F	**G947S**	E1020Q
BE-47						
BE-AZ						
BE-32						
BE-48						
09-297						
10-166						
10-294						
15-158						
15-178						
SC5314						
BE-90						
06-116						
10-169						
10-295						
15-153						
15-155						
15-161						
15-179						
10-171						
10-280						
08-187						
08-105						
15-160						
06-100						
16-133						
16-135*						
16-132*						
15-159						
16-122						
16-123						
10-168						
06-114						
BE-114						
10-221						
16-134						
15-156						
15-157						
10-170						
BE-113						
16-091						
ATCC 64550						
15-154						
15-176						
ATCC 64124						
16-092						
16-138						

Blue: previously described mutations; green: previously described mutations associated to resistance; red: new mutations found in this work; light colour: mutations in heterozygosis; dark colour: mutations in homozygosis; grey: not sequenced. [a] Reference strains are higlighted in purple.

4.3.5. Mrr2 amino acid substitutions

We sequenced the *MRR2* gene of the isolates that overexpressed *CDR1* (BE-113, BE-114, 15-157, 15-159, 15-176, 16-091, 16-132, 16-138, ATCC 64450 and ATCC 64124) as well as of six susceptible isolates (BE-AZ, BE-47, 06-116, 08-105, 15-153 and 15-158). As for *MRR1*, the *MRR2* gene of resistant isolates 16-134 and 16-135 were also sequenced. Three out of the 11 amino acid substitutions identified are described for the first time in this study (A311V, D442E and A627V) (Table 4.6). D442E and A627V were found in resistant and susceptible strains so they are unlikely to be involved in resistance. On the contrary, A311V was found in homozygosis only in the BE-114 resistant isolate. In addition, in *MRR2* we also found many synonymous mutations in the selected strains (Supplementary material Table V).

Table 4.6. Amino acid substitutions found in Mrr2 of azole susceptible and resistant isolates of the UPV/EHU collection.

Strain[a]	S143P	L144V	T145A	S165N	A311V	D442E	V451A	A459T	S480P	V582L	A627V
BE-47											
BE-AZ											
BE-32											
BE-48											
09-297											
10-166											
10-294											
15-158											
15-178											
SC5314											
BE-90											
06-116											
10-169											
10-295											
15-153											
15-155											
15-161											
15-179											
10-171											
10-280											
08-187											
08-105											
15-160											
06-100											
16-133											
16-135*											
16-132*											
15-159											
16-122											
16-123											
10-168											
06-114											
BE-114											
10-221											
16-134											
15-156											
15-157											
10-170											
BE-113											
16-091											
ATCC 64550											
15-154											
15-176											
ATCC 64124											
16-092											
16-138											

Blue: previously described mutations; green: previously described mutations associated to resistance; red: new mutations found in this work; light colour: mutations in heterozygosis; dark colour: mutations in homozygosis; grey: not sequenced. [a] Reference strains are highlighted in purple.

4.4. Analysis of the role in azole resistance of the new mutations identified

The sequencing of *ERG11*, *TAC1*, *UPC2*, *MRR1* and *MRR2* genes revealed 18 amino acid substitutions that are first described in this study. Among these, three were only found in resistant isolates, while the others were harboured either by just susceptible isolates or by both susceptible and resistant strains.

The three mutations found only among resistant isolates were Erg11 Y477C in 16-134, Tac1 S758F in BE-113, and Mrr2 A311V in BE-114. All three were considered promising candidates for playing a role in azole resistance. In the first case, the 16-134 isolate exhibited FLC-resistance but did not harbour any of the described GOF mutations in the gene fragments studied in this work. Secondly, the BE-113 isolate had reduced susceptibility to azoles, which could be due to the two resistance-associated mutations found in Erg11. Nonetheless, this strain also exhibited overexpression of *CDR1* and *CDR2* genes but did not show any GOF mutations in either the *TAC1* or the *MRR2* sequenced fragments that could account for their higher expression levels. Lastly, the BE-114 isolate was also FLC-resistant and showed overexpression of *CDR1*, but we could not find any GOF mutations that could explain its phenotype. Therefore, we tried to characterize the three new mutations found in resistant strains by introducing them into *C. albicans* SC5314 reference isolate by CRISPR-Cas9 methodology and analysing the resistant phenotype of the mutants and their corresponding control.

4.4.1. Design of gRNAs to direct Cas9 to *TAC1*, *ERG11* and *MRR2* genes

Among all the possible guide-RNAs (gRNAs), the closest to each mutation site were first examined (Table 4.7). Five gRNAs were studied for *TAC1*, four for *ERG11* and seven for *MRR2*. The guides used to carry out the gene editing were selected based on their distance to the mutation, the hairpin formation, and the recognition of off-target sites.

BLAST searches of the selected gRNAs allowed us to check the specificity of each of them. These alignment hits could be classified into three types: 1) homology between the off-target site and the first 12 (or more) nucleotides (nt) of the gRNA, which are essential for target recognition and cleaving (DiCarlo et al., 2013; Jiang et

al., 2013; Jinek et al., 2012); 2) homology between the off-target site and less than the first 12 nt of the gRNA; and 3) no homology between the off-target site and the first nt of the gRNA (Figure 4.2). Only the first one, if encountered adjacent to a PAM site, could represent a greater possibility of unspecific cutting.

For the simplicity of design, guides located on the sense strand were favoured against those on the complementary strand. Therefore, Tac1-758-g2 gRNA was chosen for editing the *TAC1* gene, Erg11-477-g4 for *ERG11* and Mrr2-311-g1 for *MRR2* (underlined guides in Table 4.7).

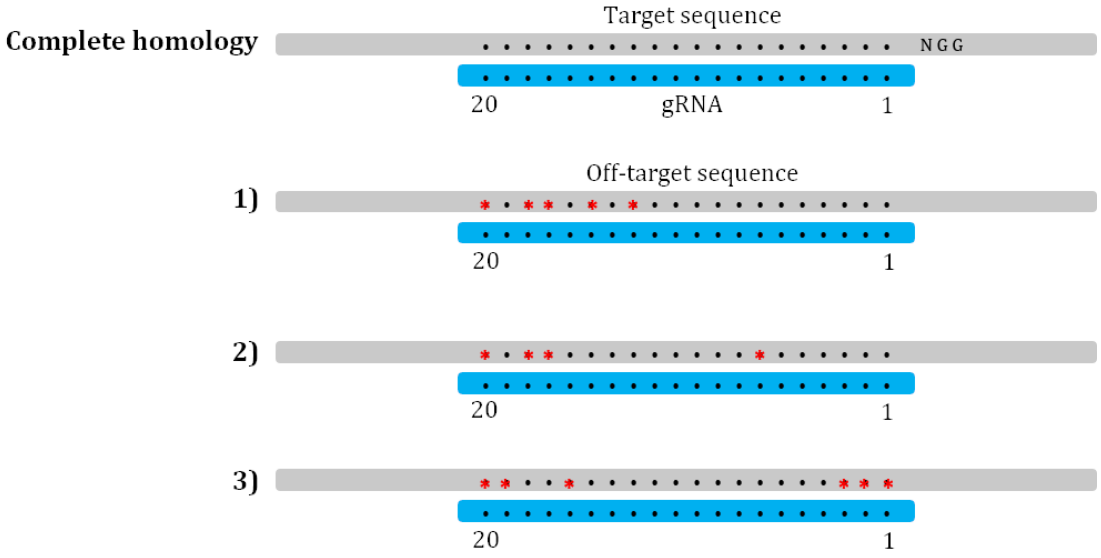

Figure 4.2. Schematic representation of the complete homology between the gRNA (blue bar), and the target sequence of *C. albicans* SC5314 which is adjacent to the PAM site NGG, and three categories of partial alignments, as described in the text. Red asterisks indicate no nucleotide homology between the gRNA and *Candida*'s sequence. NGG, PAM site.

Table 4.7. gRNAs designed for CRISPR-Cas9 editing of *C. albicans*.

gRNA	Target gene	Sequence (5'-3')	Distance to mutation	Probable off-targets	Hairpin
Tac1-758-g1	*TAC1*	CATCCTCAATTACCAGAGTC	32 nt (upstream)	2	ΔG=-0.23 Kcal/mole Tm = 27.5°C
Tac1-758-g2		TTTTTAAAAGTAGTAAACAA	28 nt (downstream)	7	ΔG=-0.28 Kcal/mole Tm = 29.1°C
Tac1-758-g3[a]		TTCAATCAATAGATTCAAAT	24 nt (upstream)	10	ΔG=-0.76 Kcal/mole Tm = 35.1°C
Tac1-758-g4[a]		TTCAAATTGGTTCCTGACTC	37 nt (upstream)	0	ΔG=0.01 Kcal/mole Tm = 24.9°C
Tac1-758-g5[a]		TAATCTAACAATCAATTCAA	98 nt (downstream)	41	ΔG=1.17 Kcal/mole Tm = 10.3°C
Erg11-477-g1	*ERG11*	TGGTAGACATAGATGTATTG	15 nt (upstream)	8	ΔG=-1.02 Kcal/mole Tm = 39.8°C
Erg11-477-g2		GTGGTAGACATAGATGTATT	16 nt (upstream)	1	ΔG=-1.02 Kcal/mole Tm = 39.8°C
Erg11-477-g3[b]		TCTTCACCTTATTTACCATT	38 nt (upstream)	12	ΔG=1.38 Kcal/mole Tm = -9.9°C
Erg11-477-g4		CAATTTGCTTATGTTCAATT	9 nt (downstream)	7	ΔG=1.07 Kcal/mole Tm = -1.7°C
Mrr2-311-g1	*MRR2*	CCACTCGCTCACTGCCCTCC	Adjacent (upstream)	1	ΔG=-0.65 Kcal/mole Tm = 34.4°C
Mrr2-311-g2		TCCAGGCAGAAATCATGCTT	13 nt (downstream)	1	ΔG=-1.21 Kcal/mole Tm = 37.5°C
Mrr2-311-g3		GCTTAGGTTCTATAAAATCG	27 nt (downstream)	1	ΔG=1 Kcal/mole Tm = 0.9°C
Mrr2-311-g4[a]		ACCTAAGCATGATTTCTGCC	2 nt (upstream)	2	ΔG=-0.63 Kcal/mole Tm = 32°C
Mrr2-311-g5[a]		TAAGCATGATTTCTGCCTGG	5 nt (upstream)	1	ΔG=-0.63 Kcal/mole Tm = 32°C
Mrr2-311-g6[a]		CCTGGAGGGCAGTGAGCGAG	20 nt (upstream)	0	ΔG=-1.44 Kcal/mole Tm = 39.8°C
Mrr2-311-g7[a]		TTGCTCTGGGTGTACAGTTC	37 nt (downstream)	0	ΔG=-0.76 Kcal/mole Tm = 33.1°C

[a]gRNA sequence is located in the complementary sequence
[b]gRNA sequence is adjacent to 3 consecutive PAMs
The selected gRNAs for CRISPR-Cas9 editing are underlined

4.4.2. Design of RTe's to introduce the putative GOF mutations in *TAC1*, *ERG11* and *MRR2*

The mutated and WT repair templates (RTe's) designed to introduce the newly described mutations are presented in Table 4.8.

Table 4.8. Repair templates designed for CRISPR-Cas9 editing in *C. albicans*.

Repair template	Associated gRNA	Sequence (5'-3')
Tac1-758-RT2	Tac1-758-g2	TTGAATCTATTGATTGAAACTTTTTTAAGTTTTTTTAAAAG TAGTAAGCAGTGGAATAGTTCTAATGACAGTCAAGACAAAC AACAAAATAGTACAATAT
Tac1-WT-RT2		TTGAATCTATTGATTGAAACTTCTTTAAGTTTTTTTAAAAG TAGTAAGCAGTGGAATAGTTCTAATGACAGTCAAGACAAAC AACAAAATAGTACAATAT
Erg11-477-RT4	Erg11-477-g4	TTTGGTGGTGGTAGACATAGA TGTATTGGGGAACAATTTGCTTGTGTCCAGTTAGGAACCAT TTTAACTACTTTTGTTTATAATTTAAGATGGACTATTG
Erg11-WT-RT4		TTTGGTGGTGGTAGACATAGATGTATTGGGGAACAATTTGC TTATGTCCAGTTAGGAACCATTTTAACTACTTTTGTTTATA ATTTAAGATGGACTATTG
Mrr2-311-RT1	Mrr2-311-g1	AACCATCATGAAAGAGTTTGACATTACCAAAACCCACTCGC TCACTGCTCTTCAGGTAGAAATCATGCTTAGGTTCTATAAA ATCGTGGCACCAGAACTG
Mrr2-WT-RT1		AACCATCATGAAAGAGTTTGACATTACCAAAACCCACTCGC TCACTGCTCTTCAGGCAGAAATCATGCTTAGGTTCTATAAA ATCGTGGCACCAGAACTG

Bold red, mutated base; yellow shade, coding triplet for the amino acid change; bold pink, silent mutations; green, PAM.

4.4.3. Transformation with CRISPR-Cas9 system

To analyse each mutation we performed two transformations, one to introduce the desired mutation and another one that would leave the SC5314 strain as WT but that had gone through the whole editing process (Figure 4.3). In addition, electroporated cells were divided into two tubes in order to obtain two replicates of the transformation (Transformation 1 and 2; T1 and T2).

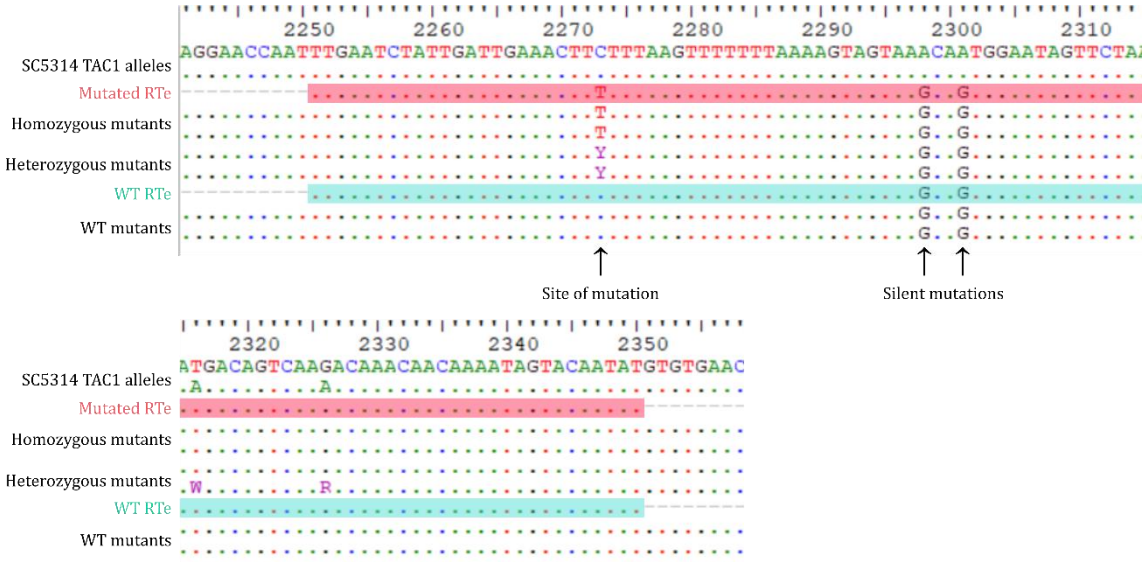

Figure 4.3. Alignment of SC5314 *TAC1* alleles, repair templates and mutated *TAC1* gene fragments from six transformants. The mutated RTe for Tac1 is highlighted in red while the WT RTe is in blue.

4.4.3.1. Transformants for Tac1 S758F (Tac1-758-RTe2 and Tac1-WT-RTe2)

To obtain Tac1 mutants we had to do four transformations with the mutated RTe, from which we obtained 82 transformants (44 from T1 and 38 from T2) and three transformations with the WT RTe obtaining 10 transformants (3 from T1 and 7 from T2). The difference in the transformation yield between the two RTe's is due to the extra transformation performed with the mutated RTe that achieved a much better efficiency. Each transformant was labelled with the letter D (for Double transformation, since they were transformed simultaneously with the digested pV1524 plasmid and the RTe) followed by a number according to the order they were picked.

Each transformant was checked for integration into the *NEUT5L* locus and acquisition of the mutation as stated in the Material and Methods section 3.7.11. Usually, we first checked if the transformants had integrated the plasmid into their genome and, if positive, then we also checked if the integration had occurred in homozygosis or heterozygosis. We also performed allele-specific PCR in order to determine whether they had acquired the mutation or not (Figure 4.4). The characteristics of the PCR amplicons of each transformant are registered in Table 4.9.

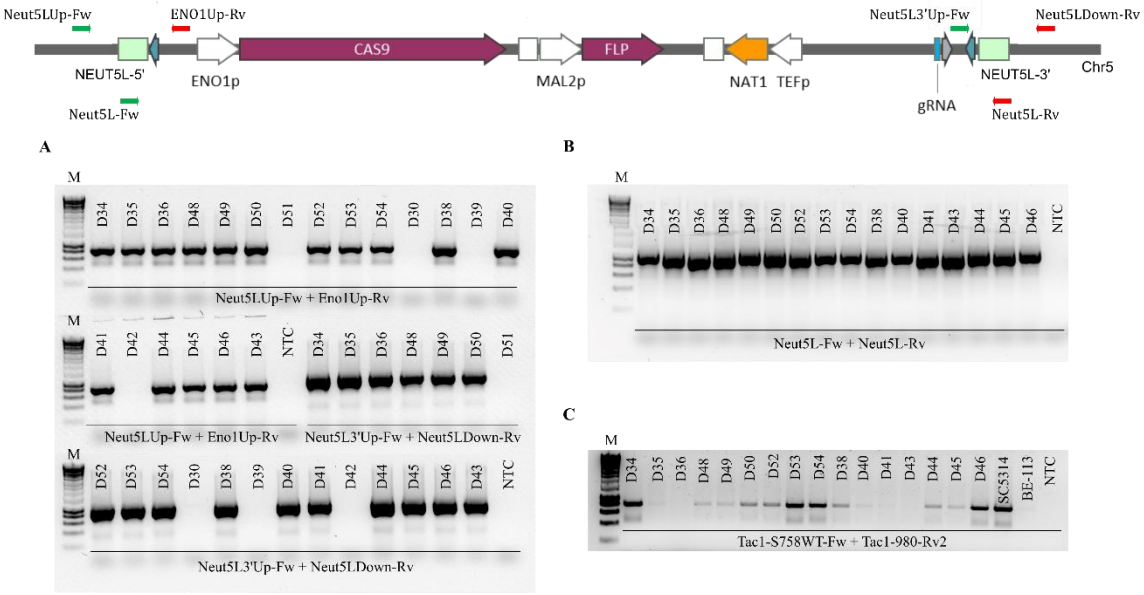

Figure 4.4. Representative image for the PCRs characterizing the Tac1 transformants directed to assess the integration of the CRISPR cassette into the *NEUT5L* locus and the acquisition of mutation. A) Integration at the *NEUT5L* locus, B) Integration zygosity, and C) Mutation acquisition.

Most transformants (75%) integrated the plasmid, and all but two integrated it in heterozygosis (Table 4.9).

Detection of the S758F mutation in Tac1 was done by a specific PCR for the WT allele. The transformants were classified as homozygous, heterozygous or WT according to the intensity of the bands in an agarose gel (Figure 4.4C; D34, D53, D54 and D46 were considered to be WT; D50 and D52 heterozygous; and D35 and D36 homozygous). Among the mutant transformants, 24 were identified as homozygous mutants, 15 as heterozygous and 19 as WT. On the other hand, PCR of the WT transformants gave unspecific results, classifying 3 as homozygous, one as heterozygous and the rest as WT (Table 4.9).

We sequenced the *TAC1* gene fragment harbouring the desired mutation for 48 transformants (41 mutant and 7 WT), of which 7 (17.1%) had incorporated the mutation in homozygosis (one of them also had other mutations), 9 (22%) in heterozygosis, one (2.4%) had repaired the DSB with a repair mechanism distinct from HR, and 4 showed only the silent mutations. The rest of the mutant transformants seemed not to have incorporated the RT. As for the WT transformants, five (71.4%) were correctly modified, while two seemed unmodified. A summary of the sequencing results is listed in Supplementary material Table VI.

Table 4.9. Screening of Tac1 transformants for integration of the CRISPR-Cas9 cassette into the *NEUT5L* locus and gene editing by PCR.

	Transformant	5'/3' Integration	Neut5L	Mutation		Transformant	5'/3' Integration	Neut5L	Mutation		Transformant	5'/3' Integration	Neut5L	Mutation
Tac1-758-RT2	D1	Yes/Yes	-	WT		D42	No/No	-	-		D73	Yes/Yes	Yes	WT
	D2	Yes/Yes	Yes	Mut		D43	Yes/Yes	Yes	Mut		D74	No/-	-	-
	D3	Yes/Yes	Yes	WT		D44	Yes/Yes	Yes	Het		D75	Yes/Yes	Yes	WT
	D4	Yes/Yes	-	Mut		D45	Yes/Yes	Yes	Het		D76	Yes/Yes	Yes	Mut
	D5	No/No	Yes	-		D46	Yes/Yes	Yes	WT		D77	No/-	-	-
	D6	Yes/Yes	Yes	WT		D47	No/-	-	-		D78	Yes/Yes	Yes	Mut
	D7	-/-	-	WT		D48	Yes/Yes	Yes	Het		D79	Yes/Yes	Yes	Mut
	D8	Yes/Yes	-	Mut		D49	Yes/Yes	Yes	Het		D80	Yes/Yes	Yes	Mut
	D14	No/No	Yes	Het		D50	Yes/Yes	Yes	Het		D81	Yes/Yes	Yes	WT/Het
	D16	Yes/Yes	No	Mut		D51	No/No	Yes	-		D82	Yes/Yes	Yes	WT/Het
	D17	Yes/Yes	Yes	Mut		D52	Yes/Yes	Yes	Het		D83	No/-	-	-
	D18	Yes/Yes	Yes	Mut		D53	Yes/Yes	Yes	WT		D84	Yes/Yes	Yes	WT/Het
	D19	Yes/Yes	No	Mut		D54	Yes/Yes	Yes	WT		D85	Yes/Yes	Yes	WT
	D20	No/No	Yes	Mut		D55	Yes/Yes	Yes	WT		D86	Yes/Yes	Yes	WT
	D21	Yes/Yes	Yes	Het		D56	Yes/Yes	Yes	WT		D87	Yes/Yes	Yes	Mut
	D22	Yes/Yes	Yes	Mut		D57	No/-	-	-		D88	Yes/Yes	Yes	Mut
	D23	Yes/Yes	Yes	Het		D58	No/-	-	-		D89	Yes/Yes	Yes	Mut
	D28	No/No	-	-		D59	No/-	-	-		D90	Yes/Yes	Yes	WT
	D29	No/No	-	-		D60	Yes/Yes	Yes	WT		D91	No/-	-	-
	D30	No/No	-	-		D61	Yes/Yes	Yes	Mut		D92	No/-	-	-
	D31	No/No	-	-		D62	Yes/Yes	Yes	Mut					
	D32	No/No	-	-		D63	Yes/Yes	Yes	Mut	Tac1-WT-RT2	D9	No/No	-	-
	D33	No/No	-	-		D64	Yes/Yes	Yes	Het		D10	No/No	-	-
	D34	Yes/Yes	Yes	WT		D65	Yes/Yes	Yes	WT		D11	Yes/Yes	-	-
	D35	Yes/Yes	Yes	Mut		D66	Yes/Yes	Yes	Mut		D12	Yes/Yes	-	-
	D36	Yes/Yes	Yes	Mut		D67	No/-	-	-		D13	Yes/Yes	Yes	-
	D37	NG				D68	Yes/Yes	Yes	Het		D15	No/No	Yes	WT/Het
	D38	Yes/Yes	Yes	Het		D69	Yes/Yes	Yes	Het		D24	Yes/Yes	Yes	Mut
	D39	No/No	-	-		D70	Yes/Yes	Yes	Het		D25	Yes/Yes	Yes	Mut
	D40	Yes/Yes	Yes	Het		D71	Yes/Yes	Yes	Het		D26	Yes/Yes	Faint	Mut
	D41	Yes/Yes	Yes	Mut		D72	No/-	-	-		D27	Yes/Yes	Yes	WT

Mut, homozygous for the mutation; Het, heterozygous for the mutation; WT, wild-type sequence; NG, no growth in YEPD+NT; -, not performed

4.4.3.2. Transformants for Erg11 Y477C (Erg11-477-RTe4 and Erg11-WT-RTe4)

In the case of Erg11 mutants we performed two independent transformation reactions with the mutation containing RTe, after which we obtained 304 transformants (65 from T1 and 31 from T2 of the first transformation, and 104 from T1 and 104 from T2 of the second transformation), and one transformation with the WT RTe, from which we obtained 289 transformants (147 from T1 and 142 from T2). Erg11 transformants were labelled with an E for the ones that were transformed with the mutated RTe or EW for the WT RTe, and a number corresponding to the order they were picked followed by the transformation replicate number (for example, E23.2, Erg11 transformant number 23 from T2 transformation).

In this way, we analysed 131 transformants from the mutated RTe and 30 from the WT, of which only 36 out of the mutated transformants (27%) and half of the WT transformants had integrated the pV1524. All integrative mutants underwent integration in heterozygosis (Table 4.10).

As for Tac1 transformants, detection of the Y477C mutation was performed with a PCR specific for the WT allele. Of the 36 transformants that had undergone integration obtained from the transformation with the mutated RTe, 21 (58.3%) were classified as homozygous, 9 (25%) as heterozygous and 6 (16.7%) as WT. Whereas all of the integrative WT transformants were identified correctly as WT (Table 4.10). The results of this PCR were used to select the transformants to be sequenced.

We sequenced the *ERG11* gene fragment harbouring the desired mutation for 31 transformants (27 mutant and 4 WT). Out of the 27 mutant transformants, 18 (66.7%) incorporated the mutation in homozygosis (homozygous transformant), 4 (14.8%) in heterozygosis (heterozygous transformant) and 5 (18.5%) had repaired the double strand break (DSB) with a mechanism distinct from homologous recombination (HR). On the other hand, the four WT transformants were correctly modified. Of note, two of the homozygous and one of the heterozygous mutant transformants, and one of the WT transformants carried unintended mutations, so they were discarded together with those that had not used the RTe for repairing. A summary of the sequencing results is listed in Supplementary material Table VII.

Table 4.10. Screening of Erg11 transformants for integration of the CRISPR-Cas9 cassette into the *NEUT5L* locus and gene editing by PCR.

	Transformant	5'/3' Integration	Neut5L	Mutation	Transformant	5'/3' Integration	Neut5L	Mutation	Transformant	5'/3' Integration	Neut5L	Mutation
Erg11-477-RT4	E1.1	No/Yes	Yes	-	E32.1	Yes/Faint	-	-	E63.1	Yes/Yes	Yes	Mut
	E2.1	No/No	Yes	-	E33.1	No/-	-	-	E64.1	Yes/Yes	Yes	Het
	E3.1	No/No	Yes	-	E34.1	No/-	-	-	E65.1	No/-	-	-
	E4.1	No/No	Yes	-	E35.1	Faint/Faint	-	-	E66.1	Yes/No	-	-
	E5.1	No/No	Yes	-	E36.1	Faint/Faint	-	-	E67.1	Yes/No	-	-
	E6.1	No/No	Yes	-	E37.1	Yes/Faint	-	-	E68.1	Yes/No	-	-
	E7.1	Yes/Yes	Yes	Mut	E38.1	No/-	-	-	E69.1	Yes/No	-	-
	E8.1	No/No	Yes	-	E39.1	No/-	-	-	E70.1	Yes/Yes	Yes	Het
	E9.1	No/Yes	Yes	-	E40.1	No/-	-	-	E71.1	Faint/No	-	-
	E10.1	Yes/No	Yes	-	E41.1	Faint/No	-	-	E72.1	Faint/No	-	-
	E11.1	Yes/Yes	Yes	Mut	E42.1	Yes/Yes	Yes	Mut	E73.1	Yes/Yes	Yes	WT
	E12.1	Yes/Yes	Yes	Mut	E43.1	Yes/-	-	-	E75.1	Faint/Faint	Yes	Het
	E13.1	No/No	Yes	-	E45.1	Yes/Yes	Yes	Het	E76.1	-	-	Het
	E15.1	Yes/Yes	Yes	Mut	E46.1	No/-	-	-	E77.1	-	-	Het
	E16.1	No/-	-	-	E47.1	Yes/Yes	Yes	Het	E78.1	-	-	Het
	E17.1	No/-	-	-	E48.1	Yes/No	-	-	E79.1	-	-	Mut
	E18.1	No/-	-	-	E49.1	No/-	-	-	E80.1	-	-	Mut
	E19.1	No/-	-	-	E50.1	Yes/Yes	Yes	Het	E81.1	-	-	Mut
	E20.1	Yes/Yes	Yes	WT	E51.1	No/-	-	-	E82.1	No/No	-	WT
	E21.1	Yes/No	-	-	E52.1	NG			E83.1	-	-	Mut
	E22.1	NG			E53.1	NG			E84.1	-	-	Mut
	E23.1	NG			E54.1	NG			E85.1	-	-	Mut
	E24.1	No/-	-	-	E55.1	No/-	-	-	E86.1-E117.1	-	-	-
	E25.1	Yes/No	-	-	E56.1	Yes/Yes	Yes	Mut	E118.1	Yes/No	-	-
	E26.1	Yes/Yes	Yes	Mut	E57.1	Yes/Yes	Yes	Mut	E119.1	Yes/Yes	Yes	Het
	E27.1	No/-	-	-	E58.1	No/-	-	-	E120.1	Yes/No	-	-
	E28.1	No/-	-	-	E59.1	Yes/Yes	Yes	Het	E121.1	Yes/No	-	-
	E29.1	No/-	-	-	E60.1	NG			E122.1	Yes/No	-	-
	E30.1	Yes/Faint	-	-	E61.1	Yes/Yes	Yes	Mut	E123.1	Faint/No	-	-
	E31.1	No/-	-	-	E62.1	Yes/Yes	Yes	Mut	E124.1	Yes/Yes	Yes	Mut

Mut, homozygous for the mutation; Het, heterozygous for the mutation; WT, wild-type sequence; NG, no growth in YEPD+NT; -, not performed

Table 4.10. Continued.

	Transformant	5'/3' Integration	Neut5L	Mutation	Transformant	5'/3' Integration	Neut5L	Mutation	Transformant	5'/3' Integration	Neut5L	Mutation
Erg11-477-RT4	E125.1	Yes/Yes	Yes	Mut	E19.2	No/-	-	-	E50.2	-	-	Mut
	E126.1	Yes/Faint	Yes	Mut	E20.2	No/-	-	-	E51.2	-	-	Het
	E127.1	No/No	-	-	E21.2	Yes/Yes	Yes	Mut	E52.2-E83.2	-	-	-
	E128.1	-	-	Mut	E22.2	NG			E84.2	No/No	-	-
	E129.1	-	-	Het	E23.2	No/-	-	-	E85.2	Yes/Yes	Yes	Mut
	E130.1	-	-	Mut	E24.2	No/-	-	-	E86.2	Yes/No	-	-
	E131.1	-	-	Mut	E25.2	No/-	-	-	E87.2	Yes/Yes	Yes	Mut
	E132.1	-	-	Mut	E26.2	No/-	-	-	E88.2	Yes/No	-	-
	E133.1	-	-	Mut	E27.2	Yes/Yes	Yes	WT	E89.2	Yes/Yes	Yes	Mut
	E134.1	-	-	Het	E28.2	No/-	-	-	E90.2	No/-	-	-
	E136.1	-	-	Het	E29.2	No/-	-	-	E91.2	No/-	-	-
	E137.1	No/No	-	WT	E30.2	No/-	-	-	E92.2	No/-	-	-
	E138.1-E169.1	-	-	-	E31.2	No/-	-	-	E93.2	No/-	-	-
	E1.2	No/No	Yes	-	E32.2	Yes/No	-	-	E94.2	-	-	Mut
	E2.2	Yes/Yes	Yes	Mut	E33.2	Yes/No	-	-	E95.2	-	-	Mut
	E3.2	Yes/Yes	Yes	Mut	E35.2	Yes/No	-	-	E96.2	-	-	Mut
	E4.2	No/No	Yes	-	E34.2	Yes/No	-	-	E97.2	-	-	Mut
	E5.2	No/No	Yes	-	E36.2	Yes/No	-	-	E98.2	-	-	Mut
	E6.2	No/No	Yes	-	E37.2	No/-	-	-	E101.2	-	-	Mut
	E7.2	No/No	Yes	-	E38.2	Faint/No	-	-	E99.2	-	-	Mut
	E8.2	Yes/No	Yes	-	E39.2	Yes/Faint	Yes	Het	E100.2	-	-	Mut
	E9.2	Yes/Yes	Yes	Mut	E40.2	Yes/Faint	Yes	WT	E102.2	-	-	Mut
	E10.2	Yes/Yes	Yes	WT	E41.2	Faint/-	-	-	E103.2	-	-	Mut
	E11.2	Yes/No	Yes	-	E42.2	-	-	Mut	E104.2-E135.2	-	-	-
	E13.1	No/-	-	-	E44.2	-	-	Mut				
	E14.2	No/-	-	-	E45.2	-	-	Mut				
	E15.2	No/-	-	-	E46.2	Yes/No	-	WT				
	E16.2	No/-	-	-	E47.2	-	-	Mut				
	E17.2	No/-	-	-	E48.2	-	-	Mut				
	E18.2	No/-	-	-	E49.2	-	-	Mut				

Mut, homozygous for the mutation; Het, heterozygous for the mutation; WT, wild-type sequence; NG, no growth in YEPD+NT; -, not performed

Table 4.10. Continued.

Transformant		5'/3' Integration	Neut5L	Mutation
Erg11-WT-RT4	EW1.1	No/No	Yes	-
	EW2.1	No/No	Yes	-
	EW3.1	No/No	Yes	-
	EW4.1	No/No	Yes	-
	EW5.1	No/No	Yes	-
	EW6.1	Yes/Yes	Yes	WT
	EW7.1	Yes/Yes	Yes	WT
	EW8.1	No/No	Yes	-
	EW9.1	Yes/Yes	Yes	WT
	EW10.1	No/No	Yes	-
	EW11.1	Yes/Yes	Yes	WT
	EW12.1	Yes/Yes	Yes	WT
	EW13.1	Yes/Yes	Yes	WT
	EW14.1	Yes/Yes	Yes	WT
	EW15.1	Yes/Yes	Yes	WT
	EW16.1-EW147.1	-	-	-
	EW1.2	No/No	Yes	-
	EW2.2	Yes/No	Yes	-
	EW3.2	No/No	Yes	-
	EW4.2	No/No	Yes	-
	EW5.2	No/No	Yes	-
	EW6.2	Yes/Yes	Yes	WT
	EW7.2	No/No	Yes	-
	EW8.2	Yes/Yes	Yes	WT
	EW9.2	Yes/Yes	Yes	WT
	EW10.2	No/No	Yes	-
	EW11.2	Yes/Yes	Yes	WT
	EW12.2	Yes/Yes	Yes	WT
	EW13.2	Yes/Yes	Yes	WT
	EW14.2	No/Yes	Yes	-
	EW15.2	Yes/Yes	Yes	WT
	EW16.2-EW142.2	-	-	-

WT, wild-type sequence; -, not performed

4.4.3.3. Transformants for Mrr2 A311V (Mrr2-311-RT1 and Mrr2-WT-RT1)

We carried out two transformations for Mrr2 with the mutated RTe where we obtained 341 transformants (166 from T1 and 175 from T2) and we had to do five transformations with the WT RTe in order to get a large number of transformants, 156 in total (101 from T1 and 55 from T2). The transformants were labelled similarly to Erg11 ones, and we used M or MW to refer to mutagenic or WT RTe-derived transformants.

We analysed 235 mutated and 71 WT RTe transformants of which 32 (13.6%) and 9 (12.7%) had integrated pV1524, respectively, and only one of them did it in homozygosis. In order to detect the A311V mutation we carried out a PCR specific for the mutated allele. Thirteen integrative transformants from the mutated RTe were identified as homozygous, another 13 as heterozygous and 9 as WT. All of the integrative WT transformants were correctly identified as WT (Table 4.11).

We sequenced the *MRR2* gene fragment harbouring the desired mutation of 22 transformants (18 mutant and 4 WT) of which 9 (50%) had the mutation in homozygosis, 2 (11.1%) were heterozygous, 7 (38.9%) had repaired the DSB with a repair mechanism distinct from HR. Half of the WT transformants were correctly modified. A summary of the sequencing results is listed in Supplementary material Table VIII.

Table 4.11. Screening of Mrr2 transformants for integration of the CRISPR-Cas9 cassette into the NEUT5L locus and gene editing by PCR.

	Transformant	5'/3' Integration	Neut5L	Mutation	Transformant	5'/3' Integration	Neut5L	Mutation	Transformant	5'/3' Integration	Neut5L	Mutation
Mrr2-311-RT1	M1.1	No/No	Yes	-	M32.1	No/No	-	-	M64.1	No/No	-	-
	M2.1	No/No	Yes	-	M33.1	No/No	-	-	M65.1	No/No	-	-
	M3.1	No/No	Yes	-	M35.1	No/No	-	-	M66.1	No/No	-	-
	M4.1	No/No	Yes	-	M36.1	No/No	-	-	M67.1	Yes/Yes	Yes	Mut
	M5.1	No/No	Yes	-	M37.1	No/No	-	-	M69.1	Yes/Yes	Yes	WT
	M6.1	No/No	Yes	-	M38.1	No/No	-	-	M68.1	Yes/Yes	Yes	Mut
	M7.1	No/No	Yes	-	M39.1	No/No	-	-	M70.1	Yes/Yes	Yes	Mut
	M8.1	No/No	Yes	-	M40.1	No/No	-	-	M71.1	Yes/Yes	Yes	WT
	M9.1	No/No	Yes	-	M41.1	No/No	-	-	M72.1	Yes/Yes	Yes	WT
	M10.1	No/No	Yes	-	M42.1	Yes/Yes	Yes	Het	M73.1	No/-	-	-
	M11.1	No/No	-	-	M43.1	No/No	-	-	M74.1	No/-	-	-
	M12.1	No/No	-	-	M44.1	No/No	-	-	M75.1	No/-	-	-
	M13.1	No/No	-	-	M45.1	No/No	-	-	M76.1	No/-	-	-
	M14.1	No/No	-	-	M46.1	No/No	-	-	M77.1	NG		
	M15.1	No/No	-	-	M47.1	No/No	-	-	M78.1	No/-	-	-
	M16.1	No/No	-	-	M48.1	Yes/Yes	Yes	Het	M79.1	No/No	Yes	Mut
	M17.1	No/No	-	-	M49.1	No/No	-	-	M80.1	NG		
	M18.1	Yes/Yes	Yes	Mut	M50.1	No/No	-	-	M81.1	-	-	WT
	M19.1	No/No	-	-	M51.1	NG			M82.1	-	-	Mut
	M20.1	No/No	-	-	M52.1	No/No	-	-	M83.1	-	-	Mut
	M21.1	No/No	-	-	M53.1	No/No	-	-	M84.1	-	-	WT
	M22.1	No/No	-	-	M54.1	No/No	-	-	M85.1	No/No	Yes	Mut
	M23.1	No/No	-	-	M55.1	Yes/Yes	Yes	Het	M86.1	No/No	Yes	Mut
	M24.1	No/No	-	-	M56.1	No/No	-	-	M87.1	-	-	Mut
	M25.1	No/No	-	-	M57.1	No/No	-	-	M88.1	-	-	Mut
	M26.1	No/No	-	-	M58.1	No/No	-	-	M89.1	Yes/No	No	-
	M27.1	No/No	-	-	M59.1	Yes/Yes	Yes	Het	M90.1	NG		
	M28.1	Yes/Yes	Yes	Het	M60.1	No/No	-	-	M91.1	No/-	-	-
	M29.1	No/No	-	-	M61.1	No/No	-	-	M92.1-M98.1	NG		
	M30.1	No/No	-	-	M62.1	Yes/Yes	Yes	Mut	M99.1	No/-	-	-
	M31.1	No/No	-	-	M63.1	No/No	-	-	M100.1	No/-	-	-

Mut, homozygous for the mutation; Het, heterozygous for the mutation; WT, wild-type sequence; NG, no growth in YEPD+NT; -, not performed

Table 4.11. Continued.

	Transformant	5'/3' Integration	Neut5L	Mutation	Transformant	5'/3' Integration	Neut5L	Mutation	Transformant	5'/3' Integration	Neut5L	Mutation
Mrr2-311-RT1	M101.1	No/-	-	-	M159.1	Yes/Yes	Yes	Mut	M25.2	No/No	-	-
	M102.1-M105.1	NG			M160.1	No/-	-	-	M26.2	Yes/Yes	Yes	WT
	M106.1	No/-	-	-	M161.1	No/-	-	-	M27.2	No/No	-	-
	M107.1	NG			M162.1	No/-	-	-	M28.2	No/No	-	-
	M108.1	No/-	-	-	M163.1	No/-	-	-	M29.2	No/No	-	-
	M109.1-M119.1	NG			M164.1	No/-	-	-	M30.2	No/No	-	-
	M120.1	No/-	-	-	M165.1	No/-	-	-	M31.2	No/No	-	-
	M121.1	No/-	-	-	M1.2	Yes/Yes	Yes	WT	M32.2	Yes/Yes	Yes	WT
	M122.1-M126.1	NG			M2.2	Yes/Yes	Yes	WT	M33.2	No/No	-	-
	M127.1	No/-	-	-	M3.2	No/No	Yes	-	M34.2	No/No	-	-
	M128.1	NG			M4.2	No/No	Yes	-	M35.2	No/No	-	-
	M129.1	NG			M5.2	No/No	Yes	-	M36.2	No/No	-	-
	M130.1	Yes/No	Yes	-	M6.2	No/No	Yes	-	M37.2	No/No	-	-
	M131.1-M133.1	NG			M7.2	No/No	Yes	-	M38.2	No/No	-	-
	M134.1	Yes/No	Yes	-	M8.2	No/No	Yes	-	M39.2	No/No	-	-
	M135.1	No/-	-	-	M9.2	No/No	Yes	-	M40.2	No/No	-	-
	M136.1-M141.1	NG			M10.2	No/No	Yes	-	M41.2	No/No	-	-
	M142.1	No/-	-	-	M11.2	Yes/Yes	Yes	Mut	M42.2	No/No	-	-
	M143.1	No/-	-	-	M12.2	Yes/Yes	Yes	Mut	M43.2	No/No	-	-
	M144.1	NG			M13.2	No/No	-	-	M44.2	No/No	-	-
	M145.1	No/-	-	-	M14.2	No/No	-	-	M45.2	No/No	-	-
	M146.1	NG			M15.2	Yes/Yes	Yes	Het	M46.2	No/No	-	-
	M147.1	NG			M16.2	No/No	-	-	M47.2	No/No	-	-
	M148.1	No/-	-	-	M17.2	No/No	-	-	M48.2	No/No	-	-
	M149.1	NG			M18.2	No/No	-	-	M49.2	Yes/Yes	Yes	Het
	M150.1	NG			M19.2	No/No	-	-	M50.2	No/No	-	-
	M151.1	No/-	-	-	M20.2	No/No	-	-	M51.2	No/-	-	-
	M152.1	NG			M21.2	No/No	-	-	M52.2	No/-	-	-
	M153.1	NG			M22.2	Yes/Yes	Yes	Het	M53.2	No/-	-	-
	M154.1	No/-	-	-	M23.2	No/No	-	-	M54.2	No/-	-	-
	M155.1-M158.1	NG			M24.2	No/No	-	-	M55.2	No/-	-	-

Mut, homozygous for the mutation; Het, heterozygous for the mutation; WT, wild-type sequence; NG, no growth in YEPD+NT; -, not performed

Table 4.11. Continued.

	Transformant	5'/3' Integration	Neut5L	Mutation	Transformant	5'/3' Integration	Neut5L	Mutation	Transformant	5'/3' Integration	Neut5L	Mutation
Mrr2-311-RT1	M56.2	Yes/Yes	Yes	WT	M87.2	No/-	-	-	M121.2	NG		
	M57.2	No/-	-	-	M88.2	NG			M122.2	No/-	-	-
	M58.2	No/-	-	-	M89.2	No/-	-	-	M123.2	No/-	-	-
	M59.2	No/-	-	-	M90.2	NG			M124.2	No/-	-	-
	M60.2	No/-	-	-	M91.2	NG			M125.2	No/-	-	-
	M61.2	NG			M92.2	No/-	-	-	M126.2	No/-	-	-
	M62.2	NG			M93.2	No/-	-	-	M127.2-M131.2	NG		
	M63.2	NG			M94.2	No/-	-	-	M132.2	No/-	-	-
	M64.2	No/-	-	-	M95.2	NG			M133.2-M135.2	NG		
	M65.2	NG			M96.2	No/-	-	-	M136.2	No/-	-	-
	M66.2	No/-	-	-	M97.2	NG			M137.2	NG		
	M67.2	No/-	-	-	M98.2	No/-	-	-	M138.2	No/-	-	-
	M68.2	NG			M99.2	NG			M139.2	NG		
	M69.2	No/-	-	-	M100.2	NG			M140.2	NG		
	M70.2	No/-	-	-	M101.2	No/-	-	-	M141.2	No/-	-	-
	M71.2	No/-	-	-	M102.2	No/-	-	-	M142.2	NG		
	M72.2	NG			M103.2	No/-	-	-	M143.2	No/-	-	-
	M73.2	NG			M104.2	No/-	-	-	M144.2	NG		
	M74.2	No/-	-	-	M105.2	No/-	-	-	M145.2	No/-	-	-
	M75.2	No/-	-	-	M106.2	No/-	-	-	M146.2	Yes/Yes	No	Het
	M76.2	No/-	-	-	M107.2	No/-	-	-	M147.2	Yes/-	-	-
	M77.2	NG			M108.2	NG			M148.2	Yes/Yes	Yes	Het
	M78.2	NG			M109.2	Yes/No	Yes	-	M149.2-M153.2	NG		
	M79.2	No/-	-	-	M110.2	NG			M154.2	No/-	-	-
	M80.2	No/-	-	-	M111.2	NG			M155.2	NG		
	M81.2	NG			M112.2	No/-	-	-	M156.2	No/-	-	-
	M82.2	NG			M113.2-M116.2	NG			M157.2	No/-	-	-
	M83.2	No/-	-	-	M117.2	Yes/Yes	Yes	Mut	M158.2	NG		
	M84.2	NG			M118.2	NG			M159.2	Yes/Yes	Yes	Het
	M85.2	No/-	-	-	M119.2	No/-	-	-	M160.2	No/-	-	-
	M86.2	No/-	-	-	M120.2	NG			M161.2	No/-	-	-

Mut, homozygous for the mutation; Het, heterozygous for the mutation; WT, wild-type sequence; NG, no growth in YEPD+NT; -, not performed

Table 4.11. Continued.

	Transformant	5'/3' Integration	Neut5L	Mutation
Mrr2-311-RT1	M162.2	No/-	-	-
	M163.2	Yes/Yes	Yes	Het
	M164.2	No/-	-	-
	M165.2	Yes/Yes	Yes	Het
	M166.2	No/-	-	-
	M167.2	No/-	-	-
	M168.2	No/-	-	-
	M169.2	NG		
	M170.2	NG		
	M171.2	Yes/Yes	Yes	Mut
	M172.2	No/-	-	-
	M173.2	No/-	-	-
	M174.2	Yes/Yes	Yes	WT
	M175.2	NG		
Mrr2-WT-RT1	MW1.1	No/No	-	WT
	MW2.1	No/No	-	WT
	MW3.1	NG		
	MW4.1	No/No	Yes	-
	MW5.1	No/No	Yes	-
	MW6.1	No/No	Yes	-
	MW7.1	No/No	Yes	-
	MW8.1	No/No	Yes	-
	MW9.1	No/No	Yes	-
	MW10.1	No/No	Yes	-
	MW11.1	No/No	Yes	-
	MW12.1	No/No	Yes	-
	MW13.1	No/No	Yes	-
	MW14.1	No/No	Yes	-
	MW15.1	No/No	Yes	-
	MW16.1	No/No	Yes	-
	MW17.1	No/No	Yes	-
Mrr2-WT-RT1	MW18.1	Yes/Yes	Yes	WT
	MW19.1	No/No	Yes	-
	MW20.1	No/No	Yes	-
	MW21.1	No/No	Yes	-
	MW22.1	No/No	Yes	-
	MW23.1	No/No	Yes	-
	MW24.1	No/No	Yes	-
	MW25.1	No/No	Yes	-
	MW26.1	No/No	Yes	-
	MW27.1	No/No	Yes	-
	MW28.1	No/No	Yes	-
	MW29.1	No/No	Yes	-
	MW30.1	No/No	Yes	-
	MW31.1	No/No	Yes	-
	MW32.1	No/No	Yes	-
	MW33.1	NG		
	MW34.1	No/No	-	-
	MW35.1	No/No	-	-
	MW36.1	No/No	-	-
	MW37.1	No/No	Yes	-
	MW38.1	No/No	Yes	-
	MW39.1	No/-	-	-
	MW40.1	No/-	-	-
	MW41.1	NG		
	MW42.1	Yes/Yes	Yes	WT
	MW43.1	Yes/Yes	Yes	WT
	MW44.1	Yes/Yes	Yes	WT
	MW45.1	No/-	-	-
	MW46.1	NG		
	MW47.1	No/-	-	-
	MW48.1	No/-	-	-
	MW49.1	Yes/Yes	Yes	WT
	MW50.1	No/-	-	-
	MW51.1-MW101.1	-	-	-
	MW1.2	No/No	-	WT
	MW2.2	No/No	No	-
	MW3.2	No/No	Yes	-
	MW4.2	No/No	Yes	-
	MW5.2	No/No	Yes	-
	MW6.2	No/No	Yes	-
	MW7.2	No/No	Yes	-
	MW8.2	No/No	Yes	-
	MW9.2	No/No	Yes	-
	MW10.2	No/No	Yes	-
	MW11.2	No/No	Yes	-
	MW12.2	No/No	Yes	-
	MW13.2	No/No	Yes	-
	MW14.2	NG		
	MW15.2	NG		
	MW16.2	NG		
	MW17.2	No/No	Yes	-
	MW18.2	No/No	Yes	-
	MW19.2	No/-	-	-
	MW20.2	No/-	-	-
	MW21.2	Yes/Yes		WT
	MW22.2	Yes/Yes	-	WT
	MW23.2	Yes/Yes		WT
	MW24.2	No/-	-	-
	MW25.2	No/-	-	-
	MW26.2	No/-	-	-
	MW27.2	No/-	-	-
	MW28.2	Yes/Yes		WT
	MW29.2-MW55.2	-	-	-

Mut, homozygous for the mutation; Het, heterozygous for the mutation; WT, wild-type sequence; NG, no growth in YEPD+NT; -, not performed

All the transformants that had correctly incorporated the repair template were then selected for flip-out (FO) induction. After FO confirmation, they were sequenced again to check if they retained the desired mutation. Finally, two transformants of each type were selected for phenotypic analysis and were renamed as detailed in Table 4.12.

A duplicate for the heterozygous mutant of Mrr2 could not be obtained because the one initially identified as heterozygous became homozygous after FO induction.

Table 4.12. New nomenclature of the transformants selected for phenotypic analysis.

Erg11 transformant	New name
E7.1_19	SC5314_Erg11^{Y477C}-1
E3.2_1	SC5314_Erg11^{Y477C}-2
E10.2_315	SC5314_Erg11$^{Y477C(h)}$-1
E82.1_2	SC5314_Erg11$^{Y477C(h)}$-2
EW6.1_78	SC5314_Erg11^{WT}-1
EW6.2_57	SC5314_Erg11^{WT}-2

Tac1 transformant	New name
D22.100	SC5314_Tac1^{S758F}-1
D61.241	SC5314_Tac1^{S758F}-2
D38.2	SC5314_Tac1$^{S758F(h)}$-1
D43.1	SC5314_Tac1$^{S758F(h)}$-2
D24.37	SC5314_Tac1^{WT}-1
D25.48	SC5314_Tac1^{WT}-2

Mrr2 transformant	New name
M55.1_240	SC5314_Mrr2^{A311V}-1
M12.2_269	SC5314_Mrr2^{A311V}-2
M28.1_358	SC5314_Mrr2$^{A311V(h)}$-1
-	-
MW43.1_97	SC5314_Mrr2^{WT}-1
MW22.2_98	SC5314_Mrr2^{WT}-2

(h) indicates the heterozygous mutants

4.4.4. Susceptibility to fluconazole of *C. albicans* mutants generated by CRISPR-Cas9

Susceptibility against fluconazole was tested by CLSI's broth microdilution method at 37 and 25°C for two replicates of each mutant (homozygotic, heterozygotic and WT) together with the parental strain (SC5314) and the azole resistant isolate that originally harboured the mutation. The isolate 16-134 could not be subjected to the subsequent analysis because we could not recover it from the stock.

4.4.4.1. Tac1 transformants

We could not observe any significant changes in fluconazole susceptibility for the Tac1 mutants, although the homozygous mutants seem to have slightly higher MIC after 24h of incubation than the SC5314 parental strain and the heterozygous and control mutants. Nonetheless, after 48h this difference is less apparent (Figure 4.5).

4.4.4.2. Erg11 transformants

In the case of Erg11 transformants, none showed higher MIC than the parental strain after 24h of incubation, neither at 37°C nor at 25°C. However, after 48h one of the homozygous mutants (SC5314-Erg11^{Y477C}-1) showed a significant increase in its fluconazole MIC at both temperatures (Figure 4.6).

4.4.4.3. Mrr2 transformants

As with the Tac1 transformants, the Mrr2 homozygous mutants showed a slight decrease in their susceptibility to FLC at 37°C, but not at 25°C. Interestingly, after 48h of incubation at 25°C the homozygous mutants showed such a heavy trailing growth that MIC could not be determined or would be established as more than 64 µg/ml (the highest FLC concentration in the CLSI assay) (Figure 4.7).

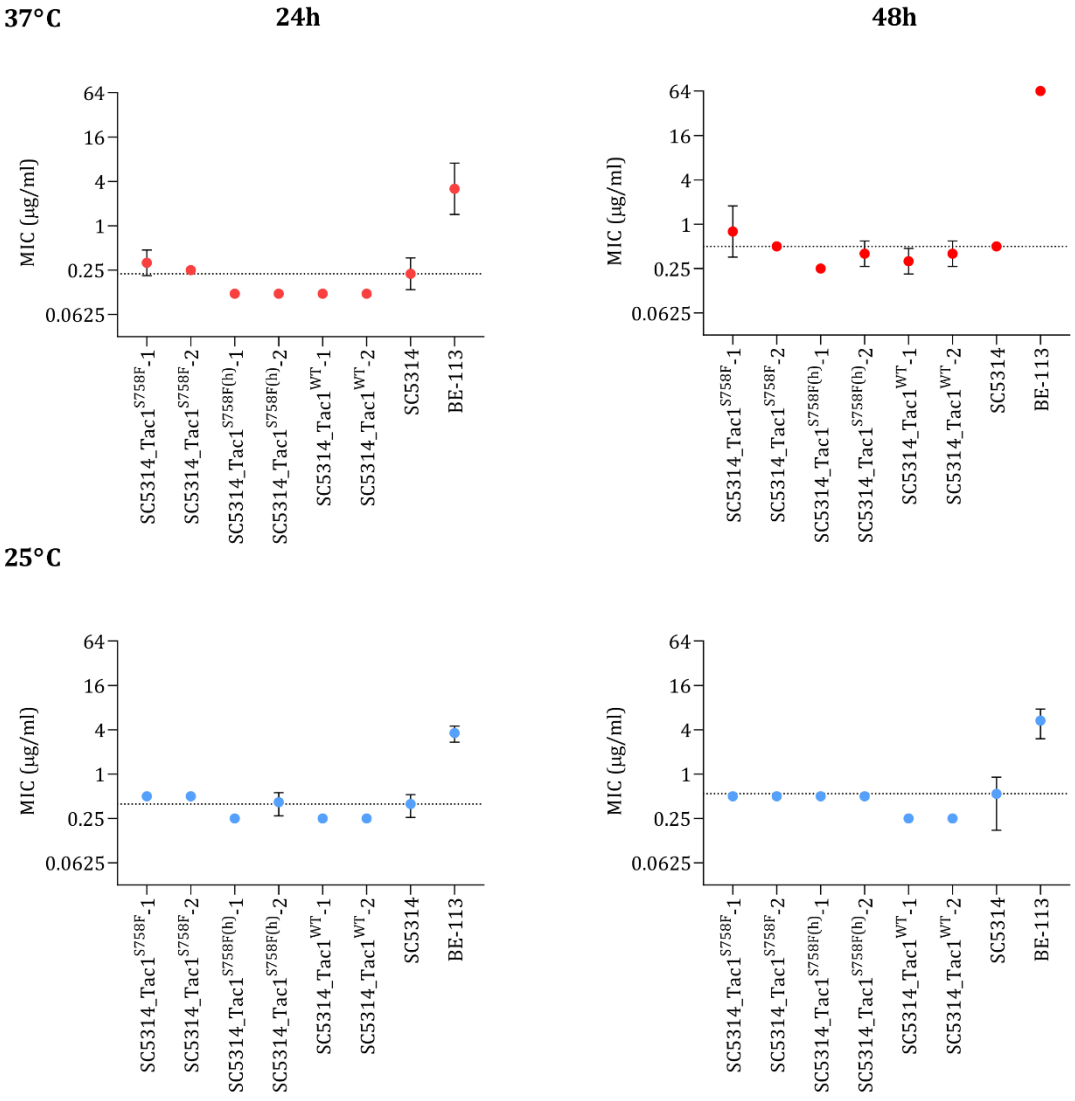

Figure 4.5. Fluconazole MIC values for Tac1 transformants after 24 and 48h of incubation at 37 and 25°C. The dotted line marks the mean MIC value for the SC5314 *C. albicans* parental strain.

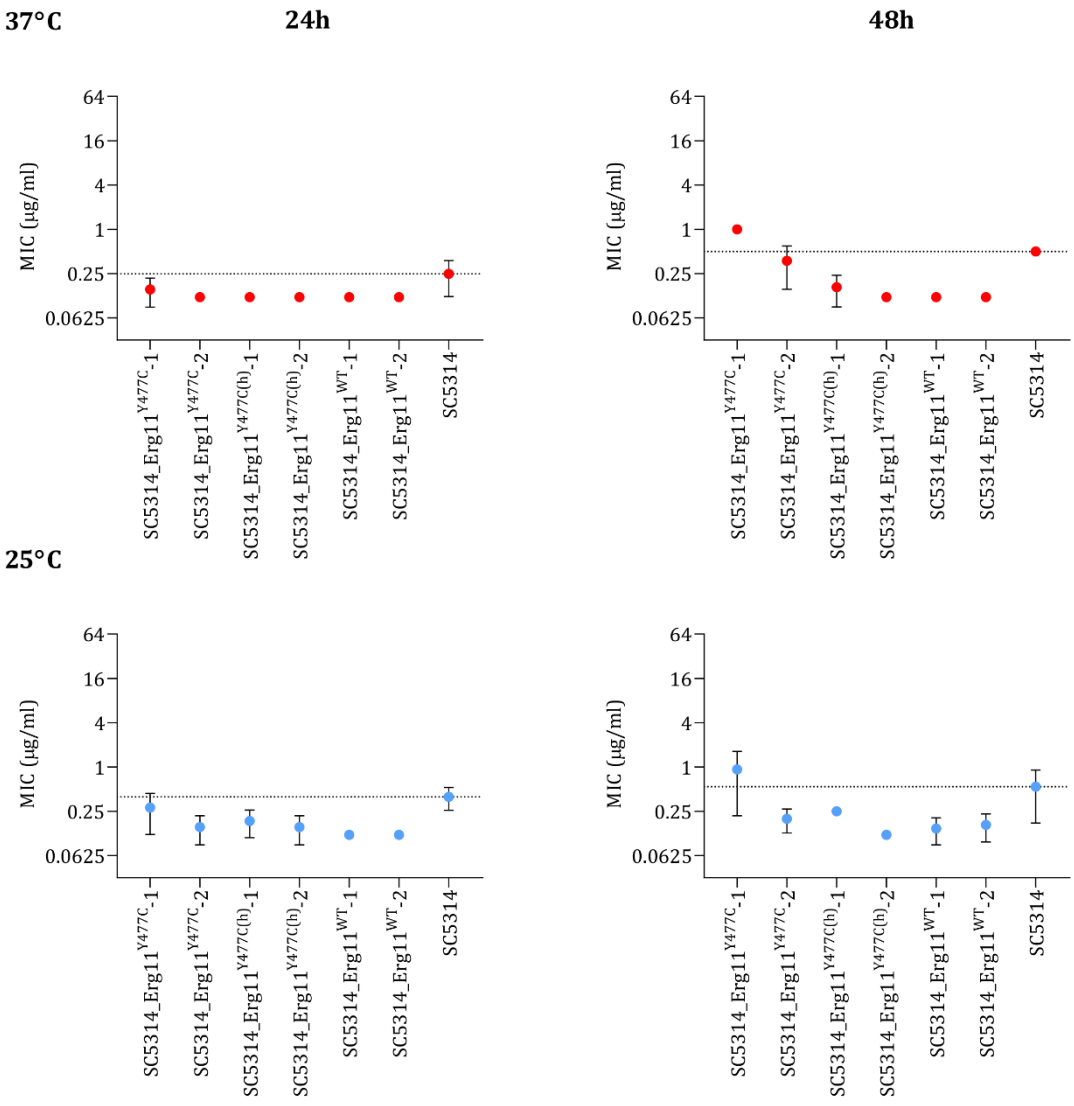

Figure 4.6. Fluconazole MIC values for Erg11 transformants after 24 and 48h of incubation at 37 and 25°C. The dotted line marks the mean MIC value for the SC5314 *C. albicans* parental strain.

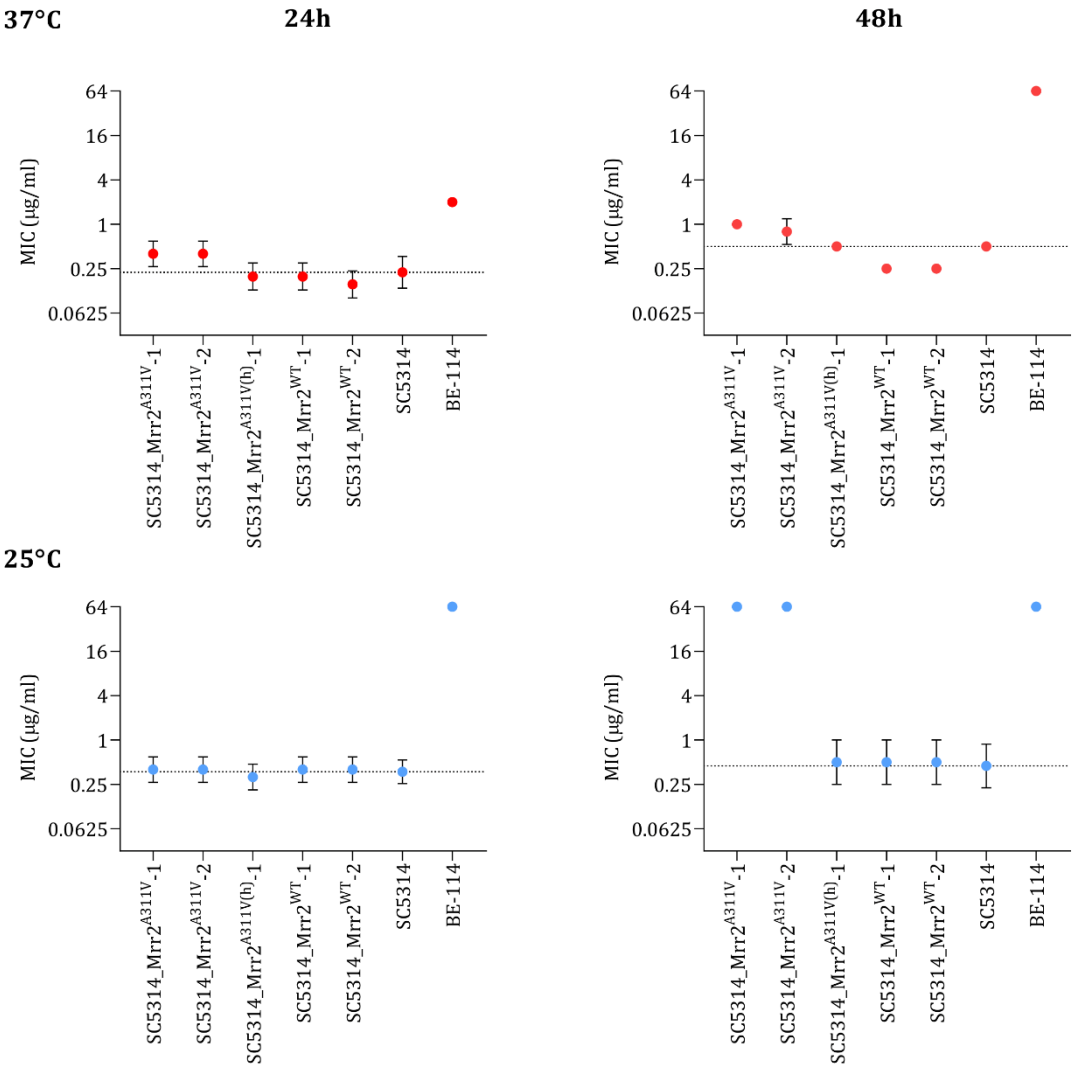

Figure 4.7. Fluconazole MIC values for Mrr2 transformants after 24 and 48h of incubation at 37 and 25°C. The dotted line marks the mean MIC value for the SC5314 *C. albicans* parental strain.

4.4.5. Spot Assay

Spot assay was carried at 37 and 25°C to compare the results with the ones obtained by CLSI's method.

4.4.5.1. Tac1 transformants

Tac1 transformants did not show any differences in growth between the mutants and the WT transformants at 37°C, while at 25°C the mutants showed a slightly higher growth (Figure 4.8). This observation is in agreement with the results of the CLSI's susceptibility assays at both temperatures. In addition, it has to be noted that specially at 37°C the parental strain has a faint growth compared to the engineered WT strain.

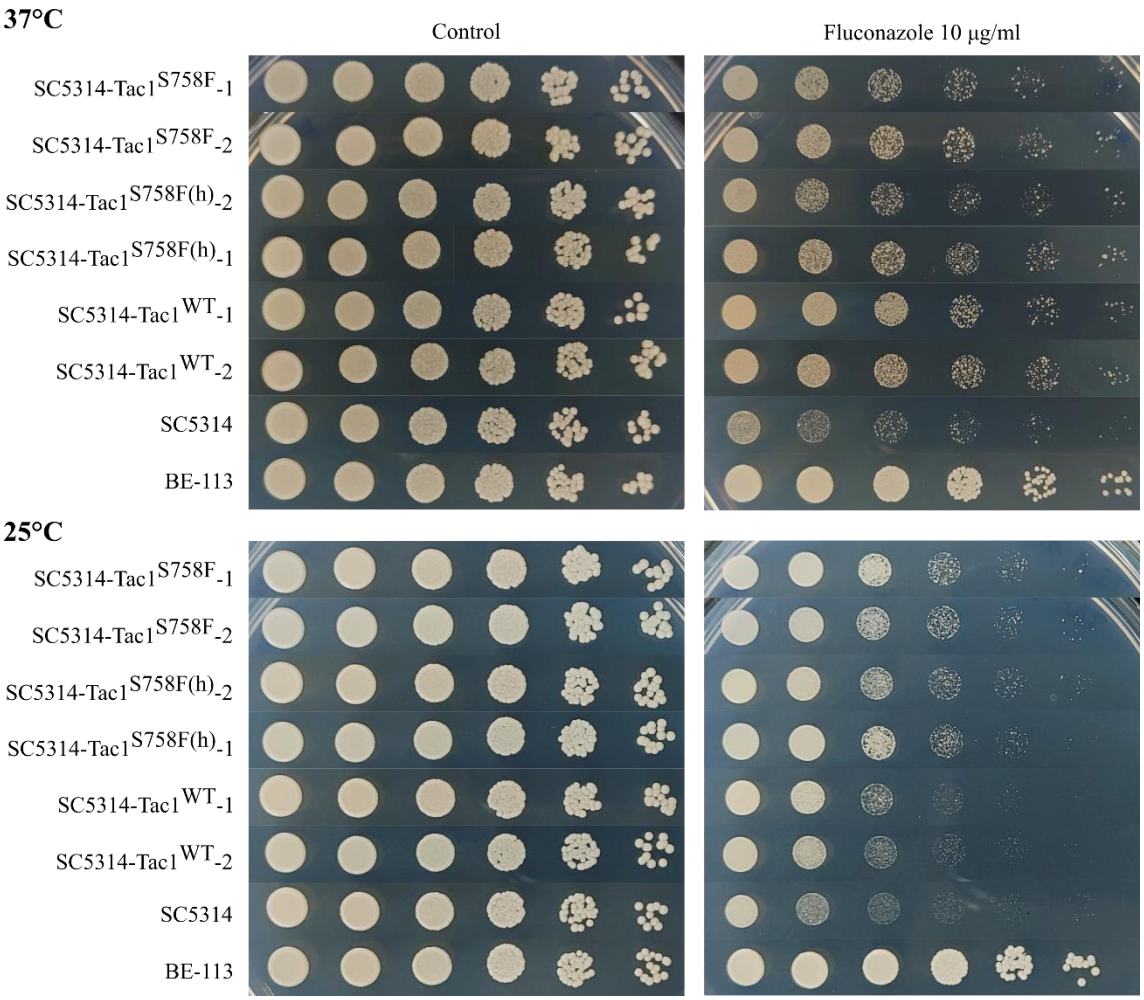

Figure 4.8. Spot assay for Tac1 transformants, BE-113 and parental SC5314 *C. albicans* strains at 37 and 25°C after 48 and 72h of incubation.

4.4.5.2. Erg11 transformants

For the Erg11 transformants we did not observe any apparent differences between the Erg11 homozygous and heterozygous mutants and the WT and parental strain, either at 37 or 25°C (Figure 4.9). These results are in accordance with CLSI at 24h of incubation, but in this assay, we could not confirm the slight reduction in fluconazole susceptibility of the SC5314-Erg11^{Y477C}-1 mutant detected after 48h.

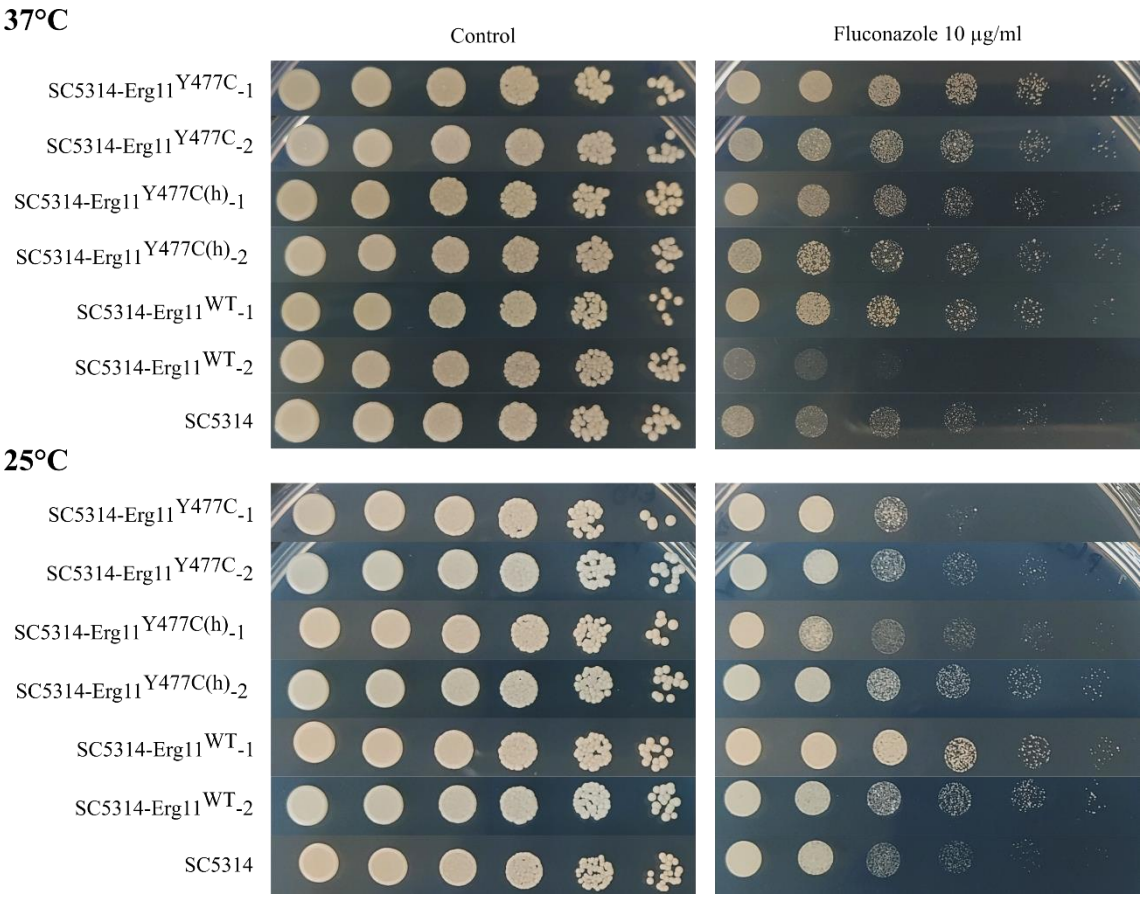

Figure 4.9. Spot assay of Erg11 transformants and SC5314 *C. albicans* parental strain at 37 and 25°C after 48 and 72h of incubation.

4.4.5.3. Mrr2 transformants

For the Mrr2 transformants there were not observable differences in the growth of the mutants with reference to the WT transformants and parental strains when grown at 37°C (Figure 4.10), contrarily to the results obtained by CLSI. However, at 25°C a slightly increased growth of the Mrr2 homozygous mutants was registered, which could be related to the heavy trailing growth described in the CLSI assay.

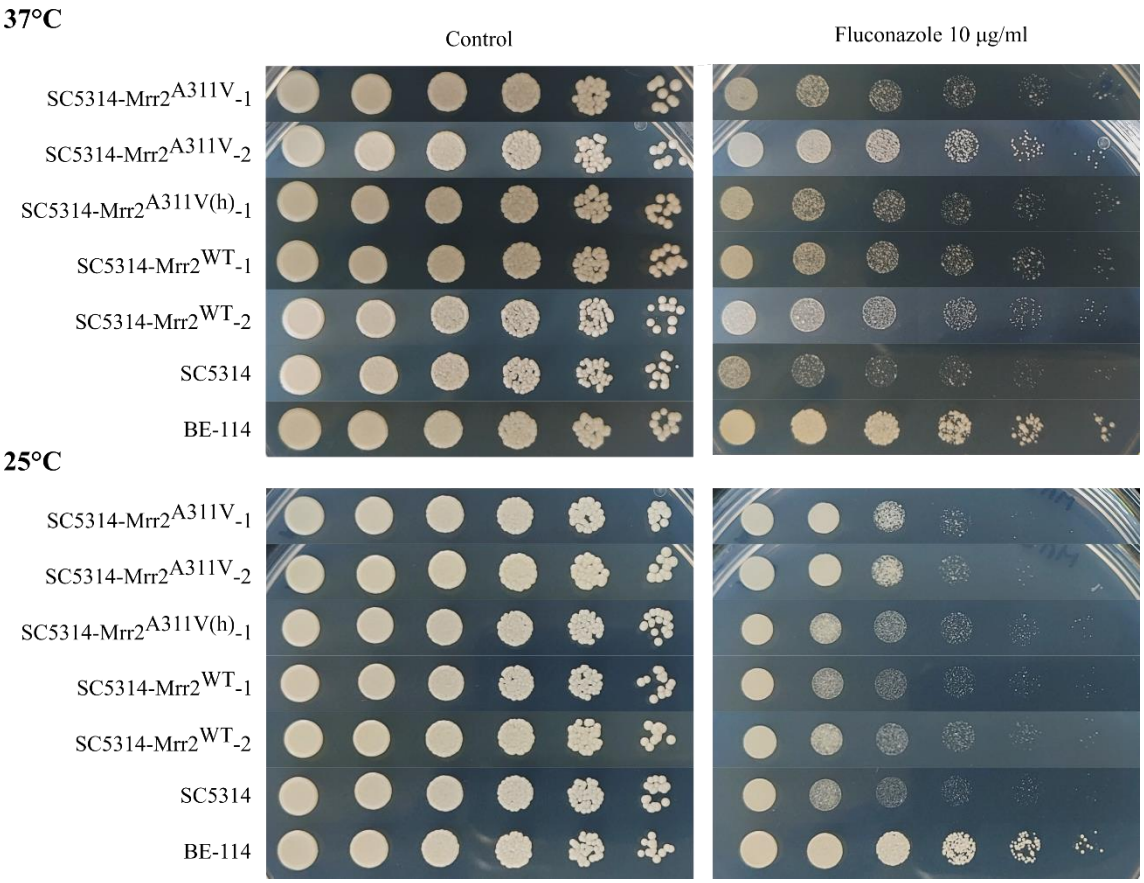

Figure 4.10. Spot assay for Mrr2 transformants, BE-114 and parental SC5314 *C. albicans* strains at 37 and 25°C after 48 and 72h of incubation.

4.4.6. Gene expression analysis

Since both Tac1 and Mrr2 are transcription factors that regulate the ABC efflux pumps Cdr1 and Cdr2 (only Tac1), expression levels of these genes were measured by RT-qPCR.

4.4.6.1. Tac1 transformants

The *CDR1* and *CDR2* genes expression was not significantly altered in the mutant or WT transformants in reference to the SC5314 parental strain. Nonetheless, we confirmed that the BE-113 clinical isolate exhibited higher expression of *CDR1* (x1.7) and *CDR2* (x71), even though it did not harbour any of the previously described GOF mutations in Tac1 or Mrr2 (Figure 4.11 A).

4.4.6.2. Mrr2 transformants

In this case, *CDR1* and *CDR2* expression was also unaltered. In addition, the BE-114 clinical isolate when compared only to SC5314 did not exhibit increased expression of either of the genes, which did when was compared to a pool of susceptible isolates. Surprisingly, it even showed a significant downregulation of *CDR1* (x-1.9) (Figure 4.11 B).

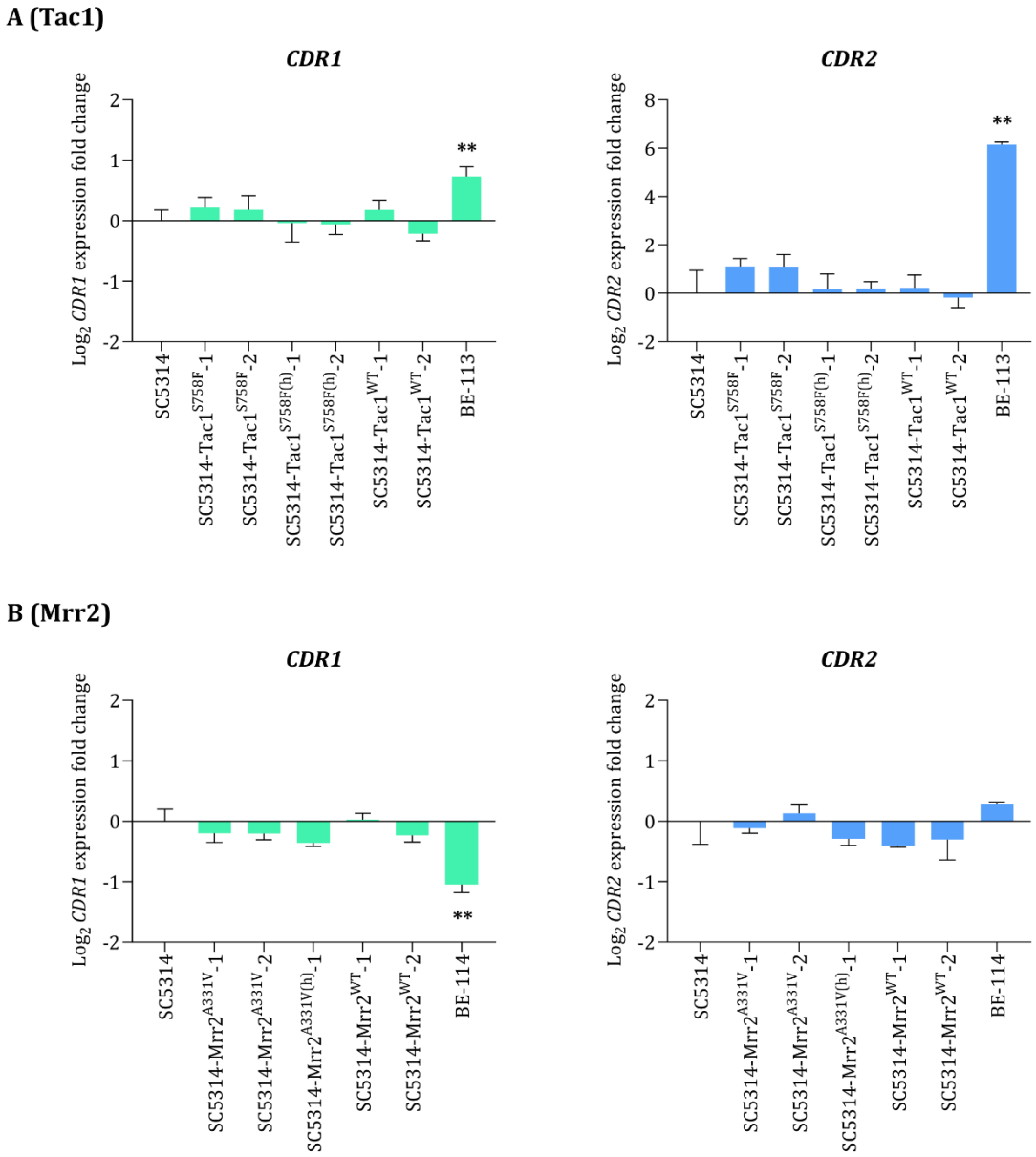

Figure 4.11. *CDR1* and *CDR2* mRNA expression level in CRISPR-Cas9-obtained transformants for Tac1 (A) and Mrr2 (B) measured by RT-qPCR relative to *C. albicans* SC5314. Error bars indicate standard deviations (SD) of three RNA extraction replicates. **Statistical significance with reference to the *C. albicans* SC5314 strain P<0.01.

4.5. In vitro evolution of *C. albicans* in the presence of increasing concentrations of fluconazole

The azole-susceptible *C. albicans* SC5314 and BE-47 strains were exposed to increasing concentrations of FLC (from 0.25 to 64 μg/ml) for 23 days, after which they were subcultured for an additional 32 days-period in the absence of the antifungal drug. In parallel, control populations grown in medium without FLC were maintained throughout the whole experiment. Samples from both the exposed (experimental) and the control populations were taken at different time points of the experiment and stored at -80°C for subsequent analysis.

4.5.1. Susceptibility to azoles

MIC values of five azoles were estimated by broth microdilution methods. MIC values were estimated for the experimental and control populations of time spots 4, 7, 15, 23, 26 and 55 days for the SC5314 strain, and 7 and 23 days for BE-47 (Figure 4.12).

The SC5314 strain exhibited a decrease in susceptibility for all the azoles tested, becoming resistant to FLC, CLT and POS, SDD to ITC, while remaining sensitive to VRC, even though we recorded a 4-fold increase in MIC for this antifungal agent (Figure 4.12 A). It has to be noted that the experimental population of the 7th day (SC5314_t7, 4 μg/ml FLC) exhibited the highest increase in MIC values. From this point onwards, the experimental populations retained the achieved resistance level that was maintained even after removing fluconazole from the media.

On the other hand, the BE-47 only acquired resistance to CLT, while FLC, ITC and VRC MIC values only registered a slight increase (Figure 4.12 B).

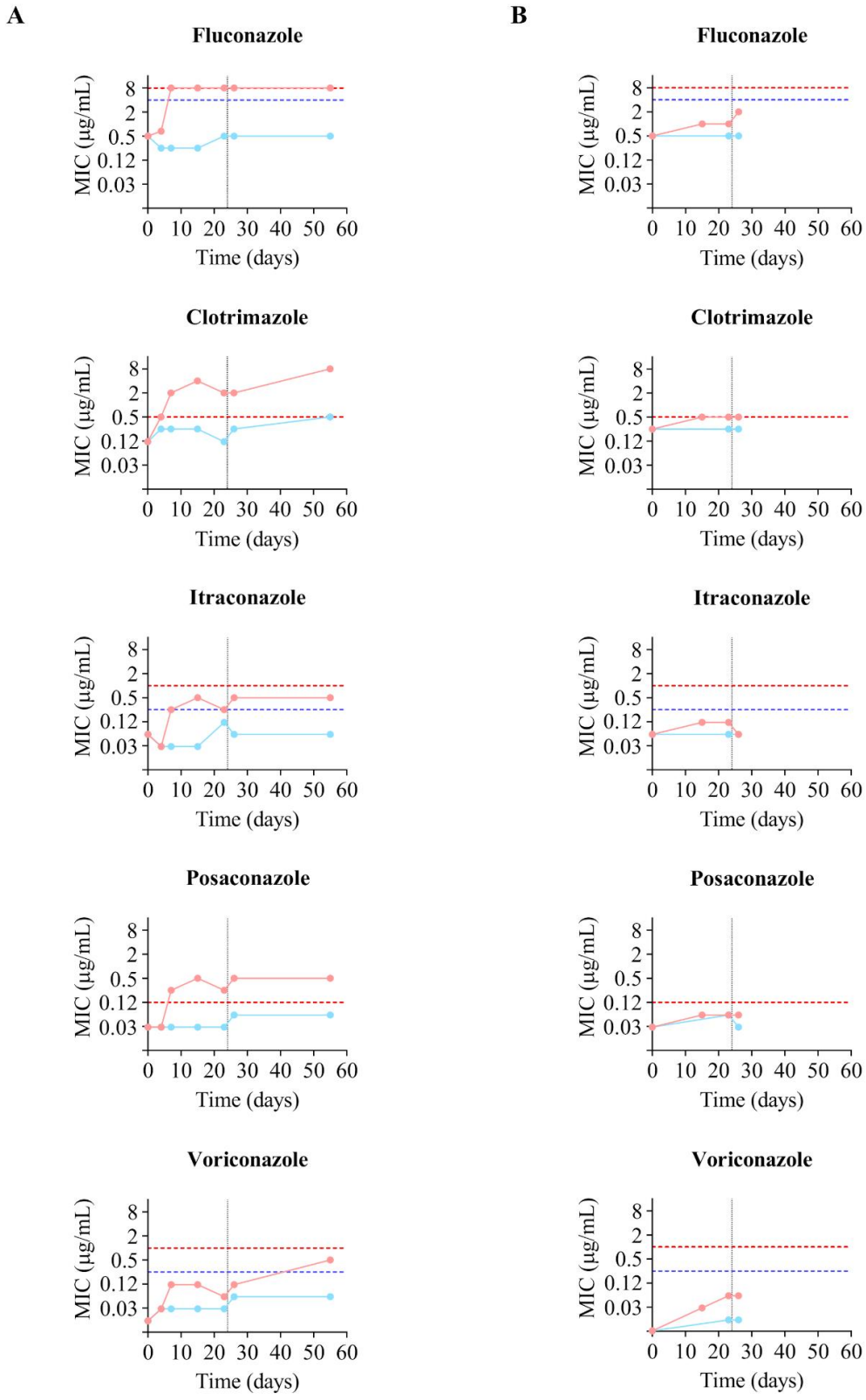

Figure 4.12. Evolution of azoles MIC for the SC5314 (A) and BE-47 (B) populations. Pink line, experimental populations; light blue line, control populations. The horizontal red and blue dashed lines indicate the antifungal drug cut-off values for resistant and susceptible-dose dependent *C. albicans* strains, respectively. The vertical dotted line denotes the time of fluconazole removal in the evolution experiment.

4.5.2. Mutations in Erg11, Tac1, Upc2, Mrr1, Mrr2 and Erg3

The SC5314 derived populations presented two amino acid substitutions in heterozygosis in Erg11 (D116E and K128T), which have been previously described as not being linked to azole resistance (Table 4.13).

The *TAC1* gene showed more polymorphisms leading to amino acid substitutions. The initial and control populations exhibited six heterozygous mutations not associated to azole resistance (N396S, N772K, D776N, E829Q, S935L and S941P). These mutations were also present in the experimental populations of days 4 (SC5314_t4, 0.5 μg/ml FLC) and 5 (SC5314_t5, 1 μg/ml), but they were absent in the subsequent populations. Besides, we also found the N977D azole resistance-associated mutation (Coste et al., 2006), first in heterozygosis in experimental populations t4 and t5, and turning homozygous from day 7 population onwards. The loss of heterozygosity (LOH) of the latter mutation was accompanied with the loss of the other amino acid heterozygotic substitutions present in the control and previous experimental populations (Table 4.13). We did not find any mutations in *UPC2*, and the *MRR1*, *MRR2* and *ERG3* genes were not sequenced for the SC5314-derived populations.

In the case of the BE-47, the mutations found in Erg11 and Tac1 of the control and experimental populations of day 23 did not exhibit any changes with respect to the initial population (BE-47_t0) and coincided with those presented by SC5314 control populations. Therefore, intermediate time-points were not analysed (Table 4.13). Concerning Upc2, Mrr1 and Mrr2, no amino acid substitutions were found in BE-47 populations. Since no relevant mutations were detected for BE-47 in the studied genes, *ERG3* was sequenced and the V351A mutation was identified, which was again shared by the initial and the day 23 populations. In addition, this amino acid substitution was already reported as not significant for azole resistance (Morio et al., 2012)(Table 4.13).

Table 4.13. Erg11, Tac1 and Erg3 amino acid substitutions detected in experimental and control populations of *C. albicans* SC5314 and BE-47 strains derived from different times along the exposition to FLC.

Population	Erg11		Tac1							Erg3
	D116E	K128T	N396S	N772K	D776N	E829Q	S935L	S941P	N977D	V351A
SC5314_t0										NA
SC5314_t4C										NA
SC5314_t4										NA
SC5314_t5C										NA
SC5314_t5										NA
SC5314_t7C										NA
SC5314_t7										NA
SC5314_t15C										NA
SC5314_t15										NA
SC5314_t23C										NA
SC5314_t23										NA
SC5314_t26C										NA
SC5314_t26										NA
SC5314_t55C										NA
SC5314_t55										NA
BE-47_t0										
BE-47_t23C										
BE-47_t23										

t0, t4, t5, ...: days of exposition to FLC. C indicates control populations that were grown without FLC in parallel to the exposed populations. NA, not analysed. Blue: previously described mutations; green: previously described mutations associated to resistance; light colour: mutations in heterozygosis; dark colour: mutations in homozygosis.

4.5.3. Expression of *CDR1*, *CDR2*, *MDR1* and *ERG11* genes

We also examined other well-described resistance mechanisms like the overexpression of efflux pumps and azoles' target enzyme Erg11, and measured the relative expression level of *CDR1*, *CDR2*, *MDR1* and *ERG11* genes by RT-qPCR of different populations obtained after FLC exposure.

4.5.3.1. RT-qPCR efficiency

The efficiency values for each gene are listed in Table 4.14. Again, we were unable to determine the efficiency for *CDR2* gene due to its low expression level.

Table 4.14. Efficiency values of the amplification reaction for each gene.

Gene	Gene name	Efficiency
CDR1	Candida Drug Resistance 1 – ABC efflux pump	1.02
CDR2	Candida Drug Resistance 2 – ABC efflux pump	-
MDR1	Multidrug Resistance 1 – Major Facilitator pump	1.06
ERG11	Cytochrome P450 lanosterol 14α-demethylase	1.06
ACT1	Actin	1.03
PMA1	Plasma membrane H^+-ATPase	1.13
RPP2B	Cytosolic ribosomal acidic protein P2B	1.06
LSC2	Succinyl-CoA synthetase β-subunit fragment	1.10
CPA1	Carbamoyl-phosphate synthetase small subunit	1.01
IMH3	Inosine-5'-monophosphate dehydrogenase fragment	0.93
RIP	Ubiquinol cytochrome-c reductase complex component	1.04

4.5.3.2. Reference genes' stability

The results of the stability calculations displayed in Figure 4.13 revealed that *ACT1*, *PMA1* and *RPP2B* were the most stable genes, so they were selected for normalization.

A

Gene name	Stability value
ACT1 | PMA1	0.260
RPP2B	0.350
CPA1	0.572
IMH3	0.699
RIP1	0.849
LSC2	1.023

B

Gene name	Stability value
PMA1	0.098
RPP2B	0.189
ACT1	0.324
CPA1	0.604
IMH3	0.744
RIP1	1.216
LSC2	1.395

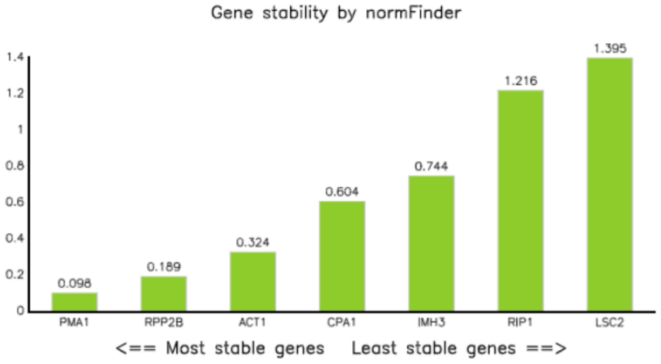

C

	Pearson correlation coefficient (r)						
BestKeeper vs.	ACT1	PMA1	RPP2B	LSC2	CPA1	IMH3	RIP1
coeff. of corr. [r]	0.227	0.564	0.547	0.001	0.502	0.548	0.810
p-value	0.416	0.028	0.035	0.900	0.056	0.034	0.001

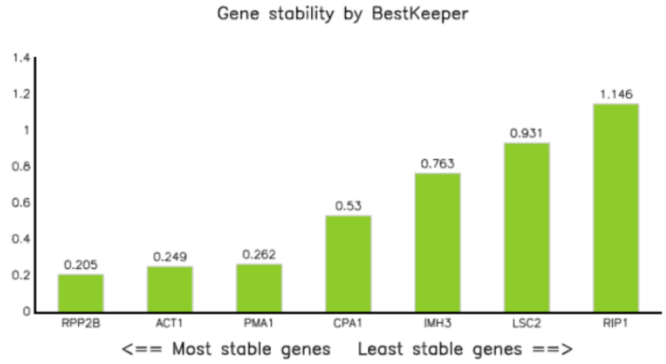

Figure 4.13. Stability analysis of the reference genes by A) GeNorm, B) normFinder, and C) BestKeeper.

4.5.3.3. Level of expression of the selected genes

The SC5314 experimental populations revealed an increased expression of Cdr1 and Cdr2 efflux pumps. In both cases, the highest increase was observed in populations of days 7 (SC5314_t7, 4 μg/ml FLC) and 15 (SC5314_t15, 64 μg/ml FLC), where a 4 and 7 fold-change were registered for *CDR1*, and 320 and 1000 fold-change for *CDR2*, respectively (Figure 4.14 A). The subsequent experimental populations experienced a reduction in expression going down to around 3 and 200 fold-change, respectively for *CDR1* and *CDR2*. Regarding *MDR1* expression, only t15 population presented higher expression levels than control. Finally, no changes in *ERG11* were detected.

Conversely, BE-47 did not experience any increase in expression levels of the studied genes (Figure 4.14 B).

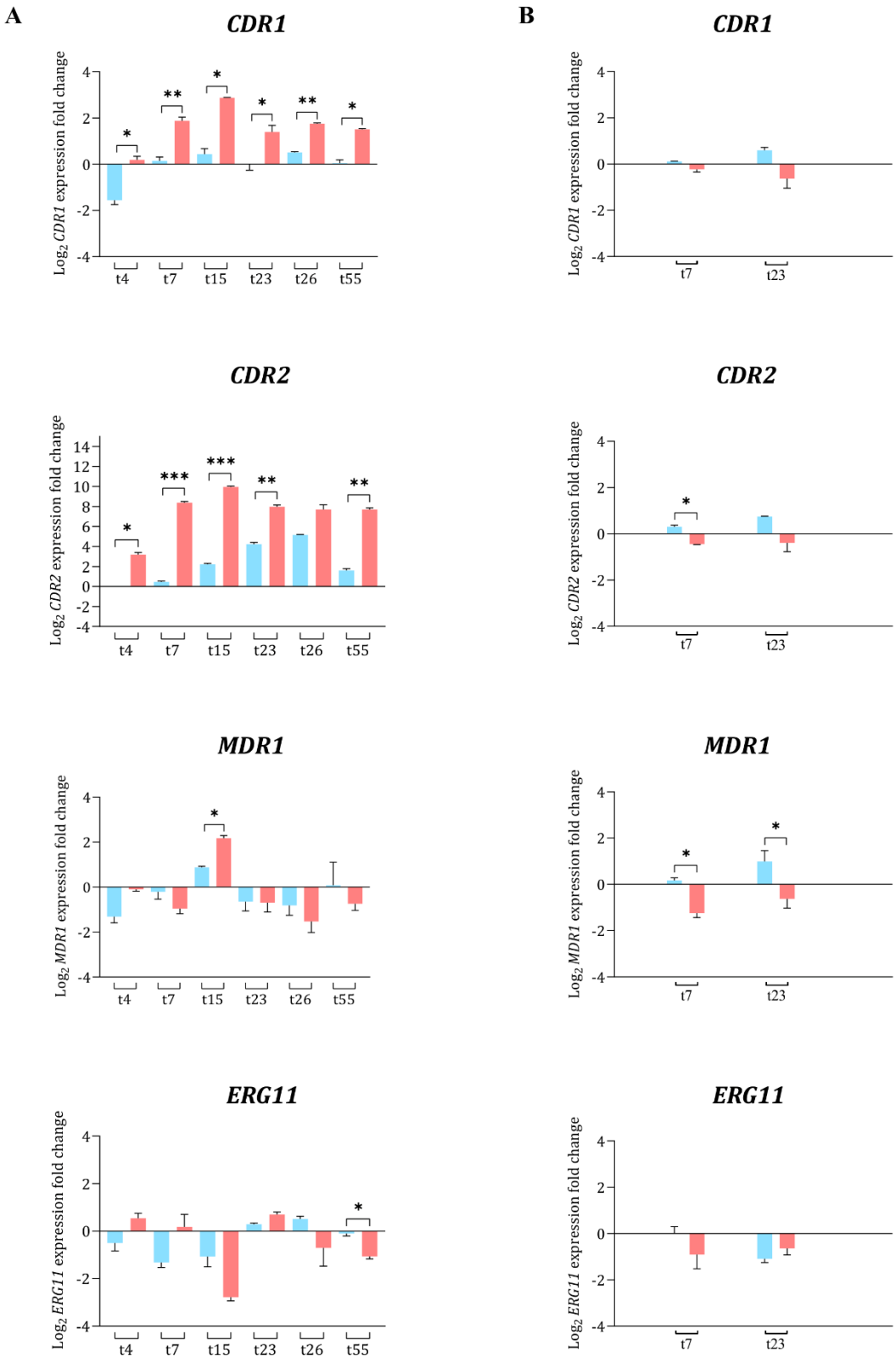

Figure 4.14. Relative mRNA expression levels of *CDR1*, *CDR2*, *MDR1* and *ERG11* genes in experimental and control populations derived from *C. albicans* SC5314 (A) and BE-47 (B) by reference to their respective initial populations (t0), expression measured by RT-qPCR. Pink bars represent the experimental populations and blue bars stand for the control populations. Statistical significance: *P <0.05; **P<0.01; ***P<0.001.

4.5.4. Zygosity of the *MTL* locus

The analysis of the mating-type like locus (*MTL*) revealed that both the a and the α *MTL* alleles were present in all populations (Figure 4.15 A). When we looked at 10 random clones (colonies) of every population of the FLC exposure experiment, all of them appeared heterozygous for *MTL* with the exception of three clones from SC5314_t23 population (lanes 11, 14 and 15 of Figure 4.15 B) and two from SC5314_t26 (lanes 32 and 37), that carried only the *MTLa1* allele.

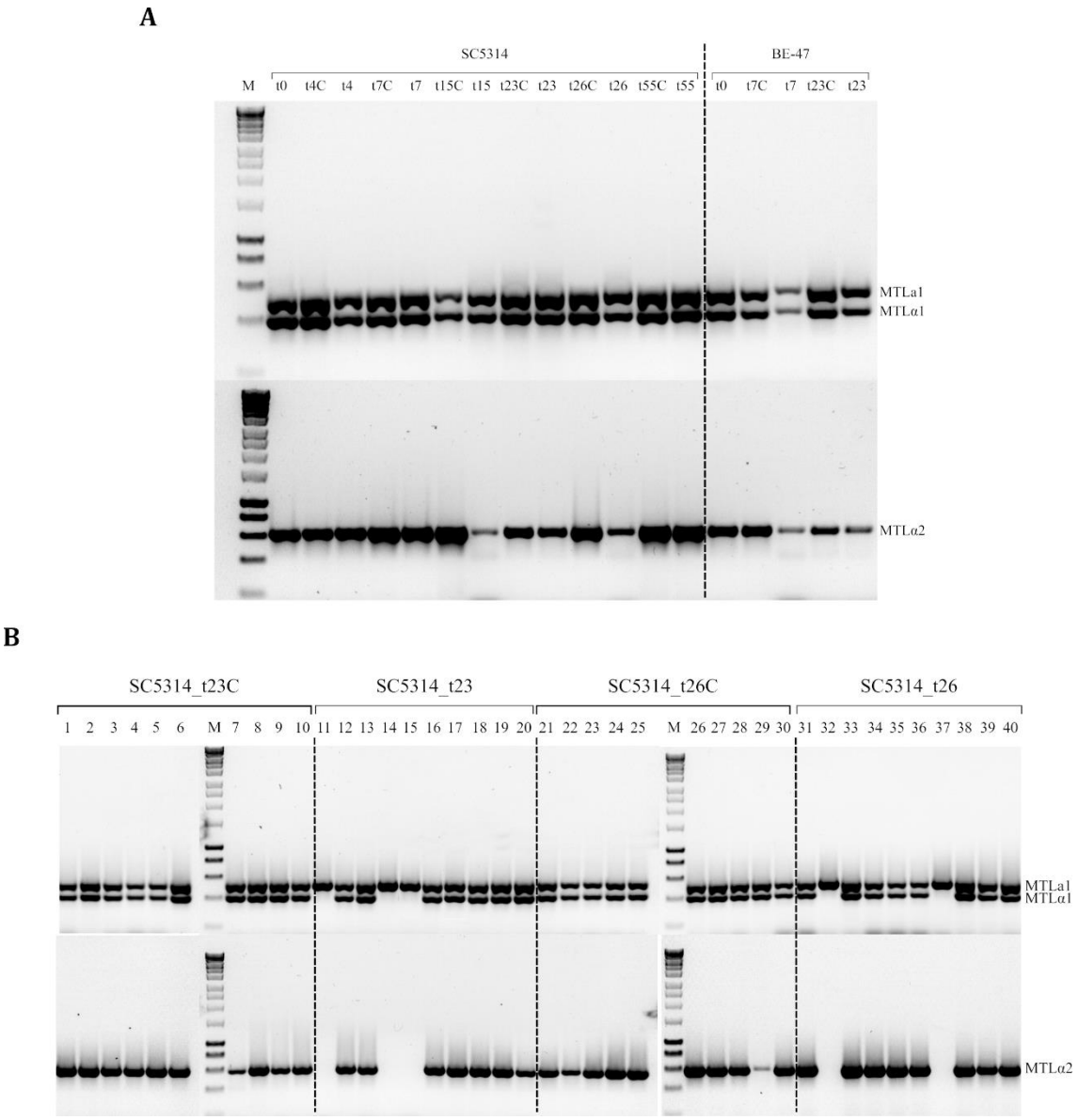

Figure 4.15. *MTL* genotype. A) Control and experimental populations of *C. albicans* SC5314 and BE-47. The dotted line separates SC5314 and BE47-derived populations. B) Ten clones representing SC5314_t23 and t26 control(C) and experimental populations, separated by dotted lines. M, molecular size marker.

4.5.5. Fitness

The fitness, calculated as the reverse value of the doubling time, of all derived populations analysed in this study in reference to their respective initial population (t0) is represented in Figure 4.16

For SC5314, only the t4 population showed a significant decrease in its fitness at both temperatures when compared to the initial population, but it did not when compared with its corresponding control. In addition, there is an evident decrease in the fitness of both t4 populations compared to the subsequent populations. This observation was more pronounced at 37°C.

For BE-47, there was a striking difference between the results at 37 and 30°C. At 37°C, there was no difference between the experimental and their corresponding control population or the initial one (Figure 4.16). On the contrary, at 30°C, we observed a significant increase in fitness of the t7 and t23 experimental populations compared to their control and initial populations (Figure 4.16).

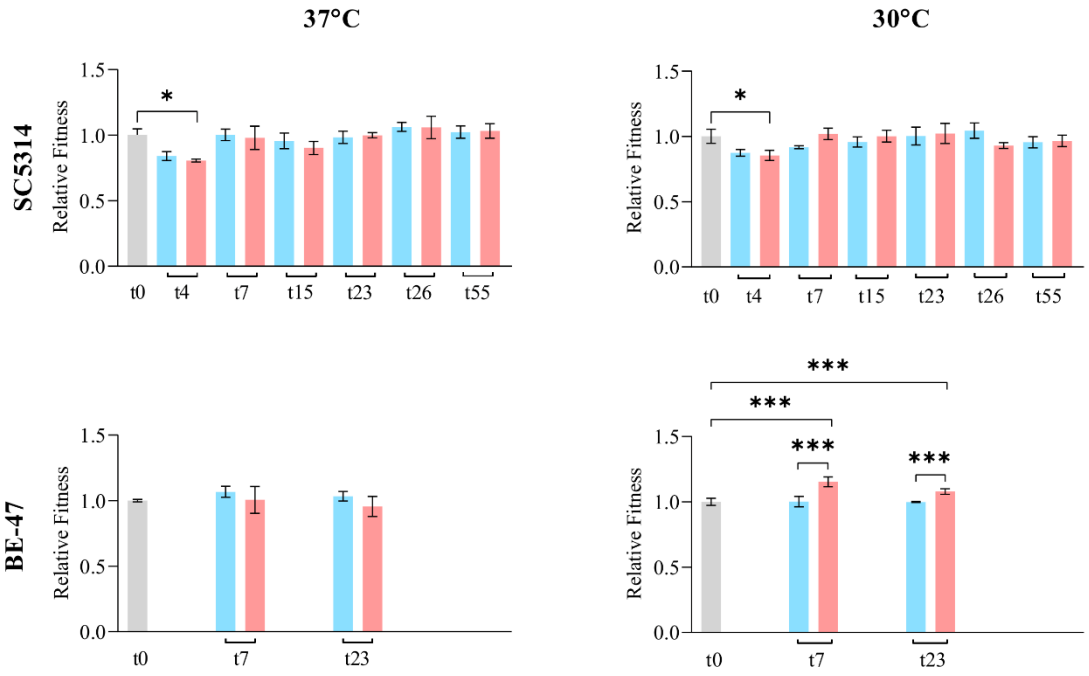

Figure 4.16. Fitness for experimental (pink bars) and control (light blue bars) populations of *C. albicans* SC5314 and BE47. The grey bar represents the population at time 0. Statistical significance: *P<0.05; ***P<0.001.

4.5.6. Tolerance

Although BE-47 populations did not seem to have acquired resistance to fluconazole and did not show any of the most common azole resistance mechanisms described in the literature, they were able to grow at the highest azole concentration in our experiment, 64 μg/ml. A possible explanation could be that BE-47 had a higher tolerance level to fluconazole than SC5314. In order to assess the tolerance of the initial, control and experimental populations of both strains we performed a variation of the CLSI broth microdilution assay in which we measured the OD after 24 and 48h of incubation at either 25 or 37°C. Measurements after 24h were used for MIC calculations and after 48h for supra-MIC-growth (SMG) as a numerical representation of the tolerance level.

When grown at 37°C, the SC5314 experimental populations exhibited higher SMG values than their corresponding controls (Figure 4.17 A), while at 25°C these differences were less evident and the control populations showed even higher SMG values than their corresponding experimental populations (Figure 4.18 A). It has to be noted that in general the SMG was higher at 37°C than at 25°C.

For BE-47, the experimental population of time 23 showed a big increase in its SMG value compared to the rest of populations at 37°C (Figure 4.17 B), while at 25°C did not exhibit any noticeable growth above its MIC (Figure 4.18 B). In the rest of the populations the SMG was also lower at 25°C than at 37°C.

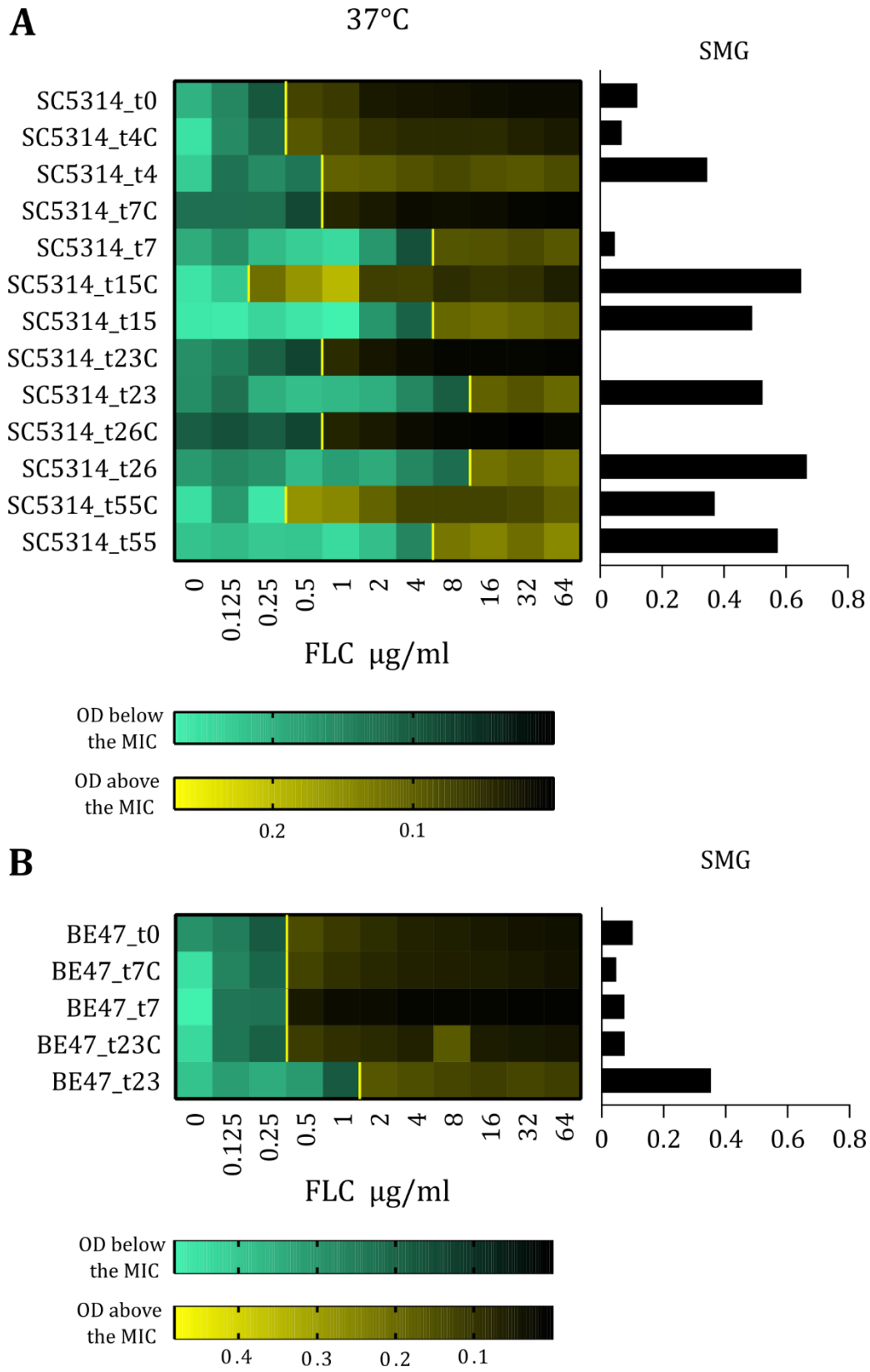

Figure 4.17. Representation of OD measurements at 450 nm of the tolerance plates incubated at 37°C for 48h for SC5314 (A) and BE-47 (B) experimental and control populations, and their supra-MIC growth (SMG) associated values. The wells corresponding to FLC concentrations below the MIC are represented in green and the wells above the MIC are in yellow. The yellow vertical bars indicate the MIC value calculated at 24h.

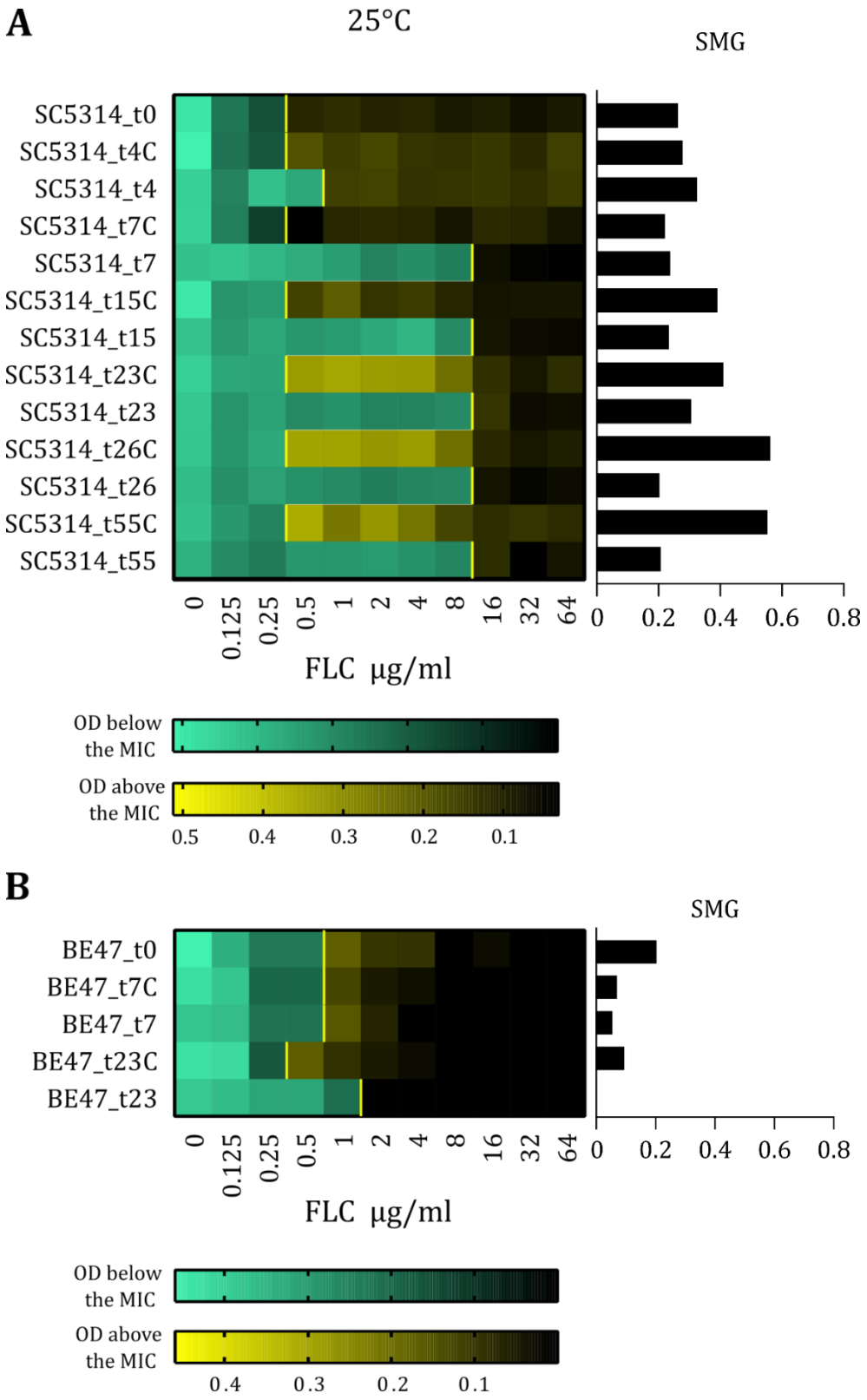

Figure 4.18. Representation of OD measurements at 450 nm of the tolerance plates incubated at 25°C for 72h for SC5314 (A) and BE-47 (B) experimental and control populations and their supra-MIC growth (SMG) associated values. The wells corresponding to FLC concentrations below the MIC are represented in green and the wells above the MIC are in yellow. The yellow vertical bars indicate the MIC value, calculated at 24h.

4.5.7. Spot Assay

In order to have a more visual representation of the different responses to fluconazole of the evolved populations we performed a spot assay in which all populations were spotted on YNB agar supplemented with the FLC concentrations used for CLSI susceptibility testing and tolerance measurement. Also, growth at 37 and 25°C was assessed to further elucidate if tolerance mechanisms could be playing a role in the adaptation to azole pressure of both strains.

After 24h of incubation at 37°C (Figure 4.19, left panel) SC5314 experimental populations showed evident growth at higher FLC concentrations than their corresponding controls, more significantly from population of time 7 (SC5314_t7) onwards. Curiously, BE-47 experimental populations had none or little growth at any concentration, while the initial and control populations exhibited normal growth at the lower concentrations. On the other hand, at 25°C all populations had very weak growth.

After 48h the differences in growth are far more evident both at 37°C (Figure 4.20, up) and 25°C (Figure 4.20, down) in the SC5314 derived populations. We also observed that at 37°C all populations presented small colonies at concentrations around and above their MIC, while at 25°C they disappeared. In the case of BE-47, the initial and control populations appeared to have stronger growth than SC5314 populations at 37°C. Intriguingly, the experimental population of time 7 (BE47-t7) showed persistent growth at high concentrations but weaker than its corresponding control. As observed for SC5314, growth above MIC was completely abolished at 25°C.

The results after 72h of incubation (Figure 4.21) are practically identical to the ones observed at 48h, only revealing that SC5314 experimental and BE47-t23 populations presented small colonies above their MICs even at 25°C.

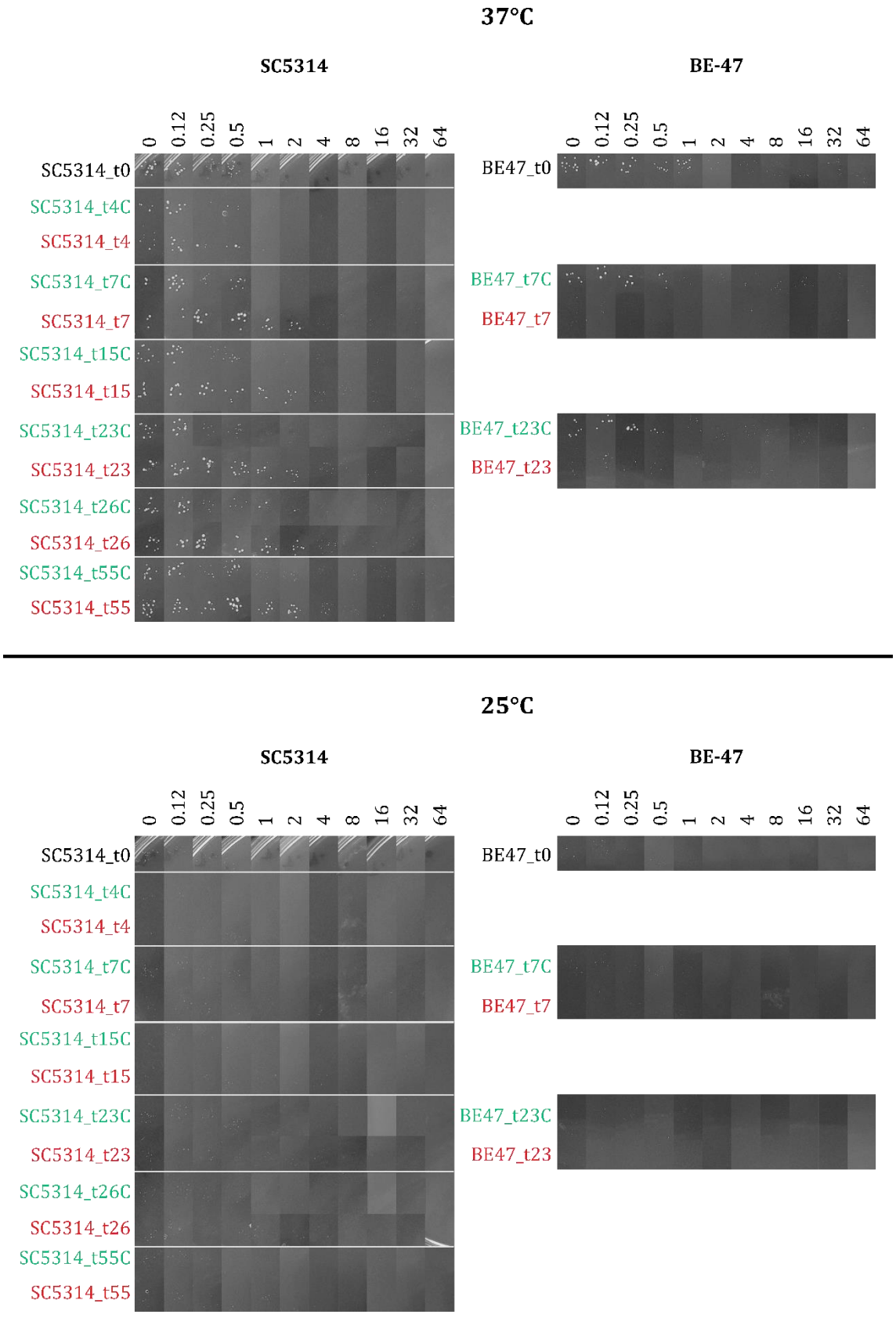

Figure 4.19. Spot Assay of SC5314 and BE-47 control and experimental populations after incubation for 24h in YNB agar with different FLC concentration at 37°C (up) or 25°C (down). The initial population is marked in black; the control populations are in green and the experimental populations in red. FCZ concentration (0 to 64 µg/ml) is indicated on top of the pictures.

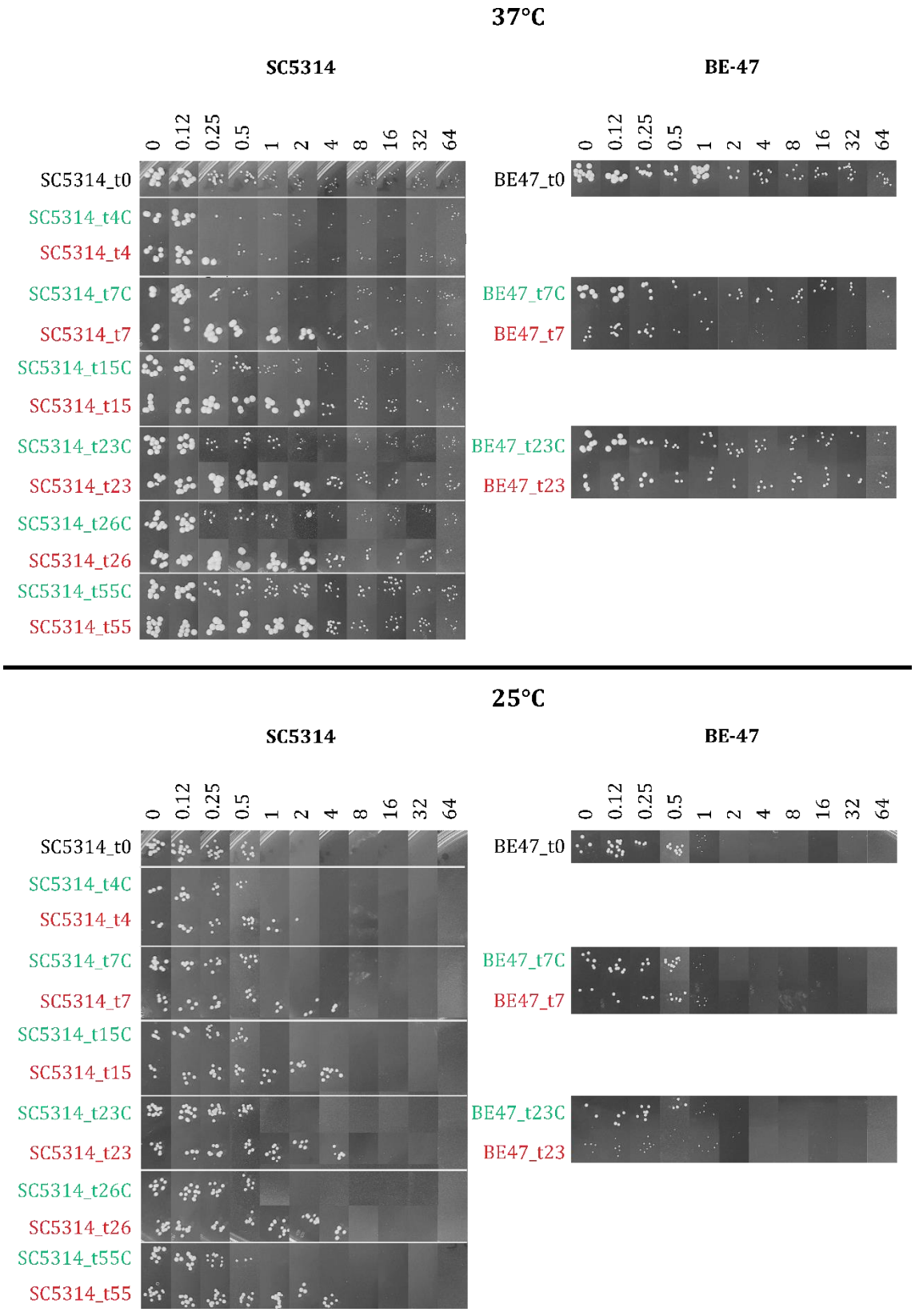

Figure 4.20. Spot Assay of SC5314 and BE-47 control and experimental populations after incubation for 48h in YNB agar with different FLC concentration at 37°C (up) or 25°C (down). The initial population is marked in black; the control populations are in green and the experimental populations in red. FCZ concentration (0 to 64 μg/ml) is indicated on top of the pictures

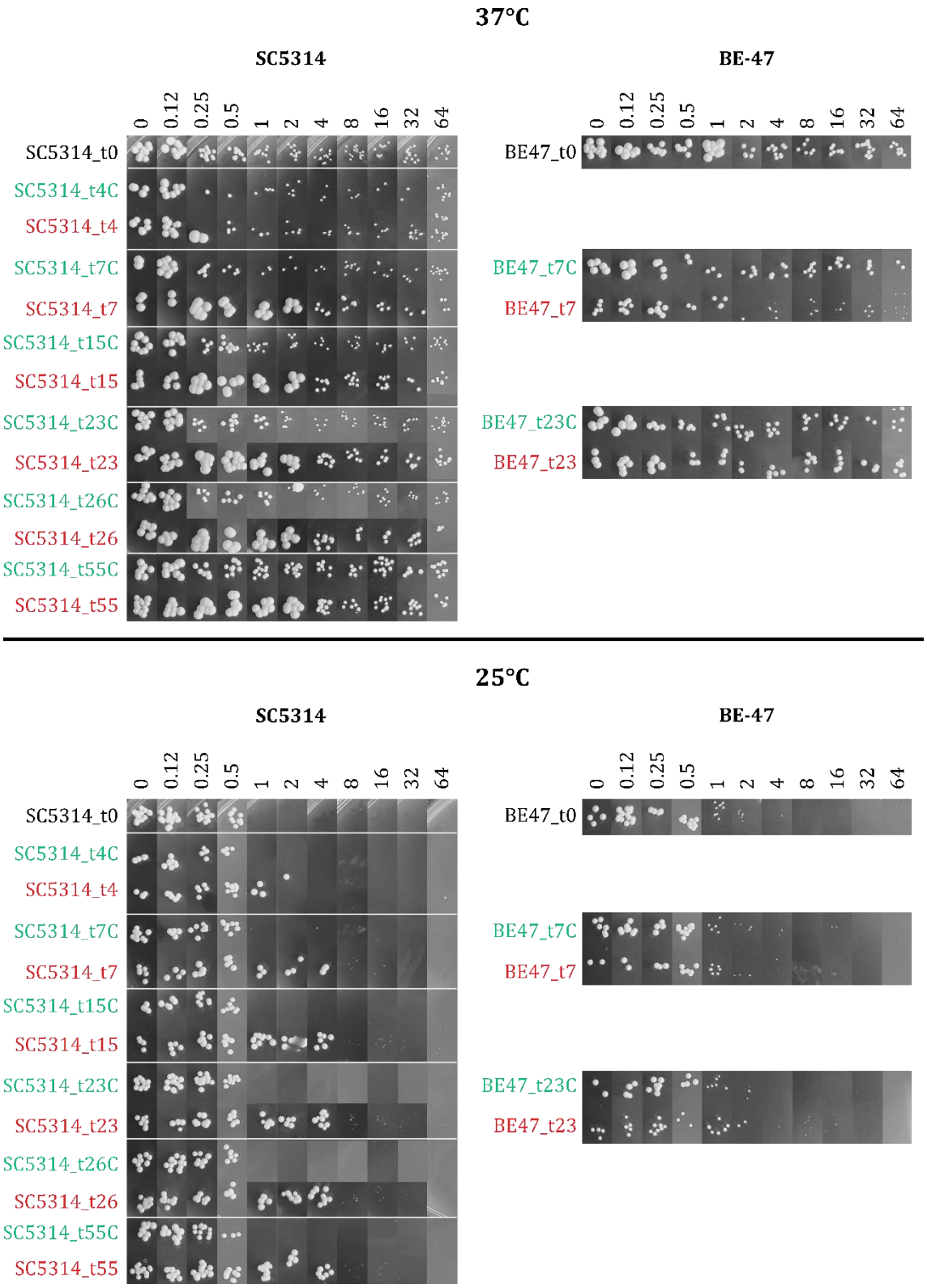

Figure 4.21. Spot Assay of SC5314 and BE-47 control and experimental populations after incubation for 72h in YNB agar with different FLC concentration at 37°C (up) or 25°C (down). The initial population is marked in black; the control populations are in green and the experimental populations in red. FCZ concentration (0 to 64 µg/ml) is indicated on top of the pictures.

DISCUSSION

5. DISCUSSION

Invasive fungal infections caused by *Candida* species are the fourth cause of nosocomial bloodstream infections (Lamoth et al., 2018; McCarty & Pappas, 2016) and have associated high mortality rates (Brown et al., 2012; Cleveland et al., 2012; Doi et al., 2016; Kreusch & Karstaedt, 2013; Puig-Asensio et al., 2014). Among *Candida* species, *Candida albicans* is the most frequently isolated one (McTaggart et al., 2020; Pfaller et al., 2019) and despite usually showing high susceptibility to antifungal drugs (Lockhart et al., 2012; McTaggart et al., 2020; Pfaller et al., 2019) there are reports of increasing azole resistance, limiting the therapeutic choices for fungal infections (Arendrup, 2014; Cuenca-Estrella et al., 2011; Perlin et al., 2017). There are a few well established resistance mechanisms, such as drug target modification or overexpression, enhanced efflux of the drug and alteration of the target biosynthetic pathway (Berkow & Lockhart, 2017; Bhattacharya et al., 2020; Hokken et al., 2019; Ksiezopolska & Gabaldón, 2018; Morio et al., 2017; Murphy & Bicanic, 2021; Perlin et al., 2017; Robbins et al., 2017; Whaley et al., 2017). Nonetheless, there are many *C. albicans* azole-resistant strains lacking these described mechanisms (Berkow & Lockhart, 2017; Ksiezopolska & Gabaldón, 2018; McTaggart et al., 2020) and new mutations are still being reported (Garnaud et al., 2015; Sitterlé et al., 2020; Spettel et al., 2019), strengthening the need for further research in this area.

With this background, we selected 43 clinical isolates of *C. albicans* from the fungal collection of the Department of Immunology, Microbiology and Parasitology of the UPV/EHU, and three reference strains (the azole-susceptible SC5314 and two azole-resistant strains ATCC 64124 and ATCC 64550) in which possible resistance mechanisms were analysed, as well as their associated genes, in search of significant mutations that could be used for diagnostic purposes. First, we determined their susceptibility to fluconazole (FLC) and clotrimazole (CLT) following CLSI's (Clinical and Laboratory Standards Institute) procedure, and those strains showing resistance to one or both azoles and/or showing inconsistent results in replicated experiments were re-evaluated with the commercial Sensititre YeastOne® method. There were some discrepancies in the FLC susceptibility results of both methods. Eight of the FLC-resistant strains that showed strong resistance to FLC (MIC ≥ 64)

with the CLSI method, appeared susceptible by Sensititre. This discrepancy can be due to the subjective evaluation of growth inhibition used in these methods and the fungistatic nature of azole drugs, which allows the fungus to grow above its MIC and making it difficult to be determined (Berkow et al., 2020). In fact, Sensititre YeastOne protocol, in order not to overestimate MICs, recommends establishing the MIC as the first well with a less intense colour than the control well (Kidd et al., 2021), whereas for CLSI the 50% of growth inhibition compared to the control well is determined visually, therefore rendering the first method as easier to interpret (Berkow et al., 2020). Moreover, many of these isolates exhibited trailing growth even after 24h of incubation and MICs varied between replicate experiments. Interestingly, the strains showing inconsistent results between the two methods account for around half of the strains without any of the major resistance mechanisms addressed in this work. The clinical isolates 16-132 and 16-135 were also included in the resistant category due to their intense above the MIC growth exhibited after 48h of incubation in both methods.

We then focused on elucidating the azole resistance mechanisms harboured by the azole-resistant strains. The most common azole resistance mechanisms described in the literature include mutations in the azole target encoding gene *ERG11* (Nishimoto et al., 2020; Perlin et al., 2017; Robbins et al., 2017), and overexpression of Cdr1, Cdr2 and Mdr1 efflux pumps due to gain-of-function (GOF) mutations in their corresponding transcription factors, Tac1 for Cdr1 and Cdr2 (Coste et al., 2006), Mrr1 for Mdr1 (Morschhäuser et al., 2007) and Mrr2 for Cdr1 (Schillig & Morschhäuser, 2013). Consequently, we measured the expression levels of *CDR1*, *CDR2* and *MDR1* genes and sequenced *TAC1*, *ERG11*, and the transcriptional activator of *ERG11*, *UPC2*, that also becomes hyperactivated due to GOF mutations (Dunkel et al., 2008; Flowers et al., 2012; Silver et al., 2004) for all isolates and *MRR1* and *MRR2* for the corresponding overexpressing strains.

A gene was considered significantly overexpressed when it showed a twofold-change in expression compared to that of a group of susceptible isolates, resulting in 53% (10/19) of the isolates overexpressing *CDR1*, five of them also overexpressed *CDR2*, and 21% (4/19) overexpressing *MDR1*, of which three were also overexpressing the other two pumps. It is worth mentioning that *C. albicans* clinical

isolates exhibiting simultaneous enhanced expression of the three efflux pumps are rarely encountered, probably linked to a high fitness cost (Sasse et al., 2012). These results are in agreement with many other reports for *C. albicans* azole-resistant isolates, which also found that overexpression of *CDR* genes is a more common mechanism than *MDR1* overexpression (Chau et al., 2004; Fuentes et al., 2014; Goldman et al., 2004; Khosravi Rad et al., 2016; Kumar et al., 2020; Liu et al., 2015; Mane et al., 2016; Morio et al., 2013; Park & Perlin, 2005; Rojas et al., 2020; Salari et al., 2016; Sanglard et al., 2003; Teo et al., 2019; White et al., 2002; Wu et al., 2018; Xu et al., 2015).

Interestingly, most of the strains overexpressing either *CDR1, CDR2* and/or *MDR1* (9/11) did not harbour any of the previously described GOF mutations in their associated transcription factors Tac1, Mrr1 and Mrr2. Of particular interest is the ATCC 64550 reference strain, which exhibited a highly increased expression of the three efflux pumps, the BE-113 isolate that harboured a new Tac1 mutation in homozygosis (S758F), and the BE-114 isolate presenting also a new mutation in homozygosis in Mrr2 (A311V).

The other two overexpressing strains, ATCC 64124 and 15-176, were among the highly resistant strains of our study and harboured known GOF mutations. The former showed strong overexpression of *CDR1* and *CDR2*, probably linked to the presence of two GOF mutations in Tac1, H839Y and N977D, both in heterozygosis. While the N977D was the first GOF mutation reported in Tac1 (Coste et al., 2006), the H839Y mutation has been recently associated to high resistance levels to FLC and itraconazole (ITC) and decreased susceptibility to voriconazole (VRC) (Sitterlé et al., 2020). This strain also harboured two resistance-associated mutations in Erg11, Y132H (Sanglard et al., 1998) and G450E (Flowers et al., 2015), both frequently reported in the literature in *C. albicans* azole-resistant isolates (Asai et al., 1999; Chau et al., 2004; Coste et al., 2007; Favre et al., 1999; Flowers et al., 2015; Garnaud et al., 2015; Goldman et al., 2004; Jensen et al., 2015; Kamai et al., 2004; Li et al., 2004; Liu et al., 2015; Löffler et al., 1997; Manavathu et al., 1999; Marichal et al., 1999; Morio et al., 2010; Park & Perlin, 2005; Sanglard et al., 1998; Siikala et al., 2010; Wang et al., 2009; Xiang et al., 2013; Xu et al., 2008; Ying et al., 2013). Moreover, when found together, these mutations have been associated to FLC, ITC

and VRC resistance (Chau et al., 2004). On the other hand, strain 15-176 showed a high overexpression of *CDR2* and *MDR1*, in addition to a 5-fold-increase in *CDR1* expression. The ABC efflux pumps expression is most certainly correlated to two GOF mutations found in Tac1, A736V and a deletion between amino acids 962 and 969 (ΔL962-N969) (Coste et al., 2007), both in heterozygosis, whereas *MDR1* enhanced expression is linked to the Mrr1 GOF mutation G947S (Lohberger et al., 2014). Additionally, it presented the R467K Erg11 mutation, previously associated to FLC resistance (Sanglard et al., 1998), and the Upc2 GOF mutation A643V (Hoot et al., 2011) in heterozygosis. The high azole resistance exhibited by these two isolates agrees with the literature reporting that the highest levels of azole resistance are obtained when several resistance mechanisms are combined in the same isolate (Sasse et al., 2012). Nevertheless, even though it has been demonstrated that homozygous GOF mutations implicate higher resistance than in heterozygosis (Morschhäuser, 2016; Sasse et al., 2012), our strains were heterozygous for Tac1 and Upc2.

Other isolates with lower resistance levels were either those exhibiting variable susceptibility results, some of them probably being tolerant rather than resistant (higher MICs after 48h of incubation) (Berman & Krysan, 2020; Rosenberg et al., 2018), or those that only harboured mutations in Erg11 and Upc2, which is consistent with the study of Sasse and collaborators (Sasse et al., 2012) claiming that the combination of these two mechanisms had the lowest effect on resistance. Interestingly, strain 16-132, one of the two isolates that exhibited elevated MICs after 48h of incubation, showed increased expression of the three efflux pumps despite not presenting any GOF mutations in the corresponding transcription factors. There are different theories for this behaviour, some subpopulations might have undergone a duplication of the right arm of chromosome 3, which contains the *CDR1*, *CDR2* and *MRR1* genes (Selmecki et al., 2009), coupled with trisomy of chromosome 7, where the Hsp90 tolerance mediator encoding gene is located (Mount et al., 2018). Moreover, drug uptake and efflux have also been associated to azole tolerance. In fact, tolerant isolates were shown to contain lower amounts of azole drugs than non-tolerant ones, while azole-resistant isolates had very low intracellular drug concentrations (Rosenberg et al., 2018). This may be associated to mechanistic differences between azole resistance and azole tolerance. In a

resistant strain harbouring GOF mutations in efflux pumps transcription factors, all or most cells would overexpress Cdr1 and Cdr2, greatly reducing intracellular azole levels. On the contrary, in a tolerant strain, the amount of efflux pump expression would vary among subpopulations, with those having higher expression being able to moderately decrease the intracellular azole concentration (Berman & Krysan, 2020).

The remaining resistant isolates can be divided into two groups, the ones that did not present any of the described mechanisms, including the highly resistant isolates 16-092 and 15-154, or those that overexpressed efflux pumps but did not harbour GOF mutations in their transcription factors, like strains 16-138, ATCC 64550 and 15-159. Because we only sequenced the gene regions where the majority of the GOF mutations had been described for *ERG11*, *TAC1*, *UPC2* and *MRR1* genes, we may have missed some mutations that could account for the resistance of these strains. Alternatively, they may have acquired other resistance mechanisms that we did not contemplate in our study or are still to be discovered (Berkow & Lockhart, 2017; Ksiezopolska & Gabaldón, 2018). As indicated in the next paragraph some other transcription factors implicated in regulation of ABC efflux pumps expression have been identified and are under study, such as Fcr1, Ndt80, Ncb2 or even mRNA stability.

Deletion of the zinc cluster transcription factor *FCR1* in *C. albicans* resulted in increased azole resistance, so loss-of-function (LOF) mutations in this transcription factor could confer azole resistance (Talibi & Raymond, 1999), but this mechanism has not yet been reported in *C. albicans* azole-resistant isolates (Morschhäuser, 2010). Another transcription factor involved in regulating *CDR1* expression is Ndt80, whose overexpression in *S. cerevisiae* induced that of *CDR1*, which in turn reduced azole susceptibility (Chen et al., 2004). Nonetheless, in a more recent study, Tac1- and Mrr1-mediated expression of their respective target efflux pumps Cdr1/Cdr2 and Mdr1 was independent of Ndt80 (Sasse et al., 2011). Finally, Ncb2, the β-subunit of the negative RNA polymerase II regulator NC2, plays an important role in basal and activated transcription of *CDR1* in *C. albicans*. This cofactor binds to the NRE (negative regulator element) of the *CDR1* promoter and, when repressed, it enhanced FLC resistance together with increased *CDR1* expression. Moreover,

azole-resistant *C. albicans* strains showed increased recruitment of Ncb2 at their promoter and, while in resistant strains it was localized to the core TATA box promoter region, eliciting transcription, in susceptible strains it was found upstream inhibiting transcription. Tac1 was proposed to be essential for this positional change, supported by the observation that in a *C. albicans* azole-resistant strain Ncb2 recruitment to other Tac1 regulated genes was increased (Shukla et al., 2011). In addition to alternative *CDR1* transcription factors, increased mRNA stability of *CDR1* transcripts was linked to increased amounts of Cdr1 transporters (Manoharlal et al., 2008).

On the other hand, regulation of *MDR1* expression has also been associated to different transcription factors other than Mrr1, such as Mcm1, Cap1 and Rep1. The Mcm1 regulator, involved in cell morphology, was proposed to bind to the BRE (benomyl responsive element) *cis*-acting element of the *MDR1* promoter, which was essential for high constitutive expression of the gene in a *C. albicans* azole-resistant strain (Rognon et al., 2006). Riggle and Kumamoto (Riggle & Kumamoto, 2006) showed that Mcm1 also bound to a region of the *MDR1* promoter, which is necessary for *MDR1* overexpression in FLC-resistant strains. Additionally, mutations in this region abolished binding of Mcm1, abrogating *MDR1* overexpression too. Mcm1 was also shown to be required for *MDR1* Mrr1-mediated overexpression (Mogavero et al., 2011).

The Cap1 (*C. albicans AP-1*, homologous to the AP-1 bZip transcription factor of *Saccharomyces cerevisiae*) has been linked to *MDR1* transcriptional regulation. Either this transcription factor is overexpressed or hyperactivated in *S. cerevisiae* there is an increase in azole resistance (Alarco et al., 1997; Alarco & Raymond, 1999). However, studies in *C. albicans* reported conflicting results. Alarco and Raymond (Alarco & Raymond, 1999) showed that deletion of Cap1 in a *C. albicans* azole-resistant strain did not decrease *MDR1* expression, so another transcription factor was involved in its high constitutive expression. In contrast, Znaidi et al. (Znaidi et al., 2009) demonstrated that increasing Cap1 expression in *C. albicans* resulted in increased FLC resistance and *MDR1* expression. Furthermore, the study of Schubert et al. (Schubert, Barker et al., 2011) highlighted a more complex regulation of *MDR1* expression involving both Cap1 and Mrr1. While hyperactivated

CAP1 and *MRR1* alleles were shown to act synergistically on *MDR1* expression and azole resistance, only the activity of Mrr1 was linked to FLC resistance. Moreover, if hyperactive forms of either transcription factor were introduced into mutants lacking *MDR1*, only a moderate decrease of azole resistance was seen, suggesting that other Cap1 or Mrr1 target genes contributed to azole resistance together with *MDR1*. Besides *MDR1*, Cap1 was also implicated in the modulation of other genes involved in azole resistance, which suggests that this transcription factor could play a role, directly or indirectly, in azole susceptibility (Znaidi et al., 2009).

An alternative transcription factor involved in *MDR1* regulation is Rep1 (Regulator of Efflux Pump 1), which was identified as a negative regulator in *C. albicans*. Deletion of the Rep1 encoding gene in *C. albicans* resulted in increased resistance to FLC and VRC. In addition, it enhanced the expression of *MDR1* in the presence of 4-NQO (4-nitroquinoline-N-oxide), a known inducer of *MDR1*, beyond that of wild-type cells. So, Chen et al. (Chen et al., 2009) proposed an interaction with Mrr1, in which Rep1 either occupies the promoter blocking access for Mrr1 or binds this transcription factor directly or indirectly, being released in the presence of the drug.

Interestingly, Upc2 has also been shown to regulate expression of both ABC and MFS pumps, either acting as an inducer or a repressor depending upon the target or activating signal (Znaidi et al., 2008), although its influence in azole resistance is mainly attributed to its key role as a sterol biosynthesis regulator (Paul & Moye-Rowley, 2014). In fact, expression of *UPC2* GOF-containing alleles in a strain lacking Mrr1 failed to induce *MDR1* expression, and when introduced in a Δ*mdr1* deletion mutant there was no change in azole susceptibility (Schubert et al., 2011).

Even though these transcriptional activators have not been reported to be directly involved in azole resistance exhibited by *C. albicans* clinical isolates, they may have been overlooked because many studies on azole resistance did not contemplate them (Morschhäuser, 2016).

Another interesting observation came from the analysis of the overall mutation rate in the 5 genes we studied in our clinical isolates. Besides the non-synonymous mutations reported in this thesis, many synonymous single nucleotide polymorphisms (SNPs) were detected. In *ERG11*, 27 different SNPs leading to amino acid substitutions were identified, while 23 did not entail amino acidic changes.

Most of the strains exhibited between 8 and 16 SNPs, of which the majority were synonymous. Interestingly, the strains harbouring resistance-associated mutations presented very few or none additional mutations, either synonymous or non-synonymous, and were always homozygous, except for strain 15-159. This observation suggests that if *ERG11* presents many polymorphisms, it is highly probable that none of them contributes to azole resistance, whereas the detection of very few and homozygous is associated with a high probability of azole-resistance.

Similarly, 27 non-synonymous SNPs were detected in *TAC1*, but we found up to 41 synonymous nucleotide changes. Almost all strains had around 20 substitutions of both types and differently to what was observed in Erg11, all the GOF mutations identified were heterozygous. The high number of SNPs detected agrees with the heterozygosity rate reported for chromosome 5, where *TAC1* is located (Hirakawa et al., 2015; Jones et al., 2004). However, the presence of heterozygous GOF mutations disagrees with the prevalence of loss of heterozygosity (LOH) events in *C. albicans* resistant isolates (Coste et al., 2006; Coste et al., 2007; Ford et al., 2015; Franz et al., 1998; Goldman et al., 2004; Morio et al., 2013; Siikala et al., 2010; Sitterlé et al., 2020). LOH turns the acquired GOF mutations homozygous, thus gaining higher resistance levels (Coste et al., 2006; Sasse et al., 2012). In our case, the strains with homozygous resistance-associated mutations in Erg11 were all heterozygous for *TAC1,* revealing that, if that were the case, LOH at the *ERG11* locus did not involve *TAC1.*

MRR1 and *MRR2* genes were also highly polymorphic, exhibiting 28 and 26 synonymous substitutions, respectively. Nonetheless, the number of non-synonymous polymorphisms was quite lower, only 4 in *MRR1* and 11 in *MRR2*. Since only some of the strains were sequenced for these genes, we cannot exclude that the proportion of non-synonymous SNPs could be higher. Only one GOF mutation was identified in Mrr1, harboured by one highly resistant strain, but it was accompanied by several other substitutions. On the other hand, we were not able to find any GOF mutations in Mrr2 which, combined with the Tac1 results, opens the possibility of alternative mechanisms being involved, such as those explained above.

Altogether, the results obtained in the first part of this thesis project further reinforce the need to continue investigating the mechanisms of azole resistance, as there are still many resistant isolates with unknown mechanisms (Berkow & Lockhart, 2017; Ksiezopolska & Gabaldón, 2018; McTaggart et al., 2020).

In a study carried out by Sitterlé and collaborators (Sitterlé et al., 2020) a panel of non-synonymous SNPs found in *TAC1*, *ERG11*, *UPC2*, *MRR1* and *FKS1* genes of 151 unrelated azole and echinocandin-susceptible *C. albicans* strains was established, which they proved reflected the natural variability between strains. Therefore, they postulated that new mutations found in resistant isolates, if not present in their panel of neutral polymorphisms, were more likely to be related to possible azole or echinocandin resistance. In our study, we found 11 new mutations in Erg11, 8 in Tac1 and 3 in Mrr2. Most Erg11 and Tac1 mutations were present in heterozygosis and either solely in susceptible isolates or both in susceptible and resistant isolates.

In Erg11, three mutations were present only in resistant strains, W57L, F217L, both in heterozygosis, and Y477C in homozygosis. The first two were in the same strain, together with two other Erg11 mutations that had been previously linked to azole resistance. Therefore, they were not considered for further analysis. The remaining Y477C was in an isolate exhibiting variable azole susceptibility between CLSI and Sensititre assays. Nonetheless, after 48h of incubation it showed increased resistance for FLC and ITC by Sensititre, so it was selected for studying its role in azole resistance.

Regarding Tac1, S758F in homozygosis was the only new mutation found among resistant isolates, in a highly resistant strain overexpressing *CDR1* and *CDR2* (target genes of Tac1) with no other mutations in this transcription factor. Consequently, the Tac1 S758F mutation was also selected for further studies.

Lastly, only one of the three new mutations found in Mrr2, A311V in homozygosis, was exclusively in resistant isolates. As well as S758F, A311V was found in a strain overexpressing *CDR1* and with no other mutations in any of the genes studied. Thus, this mutation was included for subsequent study.

In summary, from the 22 new mutations identified in *ERG11*, *TAC1* and *MRR2* genes we selected three of them, each in a different gene, for further characterization: Y477C in Erg11, S758F in Tac1 and A311V in Mrr2.

In order to study the role of these three new putative GOF mutations in azole-resistance, they were introduced into *C. albicans* SC5314 azole-susceptible reference strain by CRISPR-Cas9 methodology. As far as we know, this is the first study to use this technology for introducing SNPs in azole-resistance associated genes in *C. albicans*.

Due to the diploid nature of *C. albicans*, generating homozygous mutants was a cumbersome process, which in addition to the lack of meiosis and self-replicating plasmids, represented a great constraint for gene editing (Evans et al., 2018; Vyas et al., 2015). Advances in CRISPR technology helped to overcome these limitations (Vyas et al., 2018). Vyas and colleagues developed in 2015 a method for CRISPR-Cas9 editing in *C. albicans* that enabled the construction of homozygous mutants in a single transformation. Moreover, they obtained a high frequency of CRISPR-induced mutations, and 60 to 80% of the transformants had been correctly edited (Vyas et al., 2015). Later, in 2018, they optimized this system by improving guide expression, changing the integration locus from *ENO1* to *NEUT5L*, whose disruption does not impact growth (Gerami-Nejad et al., 2013), and excision of the whole CRISPR-Cas9 cassette, which contains the Cas9 encoding gene, the guide-RNA, the NAT (nourseothricin N-acetyl transferase) resistance marker and the flippase encoding gene (*FLP*), by induction of the latter with maltose (Vyas et al., 2018). Therefore, due to our need to create homozygous mutants resembling the parental strain, we selected this methodology to introduce the three new mutations into *C. albicans* SC5314 reference strain.

Compared to other studies in *C. albicans* where CRISPR-Cas9 elements, such as *CAS9* gene and guide-RNA (gRNA), and the selection marker are integrated into the yeast genome, we generally achieved increased transformation efficiencies by using electroporation. Evans et al. (Evans et al., 2018), following a lithium acetate transformation procedure (Gietz & Woods, 2002), obtained dozens of colonies in each transformation, whereas we reached hundreds in a single reaction. However, Nguyen et al. (Nguyen et al., 2017), with an edition strategy very similar to ours, but

again with a different transformation protocol, obtained around 50 transformants per reaction, comparable to some of our results.

Several other publications applied another methodology developed by Min et al. (Min et al., 2016), who demonstrated that both the *CAS9* gene and the gRNA cassette could be expressed inside the yeast cell without the need of integration, thus overcoming the problems associated with Vyas's method. The transformation rates in these studies were also variable, ranging from 50 transformants to thousands in a single reaction (Huang & Mitchell, 2017; Huang et al., 2018).

On the other hand, CRISPR-Cas9-mediated editing has also been performed in other species of *Candida* and yeasts, with two different approaches. The first one involves CRISPR RNA-Cas9 protein complexes (RNPs) consisting of the purified Cas9 enzyme complexed in vitro with the gRNA and the trans-activating RNA (tracrRNA) and then transformed into the yeast with or without a repair template (RTe) (Grahl et al., 2017; Kapoor et al., 2019; Liu et al., 2022); and the second approach involves a self-replicating plasmid containing all the genes necessary for CRISPR (Lombardi et al., 2017; Morio et al., 2019). The transformation efficiency seems not to be dependent on the gene editing method, but more on the transformation protocol and the yeast species, or even the strain. Our results were comparable to those obtained by Morio and collaborators (Morio et al., 2019), who studied the role in azole resistance of two newly identified Erg11 mutations in *Candida orthopsilosis*. Following Lombardi et al. method (Lombardi et al., 2017; Lombardi et al., 2019) they obtained two transformants from the transformation for one of the mutations, while for the other they got 63, even though they were working with the same strain and applying the same procedure. Similarly, we also observed varying transformation outcomes depending on the gene to be modified, especially for *TAC1* and *MRR2*. Moreover, it has been reported that Cas9 constitutive expression lowers transformation yields due to cell toxicity (DiCarlo et al., 2013). Nonetheless, we have to clarify that efficiency rates improved along with the experience and the latest transformations were the most efficient. We also noticed that time was an in important factor in the transformation protocol, thus longer processing times had a negative impact on the outcome.

Comparison of integration rates into *C. albicans* genome was not possible due to the lack of information, since all the studies focused on mutation frequencies disregarding if the plasmid was correctly introduced into the intended locus. However, in the study of Grahl et al. (Grahl et al., 2017) they compare transformation and mutation efficiencies between introduction of the RTe alone and co-transformed with the RNP. They observed that both transformation and mutation rates increased with the addition of RNPs. Edition rates with the RTe alone could be compared to our integration rates since both depend on Cas9-independent homologous recombination (HR). In our experiments we achieved between 13 and 70% of integration mutants, while they also had variable rates depending on the *Candida* species involved, for *Candida lusitaniae* 10% of the transformants had incorporated the RTe, 20% in *Candida auris* and 50% in *Nakaseomyces glabrata* (formerly known as *Candida glabrata*). It has to be noted that these three species are haploid, which may account for the higher integration rates reported in some of the cases. Another study carried out by Huang et al. (Huang et al., 2018) compared the mutation rates between introduction of the RTe alone and in combination with CRISPR elements following the transient system developed by Min et al. (Min et al., 2016); when the RTe was transformed without a gRNA cassette they only obtained 7 transformants from three separate transformations, and 5 of them were correctly modified. We can therefore agree with Min et al. (Min et al., 2016) and Nguyen et al. (Nguyen et al., 2017) that Vyas's methodology is limited by the integration of the Cas9- and gRNA-containing plasmid into the genome. Moreover, in the vast majority of the mutants, integration occurred in heterozygosis, which is in agreement with reports prior to CRISPR-Cas9-based methods, in which gene knock-outs or knock-ins relied on HR (Marton et al., 2020).

The analysis of the edition efficiency revealed that, in general, we obtained lower efficiency rates than those reported in various studies (Gao et al., 2016; Huang & Mitchell, 2017; Huang et al., 2018; Lombardi et al., 2017; Morio et al., 2019), that used either the transient method (Min et al., 2016) or the plasmid-based approach (Lombardi et al., 2017; Lombardi et al., 2019), except for the report of Grahl et al. (Grahl et al., 2017) that obtained efficiency rates of 60-70%. However, when compared to studies that followed Vyas's method, we achieved comparable efficiency rates (Nguyen et al., 2017) or even higher (Evans et al., 2018). These

differences can be attributable to different factors, such as the gRNA efficiency (Grahl et al., 2017; Ng & Dean, 2017), the HR efficiency (Paquet et al., 2016) or even the expression level of the gRNAs. In fact, Ng and Dean (Ng & Dean, 2017) and Lombardi et al. (Lombardi et al., 2017) reported that gRNAs expressed under the *SNR52* promoter, as in Vyas's method, yield lower mutation efficiency rates than with other promoters, such as tRNAs promoters.

Among the correctly edited transformants, we found that the mutation was introduced in homozygosis and heterozygosis at different proportions in each case, 81.8% of the mutants were homozygous for Erg11 and Mrr2 and 40% for Tac1. This difference correlated with the distance from the site of the mutation and the point where the DSB was directed. The gRNA for both Erg11 and Mrr2 mutants was predicted to direct Cas9-mediated cleavage at 6 nt from the mutation and for Tac1 mutants at 25 nt from the mutation. This positional effect was previously demonstrated by Paquet et al. (Paquet et al., 2016) and Lombardi et al. (Lombardi et al., 2019), and also observed by Morio et al. (Morio et al., 2019). Besides the correctly modified mutants, those that had introduced the RTe, we also found transformants that had not repaired the DSB with the RTe or had introduced additional modifications, like undesired insertions, deletions (indels) or mutations. *Candida albicans* can repair the Cas9-induced double-stranded break (DSB) through different repair mechanisms, like the error prone non-homologous end joining (NHEJ) system or the homology-directed repair (HDR). The latter is preferentially used by this yeast (Vyas et al., 2018), and that is why the RTe, that includes homology regions to both ends of the DSB, is incorporated into the yeast genome. We would expect to obtain transformants that had introduced the RTe, but when this does not occur, it can be due to deficient Cas9-mediated cleaving of DNA or to repair of the Cas9-induced DSB by HR with the sister chromatid, thus maintaining the original sequence. In the other case, the occurrence of undesired indels or mutations in the transformant's sequence can be attributed to alternative repair mechanisms like NHEJ (Ng & Dean, 2017). These kinds of modification were less common than the introduction of the RTe as reported by Evans et al. (Evans et al., 2018). It has to be noted that regardless of the zygosity of the mutation, the silent mutations were always found in homozygosis, agreeing with Morio et al. (Morio et al., 2019). This observation correlates better with the hypothesis that RTe's were

introduced in homozygosis through gene conversion or crossing over rather than through two independent integrations at each allele (Min et al., 2016).

From all the correct mutants we selected two independent transformants of each type; two homozygous, two heterozygous and two WT mutants, except for Mrr2 transformants, from which only one correctly modified heterozygous mutant could be obtained. In order to investigate if the proposed mutations were involved in azole resistance, susceptibility to azole antifungals was assayed by CLSI methodology and spot assay. The *CDR1* and *CDR2* expression levels were also measured for the Tac1 and Mrr2 mutants.

The Erg11 amino acid change from tyrosine (Y) to cysteine (C) in position 477 (Y477C) was found in the *C. albicans* 16-134 clinical isolate of vaginal origin. This strain exhibited variable susceptibility results and, to the best of our knowledge, this mutation has not been previously reported in the literature. The Erg11 enzyme is known to be highly permissive to amino acid changes, which are predominantly distributed in three hot spots (Morio et al., 2010). Erg11 Y477C is located within the Hot Spot III and in close proximity to the I471T substitution, which is associated to azole resistance (Kakeya et al., 2000). Moreover, the Hot Spot III comprises the external fungus-specific loop (FSL) that includes residues involved in heme iron binding, and amino acid changes surrounding this region are believed to have a significant impact on azole resistance. Specifically, the I471T was proposed to mediate azole resistance due to an increase of the polarity near the surface of the ligand-binding pocket (Keniya et al., 2018). The Y477C substitution could exert a similar effect on the protein environment due to a similar change in amino acid polarity, from the hydrophobic tyrosine residue to the polar cysteine. However, the susceptibility assays did not support this hypothesis; neither the homozygous nor the heterozygous mutants exhibited reduced susceptibility to FLC. We did observe a two-fold increase in FLC resistance of one of the homozygous mutants in the CLSI assay, but since it is usually considered within the expected range of variation between CLSI MIC values (Berkow et al., 2020), and it was not reproduced in the spot assay, we discarded the involvement of Erg11 Y477C mutation in azole resistance.

The *TAC1* new mutation reported in this study, implied a change from serine (S) to phenylalanine (F) in the residue 758 (S758F) and was identified in the *C. albicans* vulvovaginal isolate BE-113. This isolate was classified as resistant to all azole classes, harboured two mutations in Erg11 already linked to azole resistance (A114S and Y257H) (Chau et al., 2004; Xiang et al., 2013; Zhao et al., 2013), and overexpressed *CDR1* and *CDR2*. Since mutations in Tac1 have been associated to increased expression of those efflux pumps (Coste et al., 2006), and no other mutations in Tac1 or Mrr2 were identified, S758F was further investigated for its possible contribution to azole resistance. Although a slight increase in FLC MIC was perceived for the S758F homozygous SC5314 transformants after 24h of incubation at both 37 and 25°C, this difference between mutated transformants and WT and parental strains diminished at 48h. Regarding the spot assay, both homozygous and heterozygous mutants were slightly less susceptible to FLC only at 25°C. This apparent disagreement between assays may be explained by the effect of temperature on trailing growth (Agrawal et al., 2007) and the different conditions of each assay. As seen in the spot assay images, all transformants grew to a less extent at 25°C when compared to 37°C. In fact, due to the trailing growth often seen in CLSI susceptibility assays with azoles, lowering the incubation temperature at 25°C has been proposed as a way to better estimate MIC values for azole drugs in *C. albicans* (Rosenberg et al., 2018). Moreover, the above-the-MIC growth has been linked to azole tolerance (Berman & Krysan, 2020). Thus, the FCZ 8-fold MIC increase registered by *C. albicans* BE-113 growing at 37°C for 48h, compared to MIC values at 25°C, may indicate that this clinical isolate gathers mechanisms of both resistance and tolerance to azole drugs.

In addition, none of the Tac1 S758F transformants overexpressed *CDR1* and *CDR2* genes compared to the parental strain SC5314, in contrast to BE-113 that exhibited an increased expression of both genes. In light of these results, the Tac1 S758F mutation does not seem to contribute to azole resistance, and the question about the mechanism behind *CDR1* and *CDR2* genes overexpression in the *C. albicans* BE-113 clinical isolate remains open. The Erg11 mutations are probably the major contributors to BE-113 resistance, since *CDR1* was not highly overexpressed and *CDR2* has been shown to have a lower influence in azole resistance (Holmes et al., 2008).

Finally, the mutation identified for the first time in this study in the *MRR2* gene implicated a change from alanine (A) to valine (V) in the amino acid 311 (A311V) and was present in *C. albicans* BE-114. This clinical isolate exhibited variable FLC MICs depending on the susceptibility testing methods, and it showed a slight increase in *CDR1* expression when compared to azole-susceptible isolates; nevertheless, the only mutation found in the five genes studied was A311V in Mrr2. Since Mrr2 has been associated to regulation of *CDR1* expression (Schillig & Morschhäuser, 2013) and there is some controversy on the role of Mrr2 mutations in azole resistance and *CDR1* overexpression (Feng et al., 2019; Nishimoto et al., 2019; Wang et al., 2015), we studied the effect of introducing the Mrr2 A311V mutation in the *C. albicans* azole-susceptible SC5314 strain. The CLSI assay showed again a slight increase in FLC MICs for the homozygous mutants only at 37°C after 24h of incubation, while BE-114 showed an 8-fold difference in FLC MIC compared to SC5314, confirming previous results. Interestingly, after 48h of incubation at 25°C the homozygous mutants exhibited growth at 64 μg/ml, the highest FLC concentration of the assay. The BE-114 MIC at 25°C was also significantly higher than at 37°C. Even though we would expect an increased growth at 37°C compared to 25°C, due to the temperature effect on azole tolerance already observed for strain BE-113, Rosenberg et al. (Rosenberg et al., 2018) reported that the effect of temperature on tolerance was variable for the different strains. Therefore, BE-114 and Mrr2 homozygous mutants seem to be more susceptible to azole drugs at higher temperatures. Similarly, in the spot assay there were no apparent differences between mutants at 37°C, whereas at 25°C the homozygous mutants were less affected by FLC.

Nonetheless, this increased resistance was not accompanied by an increased expression of either *CDR1* or *CDR2*. Surprisingly, in this experiment the BE-114 strain did not overexpress *CDR1* when compared to SC5314, as opposed to what was observed when gene expression was compared to a pool of susceptible isolates. Consequently, we believe that SC5314 may have higher basal expression levels of *CDR1* than the azole-susceptible isolates used in this study, which in turn can also explain the reports of the significant tolerance exhibited by this strain (Fiori & Van Dijck, 2012; Rosenberg et al., 2018). Despite the surprising results obtained by CLSI after 48h of incubation at 25°C, if we take into account that neither the homozygous

nor the heterozygous mutants increased *CDR1* expression and their MICs were not altered, we can conclude that the Mrr2 A311V mutation is not involved in azole resistance. Nonetheless, further studies on the influence of temperature in azole susceptibility of *C. albicans* Mrr2 homozygous mutants and BE-114 are warranted.

In summary, we identified three mutations not previously reported, but none of them was found to be associated to azole resistance. Nevertheless, our results highlight the need to continue the research on azole resistance mechanisms since, as reported in other studies, some of the azole-resistant strains selected from the UPV/EHU collection did not harbour any of the most commonly described mechanisms addressed in this study.

Another interesting aspect of azole resistance is the evolutionary trajectories followed to adapt to azole pressure. In the past, azole resistance mechanisms have been studied using sequential clinical or laboratory isolates that progressively acquired azole resistance (Albertson et al., 1996; Calabrese et al., 2000; Coste et al., 2004; de Micheli et al., 2002; Dunkel et al., 2008; Dunkel, Blaß et al., 2008; Franz et al., 1998; Franz et al., 1999; Hiller et al., 2006; Karababa et al., 2004; Lopez-Ribot et al., 1998; Marichal et al., 1999; Marr et al., 1998; Morschhäuser et al., 2007; Perea et al., 2001; Saidane et al., 2006; Sanglard et al., 1995; White, 1997; White, 1997a; Wirsching et al., 2000). Since we had not sequential clinical isolates available, we carried out an in vitro evolution experiment in which two different azole-susceptible strains of *C. albicans* were exposed to increasing concentrations of FLC, the SC5314 reference strain and the vulvovaginal clinical isolate BE-47.

Both strains were exposed to increasing concentrations of FLC during 23 days (from 0.25 to 64 μg/ml), and then they were subcultured without FLC for 32 additional days. Remarkably, the reference *C. albicans* SC5314 strain rapidly adapted to FLC under the pressure of low concentrations of the antifungal compound (0.25 μg/ml for 3 days and 0.5 μg/ml during the fourth day). In these conditions, the transcription factor Tac1 of the experimental population SC5314_t4 (after 4 days of exposure) acquired the GOF mutation N977D in heterozygosis, which was already described and associated to Tac1 hyperactivity and azole resistance by Coste et al. (Coste et al., 2006). By the seventh day of exposure, once reached a FLC concentration of 4 μg/ml, the population SC5314_t7 became homozygous for this

mutation and its neighbouring sequence of the *TAC1* gene, and this GOF mutation was maintained throughout the experiment even after eliminating the fluconazole pressure for an additional 32-day period of time. Nonetheless, the sequence of *ERG11* revealed that the LOH event only included the *TAC1* regionof chromosome 5. The occurrence of this mutation correlated with acquired resistance to FLC, CLT and posaconazole (POS), and reduced susceptibility to ITC and VRC, and in all cases, the highest MIC values coincided with the acquisition of the homozygous mutation, as previously observed by Sasse et al. (Sasse et al., 2012). There are reports of rapid development of resistance to antifungal drugs in other *Candida* species such as *N. glabrata* (Bordallo-Cardona et al., 2017; Borst et al., 2005), *Pichia kudriavzevii* (formerly known as *Candida krusei*) (Ricardo et al., 2014) and *Candida tropicalis* (Barchiesi et al., 2000; Khan et al., 2018) requiring from one to two passages in drug containing media or 4 to 10 days of exposure. However, as far as we know, there are no records of such a fast and stable acquisition of resistance in *C. albicans* as observed for the SC5314 strain in our experiment. Contrarily, other studies in *C. albicans* strains report that longer periods of azoles exposure were necessary for acquiring resistance (Cowen et al., 2000; Huang et al., 2011; Riggle & Kumamoto, 2006; White, 1997; Yan et al., 2008), and in some instances this resistance was transiently acquired (Calvet et al., 1997; Marr et al., 1998).

In this work, we found an association between the reduced susceptibility to azoles and the increased expression of drug-efflux pump genes *CDR1*, *CDR2* and *MDR1*, in agreement with the reported association of the N977D mutation in Tac1 with the increased expression of *CDR1* and *CDR2* genes (Coste et al., 2006). The highest increase in expression of *CDR1* was achieved in population SC5314_t15, when it was first exposed to the highest concentration of fluconazole. After retiring the FCZ challenge, the populations still overexpressed *CDR1*, though at lower levels than t7 and t15. This reduction in *CDR1* expression levels can be due to a more adjusted regulation of ABC pumps expression, which consume ATP in order to eject their substrates from the cell (Rees et al., 2009). As pointed out by Sasse et al. (Sasse et al., 2012), Tac1 mutations drive a loss of fitness, so it has been proposed that compensatory mutations may arise (Popp et al., 2017) to adjust *CDR1* expression to non-detrimental levels, but still sufficient to withstand the antifungal pressure. Similarly, Paul et al. (Paul et al., 2020) showed that after 10 passages in the presence

of FLC, *C. tropicalis* strains overexpressed *CDR1*, but then decreased after 20 passages.

On the other hand, the increased expression of *MDR1* only in the t15 population strengthens the hypothesis that survival in high FCZ concentrations requires an enhanced efflux of the drug that would return to normal levels after further adaptation (Lee et al., 2004). FLC has been reported to induce aneuploidies (Selmecki et al., 2009) so, according to these authors, an explanation for the *MDR1* overexpression could be that the SC5314_t15 experimental population gained an extra copy of chromosome 3 where Mrr1, the transcriptional regulator of Mdr1 MFS transporter, is located, and/or of chromosome 6, where *MDR1* resides (Selmecki et al., 2009). In addition, simultaneous overexpression of ABC and MFS drug-efflux pumps seems to be extremely detrimental for *C. albicans* and is rarely observed in resistant isolates (Sasse et al., 2012), thus it makes sense that the overexpression of the three efflux pumps was not maintained and only increased expression of *CDR1* and *CDR2* persisted.

Regarding *ERG11* gene expression, we did not find variations at any time point of the experiment, as opposed to the *ERG11* overexpression reported by Lee et al. (Lee et al., 2004). Nonetheless, our RNA extraction was conducted in cells grown with no FCZ, so we measured changes in gene expression associated to permanent genomic modifications and not transient responses to antifungal pressure.

Even though we might expect that the acquisition of resistance mechanisms by the experimental populations derived from SC5314 would entail a fitness-cost in the absence of the drug (Hill et al., 2015), all populations showed no substantial differences with the initial and respective control populations, both at 30 and 37°C in RPMI, except for SC5314_t4. So, our populations may have acquired compensatory mechanisms between days 4 and 7 of the experiment, that would prevent a loss of fitness (Hill et al., 2015). In any case, our results are in agreement with those of Cowen et al. (Cowen et al., 2001), who observed that the *C. albicans* strains that evolved in the presence of FLC and overexpressed *CDR1* and *CDR2* exhibited high fitness, both in the presence and in the absence of the azole. Furthermore, this absence of fitness cost was also observed in an evolution

experiment with *Saccharomyces cerevisiae*, where none of the evolved strains had lower fitness than their progenitor in the absence of FLC (Anderson et al., 2003).

Interestingly, besides increased resistance levels due to LOH, if the mating-type like (*MTL*) locus is involved, *C. albicans* could gain sexual competence and further contribute to azole resistance development. Popp et al. (Popp et al., 2019) reported that two *C. albicans* strains with opposing homozygous mating-types (*MTLa* and *MTLα*), each carrying a different resistance mechanism, were able to mate and generate a progeny with both mechanisms and therefore, higher azole resistance. LOH can involve different parts of chromosome 5 in distinct cells of the population, and some of our experimental populations were heterogeneous, with at least two genotypes, one homozygous for *TAC1* but heterozygous for *ERG11*, and the other one was homozygous for both genes and the *MTLa* allele. Loss of heterozygosis after antifungal drug exposure (Forche et al., 2011), specially LOH of the left arm of chromosome 5, has been described in association with acquired drug resistance (Coste et al., 2007; Selmecki et al., 2008) and, even though LOH of *TAC1* is usually accompanied by LOH in *MTL*, this is not always the case (Coste et al., 2007). Moreover, this phenomenon of heterogeneity has also been reported in similar experiments of FLC exposure with *C. albicans* (Selmecki et al., 2009) or *N. glabrata* (Bordallo-Cardona et al., 2017).

A particularly interesting case was that the BE-47 experimental populations showed a slight reduction of susceptibility to most of the azoles, but we could not register any changes neither in *TAC1, ERG11, UPC2, MRR1, MRR2* and *ERG3* nucleotide sequences nor in *CDR1, CDR2, MDR1* and *ERG11* expression levels. Moreover, we were unable to obtain any clone homozygous for the *MTL*, although we cannot exclude the possibility that they exist. In contrast, we did observe a significant increase in the fitness of the experimental populations BE-47_t7 and BE-47_t23 when grown at 30°C, in agreement with other authors (Cowen et al., 2001; Huang et al., 2011; Selmecki et al., 2009). According to Desai et al. (Desai et al., 2015) and Leach et al. (Leach et al., 2016) temperature can influence gene expression, so the fitness differences between control and experimental populations may be more pronounced at 30°C than at 37°C due to a differentially expressed set of genes. Similarly, the experimental populations may have suffered changes in their genome

and gene expression (Cavalheiro et al., 2019; Cowen et al., 2002) that, besides enabling growth in the presence of FLC, would also affect their ability to grow at different temperatures. On the other hand, temperature can also affect the above-the-MIC growth phenomenon, known as "trailing", commonly observed when performing susceptibility testing of *C. albicans* isolates against azoles (Agrawal et al., 2007; Luna-Tapia et al., 2019). In fact, our study illustrates that *C. albicans* can adapt to grow in the presence of FCZ concentrations above their MIC values, as is the case of BE-47, that was able to grow with FLC 64 μg/ml although its MIC was 1 μg/ml.

Trailing growth is probably a manifestation of tolerance to antifungal drugs (Berman & Krysan, 2020), but this phenomenon may have been widely overlooked (Rosenberg et al., 2018) due to the lack of correlation between trailing and clinical outcome in former studies (Arthington-Skaggs et al., 2000; Odabasi et al., 2010; Revankar et al., 1998; Rex et al., 1998; Rueda et al., 2017). Nonetheless, recent reports show that isolates with FCZ trailing were associated to recurrent infections or worse therapeutic responses (Astvad et al., 2018) and tolerance is being considered an important factor in resistance evolution (Berman & Krysan, 2020; Costa-de-Oliveira & Rodrigues, 2020).

To investigate the azole-tolerance levels of the SC5314- and BE47-derived populations, we calculated their SMG (supra-MIC-growth) values according to Rosenberg and collaborators (Rosenberg et al., 2018). Most SC5314 experimental populations exhibited higher SMG values than their respective controls at 37°C, while BE47 populations registered lower values, except for a substantial increase of the BE47-t23 population. On the other hand, at 25°C, the SC5314 populations showed moderate and more homogenous tolerance levels, while more interestingly, BE47-t23 did not exhibit any noticeable SMG, supporting that the above-the-MIC growth of the latter population was associated to a higher tolerance to FLC. While the SC5314 strain was intrinsically more azole-tolerant than BE47, enabling a faster adaptation to FLC pressure, BE47 exhibited a slower adaptation process that culminated with acquisition of tolerance to FLC rather than resistance. Similarly, Gerstein and Berman (Gerstein & Berman, 2020) have reported diverse levels of tolerance acquisition among different *C. albicans* strains. The scarce knowledge on tolerance and the factors involved, poses a challenge to systematically studying the

effects of natural variation in the genes that may affect tolerance; one informative approach could be the employment of isogenic strains that differ in tolerance levels (Berman & Krysan, 2020), as is the case of the initial and t23-evolved BE47 populations. Therefore, the availability of these populations opens up an interesting line of future research elucidating the genomic and epigenetic mechanisms involved in tolerance development.

Another interesting theory for the faster adaptation of SC5314 was reported by Selmecki and collaborators (Selmecki et al., 2009), who analysed the formation of aneuploidies in *C. albicans* populations exposed to increasing concentrations of fluconazole. They found that only after 3.3 generations (1 day) of initial exposure to fluconazole, several populations formed an isochromosome of the left arm of chromosome 5. Even though by that time they were not resistant to fluconazole, only these populations were able to become highly resistant to fluconazole at the end of the experiment.

The results of our work support the hypothesis that adaptation to stresses such as drug exposure is strain dependent as it has been extensively reported in the literature for different *Candida* species (Cowen et al., 2000; Paul et al., 2020; Selmecki et al., 2009) and other antifungal drugs (Bordallo-Cardona et al., 2017). Although they evolved differently and modified their MIC values to different extent, the experimental populations of both *C. albicans* strains shared their ability to grow at FLC concentrations above their MIC. Therefore, besides the early acquisition by the SC5314 strain of the Tac1 N977D resistance-associated mutation and the reduced susceptibility shown by BE-47, both strains must have activated complementary tolerance mechanisms (Berman & Krysan, 2020; Rosenberg et al., 2018) that contribute to the reduction of their sensitivity to azole antifungal compounds. Moreover, we cannot discard that the BE-47 clinical isolate could have adapted to the presence of FLC by other mechanisms not studied in this work or even a yet to be discovered one. We acknowledge that a limitation of our study was the reduced number of BE-47 derived populations investigated, but due to the low number of variations registered in the t23 population developed with FLC 64 μg/ml we only focused on that population and an intermediate time spot (t7).

Regarding the clinical setting in Europe, the common dose of fluconazole is 400 mg, reaching a maximum serum concentration (C_{max}) of 23 mg/l when administered intravenously (European Committee on Antimicrobial Susceptibility Testing, 2020) while oral intake achieves a C_{max} of 9.1 mg/l; if the dose is 100 mg, C_{max} drops to 1.7 mg/l (Bellmann & Smuszkiewicz, 2017). Our work shows that acquisition of drug resistance can occur very rapidly and at drug concentrations lower than therapeutic doses. Additional evidence suggests that *C. albicans* rapidly reacts to environmental stresses, like antifungal drugs, so caution must be taken when administering long-term antifungal prophylaxis (Selmecki et al., 2009).

Deeper studies on gene expression and genomic rearrangements are warranted in order to elucidate the evolutionary pathways related to the acquisition of resistance to antifungals in *C. albicans*, as well as the molecular mechanisms laying behind the reduced antifungal susceptibility shown by different strains. As an example, to further study the putative role in azole resistance of newly found mutations, editing the original isolate harbouring the mutation back to a WT sequence could shed more light into this matter. Since the genetic background of each strain can influence the phenotypic effect of mutations (Gerstein & Berman, 2020; Huang et al., 2019; Morschhäuser, 2002; Morschhäuser et al., 2007; Popp et al., 2017; Sasse et al., 2012; Schubert et al., 2011), we may have underappreciated the impact of these mutations on the resistant phenotype of its corresponding strain. In addition, the Erg11 Y477C mutation may not implicate azole resistance by itself, since many of the Erg11 mutations known to confer resistance enhance their effect when combined with others, and have even been found in susceptible isolates (Morschhäuser, 2002). Consequently, it would be interesting to investigate if this new mutation could modify others' influence in resistance. Regarding the evolution experiment, the BE-47 derived populations represent an excellent opportunity to implement transcriptome and whole-genome sequencing to investigate the genomic or transcriptional modifications that take place in azole tolerance acquisition. Moreover, ploidy analysis is also warranted due to their occurrence in *C. albicans* azole resistance development.

CONCLUSIONS

6. CONCLUSIONS

1. The occurrence of very few mutations in the *ERG11* gene can be indicative of azole resistance.

2. There are azole-resistant strains that show none of the azole resistance mechanisms previously described, such as Erg11 alterations or overexpression of *ERG11* and efflux pumps due to hyperactivation of their corresponding transcription factors Upc2, Tac1, Mrr1 and Mrr2.

3. Most *C. albicans* azole-resistant strains overexpressing the *CDR1*, *CDR2* and/or *MDR1* efflux pumps do not harbour any of the previously described gain-of-function mutations in their corresponding transcription factors.

4. The substitutions Y477C in Erg11, S758F in Tac1 and A311V in Mrr2, described for the first time in this work, are not associated to azole resistance on their own, at least when introduced into the *C. albicans* SC5314 reference strain.

5. The exposure of *C. albicans* to fluconazole concentrations as low as 0.25-0.5 μg/ml can induce azole-resistance associated strategies in a short time, as in our case after only four days of fluconazole pressure.

6. Even though azole sensitivity (MIC) is not modified, exposure of *C. albicans* to increasing concentrations of fluconazole can induce tolerance mechanisms to this drug. In the same regard, the two susceptible but azole-tolerant *C. albicans* clinical isolates of our study failed to show any of the mechanisms of azole resistance analysed, so we still need to continue searching for factors that promote tolerance.

7. The CRISPR-Cas9 methodology employed in this study proved to be an adequate system to introduce single nucleotide changes in *C. albicans*.

REFERENCES

7. REFERENCES

A

Agrawal D, Patterson TF, Rinaldi MG & Revankar SG. (2007). Trailing end-point phenotype of *Candida* spp. in antifungal susceptibility testing to fluconazole is eliminated by altering incubation temperature. *Journal of Medical Microbiology, 56*:1003-1004. https://doi.org/10.1099/jmm.0.47168-0

Alarco AM, Balan I, Talibi D, Mainville N & Raymond M. (1997). AP1-mediated multidrug resistance in *Saccharomyces cerevisiae* requires *FLR1* encoding a transporter of the major facilitator superfamily. *The Journal of Biological Chemistry, 272*:19304-19313. https://doi.org/10.1074/jbc.272.31.19304

Alarco AM & Raymond M. (1999). The bZip transcription factor Cap1p is involved in multidrug resistance and oxidative stress response in *Candida albicans*. *Journal of Bacteriology, 181*:700-708. https://doi.org/10.1128/JB.181.3.700-708.1999

Albertson GD, Niimi M, Cannon RD & Jenkinson HF. (1996). Multiple efflux mechanisms are involved in *Candida albicans* fluconazole resistance. *Antimicrobial Agents and Chemotherapy, 40*:2835-2841. https://doi.org/10.1128/AAC.40.12.2835

Andersen CL, Jensen JL & Orntoft TF. (2004). Normalization of Real-Time Quantitative Reverse Transcription-PCR data: a model-based variance estimation approach to identify genes suited for normalization, applied to bladder and colon cancer data sets. *Cancer Research, 64*:5245-5250. https://doi.org/10.1158/0008-5472.CAN-04-0496

Anderson JB, Sirjusingh C, Parsons AB, Boone C, Wickens C, Cowen LE & Kohn LM. (2003). Mode of selection and experimental evolution of antifungal drug resistance in *Saccharomyces cerevisiae*. *Genetics, 163*:1287-1298. https://doi.org/10.1093/genetics/163.4.1287

Anderson MZ, Saha A, Haseeb A & Bennett RJ. (2017). A chromosome 4 trisomy contributes to increased fluconazole resistance in a clinical isolate of *Candida albicans*. *Microbiology, 163*:856-865. https://doi.org/10.1099/mic.0.000478

Anderson TM, Clay MC, Cioffi AG, Diaz KA, Hisao GS, Tuttle MD, Nieuwkoop AJ, Comellas G, Maryum N, Wang S, Uno BE, Wildeman EL, Gonen T, Rienstra CM & Burke MD. (2014). Amphotericin forms an extramembranous and fungicidal sterol sponge. *Nature Chemical Biology, 10*:400-406. https://doi.org/10.1038/nchembio.1496

Arendrup MC. (2014). Update on antifungal resistance in *Aspergillus* and *Candida*. *Clinical Microbiology and Infection, 20*:42-48. https://doi.org/10.1111/1469-0691.12513

Arendrup MC & Patterson TF. (2017). Multidrug-resistant *Candida*: epidemiology, molecular mechanisms, and treatment. *The Journal of Infectious Diseases, 216*:S445-S451. https://doi.org/10.1093/infdis/jix131

Arrieta Aguirre, I. (2018). *Diagnóstico molecular de especies de Candida y otras levaduras. Identificación de mutaciones en los genes ERG11, TAC1 y UPC2 en relación con la sensibilidad reducida a azoles, y a equinocandinas en el gen FKS*. (ADDI). http://hdl.handle.net/10810/36125

Arthington-Skaggs BA, Warnock DW & Morrison CJ. (2000). Quantitation of *Candida albicans* ergosterol content improves the correlation between in vitro antifungal susceptibility test results and in vivo outcome after fluconazole treatment in a murine model of invasive candidiasis. *Antimicrobial Agents and Chemotherapy, 44*:2081-2085. https://doi.org/10.1128/AAC.44.8.2081-2085.2000

Asai K, Tsuchimori N, Okonogi K, Perfect JR, Gotoh O & Yoshida Y. (1999). Formation of azole-resistant *Candida albicans* by mutation of sterol 14-demethylase P450. *Antimicrobial Agents and Chemotherapy, 43*:1163-1169. https://doi.org/10.1128/AAC.43.5.1163

Astvad KMT, Sanglard D, Delarze E, Hare RK & Arendrup MC. (2018). Implications of the EUCAST trailing phenomenon in *Candida tropicalis* for the in vivo susceptibility in invertebrate and murine models. *Antimicrobial Agents and Chemotherapy, 62*:e01624-18. https://doi.org/10.1128/aac.01624-18

B

Barchiesi F, Calabrese D, Sanglard D, Di Francesco LF, Caselli F, Giannini D, Giacometti A, Gavaudan S & Scalise G. (2000). Experimental induction of fluconazole resistance in *Candida tropicalis* ATCC 750. *Antimicrobial Agents and Chemotherapy, 44*:1578-1584. https://doi.org/rg/10.1128/AAC.44.6.1578-1584.2000

Bassetti M, Righi E, Montravers P & Cornely OA. (2018). What has changed in the treatment of invasive candidiasis? A look at the past 10 years and ahead. *Journal of Antimicrobial Chemotherapy, 73*:i14-i25. https://doi.org/10.1093/jac/dkx445

Bellmann R & Smuszkiewicz P. (2017). Pharmacokinetics of antifungal drugs: practical implications for optimized treatment of patients. *Infection, 45*:737-779. https://doi.org/10.1007/s15010-017-1042-z

Bennett RJ & Johnson AD. (2003). Completion of a parasexual cycle in *Candida albicans* by induced chromosome loss in tetraploid strains. *The EMBO Journal, 22*:2505-2515. https://doi.org/10.1093/emboj/cdg235

Berkow EL & Lockhart SR. (2017). Fluconazole resistance in *Candida* species: a current perspective. *Infection and Drug Resistance, 10*:237-245. https://doi.org/10.2147/IDR.S118892

Berkow EL, Lockhart SR & Ostrosky-Zeichner L. (2020). Antifungal susceptibility testing: current approaches. *Clinical Microbiology Reviews, 33*:e00069-19. https://doi.org/10.1128/CMR.00069-19

Berman J & Hadany L. (2012). Does stress induce (para)sex? Implications for *Candida albicans* evolution. *Trends in Genetics, 28*:197-203. https://doi.org/10.1016/j.tig.2012.01.004

Berman J & Krysan DJ. (2020). Drug resistance and tolerance in fungi. *Nature Reviews Microbiology, 18*:319-331. https://doi.org/10.1038/s41579-019-0322-2

Bhattacharya S, Esquivel BD & White TC. (2018). Overexpression or deletion of ergosterol biosynthesis genes alters doubling time, response to stress agents, and drug susceptibility in *Saccharomyces cerevisiae*. *mBio, 9*:e01291-18. https://doi.org/10.1128/mBio.01291-18

Bhattacharya S, Sae-Tia S & Fries BC. (2020). Candidiasis and mechanisms of antifungal resistance. *Antibiotics, 9*:312-330. https://doi.org/10.3390/antibiotics9060312

Bolotin A, Quinquis B, Sorokin A & Ehrlich SD. (2005). Clustered regularly interspaced short palindrome repeats (CRISPRs) have spacers of extrachromosomal origin. *Microbiology, 151*:2551-2561. https://doi.org/10.1099/mic.0.28048-0

Bongomin F, Gago S, Oladele R & Denning DW. (2017). Global and multi-national prevalence of fungal diseases—estimate precision. *Journal of Fungi, 3*:57-85. https://doi.org/10.3390/jof3040057

Bordallo-Cardona MA, Escribano P, Gómez G de la Pedrosa, E, Marcos-Zambrano LJ, Cantón R, Bouza E & Guinea J. (2017). In vitro exposure to increasing micafungin concentrations easily promotes echinocandin resistance in *Candida glabrata* isolates. *Antimicrobial Agents and Chemotherapy, 61*:e01542-16. https://doi.org/https://doi.org/10.1128/aac.01542-16

Borst A, Raimer MT, Warnock DW, Morrison CJ & Arthington-Skaggs BA. (2005). Rapid acquisition of stable azole resistance by *Candida glabrata* isolates obtained before the clinical introduction of fluconazole. *Antimicrobial Agents and Chemotherapy, 49*:783-787. https://doi.org/https://doi.org/10.1128/AAC.49.2.783-787.2005

Brown GD, Denning DW, Gow NA, Levitz SM, Netea MG & White TC. (2012). Hidden killers: human fungal infections. *Science Translational Medicine, 4*:165rv13. https://doi.org/10.1126/scitranslmed.3004404

Bustin SA, Benes V, Garson JA, Hellemans J, Huggett J, Kubista M, Mueller R, Nolan T, Pfaffl MW, Shipley GL, Vandesompele J & Wittwer CT. (2009). The MIQE guidelines: minimum information for publication of Quantitative Real-Time PCR experiments. *Clinical Chemistry, 55*:611-622. https://doi.org/10.1373/clinchem.2008.112797

Butler G, Rasmussen MD, Lin MF, Santos MAS, Sakthikumar S, Munro CA, Rheinbay E, Grabherr M, Forche A, Reedy JL, Agrafioti I, Aranud MB, Bates S, Brown AJP, Brunke S, Costanzo MC, Fitzpatrick DA, de Groot, P W J, Harris D, Hoyer LL, Hube B, Klis FM, Kodira C, Lennard N, Logue ME, Martin R, Neiman AM, Nikolaou E, Quail MA, Quinn J, Santos MC, Schmitzberger FF, Sherlock G, Shah P, Silverstein KAT, Skrzypek MS, Soll D, Staggs R, Stansfield I, Stumpf MPH, Sudbery PE, Srikantha T, Zeng Q, Berman J, Berriman M, Heitman J, Gow NAR, Lorenz MC, Birren BW, Kellis M & Cuomo CA. (2009). Evolution of pathogenicity and sexual reproduction in eight *Candida* genomes. *Nature, 459*:657-662. https://doi.org/10.1038/nature08064

C

Calabrese D, Bille J & Sanglard D. (2000). A novel multidrug efflux transporter gene of the major facilitator superfamily from *Candida albicans* (*FLU1*) conferring resistance to fluconazole. *Microbiology, 146*:2743-2754. https://doi.org/10.1099/00221287-146-11-2743

Calvet HM, Yeaman MR & Filler SG. (1997). Reversible fluconazole resistance in *Candida albicans*: a potential in vitro model. *Antimicrobial Agents and Chemotherapy, 41*:535-539. https://doi.org/10.1128/AAC.41.3.535

Castanheira M, Deshpande LM, Davis AP, Rhomberg PR & Pfaller MA. (2017). Monitoring antifungal resistance in a global collection of invasive yeasts and molds: application of CLSI epidemiological cutoff values and whole-genome sequencing analysis for detection of azole resistance in *Candida albicans*. *Antimicrobial Agents and Chemotherapy, 61*:e00906-17. https://doi.org/10.1128/aac.00906-17

Cavalheiro M, Costa C, Silva-Dias A, Miranda IM, Wang C, Pais P, Pinto SN, Mil-Homens D, Sato-Okamoto M, Takahashi-Nakaguchi A, Silva RM, Mira NP, Fialho AM, Chibana H, Rodrigues AG, Butler G & Teixeira MC. (2019). A transcriptomics approach to unveiling the mechanisms of in vitro evolution towards fluconazole resistance of a *Candida glabrata* clinical isolate. *Antimicrobial Agents and Chemotherapy, 63*:e00995-18. https://doi.org/10.1128/aac.00995-18

Chang Z, Yadav V, Lee SC & Heitman J. (2019). Epigenetic mechanisms of drug resistance in fungi. *Fungal Genetics and Biology, 132*:103253. https://doi.org/10.1016/j.fgb.2019.103253

Chau AS, Gurnani M, Hawkinson R, Laverdiere M, Cacciapuoti A & McNicholas PM. (2005). Inactivation of sterol Δ5,6-Desaturase attenuates virulence in *Candida albicans*. *Antimicrobial Agents and Chemotherapy, 49*:3646-3651. https://doi.org/10.1128/AAC.49.9.3646-3651.2005

Chau AS, Mendrick CA, Sabatelli FJ, Loebenberg D & McNicholas PM. (2004). Application of Real-Time Quantitative PCR to molecular analysis of *Candida albicans* strains exhibiting reduced susceptibility to azoles. *Antimicrobial Agents and Chemotherapy, 48*:2124-2131. https://doi.org/10.1128/AAC.48.6.2124-2131.2004

Chen C, Yang Y, Shin H, Su C & Lo H. (2004). CaNdt80 is involved in drug resistance in *Candida albicans* by regulating *CDR1*. *Antimicrobial Agents and Chemotherapy, 48*:4505-4512. https://doi.org/10.1128/AAC.48.12.4505-4512.2004

Chen C, Yang Y, Tseng K, Shih H, Liou C, Lin C & Lo H. (2009). Rep1p negatively regulating *MDR1* efflux pump involved in drug resistance in *Candida albicans*. *Fungal Genetics and Biology, 46*:714-720. https://doi.org/10.1016/j.fgb.2009.06.003

Cheng S, Clancy CJ, Nguyen KT, Clapp W & Nguyen MH. (2007). A *Candida albicans* petite mutant strain with uncoupled oxidative phosphorylation overexpresses *MDR1* and has diminished susceptibility to fluconazole and voriconazole. *Antimicrobial Agents and Chemotherapy, 51*:1855-1858. https://doi.org/10.1128/AAC.00182-07

Cleveland AA, Farley MM, Harrison LH, Stein B, Hollick R, Lockhart SR, Magill SS, Derado G, Park BJ & Chiller TM. (2012). Changes in incidence and antifungal drug resistance in candidemia: results from population-based laboratory surveillance in Atlanta and Baltimore, 2008–2011. *Clinical Infectious Diseases, 55*:1352-1361. https://doi.org/10.1093/cid/cis697

Clinical and Laboratory Standards Institute. (2008). *Reference method for broth dilution antifungal susceptibility testing of yeast: Approved standard CLSI document M27-A3.* Clinical Laboratory Standards Institute.

Clinical and Laboratory Standards Institute. (2012). *Reference method for broth dilution antifungal susceptibility testing of yeasts; fourth informational supplement*. CLSI document M27-S4.

Coenye T, De Vos M, Vandenbosch D & Nelis H. (2008). Factors influencing the trailing endpoint observed in *Candida albicans* susceptibility testing using the CLSI procedure. *Clinical Microbiology and Infection, 14*:495-497. https://doi.org/10.1111/j.1469-0691.2008.01956.x

Coleman JJ & Mylonakis E. (2009). Efflux in fungi: la pièce de résistance. *PLoS Pathogens, 5*:e1000486. https://doi.org/10.1371/journal.ppat.1000486

Cornet M, Bidard F, Schwarz P, Da Costa G, Blanchin-Roland S, Dromer F & Gaillardin C. (2005). Deletions of endocytic components *VPS28* and *VPS32* affect growth at alkaline pH and virulence through both *RIM101*-dependent and *RIM101*-independent pathways in *Candida albicans*. *Infection and Immunity, 73*:7977-7987. https://doi.org/10.1128/IAI.73.12.7977-7987.2005

Costa-de-Oliveira S & Rodrigues AG. (2020). *Candida albicans* antifungal resistance and tolerance in bloodstream infections: the triad yeast-host-antifungal. *Microorganisms, 8*:154-172. https://doi.org/10.3390/microorganisms8020154

Coste AT, Crittin J, Bauser C, Rohde B & Sanglard D. (2009). Functional analysis of *cis*- and *trans*-acting elements of the *Candida albicans CDR2* promoter with a novel promoter reporter system. *Eukaryotic Cell, 8*:1250-1267. https://doi.org/10.1128/EC.00069-09

Coste AT, Karababa M, Ischer F, Bille J & Sanglard D. (2004). *TAC1*, transcriptional activator of *CDR* genes, is a new transcription factor involved in the regulation of *Candida albicans* ABC transporters *CDR1* and *CDR2*. *Eukaryotic Cell, 3*:1639-1652. https://doi.org/10.1128/EC.3.6.1639-1652.2004

Coste A, Selmecki A, Forche A, Diogo D, Bougnoux M, d'Enfert C, Berman J & Sanglard D. (2007). Genotypic evolution of azole resistance mechanisms in sequential *Candida albicans* isolates. *Eukaryotic Cell, 6*:1889-1904. https://doi.org/10.1128/ec.00151-07

Coste A, Turner V, Ischer F, Morschhäuser J, Forche A, Selmecki A, Berman J, Bille J & Sanglard D. (2006). A mutation in Tac1p, a transcription factor regulating *CDR1* and *CDR2*, is coupled with loss of heterozygosity at chromosome 5 to mediate antifungal resistance in *Candida albicans*. *Genetics, 172*:2139-2156. https://doi.org/10.1534/genetics.105.054767

Cowen LE, Kohn LM & Anderson JB. (2001). Divergence in fitness and evolution of drug resistance in experimental populations of *Candida albicans*. *Journal of Bacteriology, 183*:2971-2978. https://doi.org/10.1128/JB.183.10.2971-2978.2001

Cowen LE & Lindquist S. (2005). Hsp90 potentiates the rapid evolution of new traits: drug resistance in diverse fungi. *Science, 309*:2185-2189. https://doi.org/10.1126/science.1118370

Cowen LE, Nantel A, Whiteway M, Thomas D, Tessier D, Kohn L & Anderson J. (2002). Population genomics of drug resistance in *Candida albicans*. *Proceedings of the National Academy of Sciences of the United States of America, 99*:9284–9289. https://doi.org/10.1073/pnas.102291099

Cowen LE, Sanglard D, Calabrese D, Sirjusingh C, Anderson JB & Kohn LM. (2000). Evolution of drug resistance in experimental populations of *Candida albicans*. *Journal of Bacteriology, 182*:1515-1522. https://doi.org/rg/10.1128/JB.182.6.1515-1522.2000

Cowen LE, Sanglard D, Howard SJ, Rogers PD & Perlin DS. (2015). Mechanisms of antifungal drug resistance. *Cold Spring Harbor Perspectives in Medicine, 5*:a019752. https://doi.org/10.1101/cshperspect.a019752

Cowen LE, Singh SD, Köhler JR, Collins C, Zaas AK, Schell WA, Aziz H, Mylonakis E, Perfect JR, Whitesell L & Lindquist S. (2009). Harnessing Hsp90 function as a powerful, broadly effective therapeutic strategy for fungal infectious disease. *Proceedings of the National Academy of Sciences, 106*:2818-2823. https://doi.org/10.1073/pnas.0813394106

Cruz MC, Goldstein AL, Blankenship JR, Del Poeta M, Davis D, Cardenas ME, Perfect JR, Mccusker JH & Heitman J. (2002). Calcineurin is essential for survival during membrane stress in *Candida albicans*. *The EMBO Journal, 21*:546-559. https://doi.org/10.1093/emboj/21.4.546

Cuenca-Estrella M, Gomez-Lopez A, Cuesta I, Zaragoza O, Mellado E & Rodriguez-Tudela JL. (2011). Frequency of voriconazole resistance *in vitro* among Spanish clinical isolates of *Candida* spp. according to breakpoints established by the antifungal subcommittee of the European Committee on Antimicrobial Susceptibility Testing. *Antimicrobial Agents and Chemotherapy, 55*:1794-1797. https://doi.org/10.1128/aac.01757-10

Cuomo CA, Fanning S, Gujja S, Zeng Q, Naglik JR, Filler SG & Mitchell AP. (2019). Genome sequence for *Candida albicans* clinical oral isolate 529L. *Microbiology Resource Announcements, 8*:e00554-19. https://doi.org/10.1128/MRA.00554-19

D

de Micheli M, Bille J, Schueller C & Sanglard D. (2002). A common drug-responsive element mediates the upregulation of the *Candida albicans* ABC transporters *CDR1* and *CDR2*, two genes involved in antifungal drug resistance. *Molecular Microbiology, 43*:1197-1214. https://doi.org/10.1046/j.1365-2958.2002.02814.x

de Oliveira Santos GC, Vasconcelos CC, Lopes AJO, de Sousa Cartágenes MdS, Filho AKDB, do Nascimento FRF, Ramos RM, Pires ERRB, de Andrade MS, Rocha FMG & de Andrade Monteiro C. (2018). *Candida* infections and therapeutic strategies: mechanisms of action for traditional and alternative Agents. *Frontiers in Microbiology, 9*:1351. https://doi.org/10.3389/fmicb.2018.01351

Delarze E & Sanglard D. (2015). Defining the frontiers between antifungal resistance, tolerance and the concept of persistence. *Drug Resistance Updates, 23*:12-19. https://doi.org/10.1016/j.drup.2015.10.001

Desai PR, van Wijlick L, Kurtz D, Juchimiuk M & Ernst JF. (2015). Hypoxia and temperature regulated morphogenesis in *Candida albicans*. *PLoS Genetics, 11*:e1005447. https://doi.org/10.1371/journal.pgen.1005447

DiCarlo JE, Norville JE, Mali P, Rios X, Aach J & Church GM. (2013). Genome engineering in *Saccharomyces cerevisiae* using CRISPR-Cas systems. *Nucleic Acids Research, 41*:4336-4343. https://doi.org/10.1093/nar/gkt135

Doi AM, Pignatari ACC, Edmond MB, Marra AR, Camargo LFA, Siqueira RA, da Mota VP & Colombo AL. (2016). Epidemiology and microbiologic characterization of nosocomial candidemia from a Brazilian National Surveillance Program. *PLoS ONE, 11*:e0146909. https://doi.org/10.1371/journal.pone.0146909

Douglas CM, Foor F, Marrinan JA, Morin N, Nielsen JB, Dahl AM, Mazur P, Baginsky W, Li W, El-Sherbeini M, Clemas JA, Mandala SM, Frommer BR & Kurtz MB. (1994). The *Saccharomyces cerevisiae FKS1* (*ETG1*) gene encodes an integral membrane protein which is a subunit of 1,3-β-D-glucan synthase. *Proceedings of the National Academy of Sciences, 91*:12907-12911. https://doi.org/10.1073/pnas.91.26.12907

Dunkel N, Blaß J, Rogers PD & Morschhäuser J. (2008). Mutations in the multi-drug resistance regulator *MRR1*, followed by loss of heterozygosity, are the main cause of *MDR1* overexpression in fluconazole-resistant *Candida albicans* strains. *Molecular Microbiology, 69*:827-840. https://doi.org/10.1111/j.1365-2958.2008.06309.x

Dunkel N, Liu TT, Barker KS, Homayouni R, Morschhäuser J & Rogers PD. (2008). A gain-of-function mutation in the transcription factor Upc2p causes upregulation of ergosterol biosynthesis genes and increased fluconazole resistance in a clinical *Candida albicans* isolate. *Eukaryotic Cell, 7*:1180-1190. https://doi.org/10.1128/EC.00103-08

E

Eddouzi J, Parker JE, Vale-Silva LA, Coste A, Ischer F, Kelly S, Manai M & Sanglard D. (2013). Molecular mechanisms of drug resistance in clinical *Candida* species isolated from Tunisian hospitals. *Antimicrobial Agents and Chemotherapy, 57*:3182-3193. https://doi.org/10.1128/AAC.00555-13

Ellsworth M & Ostrosky-Zeichner L. (2020). Isavuconazole: mechanism of action, clinical efficacy, and resistance. *Journal of Fungi, 6*:324. https://doi.org/10.3390/jof6040324

Ene IV, Bennett RJ & Anderson MZ. (2019). Mechanisms of genome evolution in *Candida albicans*. *Current Opinion in Microbiology, 52*:47-54. https://doi.org/10.1016/j.mib.2019.05.001

European Committee on Antimicrobial Susceptibility Testing. (2020). *Fluconazole: Rationale for the clinical breakpoints, version 3.0*

Evans BA, Smith OL, Pickerill ES, York MK, Buenconsejo KJP, Chambers AE & Bernstein DA. (2018). Restriction digest screening facilitates efficient detection of site-directed mutations introduced by CRISPR in *C. albicans UME6*. *PeerJ, 6*:e4920. https://doi.org/10.7717/peerj.4920

F

Falci DR & Pasqualotto AC. (2013). Profile of isavuconazole and its potential in the treatment of severe invasive fungal infections. *Infection and Drug Resistance, 6*:163-174. https://doi.org/10.2147/IDR.S51340

Favre B, Didmon M & Ryder NS. (1999). Multiple amino acid substitutions in lanosterol 14α-demethylase contribute to azole resistance in *Candida albicans*. *Microbiology, 145*:2715-2725. https://doi.org/10.1099/00221287-145-10-2715

Feng W, Yang J, Ji Y, Xi Z, Yang L, Zhu X & Ma Y. (2019). Mrr2 mutations and upregulation are associated with increased fluconazole resistance in *Candida albicans* isolates from patients with vulvovaginal candidiasis. *Letters in Applied Microbiology, 70*:95-101. https://doi.org/10.1111/lam.13248

Fiori A & Van Dijck P. (2012). Potent synergistic effect of doxycycline with fluconazole against *Candida albicans* is mediated by interference with iron homeostasis. *Antimicrobial Agents and Chemotherapy, 56*:3785-3796. https://doi.org/10.1128/AAC.06017-11

Fling ME, Kopf J, Tamarkin A, Gorman JA, Smith HA & Koltin Y. (1991). Analysis of a *Candida albicans* gene that encodes a novel mechanism for resistance to benomyl and methotrexate. *Molecular and General Genetics MGG, 227*:318-329. https://doi.org/10.1007/BF00259685

Flowers SA, Barker KS, Berkow EL, Toner G, Chadwick SG, Gygax SE, Morschhäuser J & Rogers PD. (2012). Gain-of-function mutations in *UPC2* are a frequent cause of *ERG11* upregulation in azole-resistant clinical isolates of *Candida albicans*. *Eukaryotic Cell, 11*:1289-1299. https://doi.org/10.1128/EC.00215-12

Flowers SA, Colón B, Whaley SG, Schuler MA & Rogers PD. (2015). Contribution of clinically derived mutations in *ERG11* to azole resistance in *Candida albicans*. *Antimicrobial Agents and Chemotherapy, 59*:450-460. https://doi.org/10.1128/AAC.03470-14

Forche A, Abbey D, Pisithkul T, Weinzierl MA, Ringstrom T, Bruck D, Petersen K & Berman J. (2011). Stress alters rates and types of loss of heterozygosity in *Candida albicans*. *mBio, 2*:129. https://doi.org/10.1128/mbio.00129-11

Forche A, Alby K, Schaefer D, Johnson AD, Berman J & Bennett RJ. (2008). The parasexual cycle in *Candida albicans* provides an alternative pathway to meiosis for the formation of recombinant strains. *PLoS Biology, 6*:e110. https://doi.org/10.1371/journal.pbio.0060110

Ford CB, Funt JM, Abbey D, Issi L, Guiducci C, Martinez DA, Delorey T, Li BY, White TC, Cuomo C, Rao RP, Berman J, Thompson DA & Regev A. (2015). The evolution of drug resistance in clinical isolates of *Candida albicans*. *eLife, 4*:e00662. https://doi.org/10.7554/eLife.00662

Franz R, Kelly SL, Lamb DC, Kelly DE, Ruhnke M & Morschhäuser J. (1998). Multiple molecular mechanisms contribute to a stepwise development of fluconazole resistance in clinical *Candida albicans* strains. *Antimicrobial Agents and Chemotherapy, 42*:3065-3072. https://doi.org/10.1128/AAC.42.12.3065

Franz R, Ruhnke M & Morschhäuser J. (1999). Molecular aspects of fluconazole resistance development in *Candida albicans*. *Mycoses, 42*:453-458. https://doi.org/10.1046/j.1439-0507.1999.00498.x

Fuentes M, Hermosilla G, Alburquenque C, Falconer MA, Amaro J & Tapia C. (2014). Caracterización de los mecanismos de resistencia a azoles en aislados clínicos chilenos de *Candida albicans*. *Revista Chilena De Infectología, 31*:511-517. https://doi.org/10.4067/S0716-10182014000500001

G

Gamarra S, Morano S, Dudiuk C, Mancilla E, Nardin ME, De Los Angeles Méndez, E & Garcia-Effron G. (2014). Epidemiology and antifungal susceptibilities of yeasts causing vulvovaginitis in a teaching hospital. *Mycopathologia, 178*:251-258. https://doi.org/10.1007/s11046-014-9780-2

Gao S, Tong Y, Wen Z, Zhu L, Ge M, Chen D, Jiang Y & Yang S. (2016). Multiplex gene editing of the *Yarrowia lipolytica* genome using the CRISPR-Cas9 system. *Journal of Industrial Microbiology and Biotechnology, 43*:1085-1093. https://doi.org/10.1007/s10295-016-1789-8

Garcia-Effron G. (2020). Rezafungin—Mechanisms of action, susceptibility and resistance: similarities and differences with the other echinocandins. *Journal of Fungi, 6*:262. https://doi.org/10.3390/jof6040262

Garnaud C, Botterel F, Sertour N, Bougnoux M, Dannaoui E, Larrat S, Hennequin C, Guinea J, Cornet M & Maubon D. (2015). Next-generation sequencing offers new insights into the resistance of *Candida* spp. to echinocandins and azoles. *Journal of Antimicrobial Chemotherapy, 70*:2556-2565. https://doi.org/10.1093/jac/dkv139

Garnaud C, García-Oliver E, Wang Y, Maubon D, Bailly S, Despinasse Q, Champleboux M, Govin J & Cornet M. (2018). The Rim pathway mediates antifungal tolerance in *Candida albicans* through newly identified Rim101 transcriptional targets, including Hsp90 and Ipt1. *Antimicrobial Agents and Chemotherapy, 62*:e01785-17. https://doi.org/10.1128/AAC.01785-17

Gasiunas G, Barrangou R, Horvath P & Siksnys V. (2012). Cas9–crRNA ribonucleoprotein complex mediates specific DNA cleavage for adaptive immunity in bacteria. *Proceedings of the National Academy of Sciences, 109*:E2579-E2586. https://doi.org/10.1073/pnas.1208507109

Gaur M, Puri N, Manoharlal R, Rai V, Mukhopadhayay G, Choudhury D & Prasad R. (2008). MFS transportome of the human pathogenic yeast *Candida albicans*. *BMC Genomics, 9*:579. https://doi.org/10.1186/1471-2164-9-579

Gaur NA, Puri N, Karnani N, Mukhopadhyay G, Goswami SK & Prasad R. (2004). Identification of a negative regulatory element which regulates basal transcription of a multidrug resistance gene *CDR1* of *Candida albicans*. *FEMS Yeast Research, 4*:389-399. https://doi.org/10.1016/S1567-1356(03)00204-6

Geddes-McAlister J & Shapiro RS. (2018). New pathogens, new tricks: emerging, drug-resistant fungal pathogens and future prospects for antifungal therapeutics. *Annals of the New York Academy of Sciences, 1435*:1-22. https://doi.org/10.1111/nyas.13739

Gerami-Nejad M, Zacchi LF, Mcclellan M, Matter K & Berman J. (2013). Shuttle vectors for facile gap repair cloning and integration into a neutral locus in *Candida albicans*. *Microbiology, 159*:565-579. https://doi.org/10.1099/mic.0.064097-0

Gerstein AC & Berman J. (2020). *Candida albicans* genetic background influences mean and heterogeneity of drug responses and genome stability during evolution in fluconazole. *mSphere, 5*:e00480-20. https://doi.org/10.1128/mSphere.00480-20

Gietz DR & Woods RA. (2002). Transformation of yeast by lithium acetate/single-stranded carrier DNA/polyethylene glycol method. In C. Guthrie, & G. R. Fink (Eds.), *Methods in enzymology* (pp. 87-96). Academic Press. https://doi.org/10.1016/S0076-6879(02)50957-5

Goldman GH, da Silva Ferreira, M E, dos Reis Marques E, Savoldi M, Perlin D, Park S, Godoy Martinez PC, Goldman MHS & Colombo AL. (2004). Evaluation of fluconazole resistance mechanisms in *Candida albicans* clinical isolates from HIV-infected patients in Brazil. *Mycology, 50*:25-32. https://doi.org/10.1016/j.diagmicrobio.2004.04.009

Grahl N, Demers EG, Crocker AW & Hogan DA. (2017). Use of RNA-protein complexes for genome editing in non- *albicans Candida* species. *mSphere, 2*:e00218-17. https://doi.org/10.1128/mSphere.00218-17

H

Hamill RJ. (2013). Amphotericin B formulations: a comparative review of efficacy and toxicity. *Drugs, 73*:919-934. https://doi.org/10.1007/s40265-013-0069-4

Harrison BD, Hashemi J, Bibi M, Pulver R, Bavli D, Nahmias Y, Wellington M, Sapiro G & Berman J. (2014). A tetraploid intermediate precedes aneuploid formation in yeasts exposed to fluconazole. *PLoS Biology, 12*:e1001815. https://doi.org/10.1371/journal.pbio.1001815

Havlickova B, Czaika VA & Friedrich M. (2008). Epidemiological trends in skin mycoses worldwide. *Mycoses, 51*:2-15. https://doi.org/10.1111/j.1439-0507.2008.01606.x

Heilmann CJ, Schneider S, Barker KS, Rogers PD & Morschhäuser J. (2010). An A643T mutation in the transcription factor Upc2p causes constitutive *ERG11* upregulation and increased fluconazole resistance in *Candida albicans*. *Antimicrobial Agents and Chemotherapy, 54*:353-359. https://doi.org/10.1128/AAC.01102-09

Hill JA, O'Meara TR & Cowen LE. (2015). Fitness trade-offs associated with the evolution of resistance to antifungal drug combinations. *Cell Reports, 10*:809-819. https://doi.org/10.1016/j.celrep.2015.01.009

Hille F, Richter H, Wong SP, Bratovič M, Ressel S & Charpentier E. (2018). The biology of CRISPR-Cas: backward and forward. *Cell, 172*:1239-1259. https://doi.org/10.1016/j.cell.2017.11.032

Hiller D, Stahl S & Morschhäuser J. (2006). Multiple *cis*-acting sequences mediate upregulation of the *MDR1* efflux pump in a fluconazole-resistante clinical *Candida albicans* isolate. *Antimicrobial Agents and Chemotherapy, 50*:2300-2308. https://doi.org/10.1128/AAC.00196-06

Hirakawa MP, Martinez DA, Sakthikumar S, Anderson MZ, Berlin A, Gujja S, Zeng Q, Zisson E, Wang JM, Greenberg JM, Berman J, Bennett RJ & Cuomo CA. (2015). Genetic and phenotypic intra-species variation in *Candida albicans*. *Genome Research, 25*:413-425. https://doi.org/10.1101/gr.174623.114

Hokken MWJ, Zwaan BJ, Melchers WJG & Verweij PE. (2019). Facilitators of adaptation and antifungal resistance mechanisms in clinically relevant fungi. *Fungal Genetics and Biology, 132*:103254. https://doi.org/10.1016/j.fgb.2019.103254

Holmes AR, Lin Y, Niimi K, Lamping E, Keniya M, Niimi M, Tanabe K, Monk BC & Cannon RD. (2008). ABC transporter Cdr1p contributes more than Cdr2p does to fluconazole efflux in fluconazole-resistant *Candida albicans* clinical isolates. *Antimicrobial Agents and Chemotherapy, 52*:3851-3862. https://doi.org/10.1128/AAC.00463-08

Hoot SJ, Smith AR, Brown RP & White TC. (2011). An A643V amino acid substitution in Upc2p contributes to azole resistance in well-characterized clinical isolates of *Candida albicans*. *Antimicrobial Agents and Chemotherapy, 55*:940-942. https://doi.org/10.1128/AAC.00995-10

Huang MY & Mitchell AP. (2017). Marker recycling in *Candida albicans* through CRISPR-Cas9-induced marker excision. *mSphere, 2*:e00050-17. https://doi.org/10.1128/mSphere.00050-17

Huang MY, Woolford CA, May G, McManus CJ & Mitchell AP. (2019). Circuit diversification in a biofilm regulatory network. *PLoS Pathogens, 15*:e1007787. https://doi.org/10.1371/journal.ppat.1007787

Huang MY, Woolford CA & Mitchell AP. (2018). Rapid gene concatenation for genetic rescue of multigene mutants in *Candida albicans*. *mSphere, 3*:e00169-18. https://doi.org/10.1128/mSphere.00169-18

Huang M, McClellan M, Berman J & Kao KC. (2011). Evolutionary dynamics of *Candida albicans* during *in vitro* evolution. *Eukaryotic Cell, 10*:1413-1421. https://doi.org/rg/10.1128/EC.05168-11

Hull CM & Johnson AD. (1999). Identification of a mating-type locus in the asexual pathogenic yeast *Candida albicans*. *Science, 285*:1271-1275. https://doi.org/10.1126/science.285.5431.1271

I

Ishino Y, Krupovic M & Forterre P. (2018). History of CRISPR-Cas from encounter with a mysterious repeated sequence to genome editing technology. *Journal of Bacteriology, 200*:e00580-17. https://doi.org/10.1128/jb.00580-17

Ishino Y, Shinagawa H, Makino K, Amemura M & Nakata A. (1987). Nucleotide sequence of the *iap* gene, responsible for alkaline phosphatase isozyme conversion in *Escherichia coli*, and identification of the gene product. *Journal of Bacteriology, 169*:5429-5433. https://doi.org/10.1128/jb.169.12.5429-5433.1987

Iyer KR, Robbins N & Cowen LE. (2022). The role of *Candida albicans* stress response pathways in antifungal tolerance and resistance. *iScience, 25*:103953. https://doi.org/10.1016/j.isci

J

Jallow S & Govender NP. (2021). Ibrexafungerp: a first-in-class oral triterpenoid glucan synthase inhibitor. *Journal of Fungi, 7*:163. https://doi.org/10.3390/jof7030163

Jansen R, van Embden, J D A, Gaastra W & Schouls LM. (2002). Identification of genes that are associated with DNA repeats in prokaryotes. *Molecular Microbiology, 43*:1565-1575. https://doi.org/10.1046/j.1365-2958.2002.02839.x

Jensen RH, Astvad KMT, Silva LV, Sanglard D, Jørgensen R, Nielsen KF, Mathiasen EG, Doroudian G, Perlin DS & Arendrup MC. (2015). Stepwise emergence of azole, echinocandin and amphotericin B multidrug resistance in vivo in *Candida albicans* orchestrated by multiple genetic alterations. *Journal of Antimicrobial Chemotherapy, 70*:2551-2555. https://doi.org/10.1093/jac/dkv140

Jiang W, Bikard D, Cox D, Zhang F & Marraffini LA. (2013). RNA-guided editing of bacterial genomes using CRISPR-Cas systems. *Nature Biotechnology, 31*:233-239. https://doi.org/10.1038/nbt.2508

Jinek M, Chylinski K, Fonfara I, Hauer M, Doudna JA & Charpentier E. (2012). A programmable dual-RNA—guided DNA endonuclease in adaptive bacterial immunity. *Science, 337*:816-821. https://doi.org/10.1126/science.1225829

Jones T, Federspiel NA, Chibana H, Dungan J, Kalman S, Magee BB, Newport G, Thorston YR, Agabian N, Magee PT, Davis RW & Scherer S. (2004). The diploid genome sequence of *Candida albicans*. *Proceedings of the National Academy of Sciences, 101*:7329-7334. https://doi.org/10.1073/pnas.0401648101

K

Kakeya H, Miyazaki Y, Miyazaki H, Nyswaner K, Grimberg B & Bennett JE. (2000). Genetic analysis of azole resistance in the Darlington strain of *Candida albicans*. *Antimicrobial Agents and Chemotherapy, 44*:2985-2990. https://doi.org/10.1128/AAC.44.11.2985-2990.2000

Kamai Y, Maebashi K, Kudoh M, Makimura K, Naka W, Uchida K & Yamaguchi H. (2004). Characterization of mechanisms of fluconazole resistance in a *Candida albicans* isolate from a Japanese patient with chronic mucocutaneous candidiasis. *Microbiology and Immunology, 48*:937-943.

Kapoor M, Moloney M, Soltow QA, Pillar CM & Shaw KJ. (2019). Evaluation of resistance development to the Gwt1 inhibitor Manogepix (APX001A) in *Candida* species. *Antimicrobial Agents and Chemotherapy, 64*:e01387-19. https://doi.org/10.1128/AAC.01387-19

Karababa M, Coste AT, Rognon B, Bille J & Sanglard D. (2004). Comparison of gene expression profiles of *Candida albicans* azole-resistant clinical isolates and laboratory strains exposed to drugs inducing multidrug transporters. *Antimicrobial Agents and Chemotherapy, 48*:3064-3079. https://doi.org/10.1128/AAC.48.8.3064-3079.2004

Karnani N, Gaur NA, Jha S, Puri N, Krishnamurthy S, Goswami SK, Mukhopadhyay G & Prasad R. (2004). SRE1 and SRE2 are two specific steroid-responsive modules of *Candida* drug resistance gene 1 (*CDR1*) promoter. *Yeast, 21*:219-239. https://doi.org/10.1002/yea.1067

Kelly SL, Lamb DC & Kelly DE. (1999). Y132H substitution in *Candida albicans* sterol 14α-demethylase confers fluconazole resistance by preventing binding to haem. *FEMS Microbiology Letters, 180*:171-175. https://doi.org/10.1016/s0378-1097(99)00478-4

Kelly SL, Lamb DC, Kelly DE, Manning NJ, Loeffler J, Hebart H, Schumacher U & Einsele H. (1997). Resistance to fluconazole and cross-resistance to amphotericin B in *Candida albicans* from AIDS patients caused by defective sterol Δ5,6 -desaturation. *FEBS Letters, 400*:80-82. https://doi.org/10.1016/s0014-5793(96)01360-9

Kelly SL, Lamb DC, Loeffler J, Einsele H & Kelly DE. (1999). The G464S amino acid substitution in *Candida albicans* sterol 14α-demethylase causes fluconazole resistance in the clinic through reduced affinity. *Biochemical and Biophysical Research Communications, 262*:174-179. https://doi.org/10.1006/bbrc.1999.1136

Keniya MV, Sabherwal M, Wilson RK, Woods MA, Sagatova AA, Tyndall JDA & Monk BC. (2018). Crystal structures of full-length lanosterol 14α-demethylases of prominent fungal pathogens *Candida albicans* and *Candida glabrata* provide tools for antifungal discovery. *Antimicrobial Agents and Chemotherapy, 62*:e01134-18. https://doi.org/10.1128/AAC.01134-18

Khan Z, Ahmad S, Mokaddas E, Meis JF, Joseph L, Abdullah A & Vayalil S. (2018). Development of echinocandin resistance in *Candida tropicalis* following short-term exposure to caspofungin for empiric therapy. *Antimicrobial Agents and Chemotherapy, 62*:e01926-17. https://doi.org/rg/10.1128/aac.01926-17

Khandelwal NK, Chauhan N, Sarkar P, Esquivel BD, Coccetti P, Singh A, Coste AT, Gupta M, Sanglard D, White TC, Chauvel M, d'Enfert C, Chattopadhyay A, Gaur NA, Mondal AK & Prasad R. (2018). Azole resistance in a *Candida albicans* mutant lacking the ABC transporter *CDR6*/*ROA1* depends on TOR signaling. *Journal of Biological Chemistry, 293*:412-432. https://doi.org/10.1074/jbc.M117.807032

Khandelwal NK, Wasi M, Nair R, Gupta M, Kumar M, Mondal AK, Gaur NA & Prasad R. (2019). Vacuolar sequestration of azoles, a novel strategy of azole antifungal resistance conserved across pathogenic and nonpathogenic yeast. *Antimicrobial Agents and Chemotherapy, 63*:e01347-18. https://doi.org/10.1128/aac.01347-18

Khosravi Rad K, Falahati M, Roudbary M, Farahyar S & Nami S. (2016). Overexpression of *MDR-1* and *CDR-2* genes in fluconazole resistance of *Candida albicans* isolated from patients with vulvovaginal candidiasis. *Current Medical Mycology, 2*:24-29. https://doi.org/10.18869/acadpub.cmm.2.4.24

Kidd SE, Crawford LC & Catriona L. (2021). Antifungal susceptibility testing and identification. *Infectious Disease Clinics of North America, 35*:313-339. https://doi.org/10.1016/j.idc.2021.03.004

Kodedová M & Sychrová H. (2015). Changes in the sterol composition of the plasma membrane affect membrane potential, salt tolerance and the activity of multidrug resistance pumps in *Saccharomyces cerevisiae*. *PLoS ONE, 10*:e0139306. https://doi.org/10.1371/journal.pone.0139306

Kojic EM & Darouiche RO. (2004). *Candida* infections of medical devices. *Clinical Microbiology Reviews, 17*:255-267. https://doi.org/10.1128/CMR.17.2.255-267.2004

Komor AC, Badran AH & Liu DR. (2017). CRISPR-based technologies for the manipulation of eukaryotic genomes. *Cell, 168*:20-36. https://doi.org/10.1016/j.cell.2016.10.044

Kondoh O, Tachibana Y, Ohya Y, Arisawa M & Watanabe T. (1997). Cloning of the *RHO1* gene from *Candida albicans* and its regulation of β-1,3-glucan synthesis . *Journal of Bacteriology, 179*:7734-7741. https://doi.org/10.1128/jb.179.24.7734-7741.1997

Kreusch A & Karstaedt AS. (2013). Candidemia among adults in Soweto, South Africa, 1990–2007. *International Journal of Infectious Diseases, 17*:e621-e623. https://doi.org/10.1016/j.ijid.2013.02.010

Ksiezopolska E & Gabaldón T. (2018). Evolutionary emergence of drug resistance in *Candida* opportunistic pathogens. *Genes, 9*:461. https://doi.org/10.3390/genes9090461

Kullberg BJ & Arendrup MC. (2015). Invasive candidiasis. *The New England Journal of Medicine, 373*:1445-1456. https://doi.org/10.1056/NEJMra1315399

Kumar A, Nair R, Kumar M, Banerjee A, Chakrabarti A, Rudramurthy SM, Bagga R, Gaur NA, Mondal AK & Prasad R. (2020). Assessment of antifungal resistance and associated molecular mechanism in *Candida albicans* isolates from different cohorts of patients in North Indian state of Haryana. *Folia Microbiologica, 65*:747-754. https://doi.org/10.1007/s12223-020-00785-6

L

LaFayette SL, Collins C, Zaas AK, Schell WA, Betancourt-Quiroz M, Gunatilaka AAL, Perfect JR & Cowen LE. (2010). PKC signaling regulates drug resistance of the fungal pathogen *Candida albicans* via circuitry comprised of Mkc1, calcineurin, and Hsp90. *PLoS Pathogens, 6*:e1001069. https://doi.org/10.1371/journal.ppat.1001069

Lamb DC, Kelly DE, Schunck W, Shyadehi AZ, Akhtar M, Lowe DJ, Baldwin BC & Kelly SL. (1997). The mutation T315A in *Candida albicans* sterol 14α-demethylase causes reduced enzyme activity and fluconazole resistance through reduced affinity. *The Journal of Biological Chemistry, 272*:5682-5688. https://doi.org/10.1074/jbc.272.9.5682

Lamb DC, Kelly DE, White TC & Kelly SL. (2000). The R467K amino acid substitution in *Candida albicans* sterol 14α-demethylase causes drug resistance through reduced affinity. *Antimicrobial Agents and Chemotherapy, 44*:63-67. https://doi.org/10.1128/AAC.44.1.63-67.2000

Lamoth F, Lockhart SR, Berkow EL & Calandra T. (2018). Changes in the epidemiological landscape of invasive candidiasis. *Journal of Antimicrobial Chemotherapy, 73*:i4-i13. https://doi.org/10.1093/jac/dkx444

Leach MD, Farrer RA, Tan K, Miao Z, Walker LA, Cuomo CA, Wheeler RT, Brown AJP, Wong KH & Cowen LE. (2016). Hsf1 and Hsp90 orchestrate temperature-dependent global transcriptional remodelling and chromatin architecture in *Candida albicans*. *Nature Communications, 7*:11704. https://doi.org/10.1038/ncomms11704

Lee A. (2021). Ibrexafungerp: first approval. *Drugs, 81*:1445-1450. https://doi.org/10.1007/s40265-021-01571-5

Lee M, Williams LE, Warnock DW & Arthington-Skaggs BA. (2004). Drug resistance genes and trailing growth in *Candida albicans* isolates. *Journal of Antimicrobial Chemotherapy, 53*:217-224. https://doi.org/10.1093/jac/dkh040

Legrand M, Jaitly P, Feri A, d'Enfert C & Sanyal K. (2019). *Candida albicans*: an emerging yeast model to study eukaryotic genome plasticity. *Trends in Genetics, 35*:292-307. https://doi.org/10.1016/j.tig.2019.01.005

Li X, Brown N, Chau AS, López-Ribot JL, Ruesga MT, Quindos G, Mendrick CA, Hare RS, Loebenberg D, DiDomenico B & McNicholas PM. (2004). Changes in susceptibility to posaconazole in clinical isolates of *Candida albicans*. *Journal of Antimicrobial Chemotherapy, 53*:74-80. https://doi.org/10.1093/jac/dkh027

Liu J, Vogel AK, Miao J, Carnahan JA, Lowes DJ, Rybak JM & Peters BM. (2022). Rapid hypothesis testing in *Candida albicans* clinical isolates using a cloning-free, modular, and recyclable system for CRISPR-Cas9 mediated mutant and revertant construction. *Microbiology Spectrum, 10*:e0263021. https://doi.org/10.1128/spectrum.02630-21

Liu J, Shi C, Wang Y, Li W, Zhao Y & Xiang M. (2015). Mechanisms of azole resistance in *Candida albicans* clinical isolates from Shanghai, China. *Research in Microbiology, 166*:153-161. https://doi.org/10.1016/j.resmic.2015.02.009

Liu Z & Myers LC. (2017). Mediator tail module is required for Tac1-activated *CDR1* expression and azole resistance in *Candida albicans*. *Antimicrobial Agents and Chemotherapy, 61*:e01342-17. https://doi.org/10.1128/aac.01342-17

Livak KJ & Schmittgen TD. (2001). Analysis of relative gene expression data using real-time quantitative PCR and the $2^{-\Delta\Delta CT}$ method. *Methods, 25*:402-408. https://doi.org/10.1006/meth.2001.1262

Lockhart SR, Iqbal N, Cleveland AA, Farley MM, Harrison LH, Bolden CB, Baughman W, Stein B, Hollick R, Park BJ & Chiller T. (2012). Species identification and antifungal susceptibility testing of *Candida* bloodstream isolates from population-based surveillance studies in two U.S. cities from 2008 to 2011. *Journal of Clinical Microbiology, 50*:3435-42. https://doi.org/10.1128/JCM.01283-12

Löffler J, Kelly SL, Hebart H, Schumacher U, Lass-Flörl C & Einsele H. (1997). Molecular analysis of *cyp51* from fluconazole-resistant *Candida albicans* strains. *FEMS Microbiology Letters, 151*:263-268. https://doi.org/10.1111/j.1574-6968.1997.tb12580.x

Lohberger A, Coste AT & Sanglard D. (2014). Distinct roles of *Candida albicans* drug resistance transcription factors *TAC1*, *MRR1*, and *UPC2* in virulence. *Eukaryotic Cell, 13*:127-142. https://doi.org/10.1128/EC.00245-13

Lombardi L, Oliveira-Pacheco J & Butler G. (2019). Plasmid-based CRISPR-Cas9 gene editing in multiple *Candida* species. *mSphere, 4*:e00125-19. https://doi.org/10.1128/mSphere

Lombardi L, Turner SA, Zhao F & Butler G. (2017). Gene editing in clinical isolates of *Candida parapsilosis* using CRISPR/Cas9. *Scientific Reports, 7*:8051. https://doi.org/10.1038/s41598-017-08500-1

Lopez-Ribot JL, McAtee RK, Lee LN, Kirkpatrick WR, White TC, Sanglard D & Patterson TF. (1998). Distinct patterns of gene expression associated with development of fluconazole resistance in serial *Candida albicans* isolates from human immunodeficiency virus-infected patients with oropharyngeal candidiasis. *Antimicrobial Agents and Chemotherapy, 42*:2932-2937. https://doi.org/10.1128/AAC.42.11.2932

Luna-Tapia A, Butts A & Palmer GE. (2019). Loss of C-5 sterol desaturase activity in *Candida albicans*: azole resistance or merely trailing growth? *Antimicrobial Agents and Chemotherapy, 63*:e01337-18. https://doi.org/10.1128/aac

Luna-Tapia A, Kerns ME, Eberle KE, Jursic BS & Palmer GE. (2015). Trafficking through the late endosome significantly impacts *Candida albicans* tolerance of the azole antifungals. *Antimicrobial Agents and Chemotherapy, 59*:2410-2420. https://doi.org/10.1128/AAC.04239-14

Luna-Tapia A, Tournu H, Peters TL & Palmer GE. (2016). Endosomal trafficking defects can induce calcium dependent azole tolerance in *Candida albicans*. *Antimicrobial Agents and Chemotherapy, 60*:7170-7177. https://doi.org/10.1128/AAC.01034-16

Luna-Tapia A, Willems HME, Parker JE, Tournu H, Barker KS, Nishimoto AT, Rogers PD, Kelly SL, Peters BM & Palmer GE. (2018). Loss of Upc2p-inducible *ERG3* transcription is sufficient to confer niche-specific azole resistance without compromising *Candida albicans* pathogenicity. *mBio, 9*:e00225-18. https://doi.org/10.1128/mBio.00225-18

M

MacPherson S, Akache B, Weber S, De Deken X, Raymond M & Turcotte B. (2005). *Candida albicans* zinc cluster protein Upc2p confers resistance to antifungal drugs and is an activator of ergosterol biosynthetic genes. *Antimicrobial Agents and Chemotherapy, 49*:1745-1752. https://doi.org/10.1128/AAC.49.5.1745-1752.2005

Magill SS, Edwards JR, Bamberg W, Beldavs ZG, Dumyati G, Kainer MA, Lynfield R, Maloney M, McAllister-Hollod L, Nadle J, Ray SM, Thompson DL, Wilson LE & Fridkin SK. (2014). Multistate point-prevalence survey of health care–associated infections. *The New England Journal of Medicine, 370*:1198-1208. https://doi.org/10.1056/NEJMoa1306801

Makarova KS, Grishin NV, Shabalina SA, Wolf YI & Koonin EV. (2006). A putative RNA-interference-based immune system in prokaryotes: computational analysis of the predicted enzymatic machinery, functional analogies with eukaryotic RNAi, and hypothetical mechanisms of action. *Biology Direct, 1*:7. https://doi.org/10.1186/1745-6150-1-7

Manavathu EK, Kallakuri S, Arganoza MT & Vazquez JA. (1999). Amino acid variations of cytochrome P-450 lanosterol 14α-demethylase (CYP51A1) from fluconazole-resistant clinical isolates of *Candida albicans*. *Revista Iberoamericana De Micología, 16*:198-203. https://search.proquest.com/docview/17501059

Mane A, Vidhate P, Kusro C, Waman V, Saxena V, Kulkarni-Kale U & Risbud A. (2016). Molecular mechanisms associated with Fluconazole resistance in clinical Candida albicans isolates from India. *Mycoses, 59*:93-100. https://doi.org/10.1111/myc.12439

Manoharlal R, Gaur NS, Panwar SL, Morschhäuser J & Prasad R. (2008). Transcriptional activation and increased mRNA stability contribute to overexpression of *CDR1* in azole-resistant *Candida albicans*. *Antimicrobial Agents and Chemotherapy, 52*:1481-1492. https://doi.org/10.1128/AAC.01106-07

Manoharlal R, Gorantala J, Sharma M, Sanglard D & Prasad R. (2010). *PAP1* [poly(A) polymerase 1] homozygosity and hyperadenylation are major determinants of increased mRNA stability of *CDR1* in azole-resistant clinical isolates of *Candida albicans*. *Microbiology, 156*:313-326. https://doi.org/10.1099/mic.0.035154-0

Mansfield BE, Oltean HN, Oliver BG, Hoot SJ, Leyde SE, Hedstrom L & White TC. (2010). Azole drugs are imported by facilitated diffusion in *Candida albicans* and other pathogenic fungi. *PLoS Pathogens, 6*:e1001126. https://doi.org/10.1371/journal.ppat.1001126

Marcos-Zambrano LJ, Escribano P, Sánchez-Carrillo C, Bouza E & Guinea J. (2016). Scope and frequency of fluconazole trailing assessed using EUCAST in invasive *Candida* spp. isolates. *Medical Mycology, 54*:733-739. https://doi.org/10.1093/mmy/myw033

Marichal P, Koymans L, Willemsens S, Bellens D, Verhasselt P, Luyten W, Borgers M, Ramaekers FCS, Odds FC & Vanden Bossche H. (1999). Contribution of mutations in the cytochrome P450 14α-demethylase (Erg11p, Cyp51p) to azole resistance in *Candida albicans*. *Microbiology, 145*:2701–2713. https://doi.org/10.1099/00221287-145-10-2701

Marr KA, Lyons CN, Rustad T, Bowden RA & White TC. (1998). Rapid, transient fluconazole resistance in *Candida albicans* is associated with increased mRNA levels of *CDR*. *Antimicrobial Agents and Chemotherapy, 42*:2584-2589. https://doi.org/https://doi.org/10.1128/AAC.42.10.2584

Marr KA, Rustad TR, Rex JH & White TC. (1999). The trailing end point phenotype in antifungal susceptibility testing is pH dependent. *Antimicrobial Agents and Chemotherapy, 43*:1383-1386. https://doi.org/10.1128/AAC.43.6.1383

Marton T, Maufrais C, d'Enfert C & Legrand M. (2020). Use of CRISPR-Cas9 to target homologous recombination limits transformation-induced genomic changes in *Candida albicans*. *mSphere, 5*:e00620-20. https://doi.org/10.1128/mSphere.00620-20

Mazur P & Baginsky W. (1996). In vitro activity of 1,3-β-D-glucan synthase requires the GTP-binding protein Rho1. *The Journal of Biological Chemistry, 271*:14604-14609. https://doi.org/10.1074/jbc.271.24.14604

McCarthy MW, Kontoyiannis DP, Cornely OA, Perfect JR & Walsh TJ. (2017). Novel agents and drug targets to meet the challenges of resistant fungi. *The Journal of Infectious Diseases, 216*:S474-S483. https://doi.org/10.1093/infdis/jix130

McCarty TP & Pappas PG. (2016). Invasive candidiasis. *Infectious Disease Clinics of North America, 30*:103-124. https://doi.org/10.1016/j.idc.2015.10.013

McManus BA & Coleman DC. (2014). Molecular epidemiology, phylogeny and evolution of *Candida albicans*. *Infection, Genetics and Evolution, 21*:166-178. https://doi.org/10.1016/j.meegid.2013.11.008

McTaggart LR, Cabrera A, Cronin K & Kus JV. (2020). Antifungal susceptibility of clinical yeast isolates from a large Canadian reference laboratory and application of whole-genome sequence analysis to elucidate mechanisms of acquired resistance. *Antimicrobial Agents and Chemotherapy, 64*:e00402-20. https://doi.org/10.1128/aac.00402-20

McWilliam H, Li W, Uludag M, Squizzato S, Park YM, Buso N, Cowley AP & Lopez R. (2013). Analysis Tool Web Services from the EMBL-EBI. *Nucleic Acids Research, 41*:W597-600. https://doi.org/10.1093/nar/gkt376

Min K, Ichikawa Y, Woolford CA & Mitchell AP. (2016). *Candida albicans* gene deletion with a transient CRISPR-Cas9 system. *mSphere, 1*:e00130-16. https://doi.org/10.1128/mSphere.00130-16

Mogavero S, Tavanti A, Senesi S, Rogers PD & Morschhäuser J. (2011). Differential requirement of the transcription factor Mcm1 for activation of the *Candida albicans* multidrug efflux pump *MDR1* by its regulators Mrr1 and Cap1. *Antimicrobial Agents and Chemotherapy, 55*:2061-2066. https://doi.org/10.1128/AAC.01467-10

Mojica FJM, Díez-Villaseñor C, García-Martínez J & Soria E. (2005). Intervening sequences of regularly spaced prokaryotic repeats derive from foreign genetic elements. *Journal of Molecular Evolution, 60*:174-182. https://doi.org/10.1007/s00239-004-0046-3

Mojica FJM, Juez G & Rodriguez-Valera F. (1993). Transcription at different salinities of *Haloferax mediterranei* sequences adjacent to partially modified PstI sites. *Molecular Microbiology, 9*:613-621. https://doi.org/10.1111/j.1365-2958.1993.tb01721.x

Morio F, Pagniez F, Lacroix C, Miegeville M & Le Pape P. (2012). Amino acid substitutions in the *Candida albicans* sterol 5,6-desaturase (Erg3p) confer azole resistance: characterization of two novel mutants with impaired virulence. *Journal of Antimicrobial Chemotherapy, 67*:2131-2138. https://doi.org/10.1093/jac/dks186

Morio F, Jensen RH, Le Pape P & Arendrup MC. (2017). Molecular basis of antifungal drug resistance in yeasts. *International Journal of Antimicrobial Agents, 50*:599-606. https://doi.org/10.1016/j.ijantimicag.2017.05.012

Morio F, Loge C, Besse B, Hennequin C & Le Pape P. (2010). Screening for amino acid substitutions in the *Candida albicans* Erg11 protein of azole-susceptible and azole-resistant clinical isolates: new substitutions and a review of the literature. *Diagnostic Microbiology and Infectious Disease, 66*:373-384. https://doi.org/10.1016/j.diagmicrobio.2009.11.006

Morio F, Lombardi L, Binder U, Loge C, Robert E, Graessle D, Bodin M, Lass-Flörl C, Butler G & Le Pape P. (2019). Precise genome editing using a CRISPR-Cas9 method highlights the role of CoERG11 amino acid substitutions in azole resistance in *Candida orthopsilosis*. *Journal of Antimicrobial Chemotherapy, 74*:2230-2238. https://doi.org/10.1093/jac/dkz204

Morio F, Lombardi L & Butler G. (2020). The CRISPR toolbox in medical mycology: State of the art and perspectives. *PLoS Pathogens, 16*:e1008201. https://doi.org/10.1371/journal.ppat.1008201

Morio F, Pagniez F, Besse M, Gay-andrieu F, Miegeville M & Le Pape P. (2013). Deciphering azole resistance mechanisms with a focus on transcription factor-encoding genes *TAC1*, *MRR1* and *UPC2* in a set of fluconazole-resistant clinical isolates of *Candida albicans*. *International Journal of Antimicrobial Agents, 42*:410-415. https://doi.org/10.1016/j.ijantimicag.2013.07.013

Morschhäuser J. (2002). The genetic basis of fluconazole resistance development in *Candida albicans*. *Biochimica Et Biophysica Acta, 1587*:240-248. https://doi.org/10.1016/s0925-4439(02)00087-x

Morschhäuser J. (2010). Regulation of multidrug resistance in pathogenic fungi. *Fungal Genetics and Biology, 47*:94-106. https://doi.org/10.1016/j.fgb.2009.08.002

Morschhäuser J. (2016). The development of fluconazole resistance in *Candida albicans* – an example of microevolution of a fungal pathogen. *The Journal of Microbiology, 54*:192-201. https://doi.org/10.1007/s12275-016-5628-4

Morschhäuser J, Barker KS, Liu TT, Blaß-Warmuth J, Homayouni R & Rogers PD. (2007). The transcription factor Mrr1p controls expression of the *MDR1* efflux pump and mediates multidrug resistance in *Candida albicans*. *PLoS Pathogens, 3*:e164. https://doi.org/10.1371/journal.ppat.0030164

Mount HO, Revie NM, Todd RT, Anstett K, Collins C, Costanzo M, Boone C, Robbins N, Selmecki A & Cowen LE. (2018). Global analysis of genetic circuitry and adaptive mechanisms enabling resistance to the azole antifungal drugs. *PLoS Genetics, 14*:e1007319. https://doi.org/10.1371/journal.pgen.1007319

Murphy SE & Bicanic T. (2021). Drug resistance and novel therapeutic approaches in invasive candidiasis. *Frontiers in Cellular and Infection Microbiology, 11*:759408. https://doi.org/10.3389/fcimb.2021.759408

N

Nailis H, Coenye T, Van Nieuwerburgh F, Deforce D & Nelis HJ. (2006). Development and evaluation of different normalization strategies for gene expression studies in *Candida albicans* biofilms by real-time PCR. *BMC Molecular Biology, 7*:25. https://doi.org/10.1186/1471-2199-7-25

Ng H & Dean N. (2017). Dramatic improvement of CRISPR/Cas9 editing in *Candida albicans* by increased single guide RNA expression. *mSphere, 2*:e00385-16. https://doi.org/10.1128/mSphere.00385-16

Nguyen N, Quail MMF & Hernday AD. (2017). An efficient, rapid, and recyclable system for CRISPR-mediated genome editing in *Candida albicans*. *mSphere, 2*:e00149-17. https://doi.org/10.1128/mSphereDirect

Nishimoto AT, Sharma C & Rogers PD. (2020). Molecular and genetic basis of azole antifungal resistance in the opportunistic pathogenic fungus *Candida albicans*. *Journal of Antimicrobial Chemotherapy, 75*:257-270. https://doi.org/10.1093/jac/dkz400

Nishimoto AT, Zhang Q, Hazlett B, Morschhäuser J & Rogers PD. (2019). Contribution of clinically derived mutations in the gene encoding the zinc cluster transcription factor Mrr2 to fluconazole antifungal resistance and CDR1 expression in Candida albicans. *Antimicrobial Agents and Chemotherapy, 63*:e00078-19. https://doi.org/10.1128/AAC.00078-19

O

Odabasi Z, Paetznick VL, Rodriguez JR, Chen E, Rex JH, Leitz GJ & Ostrosky-Zeichner L. (2010). Lack of correlation of 24- vs. 48-h itraconazole minimum inhibitory concentrations with microbiological and survival outcomes in a guinea pig model of disseminated candidiasis. *Mycoses, 53*:438-442. https://doi.org/10.1111/j.1439-0507.2009.01733.x

Odds FC, Brown AJP & Gow NAR. (2003). Antifungal agents: mechanisms of action. *Trends in Microbiology, 11*:272-279. https://doi.org/10.1016/s0966-842x(03)00117-3

Oliver BG, Song JL, Choiniere JH & White TC. (2007). *cis*-Acting elements within the *Candida albicans ERG11* promoter mediate the azole response through transcription factor Upc2p. *Eukaryotic Cell, 6*:2231-2239. https://doi.org/10.1128/EC.00331-06

Ostrosky-Zeichner L, Casadevall A, Galgiani JN, Odds FC & Rex JH. (2010). An insight into the antifungal pipeline: selected new molecules and beyond. *Nature Reviews. Drug Discovery, 9*:719-727. https://doi.org/10.1038/nrd3074

P

Pappas PG, Kauffman CA, Andes DR, Clancy CJ, Marr KA, Ostrosky-Zeichner L, Reboli AC, Schuster MG, Vazquez JA, Walsh TJ, Zaoutis TE & Sobel JD. (2016). Clinical practice guideline for the management of candidiasis: 2016 update by the Infectious Diseases Society of America. *Clinical Infectious Diseases, 62*:e1-50. https://doi.org/10.1093/cid/civ933

Paquet D, Kwart D, Chen A, Sproul A, Jacob S, Teo S, Olsen KM, Gregg A, Noggle S & Tessier-Lavigne M. (2016). Efficient introduction of specific homozygous and heterozygous mutations using CRISPR/Cas9. *Nature, 533*:125-129. https://doi.org/10.1038/nature17664

Park S & Perlin DS. (2005). Establishing surrogate markers for fluconazole resistance in *Candida albicans*. *Microbial Drug Resistance, 11*:232-238. https://doi.org/10.1089/mdr.2005.11.232

Paul S & Moye-Rowley WS. (2014). Multidrug resistance in fungi: regulation of transporter-encoding gene expression. *Frontiers in Physiology, 5*:143. https://doi.org/10.3389/fphys.2014.00143

Paul S, Singh S, Sharma D, Chakrabarti A, Rudramurthy SM & Ghosh AK. (2020). Dynamics of *in vitro* development of azole resistance in *Candida tropicalis*. *Journal of Global Antimicrobial Resistance., 22*:553-561. https://doi.org/https://doi.org/10.1016/j.jgar.2020.04.018

Pelletier R, Peter J, Antin C, Gonzalez C, Wood L & Walsh TJ. (2000). Emergence of resistance of *Candida albicans* to clotrimazole in human immunodeficiency virus-infected children: in vitro and clinical correlations. *Journal of Clinical Microbiology, 38*:1563-1568. https://doi.org/10.1128/JCM.38.4.1563-1568.2000

Perea S, López-Ribot JL, Kirkpatrick WR, McAtee RK, Santillán RA, Martínez M, Calabrese D, Sanglard D & Patterson TF. (2001). Prevalence of molecular mechanisms of resistance to azole antifungal agents in *Candida albicans* strains displaying high-level fluconazole resistance isolated from human immunodeficiency virus-infected patients. *Antimicrobial Agents and Chemotherapy, 45*:2676-2684. https://doi.org/10.1128/AAC.45.10.2676-2684.2001

Perepnikhatka V, Fischer FJ, Niimi M, Baker RA, Cannon RD, Wang YK, Sherman F & Rustchenko E. (1999). Specific chromosome alterations in fluconazole-resistant mutants of *Candida albicans*. *Journal of Bacteriology, 181*:4041-4049. https://doi.org/10.1128/JB.181.13.4041-4049.1999

Perfect JR. (2017). The antifungal pipeline: a reality check. *Nature Reviews. Drug Discovery, 16*:603-616. https://doi.org/10.1038/nrd.2017.46

Perlin DS. (2011). Current perspectives on echinocandin class drugs. *Future Microbiology, 6*:441-457. https://doi.org/10.2217/fmb.11.19

Perlin DS, Rautemaa-Richardson R & Alastruey-Izquierdo A. (2017). The global problem of antifungal resistance: prevalence, mechanisms, and management. *The Lancet Infectious Diseases, 17*:e383-92. https://doi.org/10.1016/s1473-3099(17)30316-x

Pfaffl MW, Tichopad A, Prgomet C & Neuvians TP. (2004). Determination of stable housekeeping genes, differentially regulated target genes and sample integrity: BestKeeper – Excel-based tool using pair-wise correlations. *Biotechnology Letters, 26*:509-515. https://doi.org/10.1023/B:BILE.0000019559.84305.47

Pfaller MA & Castanheira M. (2016). Nosocomial candidiasis: antifungal stewardship and the importance of rapid diagnosis. *Medical Mycology, 54*:1-22. https://doi.org/10.1093/mmy/myv076

Pfaller MA, Diekema DJ, Turnidge JD, Castanheira M & Jones RN. (2019). Twenty years of the SENTRY Antifungal Surveillance Program: results for *Candida* species from 1997–2016. *Open Forum Infectious Diseases, 6*:S79-S94. https://doi.org/10.1093/ofid/ofy358

Popp C, Hampe IAI, Hertlein T, Ohlsen K, Rogers PD & Morschhäuser J. (2017). Competitive fitness of fluconazole-resistant clinical *Candida albicans* strains. *Antimicrobial Agents and Chemotherapy, 61*:e00584-17. https://doi.org/10.1128/aac.00584-17

Popp C, Ramírez-Zavala B, Schwanfelder S, Krüger I, Morschhäuser J & Berman J. (2019). Evolution of fluconazole-resistant *Candida albicans* strains by drug-induced mating competence and parasexual recombination. *mBio, 10*:e02740-18. https://doi.org/10.1128/mBio.02740-18

Pourcel C, Salvignol G & Vergnaud G. (2005). CRISPR elements in *Yersinia pestis* acquire new repeats by preferential uptake of bacteriophage DNA, and provide additional tools for evolutionary studies. *Microbiology, 151*:653-663. https://doi.org/10.1099/mic.0.27437-0

Prasad R, De Wergifosse P, Goffeau A & Balzi E. (1995). Molecular cloning and characterization of a novel gene of *C. albicans*, *CDR1*, conferring multiple resistance to drugs and antifungals. *Current Genetics, 27*:320-329. https://doi.org/10.1007/BF00352101

Prasad R & Goffeau A. (2012). Yeast ATP-binding cassette transporters conferring multidrug resistance. *Annual Review of Microbiology, 66*:39-63. https://doi.org/10.1146/annurev-micro-092611-150111

Puig-Asensio M, Padilla B, Garnacho-Montero J, Zaragoza O, Aguado JM, Zaragoza R, Montejo M, Muñoz P, Ruiz-Camps I, Cuenca-Estrella M & Almirante B. (2014). Epidemiology and predictive factors for early and late mortality in *Candida* bloodstream infections: a population-based surveillance in Spain. *Clinical Microbiology and Infection, 20*:O245-O254. https://doi.org/10.1111/1469-0691.12380

R

Rees DC, Lewinson O & Johnson E. (2009). ABC transporters: the power to change. *Nature Reviews. Molecular Cell Biology, 10*:218-227. https://doi.org/10.1038/nrm2646

Revankar SG, Kirkpatrick WR, McAtee RK, Fothergill AW, Redding SW, Rinaldi MG & Patterson TF. (1998). Interpretation of trailing endpoints in antifungal susceptibility testing by the National Committee for Clinical Laboratory Standards Method. *Journal of Clinical Microbiology, 36*:153-156. https://doi.org/10.1128/jcm.36.1.153-156.1998

Rex JH, Nelson PW, Paetznick VL, Lozano-Chiu M, Espinel-Ingroff A & Anaissie EJ. (1998). Optimizing the correlation between results of testing *in vitro* and therapeutic outcome *in vivo* for fluconazole by testing critical isolates in a murine model of invasive candidiasis. *Antimicrobial Agents and Chemotherapy, 42*:129-134. https://doi.org/10.1128/aac.42.1.129

Ricardo E, Miranda IM, Faria-Ramos I, Silva RM, Rodrigues AG & Pina-Vaz C. (2014). In vivo and in vitro acquisition of resistance to voriconazole by *Candida krusei*. *Antimicrobial Agents and Chemotherapy, 58*:4604-4611. https://doi.org/rg/10.1128/AAC.02603-14

Riggle PJ & Kumamoto CA. (2006). Transcriptional regulation of *MDR1*, encoding a drug efflux determinant, in fluconazole-resistant *Candida albicans* strains through an Mcm1p binding site. *Eukaryotic Cell, 5*:1957-1968. https://doi.org/rg/10.1128/EC.00243-06

Robbins N, Caplan T & Cowen LE. (2017). Molecular evolution of antifungal drug resistance. *Annual Review of Microbiology, 71*:753-775. https://doi.org/10.1146/annurev-micro-030117-

Robbins N, Leach MD & Cowen LE. (2012). Lysine deacetylases Hda1 and Rpd3 regulate Hsp90 function thereby governing fungal drug resistance. *Cell Reports, 2*:878-888. https://doi.org/10.1016/j.celrep.2012.08.035

Robbins N, Wright GD & Cowen LE. (2016). Antifungal drugs: the current armamentarium and development of new agents. *Microbiology Spectrum, 4*:FUNK-0002-2016. https://doi.org/10.1128/microbiolspec.FUNK-0002-2016

Roemer T & Krysan DJ. (2014). Antifungal drug development: challenges, unmet clinical needs, and new approaches. *Cold Spring Harbor Perspectives in Medicine, 4*:a019703. https://doi.org/10.1101/cshperspect.a019703

Rognon B, Kozovska Z, Coste AT, Pardini G & Sanglard D. (2006). Identification of promoter elements responsible for the regulation of *MDR1* from *Candida albicans*, a major facilitator transporter involved in azole resistance. *Microbiology, 152*:3701-3722. https://doi.org/10.1099/mic.0.29277-0

Rojas AE, Pérez JE, Hernández JS & Zapata Y. (2020). Análisis cuantitativo de la expresión de genes de resistencia a fluconazol en cepas de *Candida albicans* aisladas al ingreso de adultos mayores a una unidad de cuidados intensivos de Manizales, Colombia. *Biomédica, 40*:153-165. https://doi.org/10.7705/biomedica.4723

Rosenberg A, Ene IV, Bibi M, Zakin S, Segal ES, Ziv N, Dahan AM, Colombo AL, Bennett RJ & Berman J. (2018). Antifungal tolerance is a subpopulation effect distinct from resistance and is associated with persistent candidemia. *Nature Communications, 9*:2470-14. https://doi.org/10.1038/s41467-018-04926-x

Rueda C, Puig-Asensio M, Guinea J, Almirante B, Cuenca-Estrella M, Zaragoza O, Padilla B, Muñoz P, Guinea J, Paño Pardo JR, García-Rodríguez J, García Cerrada C, Fortún J, Martín P, Gómez E, Ryan P, Campelo C, de los Santos Gil, I, Buendía V, Gorricho BP, Alonso M, Sanz FS, Aguado JM, Merino P, González Romo F, Gorgolas M, Gadea I, Losa JE, Delgado-Iribarren A, Ramos A, Romero Y, Sánchez Romero I, Zaragoza O, Cuenca-Estrella M, Rodriguez-Baño J, Isabel Suarez A, Loza A, Aller García AI, Martín-Mazuelos E, Pérez de Pipaón, M R, Garnacho J, Ortiz C, Chávez M, Maroto FL, Salavert M, Pemán J, Blanquer J, Navarro D, Camarena JJ, Zaragoza R, Abril V, Gimeno C, Hernáez S, Ezpeleta G, Bereciartua E, Hernández Almaraz JL, Montejo M, Rivas RA, Ayarza R, Planes AM, Camps IR, Almirante B, Mensa J, Almela M, Gurgui M, Sánchez-Reus F, Martinez-Montauti J, Sierra M, Horcajada JP, Sorli L, Gómez J, Gené A, Urrea M, Valerio M, Díaz-Martín A, Puchades F & Mularoni A. (2017). Evaluation of the possible influence of trailing and paradoxical effects on the clinical outcome of patients with candidemia. *Clinical Microbiology and Infection, 23*:49.e1-49.e8. https://doi.org/10.1016/j.cmi.2016.09.016

Rustad TR, Stevens DA, Pfaller MA & White TC. (2002). Homozygosity at the *Candida albicans MTL* locus associated with azole resistance. *Microbiology, 148*:1061-1072. https://doi.org/10.1099/00221287-148-4-1061

S

Saidane S, Weber S, De Deken X, St-Germain G & Raymond M. (2006). *PDR16*-mediated azole resistance in *Candida albicans*. *Molecular Microbiology, 60*:1546-1562. https://doi.org/10.1111/j.1365-2958.2006.05196.x

Salari S, Khosravi AR, Mousavi SAA & Nikbakht-Brojeni GH. (2016). Mechanisms of resistance to fluconazole in *Candida albicans* clinical isolates from Iranian HIV-infected patients with oropharyngeal candidiasis. *Journal De Mycologie Médicale, 26*:35-41. https://doi.org/10.1016/j.mycmed.2015.10.007

Sambrook J & Russell DW. (2001). Working with synthetic oligonucleotide probes. In J. Sambrook, & D. W. Russel (Eds.), *Molecular cloning: A laboratory manual* (3rd ed., pp. 10.1-10.52). Cold Spring Harbor Laboratory Press.

Sanglard D & Coste AT. (2016). Activity of isavuconazole and other azoles against *Candida* clinical isolates and yeast model systems with known azole resistance mechanisms. *Antimicrobial Agents and Chemotherapy, 60*:229-238. https://doi.org/10.1128/AAC.02157-15

Sanglard D, Ischer F, Koymans L & Bille J. (1998). Amino acid substitutions in the cytochrome P-450 lanosterol 14α-demethylase (CYP51A1) from azole-resistant *Candida albicans* clinical isolates contribute to resistance to azole antifungal agents. *Antimicrobial Agents and Chemotherapy, 42*:241-253. https://doi.org/10.1128/AAC.42.2.241

Sanglard D, Ischer F, Marchetti O, Entenza J & Bille J. (2003). Calcineurin A of *Candida albicans*: involvement in antifungal tolerance, cell morphogenesis and virulence. *Molecular Microbiology, 48*:959-976. https://doi.org/10.1046/j.1365-2958.2003.03495.x

Sanglard D, Ischer F, Monod M & Bille J. (1996). Susceptibilities of *Candida albicans* multidrug transporter mutants to various antifungal agents and other metabolic inhibitors. *Antimicrobial Agents and Chemotherapy, 40*:2300-2305. https://doi.org/10.1128/AAC.40.10.2300

Sanglard D, Ischer F, Monod M & Bille J. (1997). Cloning of *Candida albicans* genes conferring resistance to azole antifungal agents: characterisation of *CDR2*, a new multidrug ABC transporter gene. *Microbiology, 143*:405-416. https://doi.org/10.1099/00221287-143-2-405

Sanglard D, Kuchler K, Ischer F, Pagani J-, Monod M & Bille J. (1995). Mechanisms of resistance to azole antifungal agents in *Candida albicans* isolates from AIDS patients involve specific multidrug transporters. *Antimicrobial Agents and Chemotherapy, 39*:2378-2386. https://doi.org/10.1128/AAC.39.11.2378

Sanguinetti M, Posteraro B, Beigelman-Aubry C, Lamoth F, Dunet V, Slavin M & Richardson MD. (2019). Diagnosis and treatment of invasive fungal infections: looking ahead. *Journal of Antimicrobial Chemotherapy, 74*:ii27-ii37. https://doi.org/10.1093/jac/dkz041

Sasse C, Dunkel N, Schäfer T, Schneider S, Dierolf F, Ohlsen K & Morschhäuser J. (2012). The stepwise acquisition of fluconazole resistance mutations causes a gradual loss of fitness in *Candida albicans*. *Molecular Microbiology, 86*:539-556. https://doi.org/https://doi.org/10.1111/j.1365-2958.2012.08210.x

Sasse C, Schillig R, Dierolf F, Weyler M, Schneider S, Mogavero S, Rogers PD & Morschhäuser J. (2011). The transcription factor Ndt80 does not contribute to Mrr1-, Tac1-, and Upc2-mediated fluconazole resistance in *Candida albicans*. *PLoS ONE, 6*:e25623. https://doi.org/10.1371/journal.pone.0025623

Schillig R & Morschhäuser J. (2013). Analysis of a fungus-specific transcription factor family, the *Candida albicans* zinc cluster proteins, by artificial activation. *Molecular Microbiology, 89*:1003-1017. https://doi.org/10.1111/mmi.12327

Schimoler-O'rourke R, Renault S, Mo W & Selitrennikoff CP. (2003). *Neurospora crassa* FKS protein binds to the (1,3)β-glucan synthase substrate, UDP-glucose. *Current Microbiology, 46*:408-412. https://doi.org/10.1007/s00284-002-3884-5

Schubert S, Barker KS, Morschhäuser J, Znaidi S, Schneider S, Dierolf F, Dunkel N, Aid M, Boucher G, Rogers PD & Raymond M. (2011). Regulation of efflux pump expression and drug resistance by the transcription factors Mrr1, Upc2, and Cap1 in *Candida albicans*. *Antimicrobial Agents and Chemotherapy, 55*:2212-2223. https://doi.org/10.1128/AAC.01343-10

Schubert S, Popp C, Rogers PD & Morschhäuser J. (2011). Functional dissection of a *Candida albicans* zinc cluster transcription factor, the multidrug resistance regulator Mrr1. *Eukaryotic Cell, 10*:1110-1121. https://doi.org/10.1128/EC.05100-11

Selmecki AM, Dulmage K, Cowen LE, Anderson JB & Berman J. (2009). Acquisition of aneuploidy provides increased fitness during the evolution of antifungal drug resistance. *PLoS Genetics, 5*:e1000705. https://doi.org/10.1371/journal.pgen.1000705

Selmecki A, Forche A & Berman J. (2006). Aneuploidy and isochromosome formation in drug-resistant *Candida albicans*. *Science, 313*:367-370. https://doi.org/10.1126/science.1128242

Selmecki A, Gerami-Nejad M, Paulson C, Forche A & Berman J. (2008). An isochromosome confers drug resistance *in vivo* by amplification of two genes, *ERG11* and *TAC1*. *Molecular Microbiology, 68*:624-641. https://doi.org/10.1111/j.1365-2958.2008.06176.x

Shapiro RS, Chavez A, Porter CBM, Hamblin M, Kaas CS, Dicarlo JE, Zeng G, Xu X, Revtovich AV, Kirienko NV, Wang Y, Church GM & Collins JJ. (2018). A CRISPR–Cas9-based gene drive platform for genetic interaction analysis in *Candida albicans*. *Nature Microbiology, 3*:73-82. https://doi.org/10.1038/s41564-017-0043-0

Shapiro RS, Robbins N & Cowen LE. (2011). Regulatory circuitry governing fungal development, drug resistance, and disease. *Microbiology and Molecular Biology Reviews, 75*:213-267. https://doi.org/10.1128/MMBR.00045-10

Shapiro RS, Zaas AK, Betancourt-Quiroz M, Perfect JR & Cowen LE. (2012). The Hsp90 co-chaperone Sgt1 governs *Candida albicans* morphogenesis and drug resistance. *PLoS One, 7*:e44734. https://doi.org/10.1371/journal.pone.0044734

Shaw KJ & Ibrahim AS. (2020). Fosmanogepix: a review of the first-in-class broad spectrum agent for the treatment of invasive fungal infections. *Journal of Fungi, 6*:239. https://doi.org/10.3390/jof6040239

Shukla S, Yadav V, Mukhopadhyay G & Prasad R. (2011). Ncb2 is involved in activated transcription of *CDR1* in azole-resistant clinical isolates of *Candida albicans*. *Eukaryotic Cell, 10*:1357-1366. https://doi.org/10.1128/EC.05041-11

Siikala E, Rautemaa R, Richardson M, Saxen H, Bowyer P & Sanglard D. (2010). Persistent *Candida albicans* colonization and molecular mechanisms of azole resistance in autoimmune polyendocrinopathy-candidiasis-ectodermal dystrophy (APECED) patients. *Journal of Antimicrobial Chemotherapy, 65*:2505-2513. https://doi.org/https://doi.org/10.1093/jac/dkq354

Silver PM, Oliver BG & White TC. (2004). Role of *Candida albicans* transcription factor Upc2p in drug resistance and sterol metabolism. *Eukaryotic Cell, 3*:1391-1397. https://doi.org/10.1128/EC.3.6.1391-1397.2004

Singh SD, Robbins N, Zaas AK, Schell WA, Perfect JR & Cowen LE. (2009). Hsp90 governs echinocandin resistance in the pathogenic yeast *Candida albicans* via calcineurin. *PLoS Pathogens, 5*:e1000532. https://doi.org/10.1371/journal.ppat.1000532

Sitterlé E, Coste AT, Obadia T, Maufrais C, Chauvel M, Sertour N, Sanglard D, Puel A, D'Enfert C & Bougnoux M. (2020). Large-scale genome mining allows identification of neutral polymorphisms and novel resistance mutations in genes involved in *Candida albicans* resistance to azoles and echinocandins. *Journal of Antimicrobial Chemotherapy, 75*:835-848. https://doi.org/10.1093/jac/dkz537

Sobel JD. (2007). Vulvovaginal candidosis. *The Lancet, 369*:1961-1971. https://doi.org/10.1016/s0140-6736(07)60917-9

Spettel K, Barousch W, Makristathis A, Zeller I, Nehr M, Selitsch B, Lackner M, Rath P, Steinmann J & Willinger B. (2019). Analysis of antifungal resistance genes in *Candida albicans* and *Candida glabrata* using next generation sequencing. *Plos One, 14*:e0210397. https://doi.org/10.1371/journal.pone.0210397

Strzelczyk JK, Slemp-Migiel A, Rother M, Gołąbek K & Wiczkowski A. (2013). Nucleotide substitutions in the *Candida albicans ERG11* gene of azole-susceptible and azole-resistant clinical isolates. *Acta Biochimica Polonica, 60*:547-552. https://doi.org/10.18388/abp.2013_2019

T

Talibi D & Raymond M. (1999). Isolation of a putative *Candida albicans* transcriptional regulator involved in pleiotropic drug resistance by functional complementation of a *pdr1 pdr3* mutation in *Saccharomyces cerevisiae*. *Journal of Bacteriology, 181*:231-240. https://doi.org/10.1128/JB.181.1.231-240.1999

Teo JQ, Lee SJ, Tan A, Lim RS, Cai Y, Lim T & Kwa AL. (2019). Molecular mechanisms of azole resistance in *Candida* bloodstream isolates. *BMC Infectious Diseases, 19*:63. https://doi.org/10.1186/s12879-019-3672-5

Torelli R, Posteraro B, Ferrari S, La Sorda M, Fadda G, Sanglard D & Sanguinetti M. (2008). The ATP-binding cassette transporter–encoding gene *CgSNQ2* is contributing to the *CgPDR1*-dependent azole resistance of *Candida glabrata*. *Molecular Microbiology, 68*:186-201. https://doi.org/10.1111/j.1365-2958.2008.06143.x

Tsao S, Rahkhoodaee F & Raymond M. (2009). Relative contributions of the *Candida albicans* ABC Transporters Cdr1p and Cdr2p to clinical azole resistance. *Antimicrobial Agents and Chemotherapy, 53*:1344-1352. https://doi.org/10.1128/AAC.00926-08

V

Vale-Silva LA. (2015). Molecular mechanisms of resistance of *candida* spp. to membrane-targeting antifungals. In A. T. Coste, & P. Vandeputte (Eds.), *Antifungals: From genomics to resistance and the development of novel agents* (pp. 1-26). Caister Academic Press. https://doi.org/10.21775/9781910190012.01

Vale-Silva LA, Coste AT, Ischer F, Parker JE, Kelly SL, Pinto E & Sanglard D. (2012). Azole resistance by loss of function of the sterol Δ5,6-desaturase gene (*ERG3*) in *Candida albicans* does not necessarily decrease virulence. *Antimicrobial Agents and Chemotherapy, 56*:1960-1968. https://doi.org/10.1128/AAC.05720-11

van het Hoog M, Rast TJ, Martchenko M, Grindle S, Dignard D, Hogues H, Cuomo C, Berriman M, Scherer S, Magee BB, Whiteway M, Chibana H, Nantel A & Magee PT. (2007). Assembly of the *Candida albicans* genome into sixteen supercontigs aligned on the eight chromosomes. *Genome Biology, 8*:R52. https://doi.org/10.1186/gb-2007-8-4-r52

Vandesompele J, De Preter K, Pattyn F, Poppe B, Van Roy N, De Paepe A & Speleman F. (2002). Accurate normalization of real-time quantitative RT-PCR data by geometric averaging of multiple internal control genes. *Genome Biology, 3*:research0034.1-0034.11. https://doi.org/10.1186/gb-2002-3-7-research0034

Vermes A, Guchelaar HJ & Dankert J. (2000). Flucytosine: a review of its pharmacology, clinical indications, pharmacokinetics, toxicity and drug interactions. *Journal of Antimicrobial Chemotherapy, 46*:171-179. https://doi.org/10.1093/jac/46.2.171

Vincent BM, Lancaster AK, Scherz-Shouval R, Whitesell L & Lindquist S. (2013). Fitness trade-offs restrict the evolution of resistance to amphotericin B. *PLoS Biology, 11*:e1001692. https://doi.org/10.1371/journal.pbio.1001692

Vyas VK, Barrasa MI & Fink GR. (2015). A *Candida albicans* CRISPR system permits genetic engineering of essential genes and gene families. *Science Advances, 1*:e1500248. https://doi.org/10.1126/sciadv.1500248

Vyas VK, Bushkin GG, Bernstein DA, Getz MA, Sewastianik M, Barrasa MI, Bartel DP & Fink GR. (2018). New CRISPR mutagenesis strategies reveal variation in repair mechanisms among fungi. *mSphere, 3*:e00154-18. https://doi.org/10.1128/msphere.00154-18

W

Wang H, Kong F, Sorrell TC, Wang B, McNicholas P, Pantarat N, Ellis D, Xiao M, Widmer F & Chen SC. (2009). Rapid detection of *ERG11* gene mutations in clinical *Candida albicans* isolates with reduced susceptibility to fluconazole by rolling circle amplification and DNA sequencing. *BMC Microbiology, 9*:167. https://doi.org/10.1186/1471-2180-9-167

Wang Y, Liu J, Shi C, Li W, Zhao Y, Yan L & Xiang M. (2015). Mutations in transcription factor Mrr2p contribute to fluconazole resistance in clinical isolates of *Candida albicans*. *International Journal of Antimicrobial Agents, 46*:552-559. https://doi.org/10.1016/j.ijantimicag.2015.08.001

Warrilow AGS, Mullins JGL, Hull CM, Parker JE, Lamb DC, Kelly DE & Kelly SL. (2012). S279 point mutations in *Candida albicans* sterol 14-α demethylase (CYP51) reduce *in vitro* inhibition by fluconazole. *Antimicrobial Agents and Chemotherapy, 56*:2099-2107. https://doi.org/10.1128/AAC.05389-11

Whaley SG, Berkow EL, Rybak JM, Nishimoto AT, Barker KS & Rogers PD. (2017). Azole antifungal resistance in *Candida albicans* and emerging non-albicans *Candida* species. *Frontiers in Microbiology, 7*:2173. https://doi.org/10.3389/fmicb.2016.02173

White TC. (1997a). Increased mRNA levels of *ERG16*, *CDR*, and *MDR1* correlate with increases in azole resistance in *Candida albicans* isolates from a patient infected with human immunodeficiency virus. *Antimicrobial Agents and Chemotherapy, 41*:1482-1487. https://doi.org/https://doi.org/10.1128/AAC.41.7.1482

White TC. (1997b). The presence of an R467K amino acid substitution and loss of allelic variation correlate with an azole-resistant lanosterol 14α demethylase in *Candida albicans*. *Antimicrobial Agents and Chemotherapy, 41*:1488-1494. https://doi.org/10.1128/AAC.41.7.1488

White TC, Holleman S, Dy F, Mirels LF & Stevens DA. (2002). Resistance mechanisms in clinical isolates of *Candida albicans*. *Antimicrobial Agents and Chemotherapy, 46*:1704-1713. https://doi.org/10.1128/AAC.46.6.1704-1713.2002

White TC, Marr KA & Bowden RA. (1998). Clinical, cellular, and molecular factors that contribute to antifungal drug resistance. *Clinical Microbiology Reviews, 11*:382-402. https://doi.org/10.1128/CMR.11.2.382

Wiederhold NP. (2017). Antifungal resistance: current trends and future strategies to combat. *Infection and Drug Resistance, 10*:249-259. https://doi.org/10.2147/IDR.S124918

Wilson DT, Dimondi VP, Johnson SW, Jones TM & Drew RH. (2016). Role of isavuconazole in the treatment of invasive fungal infections. *Therapeutics and Clinical Risk Management, 12*:1197-1206. https://doi.org/10.2147/TCRM.S90335

Wirsching S, Michel S, Köhler G & Morschhäuser J. (2000). Activation of the multiple drug resistance gene *MDR1* in fluconazole-resistant, clinical *Candida albicans* strains is caused by mutations in a trans-regulatory factor. *Journal of Bacteriology, 182*:400-404. https://doi.org/10.1128/JB.182.2.400-404.2000

Wirsching S, Michel S & Morschhäuser J. (2000). Targeted gene disruption in *Candida albicans* wild-type strains: the role of the *MDR1* gene in fluconazole resistance of clinical *Candida albicans* isolates. *Molecular Microbiology, 36*:856-865. https://doi.org/10.1046/j.1365-2958.2000.01899.x

Wu Y, Gao N, Li C, Gao J & Ying C. (2017). A newly identified amino acid substitution T123I in the 14α-demethylase (Erg11p) of *Candida albicans* confers azole resistance. *FEMS Yeast Research, 17*. https://doi.org/10.1093/femsyr/fox012

Wu Y, Li C, Wang Z, Gao J, Tang Z, Chen H & Ying C. (2018). Clonal spread and azole-resistant mechanisms of non-susceptible *Candida albicans* isolates from vulvovaginal candidiasis patients in three Shanghai maternity hospitals. *Medical Mycology, 56*:687-694. https://doi.org/10.1093/mmy/myx099

X

Xiang M, Liu J, Ni P, Wang S, Shi C, Wei B, Ni Y & Ge H. (2013). Erg11 mutations associated with azole resistance in clinical isolates of *Candida albicans*. *FEMS Yeast Research, 13*:386-393. https://doi.org/10.1111/1567-1364.12042

Xu Y, Chen L & Li C. (2008). Susceptibility of clinical isolates of *Candida* species to fluconazole and detection of *Candida albicans ERG11* mutations. *Journal of Antimicrobial Chemotherapy, 61*:798-804. https://doi.org/10.1093/jac/dkn015

Xu Y, Sheng F, Zhao J, Chen L & Li C. (2015). *ERG11* mutations and expression of resistance genes in fluconazole-resistant *Candida albicans* isolates. *Archives of Microbiology, 197*:1087-1093. https://doi.org/10.1007/s00203-015-1146-8

Y

Yan L, Zhang J, Li M, Cao Y, Xu Z, Gao P, Wang Y & Jiang Y. (2008). DNA microarray analysis of fluconazole resistance in a laboratory *Candida albicans* strain. *Acta Biochimica Et Biophysica Sinica, 40*:1048-1060. https://doi.org/10.1111/j.1745-7270.2008.00483.x

Yang H, Tong J, Lee CW, Ha S, Eom SH & Im YJ. (2015). Structural mechanism of ergosterol regulation by fungal sterol transcription factor Upc2. *Nature Communications, 6*:6129. https://doi.org/10.1038/ncomms7129

Ying Y, Zhao Y, Hu X, Cai Z, Liu X, Jin G, Zhang J, Liu J & Huang X. (2013). In vitro fluconazole susceptibility of 1,903 clinical isolates of *Candida albicans* and the identification of *ERG11* mutations. *Microbial Drug Resistance, 19*:266-273. https://doi.org/10.1089/mdr.2012.0204

Z

Zhao J, Xu Y & Li C. (2013). Association of T916C (Y257H) mutation in *Candida albicans ERG11* with fluconazole resistance. *Mycoses, 56*:315-320. https://doi.org/10.1111/myc.12027

Znaidi S, Barker KS, Weber S, Alarco A, Liu TT, Boucher G, Rogers PD & Raymond M. (2009). Identification of the *Candida albicans* Cap1p regulon. *Eukaryotic Cell, 8*:806-820. https://doi.org/10.1128/EC.00002-09

Znaidi S, De Deken X, Weber S, Rigby T, Nantel A & Raymond M. (2007). The zinc cluster transcription factor Tac1p regulates *PDR16* expression in *Candida albicans*. *Molecular Microbiology, 40*:440-452. https://doi.org/10.1111/j.1365-2958.2007.05931.x

Znaidi S, Weber S, Al-Abdin OZ, Bomme P, Saidane S, Drouin S, Lemieux S, De Deken X, Robert F & Raymond M. (2008). Genomewide location analysis of *Candida albicans* Upc2p, a regulator of sterol metabolism and azole drug resistance. *Eukaryotic Cell, 7*:836-847. https://doi.org/10.1128/EC.00070-08

Supplementary material

I - Synonymous and non-synonymous single nucleotide polymorphisms (SNPs) identified in azole-susceptible and resistant isolates of the UPV/EHU collection

Table I. SNPs detected in the selected regions of the *ERG11* gene and the associated amino acid substitutions of the azole-susceptible and resistant isolates of the UPV/EHU collection.

Strains	SNPs in *ERG11*	Amino acid substitutions in Erg11
BE-47	T315C, T348A, A357G, A383C, C411T, C658T, A1020G, C1110T, A1440G	F105F, D116E, K119K, K128T, S137S, L220L, L340L, L370L, L480L
BE-AZ	C125T^{h}, C411T, T549C, C658T, T996C, C1110T, T1140C, T1203C, T1257C, G1309A, A1440G	S42L^{h}, S137S, H183H, L220L, V332V, L370L, F380F, Y401Y, P419P, V437I, L480L
BE-32	C125T^{h}, A383C^{h}, C411T^{h}, C558T^{h}, C658T, A1020G^{h}, C1110T^{h}, A1440G^{h}, T1470C^{h}	S42L^{h}, K128T^{h}, S137S^{h}, A186A^{h}, L220L, L340L^{h}, L370L^{h}, L480L^{h}, N490N^{h}
BE-48	C658T^{h}, G673A^{h}, T996C, A1083G^{h}, C1110T, T1203C, T1284C, A1440G, T1470C	L220L^{h}, D225N^{h}, V332V, S361S^{h}, L370L, Y401Y, D428D, L480L, N490N
09-297	T315C^{h}, T348A^{h}, A357G^{h}, A383C^{h}, C411T^{h}, C658T^{h}, A1020G^{h}, C1110T^{h}, A1440G, T1470C	F105F^{h}, D116E^{h}, K119K^{h}, K128T^{h}, S137S^{h}, L220L^{h}, L340L^{h}, L370L^{h}, L480L, N490N
10-166	C216T^{h}, T315C, C411T, T549C^{h}, C658T, A798C, T996C, A1026G, C1110T, T1203C, C1296T, T1302C, G1462A^{h}	F72F^{h}, F105F, S137S, H183H^{h}, L220L, E266D, V332V, K342K, L370L, Y401Y, A432A, A434A, V488I^{h}
10-294	T549C, C658T, T996C, C1110T^{h}, T1140C^{h}, T1203C^{h}, C1296T^{h}, T1302C^{h}	H183H, L220L, V332V, L370L^{h}, F380F^{h}, Y401Y^{h}, A432A^{h}, A434A^{h}
15-158	C216T^{h}, T315C, C411T, T549C^{h}, C658T, A798C, T996C, A1026G, C1110T, T1203C, G1204T^{h}, C1296T, T1302C, C1435G^{h}, G1462A^{h}	F72F^{h}, F105F, S137S, H183H^{h}, L220L, E266D, V332V, K342K, L370L, Y401Y, V402F^{h}, A432A, A434A, Q479E^{h}, V488I^{h}
15-178	A126T^{h}, C216T^{h}, T315C, T348A^{h}, A357G^{h}, C411T, T549C^{h}, C658T, A798C, T996C^{h}, A1020G^{h}, A1026G^{h}, C1110T, T1203C^{h}, C1296T^{h}, T1302C^{h}, A1440G^{h}, T1470C^{h}	S42S^{h}, F72F^{h}, F105F, D116E^{h}, K119K^{h}, S137S, H183H^{h}, L220L, E266D, V332V^{h}, L340L^{h}, K342K^{h}, L370L, Y401Y^{h}, A432A^{h}, A434A^{h}, L480L^{h}, N490N^{h}
SC5314	T315C^{h}, T348A^{h}, A357G^{h}, A383C^{h}, C411T^{h}, C658T^{h}, T996C, A1083G, C1110T, T1203C, T1284C^{h}	F105F^{h}, D116E^{h}, K119K^{h}, K128T^{h}, S137S^{h}, L220L^{h}, V332V, S361S, L370L, Y401Y, D428D^{h}
BE-90	C1110T, T1203C, T1284C, A1440G, T1470C	L370L, Y401Y, D428D, L480L, N490N
06-116	T315C, C658T, T348A^{h}, A357G^{h}, C411T^{h}, T459G^{h}, T549C^{h}, T996C^{h}, A1020G^{h}, A1083G^{h}, C1110T, T1203C^{h}, C1296T^{h}, T1302C^{h}, A1440G^{h}	F105F, L220L, D116E^{h}, K119K^{h}, S137S^{h}, D153E^{h}, H183H^{h}, V332V^{h}, L340L^{h}, S361S^{h}, L370L, Y401Y^{h}, A432A^{h}, A434A^{h}, L480L^{h}
10-169	C216T^{h}, T315C, T348A^{h}, A357G^{h}, C411T, C658T, A798C, T996C^{h}, A1020G^{h}, A1026G^{h}, C1110T, T1203C^{h}, C1296T^{h}, T1302C^{h}, A1440G^{h}, G1462A^{h}, T1470C^{h}	F72F^{h}, F105F, D116E^{h}, K119K^{h}, S137S, L220L, E266D, V332V^{h}, L340L^{h}, K342K^{h}, L370L, Y401Y^{h}, A432A^{h}, A434A^{h}, L480L^{h}, V488I^{h}, N490N^{h}
10-295	T315C^{h}, C411T^{h}, T549C, C658T, A798C^{h}, T955C^{h}, T996C, A1026G^{h}, C1110T, T1140C^{h}, T1203C, C1296T, T1302C, G1462A^{h}	F105F^{h}, S137S^{h}, H183H, L220L, E266D^{h}, F319L^{h}, V332V, K342K^{h}, L370L, F380F^{h}, Y401Y, A432A, A434A, V488I^{h}
15-153	C216T^{h}, T315C, C411T, T549C^{h}, C658T, C707A^{h}, A798C, T996C, A1026G, C1110T, T1203C, C1296T, T1302C, G1462A^{h}	F72F^{h}, F105F, S137S, H183H^{h}, L220L, P236H^{h}, E266D, V332V, K342K, L370L, Y401Y, A432A, A434A, V488I^{h}

Table I. Continued.

Strains	SNPs in *ERG11*	Amino acid substitutions in Erg11
15-155	G140A^{h}, T549C^{h}, C658T^{h}, T996C^{h}, C1110T^{h}, T1140C^{h}, T1203C^{h}, C1296T^{h}, T1302C^{h}	R47K^{h}, H183H^{h}, L220L^{h}, V332V^{h}, L370L^{h}, F380F^{h}, Y401Y^{h}, A432A^{h}, A434A^{h}
15-161	C216T^{h}, T315C, T348A^{h}, A357G^{h}, T381A^{h}, C411T, C446A^{h}, C658T, A798C, T996C^{h}, A1020G^{h}, A1026G^{h}, C1110T, T1203C^{h}, C1296T^{h}, T1302C^{h}, A1440G^{h}, G1462A^{h}, T1470C^{h}	F72F^{h}, F105F, D116E^{h}, K119K^{h}, G127G^{h}, S137S, A149D^{h}, L220L, E266D, V332V^{h}, L340L^{h}, K342K^{h}, L370L, Y401Y^{h}, A432A^{h}, A434A^{h}, L480L^{h}, V488I^{h}, N490N^{h}
15-179	C216T^{h}, C226T^{h}, T315C, C411T, T549C^{h}, C658T, A798C^{h}, T996C, A1026G^{h}, C1110T, T1140C^{h}, T1203C, C1296T^{h}, T1302C^{h}, G1309A^{h}, A1440G^{h}	F72F^{h}, R76C^{h}, F105F, S137S, H183H^{h}, L220L, E266D^{h}, V332V, K342K^{h}, L370L, F380F^{h}, Y401Y, A432A^{h}, A434A^{h}, V437I^{h}, L480L^{h}
10-171	T315C^{h}, T348A^{h}, A357G^{h}, A383C^{h}, C411T^{h}, G475A^{h}, C658T, T996C^{h}, A1020G^{h}, A1083G, C1110T^{h}, T1203C^{h}, C1296T^{h}, T1302C^{h}, A1440G^{h}, T1470C^{h}	F105F^{h}, D116E^{h}, K119K^{h}, K128T^{h}, S137S^{h}, V159I^{h}, L220L, V332V^{h}, L340L^{h}, S361S, L370L^{h}, Y401Y^{h}, A432A^{h}, A434A^{h}, L480L^{h}, N490N^{h}
10-280	T549C^{h}, C658T^{h}, T996C^{h}, C1110T^{h}, T1140C^{h}, T1203C^{h}, C1296T^{h}, T1302C^{h}	H183H^{h}, L220L^{h}, V332V^{h}, L370L^{h}, F380F^{h}, Y401Y^{h}, A432A^{h}, A434A^{h}
08-187	A126T^{h}, T315C^{h}, T348A^{h}, A357G^{h}, A383C^{h}, C411T^{h}, C658T, A1020G^{h}, C1110T^{h}, A1440G^{h}, T1470C	S42S^{h}, F105F^{h}, D116E^{h}, K119K^{h}, K128T^{h}, S137S^{h}, L220L, L340L^{h}, L370L^{h}, L480L^{h}, N490N
08-105	T549C^{h}, C658T^{h}, T996C^{h}, C1110T^{h}, T1140C^{h}, T1203C^{h}, C1296T^{h}, T1302C^{h}	H183H^{h}, L220L^{h}, V332V^{h}, L370L^{h}, F380F^{h}, Y401Y^{h}, A432A^{h}, A434A^{h}
15-160	T315C, T348A^{h}, A357G^{h}, C411T, T549C^{h}, C658T, A798C^{h}, T996C^{h}, A1020G^{h}, C1110T, T1140C^{h}, T1203C^{h}, A1209G^{h}, A1440G	F105F, D116E^{h}, K119K^{h}, S137S, H183H^{h}, L220L, E266D^{h}, V332V^{h}, L340L^{h}, L370L, F380F^{h}, Y401Y^{h}, L403L^{h}, L480L
06-100	T315C, T348A, A357G, C411T, C658T, A798C, A1020G, C1110T, A1440G	F105F, D116E, K119K, S137S, L220L, E266D, L340L, L370L, L480L
16-133	T315C, T459G, T549C^{h}, C658T, T996C^{h}, A1020G^{h}, A1083G^{h}, C1110T, T1203C^{h}, C1296T^{h}, T1302C^{h}, A1440G^{h}, T1470C^{h}	F105F, D153E, H183H^{h}, L220L, V332V^{h}, L340L^{h}, S361S^{h}, L370L, Y401Y^{h}, A432A^{h}, A434A^{h}, L480L^{h}, N490N^{h}
16-135	T549C^{h}, C658T^{h}, T996C^{h}, C1110T^{h}, T1140C^{h}, T1203C^{h}, C1296T^{h}, T1302C^{h}	H183H^{h}, L220L^{h}, V332V^{h}, L370L^{h}, F380F^{h}, Y401Y^{h}, A432A^{h}, A434A^{h}
16-132	T315C^{h}, T348A^{h}, A357G^{h}, A383C^{h}, C411T^{h}, C658T^{h}, A1020G^{h}, C1110T^{h}, A1440G^{h}, T1470C^{h}	F105F^{h}, D116E^{h}, K119K^{h}, K128T^{h}, S137S^{h}, L220L^{h}, L340L^{h}, L370L^{h}, L480L^{h}, N490N^{h}
15-159	**A428G^{h}**, T549C^{h}, T996C^{h}, C1110T^{h}, T1140C^{h}, T1203C^{h}, C1296T^{h}, T1302C^{h}	**K143R^{h}**, H183H^{h}, V332V^{h}, L370L^{h}, F380F^{h}, Y401Y^{h}, A432A^{h}, A434A^{h}
16-122	G170T^{h}, **T394C**, T651A^{h}, **G1349A**	W57L^{h}, **Y132H**, F217L^{h}, **G450E**
16-123	T394C, G1349A	Y132H, G450E
10-168	T315C, T348A^{h}, A357G^{h}, C411T^{h}, T459G^{h}, T549C^{h}, C658T, T996C^{h}, A1020G^{h}, A1083G^{h}, C1110T, T1203C^{h}, C1296T^{h}, T1302C^{h}, A1440G^{h}, T1470C^{h}	F105F, D116E^{h}, K119K^{h}, S137S^{h}, D153E^{h}, H183H^{h}, L220L, V332V^{h}, L340L^{h}, S361S^{h}, L370L, Y401Y^{h}, A432A^{h}, A434A^{h}, L480L^{h}, N490N^{h}
06-114	T315C, T348A^{h}, A357G^{h}, C411T^{h}, T459G^{h}, T549C^{h}, C658T, T996C^{h}, A1020G^{h}, A1083G^{h}, C1110T, T1203C^{h}, C1296T^{h}, T1302C^{h}, A1440G^{h}	F105F, D116E^{h}, K119K^{h}, S137S^{h}, D153E^{h}, H183H^{h}, L220L, V332V^{h}, L340L^{h}, S361S^{h}, L370L, Y401Y^{h}, A432A^{h}, A434A^{h}, L480L^{h}
BE-114	T549C, C658T, T996C, C1110T, T1140C, T1203C, C1296T, T1302C	H183H, L220L, V332V, L370L, F380F, Y401Y, A432A, A434A
10-221	T315C, T459G, T549C^{h}, C658T, T996C^{h}, A1020G^{h}, A1083G^{h}, C1110T, T1203C^{h}, C1296T^{h}, T1302C^{h}, A1440G^{h}, T1470C^{h}	F105F, D153E, H183H^{h}, L220L, V332V^{h}, L340L^{h}, S361S^{h}, L370L, Y401Y^{h}, A432A^{h}, A434A^{h}, L480L^{h}, N490N^{h}
16-134	T315C, T459G, T549C^{h}, C658T, T996C^{h}, A1020G^{h}, A1083G^{h}, C1110T, T1203C^{h}, C1296T^{h}, T1302C^{h}, A1430G, A1440G^{h}	F105F, D153E, H183H^{h}, L220L, V332V^{h}, L340L^{h}, S361S^{h}, L370L, Y401Y^{h}, A432A^{h}, A434A^{h}, Y477C, L480L^{h}
15-156	T315C^{h}, T348A^{h}, A357G^{h}, A383C^{h}, C411T^{h}, G475A^{h}, C658T^{h}, A1020G^{h}, C1110T^{h}, A1440G^{h}, T1470C^{h}	F105F^{h}, D116E^{h}, K119K^{h}, K128T^{h}, S137S^{h}, V159I^{h}, L220L^{h}, L340L^{h}, L370L^{h}, L480L^{h}, N490N^{h}

Table I. Continued.

Strains	SNPs in *ERG11*	Amino acid substitutions in Erg11
15-157	C125T^{h}, T315C, T348A^{h}, A357G^{h}, C411T^{h}, T459G^{h}, T549C, C658T, T996C, A1083G, C1110T, T1203C, C1296T, T1302C	S42L^{h}, F105F, D116E^{h}, K119K^{h}, S137S^{h}, D153E^{h}, H183H, L220L, V332V, S361S, L370L, Y401Y, A432A, A434A
10-170	T315C, T348A^{h}, A357G^{h}, C411T^{h}, T459G^{h}, T549C^{h}, C658T, T996C^{h}, A1020G^{h}, A1083G^{h}, C1110T, T1203C^{h}, C1296T^{h}, T1302C^{h}, A1440G^{h}, T1470C^{h}	F105F, D116E^{h}, K119K^{h}, S137S^{h}, D153E^{h}, H183H^{h}, L220L, V332V^{h}, L340L^{h}, S361S^{h}, L370L, Y401Y^{h}, A432A^{h}, A434A^{h}, L480L^{h}, N490N^{h}
BE-113	**G340T**, **T769C**	**A114S**, **Y257H**
16-091	**T394C**, **G1349A**	**Y132H**, **G450E**
ATCC 64550	T315C, T348A, A357G, A383C, C411T, C658T, T955C^{h}, A1020G, C1110T, C1420A, A1440G	F105F, D116E, K119K, K128T, S137S, L220L, F319L^{h}, L340L, L370L, Q474K, L480L
15-154	T549C^{h}, T996C^{h}, C1110T^{h}, T1140C^{h}, T1203C^{h}, C1296T^{h}, T1302C^{h}	H183H^{h}, V332V^{h}, L370L^{h}, F380F^{h}, Y401Y^{h}, A432A^{h}, A434A^{h}
15-176	**G1400A**	**R467K**
ATCC 64124	T214C, **T394C**, **G1349A**	F72L, **Y132H**, **G450E**
16-092	T315C, C411T, T549C, C658T, A798C, T955C^{h}, T996C, A1026G, C1110T, T1203C, C1296T, T1302C, G1462A^{h}	F105F, S137S, H183H, L220L, E266D, F319L^{h}, V332V, K342K, L370L, Y401Y, A432A, A434A, V488I^{h}
16-138	C216T^{h}, T315C, C411T, T549C^{h}, A798C, T996C, A1026G, C1110T, T1203C, C1296T, T1302C, G1462A^{h}	F72F^{h}, F105F, S137S, H183H^{h}, E266D, V332V, K342K, L370L, Y401Y, A432A, A434A, V488I^{h}

*The SNPs that do not entail changes in the amino acid sequence are denoted with the symbol of the amino acid present in the reference sequence followed by the position and again the same amino acid symbol; h, heterozygous mutation. The new mutations found in this work are underlined and the mutations associated to azole resistance are indicated in bold.

Table II. SNPs detected in the selected regions of the *TAC1* gene and the associated amino acid substitutions of the azole-susceptible and resistant isolates of the UPV/EHU collection.

Strains	SNPs in *TAC1*	Amino acid substitutions in Tac1*
BE-47	T786C^{h}, G1026A^{h}, C1038T^{h}, A1187G^{h}, G1212A^{h}, T1257C^{h}, T1305C^{h}, A2202G^{h}, T2214C^{h}, T2316A^{h}, G2326A^{h}, G2485C^{h}, C2589T^{h}, A2631G^{h}, C1804T^{h}, T2822C^{h}, G2874A^{h}	F262F^{h}, R342R^{h}, L346L^{h}, N396S^{h}, Q404Q^{h}, S419S^{h}, I435I^{h}, L734L^{h}, I738I^{h}, N772K^{h}, D776N^{h}, E829Q^{h}, T863T^{h}, Q877Q^{h}, S935L^{h}, S941P^{h}, S958S^{h}
BE-AZ	T786C, C810T^{h}, A915G^{h}, T978G^{h}, G1026A, C1038T, C1122T^{h}, A1187G, G1212A^{h}, T1257C^{h}, T1305C, A2202G, T2214C, T2271A, G2326A, T2448C, G2485C, C2589T, A2631G, A2687G^{h}, T2822C^{h}, G2874A	F262F, I270I^{h}, L305L^{h}, F326F^{h}, R342R, L346L, T374T^{h}, N396S, Q404Q^{h}, S419S^{h}, I435I, L734L, I738I, T757T, D776N, A816A, E829Q, T863T, Q877Q, N896S^{h}, S941P^{h}, S958S
BE-32	C633T^{h}, T786C^{h}, G1026A^{h}, C1038T^{h}, A1187G^{h}, G1212A^{h}, T1257C^{h}, T1305C^{h}, A2202G^{h}, T2214C^{h}, T2316A^{h}, G2326A^{h}, G2485C^{h}, C2589T^{h}, A2631G^{h}, C1804T^{h}, T2822C^{h}, G2874A^{h}	N211N^{h}, F262F^{h}, R342R^{h}, L346L^{h}, N396S^{h}, Q404Q^{h}, S419S^{h}, I435I^{h}, L734L^{h}, I738I^{h}, N772K^{h}, D776N^{h}, E829Q^{h}, T863T^{h}, Q877Q^{h}, S935L^{h}, S941P^{h}, S958S^{h}
BE-48	T786C, C810T^{h}, A915G^{h}, G1026A, C1038T, C1122T^{h}, A1187G, G1212A^{h}, T1257C^{h}, T1305C, A2202G, T2214C, T2271A, G2326A, T2448C, G2485C, C2589T, A2631G, A2687G^{h}	F262F, I270I^{h}, L305L^{h}, R342R, L346L, T374T^{h}, N396S, Q404Q^{h}, S419S^{h}, I435I, L734L, I738I, T757T, D776N, A816A, E829Q, T863T, Q877Q, N896S^{h}
09-297	G1026A^{h}, C1038T^{h}, A1187G^{h}, T1257C^{h}, T1305C^{h}, A1401T, A2202G^{h}, T2214C^{h}, G2326A^{h}, G2485C^{h}, C2589T^{h}, A2631G^{h}, C1804T^{h}, T2822C^{h}, G2874A^{h}	R342R^{h}, L346L^{h}, N396S^{h}, S419S^{h}, I435I^{h}, A467A, L734L^{h}, I738I^{h}, D776N^{h}, E829Q^{h}, T863T^{h}, Q877Q^{h}, S935L^{h}, S941P^{h}, S958S^{h}
10-166	T786C, A915G^{h}, G1026A, C1038T, C1122T^{h}, A1187G, G1212A^{h}, T1257C^{h}, T1305C^{h}, C1344T^{h}, C1374T^{h}, T2271A, A2202G^{h}, T2214C^{h}, T2271A, G2326A, T2448C, G2485C, C2589T, A2631G, A2687G^{h}, T2822C^{h}, G2874A^{h}	F262F, L305L^{h}, R342R, L346L, T374T^{h}, N396S, Q404Q^{h}, S419S^{h}, I435I^{h}, N448N^{h}, F458F^{h}, T757T, L734L^{h}, I738I^{h}, T757T, D776N, A816A, E829Q, T863T, Q877Q, N896S^{h}, S941P^{h}, S958S^{h}
10-294	T777A^{h}, T786C, C810T^{h}, C831G^{h}, G1026A, C1038T, A1187G, T1305C, C1344T, C2040T^{h}, A2202G^{h}, T2214C^{h}, T2271A^{h}, T2316A^{h}, G2326A, T2448C^{h}, T2459G^{h}, G2485C, G2573A^{h}, C2589T, A2631G, A2687G^{h}, G2733A^{h}, T2822C^{h}, G2874A^{h}	P259P^{h}, F262F, I270I^{h}, P277P^{h}, R342R, L346L, N396S, I435I, N448N, T680T^{h}, L734L^{h}, I738I^{h}, T757T^{h}, N772K^{h}, D776N, A816A^{h}, N823K^{h}, E829Q, C858Y^{h}, T863T, Q877Q, N896S^{h}, Q911Q^{h}, S941P^{h}, S958S^{h}
15-158	T786C, A915G^{h}, G1026A, C1038T, C1122T^{h}, A1187G, G1212A^{h}, T1257C^{h}, T1260C^{h}, A1269C^{h}, T1305C^{h}, C1344T^{h}, A2202G^{h}, T2214C^{h}, T2271A, G2326A, T2448C, G2485C, C2589T, A2631G, A2687G^{h}, T2822C^{h}, G2874A^{h}	F262F, L305L^{h}, R342R, L346L, T374T^{h}, N396S, Q404Q^{h}, S419S^{h}, V420V^{h}, E423D^{h}, I435I^{h}, N448N^{h}, L734L^{h}, I738I^{h}, T757T, D776N, A816A, E829Q, T863T, Q877Q, N896S^{h}, S941P^{h}, S958S^{h}
15-178	T786C^{h}, G795A^{h}, G906A^{h}, C1021G, G1026A^{h}, C1038T^{h}, T1179C^{h}, A1187G^{h}, T1198C^{h}, A1211C^{h} and G1212A^{h}, T1257C^{h}, T1305C^{h}, T1345C^{h}, A2202G^{h}, T2214C^{h}, T2271A, G2326A, T2448C^{h}, G2485C^{h}, C2589T^{h}, A2631G^{h}, T2822C^{h}, G2874A^{h}	F262F^{h}, E265E^{h}, L302L^{h}, R341G, R342R^{h}, L346L^{h}, G393G^{h}, N396S^{h}, L400L^{h}, Q404P^{h}, S419S^{h}, I435I^{h}, Y449H^{h}, L734L^{h}, I738I^{h}, T757T, D776N, A816A^{h}, E829Q^{h}, T863T^{h}, Q877Q^{h}, S941P^{h}, S958S^{h}
SC5314	T786C^{h}, G1026A^{h}, C1038T^{h}, A1187G^{h}, G1212A^{h}, T1257C^{h}, T1305C^{h}, A2202G^{h}, T2214C^{h}, T2316A^{h}, G2326A^{h}, G2485C^{h}, C2589T^{h}, A2631G^{h}, C1804T^{h}, T2822C^{h}, G2874A^{h}	F262F^{h}, R342R^{h}, L346L^{h}, N396S^{h}, Q404Q^{h}, S419S^{h}, I435I^{h}, L734L^{h}, I738I^{h}, N772K^{h}, D776N^{h}, E829Q^{h}, T863T^{h}, Q877Q^{h}, S935L^{h}, S941P^{h}, S958S^{h}
BE-90	T786C^{h}, G795A^{h}, G906A^{h}, T1014A^{h}, C1038T^{h}, A1047G^{h}, A1071G^{h}, T1107C^{h}, C1122T^{h}, C1130T^{h}, A1187G^{h}, C1344T^{h}, C1374T^{h}, G2355A, G2485C^{h}, C2589T^{h}, A2631G^{h}, T2822C^{h}	F262F^{h}, E265E^{h}, L302L^{h}, A338A^{h}, L346L^{h}, L349L^{h}, L357L^{h}, S369S^{h}, T374T^{h}, A377V^{h}, N396S^{h}, N448N^{h}, F458F^{h}, V785V, E829Q^{h}, T863T^{h}, Q877Q^{h}, S941P^{h}
06-116	A1187G, A2202G, T2214C, T2271A, G2326A, T2448C^{h}, G2485C^{h}, C2589T, A2631G, A2686G^{h}, T2822C, G2874A^{h}	N396S, L734L, I738I, T757T, D776N, A816A^{h}, E829Q^{h}, T863T, Q877Q, N896S^{h}, S941P, S958S^{h}

Table II. Continued.

Strains	SNPs in *TAC1*	Amino acid substitutions in Tac1*
10-169	T786C^{h}, G793A^{h}, G1026A^{h}, C1038T^{h}, A1187G^{h}, G1212A^{h}, T1257C^{h}, T1305C^{h}, A2202G^{h}, T2214C^{h}, T2271A^{h}, G2326A^{h}, T2448C^{h}, G2485C^{h}, C2589T^{h}, A2631G^{h}, A2686G^{h}, T2822C^{h}, G2874A^{h}	F262F^{h}, E265K^{h}, R342R^{h}, L346L^{h}, N396S^{h}, Q404Q^{h}, S419S^{h}, I435I^{h}, L734L^{h}, I738I^{h}, T757T^{h}, D776N^{h}, A816A^{h}, E829Q^{h}, T863T^{h}, Q877Q^{h}, N896S^{h}, S941P^{h}, S958S^{h}
10-295	A738T, T786C, G795A, G906A, G955G^{h}, T1014A, C1038T, A1047G^{h}, A1071G^{h}, T1107C^{h}, C1122T, C1130T^{h}, A1187G, G1212A^{h}, T1257C^{h}, T1305C, C1344T, C1374T^{h}, T2316A, G2326A, T2373A, G2485C, C2589T, A2631G, T2822C	S246S, F262F, E265E, L302L, E319K^{h}, A338A, L346L, L349L^{h}, L357L^{h}, S369S^{h}, T374T, A377V^{h}, N396S, Q404Q^{h}, S419S^{h}, I435I, N448N, F458F^{h}, N772K, D776N, I791I, E829Q, T863T, Q877Q, S941P
15-153	T786C, A915G^{h}, G1026A, C1038T, C1116T^{h}, A1187G, G1212A^{h}, T1257C^{h}, T1305C^{h}, C1344T^{h}, C1374T^{h}, A2202G^{h}, T2214C^{h}, T2271A, G2326A, T2448C, G2485C, C2589T, A2631G, A2686G^{h}, T2822C^{h}, G2874A^{h}	F262F, L305L^{h}, R342R, L346L, T373T^{h}, N396S, Q404Q^{h}, S419S^{h}, I435I^{h}, N448N^{h}, F458F^{h}, L734L^{h}, I738I^{h}, T757T, D776N, A816A, E829Q, T863T, Q877Q, N896S^{h}, S941P^{h}, S958S^{h}
15-155	G617A and T618C, T620C, A624G^{h}, C633T^{h}, G734C^{h}, T777A^{h}, T786C, C810T^{h}, C831G^{h}, G1026A^{h}, C1038T, A1187G, G1212A^{h}, T1257C^{h}, T1305C, C1344T^{h}, C1374T^{h}, C2040T^{h}, A2202G^{h}, T2214C^{h}, T2271A^{h}, T2316A^{h}, G2326A, T2448C^{h}, T2459G^{h}, G2485C, G2573A^{h}, C2589T, A2631G, A2686G^{h}, G2733A^{h}, T2822C^{h}, G2874A^{h}	R206H, V207A, K208K^{h}, N211N^{h}, G245A^{h}, P259P^{h}, F262F, I270I^{h}, P277P^{h}, R342R^{h}, L346L, N396S, Q404Q^{h}, S419S^{h}, I435I, N448N^{h}, F458F^{h}, T680T^{h}, L734L^{h}, I738I^{h}, T757T^{h}, N772K^{h}, D776N, A816A^{h}, N823K^{h}, E829Q, C858Y^{h}, T863T, Q877Q, N896S^{h}, Q911Q^{h}, S941P^{h}, S958S^{h}
15-161	T786C^{h}, G1026A^{h}, C1038T^{h}, A1187G^{h}, T1260C^{h}, A1269C^{h}, A2642G^{h}	F262F^{h}, R342R^{h}, L346L^{h}, N396S^{h}, V420V^{h}, E423D^{h}, N881S^{h}
15-179	T786C^{h}, G795A^{h}, G906A^{h}, G1026A^{h}, C1038T^{h}, A1187G^{h}, A1211C^{h} and G1212A^{h}, T1257C^{h}, T1305C^{h}, A2202G^{h}, T2214C^{h}, T2271A^{h}, G2326A, T2448C^{h}, G2485C^{h}, C2589T^{h}, A2631G^{h}, T2822C^{h}, G2874A^{h}	F262F^{h}, E265E^{h}, L302L^{h}, R342R^{h}, L346L^{h}, N396S^{h}, Q404P^{h}, S419S^{h}, I435I^{h}, L734L^{h}, I738I^{h}, T757T^{h}, D776N, A816A^{h}, E829Q^{h}, T863T^{h}, Q877Q^{h}, S941P^{h}, S958S^{h}
10-171	T786C, G1026A, C1038T, A1187G, G1212A, T1257C, T1305C, C2589T^{h}, A2631G^{h}, C1804T^{h}, T2822C^{h}, G2874A^{h}	F262F, R342R, L346L, N396S, Q404Q, S419S, I435I, T863T^{h}, Q877Q^{h}, S935L^{h}, S941P^{h}, S958S^{h}
10-280	T777A^{h}, T786C, C810T^{h}, C831G^{h}, G1026A^{h}, C1038T, A1187G, G1212A^{h}, T1257C^{h}, T1305C, C1344T^{h}, C1374T^{h}, C2040T^{h}, A2202G^{h}, T2214C^{h}, T2271A^{h}, T2316A^{h}, G2326A, T2448C^{h}, T2459G^{h}, G2485C, G2573A^{h}, C2589T, A2631G, A2686G^{h}, G2733A^{h}, T2822C^{h}, G2874A^{h}	P259P^{h}, F262F, I270I^{h}, P277P^{h}, R342R^{h}, L346L, N396S, Q404Q^{h}, S419S^{h}, I435I, N448N^{h}, F458F^{h}, T680T^{h}, L734L^{h}, I738I^{h}, T757T^{h}, N772K^{h}, D776N, A816A^{h}, N823K^{h}, E829Q, C858Y^{h}, T863T, Q877Q, N896S^{h}, Q911Q^{h}, S941P^{h}, S958S^{h}
08-187	G734C^{h}, T786C^{h}, G1026A^{h}, C1038T^{h}, A1187G^{h}, G1212A^{h}, T1257C^{h}, T1305C^{h}, A2202G^{h}, T2214C^{h}, G2326A^{h}, G2485C^{h}, A2631G^{h}, C1804T^{h}, T2822C^{h}, G2874A^{h}	G245A^{h}, F262F^{h}, R342R^{h}, L346L^{h}, N396S^{h}, Q404Q^{h}, S419S^{h}, I435I^{h}, L734L^{h}, I738I^{h}, D776N^{h}, E829Q^{h}, Q877Q^{h}, S935L^{h}, S941P^{h}, S958S^{h}
08-105	T777A^{h}, T786C, C810T^{h}, C831G^{h}, G1026A^{h}, C1038T, A1187G, G1212A^{h}, T1257C^{h}, T1305C, C1344T^{h}, C1374T^{h}, C2040T^{h}, A2202G^{h}, T2214C^{h}, T2271A^{h}, T2316A^{h}, G2326A, T2448C^{h}, T2459G^{h}, G2485C, G2573A^{h}, C2589T, A2631G, A2686G^{h}, G2733A^{h}, T2822C^{h}, G2874A^{h}	P259P^{h}, F262F, I270I^{h}, P277P^{h}, R342R^{h}, L346L, N396S, Q404Q^{h}, S419S^{h}, I435I, N448N^{h}, F458F^{h}, T680T^{h}, L734L^{h}, I738I^{h}, T757T^{h}, N772K^{h}, D776N, A816A^{h}, N823K^{h}, E829Q, C858Y^{h}, T863T, Q877Q, N896S^{h}, Q911Q^{h}, S941P^{h}, S958S^{h}
15-160	T786C, G1026A, C1038T, A1187G, G1212A, T1257C, T1305C, A2202G, T2214C, T2271A, G2326A, T2448C, G2485C, C2589T, A2631G, A2686G, T2822C, G2874A	F262F, R342R, L346L, N396S, Q404Q, S419S, I435I, L734L, I738I, T757T, D776N, A816A, E829Q, T863T, Q877Q, N896S, S941P, S958S

Table II. Continued.

Strains	SNPs in *TAC1*	Amino acid substitutions in Tac1*
06-100	T786C, T972C, T1014A, C1038T, A1047G, A1071G, T1107C, C1122T, C1130T, A1187G, G1212A, C1344T, C1374T, T2316A, G2326A, T2373A, G2485C, C2589T, G2606A, A2631G	F262F, S324S, A338A, L346L, L349L, L357L, S369S, T374T, A377V, N396S, Q404Q, N448N, F458F, N772K, D776N, I791I, E829Q, T863T, R869Q, Q877Q
16-133	G617A and T618C, T620C, A624G, C633T, T786C, G1026A, C1038T, A1187G, G1212A, T1257C, T1305C, A2202G, T2214C, T2271A, G2326A, T2448C^{h}, G2485C^{h}, C2589T, A2631G, T2684C, T2822C	R206H, V207A, K208K, N211N, F262F, R342R, L346L, N396S, Q404Q, S419S, I435I, L734L, I738I, T757T, D776N, A816A^{h}, E829Q^{h}, T863T, Q877Q, I895T, S941P
16-135	T777A, T786C, C810T^{h}, C831G, G1026A^{h}, C1038T, A1187G, T1305C, C1344T, C1374T, G1998A^{h}, C2040T^{h}, A2202G^{h}, T2214C^{h}, T2271A^{h}, T2316A^{h}, G2326A, T2448C^{h}, T2459G^{h}, G2485C, G2573A^{h}, C2589T, A2631G, A2686G^{h}, G2733A^{h}, T2822C^{h}, G2874A^{h}	P259P, F262F, I270I^{h}, P277P, R342R^{h}, L346L, N396S, I435I, N448N, F458F, S666S^{h}, T680T^{h}, L734L^{h}, I738I^{h}, T757T^{h}, N772K^{h}, D776N, A816A^{h}, N823K^{h}, E829Q, C858Y^{h}, T863T, Q877Q, N896S^{h}, Q911Q^{h}, S941P^{h}, S958S^{h}
16-132	A624G^{h}, C633T^{h}, T786C^{h}, G1026A^{h}, C1038T^{h}, A1187G^{h}, G1212A^{h}, T1257C^{h}, T1305C^{h}, A2202G^{h}, T2214C^{h}, T2316A^{h}, G2326A^{h}, G2485C^{h}, C2589T^{h}, A2631G^{h}, C1804T^{h}, T2822C^{h}, G2874A^{h}	K208K^{h}, N211N^{h}, F262F^{h}, R342R^{h}, L346L^{h}, N396S^{h}, Q404Q^{h}, S419S^{h}, I435I^{h}, L734L^{h}, I738I^{h}, N772K^{h}, D776N^{h}, E829Q^{h}, T863T^{h}, Q877Q^{h}, S935L^{h}, S941P^{h}, S958S^{h}
15-159	T777A^{h}, T786C, C810T^{h}, C831G^{h}, G1026A^{h}, C1038T, A1187G, G1212A^{h}, T1257C^{h}, T1260C^{h}, T1305C, C1344T^{h}, C1374T^{h}, C2040T^{h}, A2202G^{h}, T2214C^{h}, T2271A^{h}, T2316A^{h}, G2326A, T2448C^{h}, T2459G^{h}, G2485C, G2573A^{h}, C2589T, A2631G, A2686G^{h}, G2733A^{h}, T2822C^{h}, G2874A^{h}	P259P^{h}, F262F, I270I^{h}, P277P^{h}, R342R^{h}, L346L, N396S, Q404Q^{h}, S419S^{h}, V420V^{h}, I435I, N448N^{h}, F458F^{h}, T680T^{h}, L734L^{h}, I738I^{h}, T757T^{h}, N772K^{h}, D776N, A816A^{h}, N823K^{h}, E829Q, C858Y^{h}, T863T, Q877Q, N896S^{h}, Q911Q^{h}, S941P^{h}, S958S^{h}
16-122	A2202G, T2214C, T2316A, G2326A, G2485C, C2589T, A2631G, C1804T, T2822C, G2874A	L734L, I738I, N772K, D776N, E829Q, T863T, Q877Q, S935L, S941P, S958S
16-123	T786C^{h}, G1026A^{h}, C1038T^{h}, A1187G^{h}, G1212A^{h}, T1257C^{h}, T1305C^{h}, A2202G^{h}, T2214C^{h}, T2316A^{h}, G2326A^{h}, G2485C^{h}, C2589T^{h}, A2631G^{h}, C1804T^{h}, T2822C^{h}, G2874A^{h}	F262F^{h}, R342R^{h}, L346L^{h}, N396S^{h}, Q404Q^{h}, S419S^{h}, I435I^{h}, L734L^{h}, I738I^{h}, N772K^{h}, D776N^{h}, E829Q^{h}, T863T^{h}, Q877Q^{h}, S935L^{h}, S941P^{h}, S958S^{h}
10-168	T786C, G1026A, C1038T, A1187G, G1212A, T1257C, T1305C, A2202G, T2214C, T2271A, G2326A, T2448C^{h}, G2485C^{h}, C2589T, A2631G, T2684C^{h}, A2686G^{h}, T2822C, G2874A^{h}	F262F, R342R, L346L, N396S, Q404Q, S419S, I435I, L734L, I738I, T757T, D776N, A816A^{h}, E829Q^{h}, T863T, Q877Q, I895T^{h}, N896S^{h}, S941P, S958S^{h}
06-114	G617A and T618C, T620C, A624G, C633T, T786C, G1026A, C1038T, A1187G, G1212A, T1257C, T1305C, A2202G, T2214C, T2271A, G2326A, C2589T, A2631G, T2822C	R206H, V207A, K208K, N211N, F262F, R342R, L346L, N396S, Q404Q, S419S, I435I, L734L, I738I, T757T, D776N, T863T, Q877Q, S941P
BE-114	A738T^{h}, T786C, G795A, G906A, T1014A, C1038T, A1047G^{h}, A1071G^{h}, T1107C^{h}, C1122T, C1130T^{h}, A1187G, G1212A^{h}, T1257C^{h}, T1305C, C1344T^{h}, C1374T^{h}, C2040T^{h}, C2083T^{h} and T2085A^{h}, T2316A, G2326A, T2373A, G2485C^{h}, C2589T^{h}, A2631G^{h}, T2822C^{h}	S246S^{h}, F262F, E265E, L302L, A338A, L346L, L349L^{h}, L357L^{h}, S369S^{h}, T374T, A377V^{h}, N396S, Q404Q^{h}, S419S^{h}, I435I, N448N^{h}, F458F^{h}, T680T^{h}, L695L^{h}, N772K, D776N, I791I, E829Q^{h}, T863T^{h}, Q877Q^{h}, S941P^{h}
10-221	T786C, G1026A, C1038T, A1187G, G1212A, T1257C, T1305C, A2202G, T2214C, T2271A, G2326A, T2448C^{h}, G2485C^{h}, C2589T, A2631G, T2684C^{h}, A2686G^{h}, T2822C, G2874A^{h}	F262F, R342R, L346L, N396S, Q404Q, S419S, I435I, L734L, I738I, T757T, D776N, A816A^{h}, E829Q^{h}, T863T, Q877Q, I895T^{h}, N896S^{h}, S941P, S958S^{h}

Table II. Continued.

Strains	SNPs in *TAC1*	Amino acid substitutions in Tac1*
16-134	T786C, G1026A, C1038T, A1187G, G1212A, T1257C, T1305C, A2202G, T2214C, T2271A, G2326A, T2448C^{h}, G2485C^{h}, C2589T, A2631G, T2684C^{h}, A2686G^{h}, T2822C	F262F, R342R, L346L, N396S, Q404Q, S419S, I435I, L734L, I738I, T757T, D776N, A816A^{h}, E829Q^{h}, T863T, Q877Q, I895T^{h}, N896S^{h}, S941P
15-156	C633T^{h}, T786C^{h}, G1026A^{h}, C1038T^{h}, A1187G^{h}, G1212A^{h}, T1257C^{h}, T1305C^{h}, A2202G^{h}, T2214C^{h}, T2316A^{h}, G2326A^{h}, G2485C^{h}, C2589T^{h}, A2631G^{h}, C1804T^{h}, T2822C^{h}, G2874A^{h}	N211N^{h}, F262F^{h}, R342R^{h}, L346L^{h}, N396S^{h}, Q404Q^{h}, S419S^{h}, I435I^{h}, L734L^{h}, I738I^{h}, N772K^{h}, D776N^{h}, E829Q^{h}, T863T^{h}, Q877Q^{h}, S935L^{h}, S941P^{h}, S958S^{h}
15-157	T786C, A915G, G1026A, C1038T, A1187G, G1212A, T1257C, T1305C, A2202G, T2214C, T2271A, G2326A, T2448C^{h}, G2485C^{h}, C2589T, A2631G, T2684C^{h}, A2686G^{h}, T2822C, G2874A^{h}	F262F, L305L, R342R, L346L, N396S, Q404Q, S419S, I435I, L734L, I738I, T757T, D776N, A816A^{h}, E829Q^{h}, T863T, Q877Q, I895T^{h}, N896S^{h}, S941P, S958S^{h}
10-170	T786C, G1026A, C1038T, A1187G, G1212A, T1257C, T1305C, A2202G, T2214C, T2271A, G2326A, G2485C^{h}, C2589T, A2631G, T2684C^{h}, A2686G^{h}, T2822C, G2874A^{h}	F262F, R342R, L346L, N396S, Q404Q, S419S, I435I, L734L, I738I, T757T, D776N, E829Q^{h}, T863T, Q877Q, I895T^{h}, N896S^{h}, S941P, S958S^{h}
BE-113	T786C^{h}, G1026A^{h}, C1038T^{h}, A1187G^{h}, G1212A^{h}, T1257C^{h}, T1305C^{h}, <u>C2273T</u>	F262F^{h}, R342R^{h}, L346L^{h}, N396S^{h}, Q404Q^{h}, S419S^{h}, I435I^{h}, <u>S758F</u>
16-091	T786C, G1026A^{h}, C1038T^{h}, A1187G^{h}, G1212A^{h}, T1257C^{h}, T1305C^{h}, A2202G^{h}, T2214C^{h}, T2316A^{h}, G2326A^{h}, G2485C^{h}	F262F, R342R^{h}, L346L^{h}, N396S^{h}, Q404Q^{h}, S419S^{h}, I435I^{h}, L734L^{h}, I738I^{h}, N772K^{h}, D776N^{h}, E829Q^{h}
ATCC 64550	G1026A, C1038T, A1187G, G1212A, T1257C, T1305C	R342R, L346L, N396S, Q404Q, S419S, I435I
15-154	T777A^{h}, T786C, C810T^{h}, C831G^{h}, G1026A^{h}, C1038T, A1187G, G1212A^{h}, T1257C^{h}, T1305C, C1344T^{h}, C1374T^{h}, C2040T^{h}, A2202G^{h}, T2214C^{h}, T2316A^{h}, G2326A, T2448C^{h}, T2459G^{h}, G2485C, G2573A^{h}, C2589T, A2631G, A2686G^{h}, G2733A^{h}, T2822C^{h}, G2874A^{h}	P259P^{h}, F262F, I270I^{h}, P277P^{h}, R342R^{h}, L346L, N396S, Q404Q^{h}, S419S^{h}, I435I, N448N^{h}, F458F^{h}, T680T^{h}, L734L^{h}, I738I^{h}, N772K^{h}, D776N, A816A^{h}, N823K^{h}, E829Q, C858Y^{h}, T863T, Q877Q, N896S^{h}, Q911Q^{h}, S941P^{h}, S958S^{h}
15-176	T786C, G1026A^{h}, C1038T^{h}, A1187G^{h}, G1212A^{h}, T1257C^{h}, T1305C^{h}, A2202G^{h}, **C2207T^{h}**, T2214C^{h}, T2316A^{h}, G2326A^{h}, G2485C^{h}, C2589T^{h}, A2631G^{h}, **ΔT2884-T2907^{h}**	F262F, R342R^{h}, L346L^{h}, N396S^{h}, Q404Q^{h}, S419S^{h}, I435I^{h}, L734L^{h}, **A736V**^{h}, I738I^{h}, N772K^{h}, D776N^{h}, E829Q^{h}, T863T^{h}, Q877Q^{h}, **ΔL962-N969**^{h}
ATCC 64124	T786C^{h}, G1026A^{h}, C1038T^{h}, A1187G^{h}, G1212A^{h}, T1257C^{h}, T1305C^{h}, A2202G^{h}, T2214C^{h}, T2316A^{h}, G2326A^{h}, G2485C^{h}, **C2515T^{h}**, C2589T, A2631G, C1804T^{h}, T2822C^{h}, G2874A^{h}, **A2929G^{h}**	F262F^{h}, R342R^{h}, L346L^{h}, N396S^{h}, Q404Q^{h}, S419S^{h}, I435I^{h}, L734L^{h}, I738I^{h}, N772K^{h}, D776N^{h}, E829Q^{h}, **H839Y^{h}**, T863T, Q877Q, S935L^{h}, S941P^{h}, **N977D^{h}**
16-092	T786C, A915G^{h}, G1026A, C1038T, C1122T^{h}, A1187G, G1212A^{h}, T1257C^{h}, T1305C^{h}, A2202G^{h}, T2214C^{h}, T2271A, G2326A, T2448C, G2485C, C2589T, A2631G	F262F, L305L^{h}, R342R, L346L, T374T^{h}, N396S, Q404Q^{h}, S419S^{h}, I435I^{h}, L734L^{h}, I738I^{h}, T757T, D776N, A816A, E829Q, T863T, Q877Q
16-138	T786C, A915G, G1026A, C1038T, C1122T, A1187G, C1344T, C1374T, A2202G^{h}, T2214C^{h}, T2271A, G2326A, T2448C, G2485C, C2589T, A2631G, A2686G^{h}, T2822C^{h}, G2874A^{h}	F262F, L305L, R342R, L346L, T374T, N396S, N448N, F458F, L734L^{h}, I738I^{h}, T757T, D776N, A816A, E829Q, T863T, Q877Q, N896S^{h}, S941P^{h}, S958S^{h}

*The SNPs that do not entail changes in the amino acid sequence are denoted with the symbol of the amino acid present in the reference sequence followed by the position and again the same amino acid symbol; h, heterozygous mutation. The new mutations found in this work are underlined and the mutations associated to azole resistance are indicated in bold.

Table III. SNPs detected in the selected regions of the *UPC2* gene and the associated amino acid substitutions of the azole-susceptible and resistant isolates of the UPV/EHU collection.

Strains	SNPs in *UPC2*	Amino acid substitutions in Upc2*
16-122	**G1942A^{h}**	**G648S^{h}**
16-123	**G1942A^{h}**	**G648S^{h}**
16-091	**G1942A^{h}**	**G648S^{h}**
15-176	**C1928T^{h}**	**A643V^{h}**

*The SNPs that do not entail changes in the amino acid sequence are denoted with the symbol of the amino acid present in the reference sequence followed by the position and again the same amino acid symbol; h, heterozygous mutation. The new mutations found in this work are underlined and the mutations associated to azole resistance are indicated in bold.

Table IV. SNPs detected in the selected regions of the *MRR1* gene and the associated amino acid substitutions of the azole-susceptible and resistant isolates of the UPV/EHU collection.

Strains	SNPs in *MRR1*	Amino acid substitutions in Mrr1*
BE-47	-	-
16-135	C972T^{h}, T999C^{h}, T1022A^{h}, T1134A^{h}, G1437A^{h}, A1626G^{h}, A1773T^{h}, C1774T^{h} and C1776A^{h}, T1782C^{h}, C1791T^{h}, T1806A^{h}, A1824G^{h}, T1851C^{h}, C1866T^{h}, A1872G^{h}, C2358T^{h}, C2370T^{h}, C2373T^{h}, A2385T^{h}, G2502C^{h}, T2529C^{h}, G2577A^{h}, A2589G^{h}, C1595T^{h}, G3058C	A324A^{h}, L333L^{h}, V341E^{h}, T378T^{h}, K479K^{h}, L542L^{h}, A591A^{h}, L592L^{h}, S594S^{h}, V597V^{h}, S602S^{h}, E608E^{h}, N617N^{h}, N622N^{h}, L624L^{h}, L786L^{h}, A790A^{h}, G791G^{h}, P795P^{h}, V834V^{h}, N843N^{h}, S859S^{h}, E863E^{h}, C865C^{h}, E1020Q
16-132	C972T^{h}, T999C^{h}, T1022A^{h}, T1134A^{h}, G1437A^{h}, A1626G^{h}, A1773T^{h}, C1774T^{h} and C1776A^{h}, T1782C^{h}, C1791T^{h}, T1806A^{h}, A1824G^{h}, T1851C^{h}, C1866T^{h}, A1872G^{h}, C2358T^{h}, C2370T^{h}, C2373T^{h}, A2385T^{h}, G2502C^{h}, T2529C^{h}, G2577A^{h}, A2589G^{h}, C1595T^{h}, G3058C	A324A^{h}, L333L^{h}, V341E^{h}, T378T^{h}, K479K^{h}, L542L^{h}, A591A^{h}, L592L^{h}, S594S^{h}, V597V^{h}, S602S^{h}, E608E^{h}, N617N^{h}, N622N^{h}, L624L^{h}, L786L^{h}, A790A^{h}, G791G^{h}, P795P^{h}, V834V^{h}, N843N^{h}, S859S^{h}, E863E^{h}, C865C^{h}, E1020Q
06-114	C972T^{h}, T999C^{h}, T1022A^{h}, T1134A^{h}, G1227T^{h}, G1437A^{h}, A1626G^{h}, A1773T^{h}, C1774T^{h} and C1776A^{h}, T1782C^{h}, C1791T^{h}, T1806A^{h}, T1812A^{h}, A1824G^{h}, T1851C^{h}, C1866T^{h}, A1872G^{h}, C2358T^{h}, C2370T^{h}, C2373T^{h}, A2385T^{h}, G2502C^{h}, T2529C^{h}, G2577A^{h}, A2589G^{h}, C1595T^{h}	A324A^{h}, L333L^{h}, V341E^{h}, T378T^{h}, G409G^{h}, K479K^{h}, L542L^{h}, A591A^{h}, L592L^{h}, S594S^{h}, V597V^{h}, S602S^{h}, G604G^{h}, E608E^{h}, N617N^{h}, N622N^{h}, L624L^{h}, L786L^{h}, A790A^{h}, G791G^{h}, P795P^{h}, V834V^{h}, N843N^{h}, S859S^{h}, E863E^{h}, C865C^{h}
BE-114	C972T, T999C, T1022A, T1134A, G1437A, A1626G, A1773T, C1774T and C1776A, T1782C, C1791T, T1806A, T1812A, A1824G, T1851C, C1866T, A1872G, C2358T, C2370T, C2373T, A2385T, G2502C, T2529C, C2538T, G2577A, A2589G, C1595T, G3058C	A324A, L333L, V341E, T378T, K479K, L542L, A591A, L592L, S594S, V597V, S602S, G604G, E608E, N617N, N622N, L624L, L786L, A790A, G791G, P795P, V834V, N843N, H846H, S859S, E863E, C865C, E1020Q
16-134	A2967G	S989S
BE-113	C972T^{h}, T999C^{h}, T1022A^{h}, T1134A^{h}, G1437A^{h}, A1626G^{h}, A1773T^{h}, C1774T^{h} and C1776A^{h}, T1782C^{h}, C1791T^{h}, T1806A^{h}, T1812A^{h}, A1824G^{h}, T1851C^{h}, C1866T^{h}, A1872G^{h}, C2358T^{h}, C2370T^{h}, C2373T^{h}, A2385T^{h}, G2502C^{h}, T2529C^{h}, C2538T^{h}, G2577A^{h}, A2589G^{h}, C1595T^{h}, G3058C^{h}	A324A^{h}, L333L^{h}, V341E^{h}, T378T^{h}, K479K^{h}, L542L^{h}, A591A^{h}, L592L^{h}, S594S^{h}, V597V^{h}, S602S^{h}, G604G^{h}, E608E^{h}, N617N^{h}, N622N^{h}, L624L^{h}, L786L^{h}, A790A^{h}, G791G^{h}, P795P^{h}, V834V^{h}, N843N^{h}, H846H^{h}, S859S^{h}, E863E^{h}, C865C^{h}, E1020Q^{h}
ATCC 64550	C2931T^{h}	G997G^{h}
15-176	C972T, T999C, T1022A, T1134A, G1437A, A1626G, A1773T, C1774T and C1776A, T1782C, C1791T, T1806A, T1812A, A1824G, T1851C, C1866T, A1872G, C2358T, C2370T, C2373T, A2385T, G2502C, T2529C, C2538T, G2577A, A2589G, C1595T, **G2839A**, G3058C	A324A, L333L, V341E, T378T, K479K, L542L, A591A, L592L, S594S, V597V, S602S, G604G, E608E, N617N, N622N, L624L, L786L, A790A, G791G, P795P, V834V, N843N, H846H, S859S, E863E, C865C, **G947S,** E1020Q

*The SNPs that do not entail changes in the amino acid sequence are denoted with the symbol of the amino acid present in the reference sequence followed by the position and again the same amino acid symbol; h, heterozygous mutation. The new mutations found in this work are underlined and the mutations associated to azole resistance are indicated in bold.

Table V. SNPs detected in the selected regions of the *MRR2* gene and the associated amino acid substitutions of the azole-susceptible and resistant isolates of the UPV/EHU collection.

Strains	SNPs in *MRR2*	Amino acid substitutions in Mrr2*
BE-47	C462T	A154A
BE-AZ	T1352C	V451A
15-158	C1125T^{h}, T1352C^{h}, G1503A^{h}, G1524A^{h}, T1623C^{h}, T1662C^{h}, A1797G, C1880T^{h}	R375R^{h}, V451Ah, L501L^{h}, K508K^{h}, I541I^{h}, H554H^{h}, R599R, A627V^{h}
06-116	C1266A, G1375A, T1380C, T1383C, T1480C, C1515T, T1662C, A1797G, C1878G	D442E, A459T, F460F, I464I, L494L, Y505Y, H554H, R599R, S626S
15-153	C1125T^{h}, G1503A^{h}, G1524A^{h}, T1623C^{h}, T1662C^{h}, A1797G, C1880T^{h}	R375R^{h}, L501L^{h}, K508K^{h}, I541I^{h}, H554H^{h}, R599R, A627V^{h}
08-105	G1375A, T1380C, T1383C, T1623C, T1662C, C1734T, A1797G, T2040C	A459T, F460F, I464I, I541I, H554H, F578F, R599R, Y680Y
16-135	C84T, T423C, A426G, T428C and G429A, C430G, A433G, G492C, G494A, A723G, C732T, G1375A, T1380C, T1383C, T1438C, T1480C, T1494C, T1623C, T1662C, C1734T, A1797G, T2040C	A28A, D141D, L142L, S143P, L144V, T145A, P164P, S165N, P241P, D244D, A459T, F460F, I464I, S480P, L494L, P498P, I541I, H554H, F578F, R599R, Y680Y
16-132	C462T	A154A
15-159	T423C, A426G, T428C and G429A, C430G, A433G, G492C, G494A, A723G, C732T, G1375A, T1380C, T1383C, T1438C, T1480C, T1494C, T1623C, T1662C, C1734T, A1797G, T2040C	D141D, L142L, S143P, L144V, T145A, P164P, S165N, P241P, D244D, A459T, F460F, I464I, S480P, L494L, P498P, I541I, H554H, F578F, R599R, Y680Y
BE-114	C932T, T1352C, G1744T	A311V, V451A, V582L
16-134	C84T, A228G, T423C, A426G, T428C and G429A, C430G, A433G, G492C, G494A, C1266A, G1375A, T1380C, T1383C, T1438C, T1480C, C1515T, T1662C, A1797G, C1878G	A28A, K76K, D141D, L142L, S143P, L144V, T145A, P164P, S165N, D442E, A459T, F460F, I464I, S480P, L494L, Y505Y, H554H, R599R, S626S
15-157	C84T, A228G, T423C, A426G, T428C and G429A, C430G, A433G, G492C, G494A, C1266A, G1375A, T1380C, T1383C, T1438C, T1480C, C1515T, T1662C, A1797G, C1878G	A28A, K76K, D141D, L142L, S143P, L144V, T145A, P164P, S165N, D442E, A459T, F460F, I464I, S480P, L494L, Y505Y, H554H, R599R, S626S
BE-113	C462T, A768C	A154A, S256S
16-091	C462T	A154A
ATCC 64550	C462T	A154A
15-176	C462T	A154A
ATCC 64124	T1352C	V451A
16-138	T687C, T693C, C696T, A723G, T1352C, A1797G	T229T, F231F, N232N, P241P, V451A, R599R

*The SNPs that do not entail changes in the amino acid sequence are denoted with the symbol of the amino acid present in the reference sequence followed by the position and again the same amino acid symbol; h, heterozygous mutation. The new mutations found in this work are underlined and the mutations associated to azole resistance are indicated in bold.

II – Amino acid substitutions and other modifications identified in the Erg11, Tac1 and Mrr2 transformants

Table VI. Summary of the sequencing results of *TAC1* in the *C. albicans* SC5314 and derived mutants and the corresponding amino acid residues.

Transformant	Nucleotide positions in *TAC1*[a]	Amino acid residues in Tac1[b]
SC5314	G2078, R2202, Y2214, C2273, A2298, A2300 and A2301, W2316, R2326 and A2327, T2402, A2426, T2435, S2485, Y2589, R2631, Y2804, Y2822, R2874, C2922	R693, L734, I738, S758, K766, Q767, N/K772, D/N776, V801, H809, V812, E/Q829, T863, Q877, S/L935, S/P941, S958, F974
D1	G2078, A2202, T2214, T2273, G2298, A2300 and G2301, T2316, G2326 and A2327, T2402, A2426, T2435, G2485, C2589, A2631, C2804, T2822, G2874, C2922	R693, L734, I738, S758F, K766K, Q767Q, N772, D776, V801, H809, V812, E829, T863, Q877, S935, S941, S958, F974
D2	G2078, R2202, Y2214, C2273, G2298, A2300 and G2301, T2316, G2326 and A2327, T2402, A2426, T2435, G2485, C2589, A2631, C2804, T2822, G2874, Y2922	R693, L734L, I738I, S758, K766K, Q767Q, N772, D776, V801, H809, V812, E829, T863, Q877, S935, S941, S958, F974F
D3	G2078, G2202, C2214, T2273, G2298, A2300 and G2301, T2316, G2326 and A2327, T2402, A2426, T2435, G2485, C2589, A2631, C2804, T2822, G2874, C2922	R693, L734, I738, S758F, K766K, Q767Q, N772, D776, V801, H809, V812, E829, T863, Q877, S935, S941, S958, F974
D4	G2078, R2202, Y2214, Y2273, insertion and multiple substitutions	R693, L734L, I738I, S/F758
D5	G2078, R2202, Y2214, Y2273, G2298, A2300 and G2301, T2316, G2326 and A2327, T2402, A2426, T2435, no more sequence from here onwards	R693, L734L, I738I, S/F758, K766K, Q767Q, N772, D776, V801, H809, V812
D6	G2078, R2202, Y2214, Y2273, G2298, A2300 and G2301, T2316, G2326 and A2327, T2402, A2426, T2435, no more sequence from here onwards	R693, L734L, I738I, S/F758, K766K, Q767Q, N772, D776, V801, H809, V812
D7	G2078, R2202, Y2214, C2273, G2298, A2300 and G2301, T2316, G2326 and A2327, T2402, A2426, T2435, no more sequence from here onwards	R693, L734L, I738I, S758, K766K, Q767Q, N772, D776, V801, H809, V812
D8	G2078, R2202, Y2214, C2273, A2298, A2300 and A2301, W2316, R2326 and A2327, T2402, A2426, T2435, S2485, Y2589, R2631, C2804, T2822, R2874, C2922	R693, L734L, I738I, S758, K766, Q767, N/K772, D/N776, V801, H809, V812, E/Q829, T863, Q877, S935, S941, S958, F974
D9 (WT RTe)	G2078, R2202, Y2214, C2273, G2298, A2300 and G2301, W2316, R2326 and A2327, T2402, A2426, T2435, no more sequence from here onwards	R693, L734L, I738I, S758, K766K, Q767Q, N/K772, D/N776, V801, H809, V812
D12 (WT RTe)	G2078, R2202, Y2214, C2273, A2298, A2300 and A2301, W2316, R2326 and A2327, T2402, A2426, T2435, no more sequence from here onwards	R693, L734L, I738I, S758, K766, Q767, N/K772, D/N776, V801, H809, V812
D13 (WT RTe)	G2078, G2202, C2214, C2273, G2298, A2300 and G2301, W2316, R2326 and A2327, T2402, A2426, T2435, no more sequence from here onwards	R693, L734, I738, S758, K766K, Q767Q, N/K772, D/N776, V801, H809, V812
D16	G2078, A2202, T2214, T2273, G2298, C2300 and G2301, T2316, G2326 and A2327, T2402, A2426, T2435, G2485, C2589, A2631, C2804, T2822, G2874, C2922	R693, L734, I738, S758F, K766K, Q767P, N772, D776, V801, H809, V812, E829, T863, Q877, S935, S941, S958, F974
D17	G2078, G2202, C2214, C2273, G2298, A2300 and G2301, T2316, G2326 and A2327, T2402, A2426, T2435, C2485, T2589, G2631, T2804, C2822, A2874, C2922	R693, L734, I738, S758, K766K, Q767Q, N772, D776, V801, H809, V812, Q829, T863, Q877, L935, P941, S958, F974

Table VI. Continued.

Transformant	Nucleotide positions in *TAC1*[a]	Amino acid residues in Tac1[b]
D18	G2078, G2202, C2214, C2273, A2298, A2300 and A2301, A2316, A2326 and R2327, T2402, A2426, T2435, S2485, Y2589, G2631, Y2804, Y2822, R2874, C2922	R693, L734, I738, S758, K766, Q767, K772, N/S776, V801, H809, V812, E/Q829, T863, Q877, S/L935, S/P941, S958, F974
D19	G2078, G2202, C2214, C2273, A2298, A2300 and A2301, A2316, A2326 and A2327, T2402, A2426, T2435, C2485, Y2589, R2631, C2804, T2822, G2874, C2922	R693, L734, I738, S758, K766, Q767, K772, N776, V801, H809, V812, Q829, T863, Q877, S935, S941, S958, F974
D21	G2078, A2202, T2214, C2273, G2298, A2300 and G2301, A2316, R2326 and A2327, T2402, A2426, T2435, S2485, Y2589, R2631, Y2804, Y2822, Y2874, C2922	R693, L734, I738, S758, K766K, Q767Q, K772, D/N776, V801, H809, V812, E/Q829, T863, Q877, S/L935, S/P941, S958, F974
D22	G2078, A2202, T2214, T2273, G2298, A2300 and G2301, T2316, G2326 and A2327, T2402, A2426, T2435, S2485, Y2589, R2631, Y2804, Y2822, R2874, C2922	R693, L734, I738, S758F, K766K, Q767Q, N772, D776, V801, H809, V812, E/Q829, T863, Q877, S/L935, S/P941, S958, F974
D23	G2078, R2202, Y2214, C2273, A2298, A2300 and A2301, T2316, G2326 and A2327, T2402, A2426, T2435, G2485, C2589, A2631, C2804, T2822, G2874, C2922	R693, L734L, I738I, S758, K766, Q767, N772, D776, V801, H809, V812, E829, T863, Q877, S935, S941, S958, F974
D24 (WT RTe)	G2078, G2202, C2214, C2273, G2298, A2300 and G2301, T2316, G2326 and A2327, T2402, A2426, T2435, C2485, T2589, G2631, T2804, C2822, A2874, C2922	R693, L734, I738, S758, K766K, Q767Q, N772, D776, V801, H809, V812, Q829, T863, Q877, L935, P941, S958, F974
D25 (WT RTe)	G2078, G2202, C2214, C2273, G2298, A2300 and G2301, T2316, G2326 and A2327, T2402, A2426, T2435, C2485, T2589, G2631, T2804, C2822, A2874, C2922	R693, L734, I738, S758, K766K, Q767Q, N772, D776, V801, H809, V812, Q829, T863, Q877, L935, P941, S958, F974
D26 (WT RTe)	G2078, R2202, Y2214, C2273, A2298, A2300 and A2301, W2316, R2326 and A2327, T2402, A2426, T2435, S2485, Y2589, R2631, Y2804, Y2822, R2874, C2922	R693, L734L, I738I, S758, K766, Q767, N/K772, D/N776, V801, H809, V812, E/Q829, T863, Q877, S/L935, S/P941, S958, F974
D27 (WT RTe)	G2078, A2202, T2214, C2273, G2298, A2300 and G2301, T2316, G2326 and A2327, T2402, A2426, T2435, S2485, Y2589, R2631, Y2804, Y2822, R2874, C2922	R693, L734, I738, S758, K766K, Q767Q, N772, D776, V801, H809, V812, E/Q829, T863, Q877, S/L935, S/P941, S958, F974
D34	G2078, A2202, T2214, C2273, A2298, A2300 and A2301, T2316, G2326 and A2327, T2402, A2426, T2435, G2485, C2589, A2631, C2804, T2822, G2874, C2922	R693, L734, I738, S758, K766, Q767, N772, D776, V801, H809, V812, E829, T863, Q877, S935, S941, S958, F974
D35	G2078, A2202, T2214, C2273, A2298, A2300 and A2301, T2316, G2326 and A2327, T2402, A2426, T2435, G2485, C2589, A2631, C2804, T2822, G2874, C2922	R693, L734, I738, S758, K766, Q767, N772, D776, V801, H809, V812, E829, T863, Q877, S935, S941, S958, F974
D36	G2078, A2202, T2214, T2273, G2298, A2300 and A2301, T2316, G2326 and A2327, T2402, A2426, T2435, G2485, C2589, A2631, T2804, T2822, A2874, C2922	R693, L734, I738, S758F, K766K, Q767, N772, D776, V801, H809, V812, E829, T863, Q877, L935, S941, S958, F974
D38	G2078, R2202, Y2214, Y2273, G2298, A2300 and G2301, T2316, G2326 and A2327, T2402, A2426, T2435, S2485, Y2589, G2631, Y2804, Y2822, R2874, C2922	R693, L734L, I738I, S/F758, K766K, Q767Q, N772, D776, V801, H809, V812, E/Q829, T863, Q877, S/L935, S/P941, S958, F974
D40	G2078, R2202, Y2214, C2273, A2298, A2300 and A2301, A2316, R2326 and A2327, T2402, A2426, T2435, S2485, Y2589, R2631, Y2804, Y2822, R2874, C2922	R693, L734L, I738I, S758, K766, Q767, K772, D/N776, V801, H809, V812, E/Q829, T863, Q877, S/L935, S/P941, S958, F974
D41	G2078, R2202, Y2214, Y2273, G2298, A2300 and G2301, T2316, G2326 and A2327, T2402, A2426, T2435, S2485, Y2589, R2631, Y2804, Y2822, R2874, C2922	R693, L734L, I738I, S/F758, K766K, Q767Q, N772, D776, V801, H809, V812, E/Q829, T863, Q877, S/L935, S/P941, S958, F974

Table VI. Continued.

Transformant	Nucleotide positions in *TAC1*[a]	Amino acid residues in Tac1[b]
D43	G2078, A2202, T2214, Y2273, G2298, A2300 and G2301, W2316, R2326 and A2327, T2402, A2426, T2435, S2485, Y2589, R2631, Y2804, Y2822, R2874, C2922	R693, L734, I738, S/F758F, K766K, Q767Q, N/K772, D/N776, V801, H809, V812, E/Q829, T863, Q877, S/L935, S/P941, S958, F974
D44	R2078, R2202, Y2214, C2273, A2298, A2300 and A2301, A2316, A2326 and A2327, T2402, A2426, T2435, S2485, Y2589, G2631, Y2804, Y2822, R2874, C2922	R/K693, L734L, I738I, S758, K766, Q767, K772, N776, V801, H809, V812, E/Q829, T863, Q877, S/L935, S/P941, S958, F974
D45	G2078, R2202, Y2214, Y2273, G2298, A2300 and G2301, W2316, R2326 and A2327, T2402, A2426, T2435, S2485, Y2589, G2631, Y2804, Y2822, R2874, C2922	R693, L734L, I738I, S/F758, K766K, Q767Q, N/K772, D/N776, V801, H809, V812, E/Q829, T863, Q877, S/L935, S/P941, S958, F974
D48	G2078, G2202, C2214, Y2273, G2298, A2300 and G2301, T2316, G2326 and A2327, T2402, A2426, T2435, G2485, C2589, A2631, C2804, T2822, G2874, C2922	R693, L734, I738, S758F, K766K, Q767Q, N772, D776, V801, H809, V812, E829, T863, Q877, S935, S941, S958, F974
D49	G2078, R2202, Y2214, C2273, A2298, A2300 and A2301, T2316, G2326 and A2327, T2402, A2426, T2435, G2485, C2589, A2631, C2804, T2822, G2874, C2922	R693, L734L, I738I, S758, K766, Q767, N772, D776, V801, H809, V812, E829, T863, Q877, S935, S941, S958, F974
D50	G2078, R2202, Y2214, C2273, A2298, A2300 and A2301, T2316, G2326 and A2327, A2402, C2426, G2435, no more sequence from here onwards	R693, L734L, I738I, S758, K766, Q767, K766, Q767, N772, D776, V801E, H809P, V812G
D52	G2078, A2202, T2214, Y2273, G2298, A2300 and G2301, T2316, G2326 and A2327, T2402, A2426, T2435, G2485, C2589, A2631, C2804, T2822, G2874, C2922	R693, L734, I738, S/F758, K766K, Q767Q, N772, D776, V801, H809, V812, E829, T863, Q877, S935, S941, S958, F974
D53	G2078, A2202, T2214, C2273, A2298, A2300 and A2301, T2316, G2326 and A2327, T2402, A2426, T2435, G2485, C2589, A2631, C2804, T2822, G2874, C2922	R693, L734, I738, S758, K766, Q767, N772, D776, V801, H809, V812, E829, T863, Q877, S935, S941, S958, F974
D54	G2078, R2202, Y2214, C2273, A2298, A2300 and A2301, W2316, R2326 and A2327, T2402, A2426, T2435, G2485, Y2589, A2631, C2804, Y2822, R2874, C2922	R693, L734L, I738I, S758, K766, Q767, N/K772, D/N776, V801, H809, V812, E829, T863, Q877, S935, S/P941, S958, F974
D61	G2078, G2202, C2214, T2273, G2298, A2300 and G2301, T2316, G2326 and A2327, T2402, A2426, T2435, G2485, Y2589, R2631, Y2804, Y2822, R2874, C2922	R693, L734, I738, S758F, K766K, Q767Q, N772, D776, V801, H809, V812, E829, T863, Q877, S/L935, S/P941, S958, F974
D62	G2078, R2202, Y2214, C2273, A2298, A2300 and A2301, T2316, R2326 and A2327, T2402, A2426, T2435, S2485, Y2589, R2631, C2804, T2822, R2874, C2922	R693, L734L, I738I, S758, K766, Q767, N772, D/N776, V801, H809, V812, E/Q829, T863, Q877, S935, S941, S958, F974
D63	G2078, R2202, Y2214, C2273, A2298, A2300 and A2301, A2316, A2326 and A2327, T2402, A2426, T2435, S2485, Y2589, R2631, Y2804, Y2822, R2874, C2922	R693, L734L, I738I, S758, K766, Q767, K772, N776, V801, H809, V812, E/Q829, T863, Q877, S/L935, S/P941, S958, F974
D66	G2078, A2202, T2214, Y2273, G2298, A2300 and G2301, T2316, R2326 and A2327, T2402, A2426, T2435, S2485, Y2589, R2631, Y2804, Y2822, R2874, C2922	R693, L734, I738, S/F758, K766K, Q767Q, N772, D/N776, V801, H809, V812, E/Q829, T863, Q877, S/L935, S/P941, S958, F974
D76	G2078, R2202, Y2214, C2273, A2298, A2300 and A2301, T2316, R2326 and A2327, T2402, A2426, T2435, S2485, Y2589, R2631, Y2804, T2822, R2874, C2922	R693, L734L, I738I, S758, K766, Q767, N772, D/N776, V801, H809, V812, E/Q829, T863, Q877, S/L935, S941, S958, F974
D78	G2078, R2202, Y2214, C2273, A2298, A2300 and A2301, W2316, R2326 and A2327, T2402, A2426, T2435, S2485, Y2589, R2631, Y2804, Y2822, R2874, C2922	R693, L734L, I738I, S758, K766, Q767, N/K772, D/N776, V801, H809, V812, E/Q829, T863, Q877, S/L935, S/P941, S958, F974

Table VI. Continued.

Transformant	Nucleotide positions in *TAC1*[a]	Amino acid residues in Tac1[b]
D79	G2078, R2202, Y2214, C2273, A2298, A2300 and A2301, T2316, R2326 and A2327, T2402, A2426, T2435, S2485, Y2589, R2631, Y2804, Y2822, R2874, C2922	R693, L734L, I738I, S758, K766, Q767, N772, D/N776, V801, H809, V812, E/Q829, T863, Q877, S/L935, S/P941, S958, F974
D80	G2078, R2202, Y2214, C2273, A2298, A2300 and A2301, W2316, R2326 and A2327, T2402, A2426, T2435, S2485, Y2589, G2631, Y2804, Y2822, R2874, C2922	R693, L734L, I738I, S758, K766, Q767, N/K772, D/N776, V801, H809, V812, E/Q829, T863, Q877, S/L935, S/P941, S958, F974
D87	G2078, A2202, T2214, C2273, A2298, A2300 and A2301, A2316, G2326 and A2327, T2402, A2426, T2435, G2485, T2589, G2631, T2804, C2822, A2874, C2922	R693, L734, I738, S758, K766, Q767, K772, D776, V801, H809, V812, E829, T863, Q877, L935, P941, S958, F974
D88	G2078, R2202, Y2214, T2273, G2298, A2300 and G2301, T2316, G2326 and A2327, T2402, A2426, T2435, G2485, C2589, A2631, C2804, T2822, G2874, C2922	R693, L734L, I738I, S758F, K766K, Q767Q, N772, D776, V801, H809, V812, E829, T863, Q877, S935, S941, S958, F974
D89	G2078, R2202, Y2214, Y2273, R2298, A2300 and R2301, W2316, R2326 and A2327, T2402, A2426, T2435, S2485, Y2589, R2631, Y2804, Y2822, R2874, C2922	R693, L734L, I738I, S/F758, K766K, Q767Q, N/K772, D/N776, V801, H809, V812, E/Q829, T863, Q877, S/L935, S/P941, S958, F974

Otherwise specified the transformants were obtained from the transformations carried out with the mutated RTe.

[a], the *C. albicans* SC5314 strain is heterozygous in some nucleotide positions, which are represented with the following codes: R, A and G; Y, C and T; W, A and T; S, C and G. Red, the nucleotide changes included in the mutated RTe to introduce the S758F mutation in Tac1; pink, the synonymous mutations to avoid the post-editing cleaving of Cas9.

[b], when heterozygous nucleotide positions resulted in amino acid change it was represented with the two amino acid symbols separated by a slash followed by the residue number. For homozygous mutations, if they did not entail amino acid change, they are denoted with the symbol of the amino acid present in the SC5314 strain followed by the position and again the same amino acid symbol. Conversely, if they encoded a different amino acid, they are represented with the symbol of the amino acid present in the SC5314 strain followed by the position and then the other amino acid. The S758F mutation and the amino acid residues encoded by the synonymous mutations are highlighted in red and pink, respectively.

Table VII. Summary of the sequencing results of *ERG11* in the *C. albicans* SC5314 and derived mutants and the corresponding amino acid residues.

Transformant	Nucleotide positions in *ERG11*[a]	Amino acid residues in Erg11[b]
SC5314	C837, R1020, Y1110, A1120, A1430, T1434, A1437, R1440, A1444, T1463, Y1470	S279, L340, L370, M374, Y477, V478, Q479, L480, T482, V488, N490
E7.1	C837, R1020, Y1110, A1120, G1430, C1434, G1437, A1440, A1444, T1463, T1470	S279, L340, L370, M374, Y477C, V478V, Q479Q, L480, T482, V488, N490
E12.1	Several small insertions and deletions surrounding the RTe insertion site leading to frame-shifts in the coding sequence	
E15.1	C837, A1020, C1110, A1120, G1430, C1434, no more sequence from here onwards	S279, L340, L370, M374, Y477C, V478V
E20.1	C837, R1020, Y1110, A1120, G1430, C1434, G1437, A1440, A1444, T1463, T1470	S279, L340, L370, M374, Y477C, V478V, Q479Q, L480, T482, V488, N490
E26.1	C837, R1020, Y1110, A1120, G1430, C1434, G1437, A1440, A1444, T1463, Y1470	S279, L340, L370, M374, Y477C, V478V, Q479Q, L480, T482, V488, N490
E27.1	A986, ΔT1022-G1023, from here onwards there is a frame-shift in the coding sequence	L329Stop, L341Stop
E42.1	C837, R1020, Y1110, A1120, G1430, C1434, G1437, A1440, A1444, T1463, Y1470	S279, L340, L370, M374, Y477C, V478V, Q479Q, L480, T482, V488, N490
E45.1	C837, A1020, C1110, A1120, G1430, C1434, G1437, A1440, A1444, T1463, T1470	S279, L340, L370, M374, Y477C, V478V, Q479Q, L480, T482, V488, N490
E47.1	C837, R1020, Y1110, A1120, G1430, C1434, G1437, A1440, A1444, T1463, T1470	S279, L340, L370, M374, Y477C, V478V, Q479Q, L480, T482, V488, N490
E50.1	C837, A1020, C1110, A1120, G1430, C1434, G1437, A1440, A1444, T1463, T1470	S279, L340, L370, M374, Y477C, V478V, Q479Q, L480, T482, V488, N490
E59.1	C837, A1020, C1110, A1120, G1430, C1434, G1437, A1440, A1444, T1463, T1470	S279, L340, L370, M374, Y477C, V478V, Q479Q, L480, T482, V488, N490
E64.1	Other modifications (M881, K1019, ΔT1415 leading to frame-shifts in the coding sequence)	D/A294, L/W340
E70.1	C837, R1020, Y1110, A1120, G1430, C1434, G1437, A1440, A1444, no more sequence from here onwards	S279, L340, L370, M374, Y477C, V478V, Q479Q, L480, T482
E73.1	C837, A1020, C1110, A1120, G1430, C1434, G1437, A1440, A1444, T1463, T1470	S279, L340, L370, M374, Y477C, V478V, Q479Q, L480, T482, V488, N490
E82.1	C837, A1020, C1110, A1120, R1430, C1434, G1437, A1440, A1444, T1463, Y1470	S279, L340, L370, M374, Y/C477, V478V, Q479Q, L480, T482, V488, N490
E119.1	C837, R1020, Y1110, A1120, G1430, C1434, G1437, A1440, A1444, T1463, T1470	S279, L340, L370, M374, Y477C, V478V, Q479Q, L480, T482, V488, N490
E125.1	C837, G1020, T1110, A1120, G1430, C1434, G1437, A1440, A1444, T1463, T1470	S279, L340, L370, M374, Y477C, V478V, Q479Q, L480, T482, V488, N490
E135.1	C837, R1020, Y1110, A1120, R1430, C1434, G1437, A1440, R1444, T1463, Y1470	S279, L340, L370, M374, Y/C477, V478V, Q479Q, L480, T/A482, V488, N490

Table VII. Continued.

Transformant	Nucleotide positions in *ERG11*[a]	Amino acid residues in Erg11[b]
E137.1	C837, R1020, Y1110, A1120, R1430, Y1434, G1437, A1440, A1444, T1463, T1470	S279, L340, L370, M374, Y/C477, V478V, Q479Q, L480, T482, V488, N490
E2.2	C837, R1020, Y1110, A1120, G1430, C1434, G1437, A1440, A1444, T1463, Y1470	S279, L340, L370, M374, Y477C, V478V, Q479Q, L480, T482, V488, N490
E3.2	C837, G1020, T1110, A1120, G1430, C1434, G1437, A1440, A1444, T1463, T1470	S279, L340, L370, M374, Y477C, V478V, Q479Q, L480, T482, V488, N490
E9.2	C837, R1020, Y1110, A1120, G1430, C1434, G1437, A1440, A1444, T1463, T1470	S279, L340, L370, M374, Y477C, V478V, Q479Q, L480, T482, V488, N490
E10.2	C837, A1020, C1110, A1120, R1430, Y1434, G1437, A1440, A1444, T1463, T1470	S279, L340, L370, M374, Y/C477, V478V, Q479Q, L480, T482, V488, N490
E21.2	T837, R1020, Y1110, M1120, G1430, C1434, G1437, A1440, A1444, T1463, T1470	S279, L340, L370, M/S374, Y477C, V478V, Q479Q, L480, T482, V488, N490
E40.2	C837, A1020, C1110, A1120, G1430, C1434, G1437, A1440, A1444, T1463, T1470	S279, L340, L370, M374, Y477C, V478V, Q479Q, L480, T482, V488, N490
E46.2	Several small deletions leading to frame-shifts in the coding sequence	
E89.2	Several nucleotide changes and small deletions leading to frame-shifts in the coding sequence	
EW6.1	C837, A1020, C1110, A1120, A1440, A1444, A1430, C1434, G1437, T1463, Y1470	S279, L340, L370, M374, Y477, V478V, Q479Q, L480, T482, V488, N490
EW7.1	C837, A1020, C1110, A1120, A1430, C1434, G1437, A1440, A1444, W1463, T1470	S279, L340, L370, M374, Y477, V478V, Q479Q, L480, T482, V/D488, N490
EW6.2	C837, G1020, T1110, A1120, A1430, C1434, G1437, A1440, A1444, T1463, T1470	S279, L340, L370, M374, Y477, V478V, Q479Q, L480, T482, V488, N490
EW8.2	C837, A1020, C1110, A1120, A1430, C1434, G1437, A1440, A1444, T1463, Y1470	S279, L340, L370, M374, Y477, V478V, Q479Q, L480, T482, V488, N490

[a], the *C. albicans* SC5314 strain is heterozygous in some nucleotide positions, which are represented with the following codes: R, A and G; Y, C and T; W, A and T; M, A and C; K, G and T. Red, the nucleotide changes included in the mutated RTe to introduce the Y477C mutation in Erg11; pink, the synonymous mutations to avoid the post-editing cleaving of Cas9. Δ, Deletion.

[b], when heterozygous nucleotide positions resulted in amino acid change it was represented with the two amino acid symbols separated by a slash followed by the residue number. For homozygous mutations, if they did not entail amino acid change, they are denoted with the symbol of the amino acid present in the SC5314 strain followed by the position and again the same amino acid symbol. Conversely, if they encoded a different amino acid, they are represented with the symbol of the amino acid present in the SC5314 strain followed by the position and then the other amino acid. The Y477C mutation and the amino acid residues encoded by the synonymous mutations are highlighted in red and pink, respectively. If changes in the nucleotide sequence introduced a stop codon it is represented as the amino acid symbol followed by the residue's number and Stop.

Table VIII. Summary of the sequencing results of *MRR2* in the *C. albicans* SC5314 and derived mutants and the corresponding amino acid residues.

Transformant	Nucleotide positions in *MRR2*[a]	Amino acid residues in Mrr2[b]
SC5314	C924, C927, C932	A308, L309, A311
M18.1	T924, T927, T932	A308A, L309L, A311V
M28.1	T924, T927, Y932	A308A, L309L, A/V311
M42.1	The RTe was introduced twice, the second in heterozygosis, and additional nucleotide changes were identified	
M48.1	Small insertion leading to frame-shifts in the coding sequence	
M55.1	T924, T927, T932	A308A, L309L, A311V
M59.1	Small deletion leading to frame-shifts in the coding sequence	
M67.1	Small deletion leading to frame-shifts in the coding sequence	
M68.1	T924, T927, Y932	A308A, L309L, A/V311
M70.1	T924, T927, T932	A308A, L309L, A311V
M12.2	T924, T927, T932	A308A, L309L, A311V
M15.2	Small deletion leading to frame-shifts in the coding sequence	
M22.2	Small deletion leading to frame-shifts in the coding sequence	
M49.2	Small deletion leading to frame-shifts in the coding sequence	
M146.2	T924, T927, T932	A308A, L309L, A311V
M148.2	T924, T927, T932	A308A, L309L, A311V
M159.2	T924, T927, T932	A308A, L309L, A311V
M163.2	T924, T927, T932	A308A, L309L, A311V
M165.2	T924, T927, T932	A308A, L309L, A311V
MW42.1	Small insertions and deletions leading to frame-shifts in the coding sequence and several other nucleotide changes	
MW43.1	T924, T927, C932	A308A, L309L, A311
MW21.2	Small insertion leading to frame-shifts in the coding sequence	
MW22.2	T924, T927, C932	A308A, L309L, A311

[a], Y, heterozygous position with either C or T. Red, the nucleotide changes included in the mutated RTe to introduce the A311V mutation in Mrr2; pink, the synonymous mutations to avoid the post-editing cleaving of Cas9. Δ, Deletion.

[b], when heterozygous nucleotide positions resulted in amino acid change it was represented with the two amino acid symbols separated by a slash followed by the residue number. For homozygous mutations, if they did not entail amino acid change, they are denoted with the symbol of the amino acid present in the SC5314 strain followed by the position and again the same amino acid symbol. Conversely, if they encoded a different amino acid, they are represented with the symbol of the amino acid present in the SC5314 strain followed by the position and then the other amino acid. The A311V mutation and the amino acid residues encoded by the synonymous mutations are highlighted in red and pink, respectively.